GENETIC AND EPIGENETIC TARGETS IN LIVER CANCER

A THESIS SUBMITTED TO
THE DEPARTMENT OF MOLECULAR BIOLOGY AND GENETICS
AND THE INSTITUTE OF ENGINEERING AND SCIENCE OF
BİLKENT UNIVERSITY
IN PARTIAL FULFILLMENT OF THE REQUIREMENTS
FOR THE DEGREE OF DOCTOR OF PHILOSOPHY

BY
HALUK YÜZÜGÜLLÜ
AUGUST, 2010

TO MY FAMILY

I certify that I have read this thesis and that in my opinion it is fully adequate, in scope, and in quality, as a thesis for the degree of Doctor of Philosophy.

_____
Prof. Dr. Mehmet Öztürk

I certify that I have read this thesis and that in my opinion it is fully adequate, in scope, and in quality, as a thesis for the degree of Doctor of Philosophy.

_____
Prof. Dr. Kuyaş Buğra

I certify that I have read this thesis and that in my opinion it is fully adequate, in scope, and in quality, as a thesis for the degree of Doctor of Philosophy.

_____
Prof. Dr. İhsan Çalış

I certify that I have read this thesis and that in my opinion it is fully adequate, in scope, and in quality, as a thesis for the degree of Doctor of Philosophy.

_____
Assoc. Prof. Dr. İhsan Gürsel

I certify that I have read this thesis and that in my opinion it is fully adequate, in scope, and in quality, as a thesis for the degree of Doctor of Philosophy.

_____
Assist. Prof. Dr. Uygar Tazebay

Approved for the Institute of Engineering and Science

_____
Prof. Dr. Levent Onural

Director of the Institute of Engineering and Science

ABSTRACT

Genetic and Epigenetic Targets in Liver Cancer

Haluk Yüzügüllü
Ph.D. in Molecular Biology and Genetics
Supervisor: Prof. Dr. Mehmet Öztürk
August, 2010, 143 Pages

Hepatocellular carcinoma (HCC) kills nearly 600.000 people each year and the only effective therapy for this cancer is liver transplantation or tumor ablation only when the tumor is small enough. These tumors are surprisingly resistant to conventional therapies such as chemotherapy and radiotherapy. Moreover, as HCC is almost always associated with cirrhosis, the treatment with cytotoxic agents is dangerous as they will also affect hepatic functions of the diseased liver. Therefore, there is urgent need to find novel therapeutic approaches against HCC in order to diminish death toll. Our overall goal is to discover "druggable target genes" in HCC. In other words, we wish to identify novel genes and novel mechanisms involved in these cancers in order to use them as potential therapeutic targets.

During my thesis work, I developed different approaches to find new mechanisms and novel targets:

1- Deciphering the role of canonical Wnt signaling in HCC: We classified human HCC cell lines into "well-differentiated" and "poorly differentiated" subtypes, based on the expression of hepatocyte lineage, epithelial and mesenchymal markers. Poorly differentiated cell lines lost epithelial and hepatocyte lineage markers, and overexpressed mesenchymal markers. Also, they were highly motile and invasive. We compared the expression of 45 Wnt pathway genes between two subtypes. Likewise, six Frizzled receptors, and canonical Wnt3 ligand were expressed in both subtypes. In contrast, canonical ligand Wnt8b and noncanonical ligands Wnt4, Wnt5a, Wnt5b and Wnt7b were expressed selectively in well- and poorly differentiated cell lines, respectively. Canonical Wnt signaling activity, as tested by a TCF reporter assay was detected in 80% of well-differentiated, contrary to 14% of poorly differentiated cell lines. TCF activity generated by ectopic mutant β-catenin was weak in poorly differentiated SNU449 cell line,

suggesting a repressive mechanism. We tested Wnt5a as a candidate antagonist. It strongly inhibited canonical Wnt signaling that is activated by mutant β-catenin in HCC cell lines.

2. Systematic screening of protein kinases and phosphatases as potential therapeutic targets: There is evidence of aberrant activation of several signaling cascades in HCC, and a multikinase inhibitor, sorafenib, has shown survival benefits in patients with advanced HCC. We used siRNAs to screen a large number of kinases and phosphatases to identify related genes involved in HCC cell survival. A total of 7 kinases and 5 phosphatases were identified as strong candidate targets.

3-Screening of a set of selected epigenetic regulators as potential therapeutic targets: Recent studies have indicated that senescence arrest or senescence escape could be regulated by epigenetic changes on chromatin. We wanted to identify key histone methylation and acetylation changes associated with senescence or senescence escape, and select key histone modifying enzymes, as potential targets for "pro-senescence" interventions (therapeutic interventions that allow senescence induction in cancer cells). We identified ATAD2 as an epigenetic target, and found ATAD2 gene overexpressed in HCC compared to normal liver. We also found a stepwise increase of ATAD2 protein expression in late stages with respect to pre-neoplastic and early stage during hepatocellular carcinogenesis. ATAD2 knockdown using siRNAs in cancer cells leads to increase in global histone acetylation and inhibit cell proliferation and induce caspase-3 dependent apoptosis in HCC and induce senescence in MRC5 cells. Its potentiator role (coactivator role with estrogen, androgen and myc targets) indicates ATAD2 as a potential therepeutic target for HCC.

ÖZET

Karaciğer kanserinde Genetik ve Epigenetik Hedefler

Haluk Yüzügüllü
Moleküler Biyoloji ve Genetik Doktorası
Tez Yöneticisi: Prof. Dr. Mehmet Öztürk
Ağustos, 2010, 143 sayfa

Karaciğer kanseri en sık rastlanan birincil kanserlerden olup, yılda 600.000 civarında ölüme sebep olmaktadır. Şu andaki en etkili tedavi yöntemi karaciğer transplantasyonudur ve tümör ablasyon yöntemi sadece tümör yeterince küçük ise uygulanabilmektedir. Kanserli hücreler kemoterapi ve radyoterapi gibi yöntemlere oldukça dayanıklıdırlar. Dahası, karaciğer kanseri sürekli siroz üzerine geliştiği için karaciğerin diğer hepatik fonksiyonlarını yerine getirmesini de engellediği için, sitotoksik ajanlar kullanmak oldukça tehlikelidir. Bu nedenle karaciğer kanserini yenmek için daha yeni ve geçerli terapatik yöntemlere ihtiyac duyulmaktadır.

Bizim amacımız karaciğer kanserinde yeni hedeflenebilir genleri keşfetmektir. Başka bir değişle, biz bu çalışma ile karaciğer kanserinde yeni hedefler ve yeni mekanizmalar keşfederek bunları potansiyel terapötik hedefler olarak kullanmayı amaçladık.

Tez çalışmalarım sırasında, yeni hedefler ve yeni mekanizmalar keşfetmek için değişik yöntemler kullanmaya çalıştım:

1- Karaciğer kanserinde kanonik Wnt sinyallenme yolağının rolü: karaciğer kanserı hücrelerini hepatosit spesifik, epitel ve mezenkimal markörler kullanarak “iyi diferansiye” ve “kötü diferansiye” hücre hatları olarak iki gruba ayırdık. Kötü diferansiye hücre hatlarında epitel ve hepatosit spesifik markörlerin negatif hale geldiğini, mezenkimal markörleri anlatmaya başladığını gösterdik. Wnt sinyal yolağında görev alan 45 genin, gen anlatım seviyelerini iki grupta inceledik. 6 Frizzled almaç geninin ve wnt3 ligandının her iki grupta da anlatıldığını gösterdik. Kanonik Wnt ligandı wnt8b`nin sadece iyi diferansiye grupta anlatıldığını ve Wnt4, Wnt5a, Wnt5b and Wnt7b gibi kanonik olmayan ligandların kötü diferansiye gruba spesifik olduğunu gösterdik. Kanonik Wnt

sinyallenmesinin sadece iyi diferansiye hücrelerde seçici olarak aktif olduğunu değil, aynı zamanda kötü diferansiye tümörlerde de baskılandığını gösterdik. Kanonik olmayan hücre hattı, Snu449 da mutant beta-kateninin ektopik anlatımının TCF aktivitesini arttıramaması bu gruptaki hücrelerde baskılayıcı bir mekanizma olduğuna işaret etti. Kanonik olmayan wnt5a genini aday olarak test ettik. Wnt5a geninin mutant beta-kateninin aktive ettiği TCF aktivitesini baskıladığını gösterdik. Bazı kanser tiplerinde, APC, Axin ve beta-katenin gibi genlerde oluşan mutasyonlarla Wnt-beta-katenin sinyallenmesinin, Wnt ligandlarının olmadığı ortamda anormal olarak aktifleşip, beta-kateninin sitoplazma ve çekirdekte birikmesine sebep olup hedef genlerin aktivasyonuna yol açtığı biliniyor. Bu nedenle beta-kateninin hücre zarı, sitoplazma ve çekirdekteki fraksiyonlarını tanıyabilen monoklonal antikorlar üretip, bu antikorları kanserli dokularda test ederek klinik değerlerini karakterize ettik.

2- Kinaz ve fosfataz genlerini potansiyel terapatik hedef olarak sistematik olarak taranması: Karaciğer kanserinde değişik sinyallenme yolaklarının aktif hale geldiği ve bu hastalarda multikinaz inhibitorü olan sorafenib ilacının, ileri derece hastaların ömürlerini uzattığı biliniyor. Bu amaçla yeni hedefler bulmak ve hücre yaşlanması indüklenmesi yönünde terapatik hedef gösterebilmek için çok fazla sayıda kinaz ve fosfatazları hedef alan RNA müdehalesi yöntemi ile tarama gerçekleştirdik. Toplamda 7 kinaz ve 5 fosfataz genini güçlü adaylar olarak gösterildi.

3- Seçilen epigenetik hedeflerin potansiyel terapötik hedef olarak taranması: Yakın dönemde yapılan çalışmalar, hücre yaşlanması ve bundan kaçışın kromatin üzerindeki epigenetik değişiklikler ile düzenlendiğini gösterdi. Bu amaçla hücre yaşlanması ve bundan kaçış ile uyumlu histon asetillenmesi ve metillenmesi değişiklikleri tanımladık, bundan sorumlu histon enzimlerini bulup, bunları "hücre yaşlanması öncüleyici" hedefler (kanserli hücreleri hücre yaşlanmasına götüren) olarak göstermeyi hedefledik. ATAD2 genini epigenetik hedef olarak tanımlayıp, karaciğer kanserinde normal hepatositlere göre daha fazla gen ifadesi olduğunu gösterdik. ATAD2 proteinin öncü-neoplastik ve ilk aşama karaciğer kanserlerine göre ileri aşama kanserlerde kademeli artış olduğu gösterildi.

Kanserli hücrelerde siRNA tekniği kullanarak, ATAD2 proteinini azaltıp ve buna bağlı global histon asetillenmesinin arttığını, hücre çoğalmasının azaldığını, hücreleri apoptoza götürdüğünü ve MRC5 akciğer fibroblastlarında ise hücre yaşlanmasını indüklediğini gösterdik. ATAD2 geninin potansiyel artırıcı (östrojen, androjen ve myc hedefleri üzerinde) etkisinden dolayı karaciğer kanserinde aday terapötik hedef olduğunu işaret etmektedir.

ACKNOWLEDGMENTS

I would like to begin thanking to my thesis advisor Prof. Mehmet Öztürk for all that I have learnt from him. Without his support, guidance, and patience, none of this would be possible. I am also thankful that he let me learn new techniques, introduce me to new networks and gave me more freedom in the lab. He was a lot more than a supervisor for me.

I would like to thank Dr. Rengül Çetin-Atalay, for her knowledge, experience, support and patience.

I would like to thank TUBITAK for financial supports for 2211 and 2214 programs.

I would like to thank also to all members of Equipe 2 and 5, especially Dr. Jean Luc Coll for their reagents and technical helps. To Ralph Meuwissen for his career advices, discussions, and share his experience.

I also want to thank Dr. Stephan Dimitrov for his career and scientific advices.

I am also grateful to all the other researchers and fellows in Bilkent University for providing me such a wonderful scientific and friendly environment. It will definitely be an unforgettable memory for me.

I thank all the current and former members of Ozturk Lab, for their help and experience they shared. Especially I am grateful to Nuri Ozturk for his invaluable discussion and scientific help. I want to thank also Hani Al Otaibi, Khemais Benhaj, Pelin Telkoparan and Bilge Kilic for their both technical help and advice.

I would like thank my family and especially to my parents for their never-ending support and care. I am away from them for almost 14 years and I hope it is worth it.

And throughout my journey, she is the one that believed me and always supported me even in very difficult times. A fellow and beloved, Özge, she has been always with me and I believe I cannot even thank her enough for her help and support both intellectually and technically and the wonderful meaning she gave to my life…

TABLE OF CONTENTS

LIST OF TABLES

LIST OF FIGURES

ABBREVIATIONS

AD	activation domain
AFB1	aflotoxinB1
AFP	alpha-feto protein
APC	Adenomatous polyposis coli
BRCA	breast cancer gene, early onset
BrdU	Bromodeoxyuridine
CDK	Cyclin Dependent Kinase
CK	Casein Kinase
CK19	Cytokeratin 19
CO_2	carbon dioxide
CRC	colorectal cancer
C-terminus	carboxy terminus
Dkk	Dickkopf
DNA	Deoxyribonucleic acid
DOX	Doxorubucin
Dox	Doxycycline
Dsh	Dishevelled (in Drosophila)
Dvl	Dishevelled (in vertebrates)
ED	embriyonal day
EDTA	ethylenediaminetetraacetic acid

EtBr	ethidium bromide
FAP	familial adenomatous polyposis
FBS	fetal bovine serum
Fz	Frizzled
g	gram
GAPDH	glyceraldehyde-3-phosphate dehydrogenase
GSK3β	glycogen synthase kinase 3 beta
HB	Hepatoblastoma
HBV	Hepatitis B Virus
HbX	hepatitis B virus X protein
HBXAg	Hepatitis B virus X antigen
HCC	Hepatocellular Carcinoma
HCV	Hepatitis C Virus
HDAC	histone deacetylase
HRP	horse radish peroxidase
hTERT	human Telomerase Reverse Transcriptase
ICR	Imprinting Control Regions
Ig	immunoglobulin
IGF2	insulin-like growth factor 2
IGF2R1	IGF2 Receptor
IGFBP	IGF-binding proteins
JNK	Jun Kinase
Kan	kanamycin
Kb	Kilo base
kDa	kilo dalton
LB	Luria-Bertani media
LD	Low dose
LEF	lymphoid enhancer-binding factor 1
LOH	loss of heterozygosity
LRP5	LDL-receptor related protein 5
LRP6	LDL-receptor related protein 6

LTR	long terminal repeat
M6P/IGF2R	mannose-6-phosphate/insulin-like growth factor 2 receptor
MAb	monoclonal antibody
MAP/ERK	mitogen activated protein/extracellular signal-regulated kinase
MAPK	Mitogen Activated Protein Kinase
MDM2	Mouse Double Minute 2
MET	met proto-oncogene (hepatocyte growth factor receptor)
mg	milligram
µg	microgram
$MgSO_4$	Magnesium Sulfate
$MHBS^t$	carboxyterminal truncated middle hepatitis B surface protein
ml	milliliter
µl	microliter
MMLV	Murine Maloney Leukemia Virus
MQ	MilliQ water
NaCl	Sodium Chloride
NaOH	Sodium Hydroxide
NEAA	Non-essential Amino Acid
nm	nanometer ($1/10^9$ of a meter)
NS3	Nonstructural Protein 3
NS5A	Nonstructural Protein 5A
N-terminus	amino terminus
O/N	over night
OD	Optical Density
PAb	polyclonal antibody
PAGE	Polyacrylamide gel electrophoresis
PBS	Phosphate Buffered Saline
PBS-T	Phosphate Buffered Saline with Tween-20
PCR	Polymearase chain reaction
PD	poorly-differentiated
PI-3 kinase	Phosphatidylinositol 3-kinase

PP2A	protein phosphatase 2A
PPARγ	peroxisome proliferators antigen receptor γ
pRb	Retinoblastoma protein
PS	presenescent
RD	regulatory domains
RFLP	Restriction length fragment polymorphisms
RNA	Ribonucleic acid
RNAi	RNA interference
RTK	receptor tyrosine kinases
S	senescent
S/N	supernatant
SABG	senescence associated beta galactosidase
SAP	shrimp alkaline phosphatase
SCD	small cell-dysplasia
SDS	Sodium Dodecyl Sulfate
SDS-PAGE	SDS- Polyacrylamide Gel Electrophoresis
sFRPs	secreted Frizzled-related proteins
shRNA	short hairpin RNA
siRNA	small interfering RNA
Smad	homolog of mothers against decapentaplegic (MAD)
SWI/SNF	switching-defective and sucrose nonfermenting
TBS	Tris Buffered Saline
TBS-T	Tris Buffered Saline with Tween-20
TCF	T-cell specific, HMG-box
TEMED	N, N, N, N-tetramethyl-1, 2 diaminoethane
TGFα	transforming growth factor alpha
TGF-β	Transforming growth factor
Tris	Tris (hydroxymethyl)-methylamine
TSA	Trichostatin-A
UV	Ultraviolet
WD	well-differentiated

WIF-1	Wnt-inhibitory factor-1
X-Gal	5-bromo-4-chloro-3-indolyl-b-D-galactoside
ZO-1	Zona Occludens

CHAPTER 1. INTRODUCTION

1.1 Hepatocellular malignancy

Hepatocellular carcinoma (HCC) is believed to be originated from either hepatocytes or their progenitors. It is the one of the most frequent neoplasms worldwide and causes around 600,000 deaths per year, and the incidence is steadily increasing in Europe [1]. More than 80% of HCC occur in sub-Saharan Africa and Eastern Asia. The disease incidence is decreasing in these areas due to massive Hepatitis B virus (HBV) vaccination and the control of dietary aflatoxin intake, whereas it is still increasing in low-rate area including Europe. The increase has been associated with hepatitis C virus (HCV) infection. Hepatocellular carcinoma is classified into 4 different groups; well, moderately, poorly differentiated and undifferentiated tumors, respectively. HCC arises as a well differentiated cancer and continues with a stepwise dedifferentiation process.

Indeed, well-differentiated histology is generally seen in early stage and advanced HCC is associated with dedifferentiation. Well-differentiated and moderately differentiated cells are alike hepatocytes, and they are smaller in size and they have irregular trabecular or pseudoglandular architechtural patterns. Poorly differentiated and undifferentiated HCC cells have scanty cytoplasms and pleomorphism [2]. The progenitor cells in HCC like other epithelial tumors evolve during tumor progression and become autonomous later. This is observed with changes in their morphology and behavior; cuboidal shape and polarity is lost, and become more autonomous. Finally, they invade the underlying tissue and form distant metastases. The progressive loss phenotypic and biochemical of hepatocytes is defined as "dedifferentiation" [3]. Poorly differentiated and undifferentiated HCCs are associated with portal veneous invasion and the tumor invasiveness is a crucial factor in determining the long-term clinical outcome for the patient [4-5].

1.2 Aetiological factors of Hepatocellular Carcinoma

HCC occurs after years of damage to liver with inflammatory conditions resulting with chronic hepatitis and/or cirrhosis. This leads to death of hepatocytes and attack of inflammatory cells to hepatocytes and connective tissue [6]. The major causes for HCC are: hepatitis B virus (HBV), hepatitis C virus (HCV) and chronic exposure to aflatoxinB1 (AFB1) and nearly all

cirrhosis inducing factors together are responsible for about 70% - 90% of all HCCs [7-8]. Apart from these factors, there are other aetiological factors including long term use of oral contraceptives, hereditary haemochromatosis diseases, Non-alcoholic fatty liver disorders (NAFLD) and diabetes [6, 9-11].

HCC is a slow process, and usually requires between 10-30 years from the initiation step to the fully malignant phenotype. This process is co-occurring with damage and death of hepatocytes with structurally aberrant chromosomes and genes often as a result of telomerase reactivation with marked genomic instability. The alteration of genes and chromosomes are irreversible and leads to heterogeneous malignant phenotype. [6]. Chronic inflammation, massive cell death and necrosis, fibrosis and cirrhosis, cycles of regeneration, and finally dysplasia and HCC occurs [12]. Recent studies indicate that cirrhosis is associated with senescence arrest of hepatocytes, from which HCC cells must emerge through the bypass of senescence control [13].

1.2.1 Viral induced Hepatocarcinogenesis

The two main hepatitis viruses are hepatitis B virus (HBV) and hepatitis C virus (HCV). HBV infects each year around 2 billions individuals, causes 320,000 deaths each year, and 30-50% of each attributable to HCC. Hepatitis C virus (HCV) infects each year 170,000 individuals, 20% of which develops cirrhosis [14-15]. HBV is a double stranded DNA virus and a member of *hepadnaviridae* family. HBV can integrate into the host genome and may lead to chromosomal instabilities and DNA microdeletions, may target telomerase reverse transcriptase enzyme (hTERT) and also encodes a protein so called protein x (HBx) [16-20]. The role of this protein is not fully characterized yet. HCV is a positive stranded RNA virus, a member *flaviviridae* family, thus cannot integrate into the genome. HCV is different from the HBV that it may yield a higher chronic infection rates and may cause high rates of cirrhosis (5-20%) [21-22]. HCV infected hepatocytes can escape from apoptosis by immune cells via using their HCV core protein and non structural protein NS5A interacting with TNF-α and IFN-α [23-25].

1.2.2 Alcohol and cirrhosis

Chronic alcohol intake or ethanol exposure affect hepatocyte cell signalling pathways that regulate chronic hepatocyte destruction–regeneration, stellate cell activation, cirrhosis and

eventually HCC [26]. Alcohol damages liver cells and induces oxidative stress which contributes to development of fibrosis and cirrhosis and further on HCC itself.

1.2.3 Aflatoxin B1-induced hepatocarcinogenesis

AflatoxinB1 (AFB_1) was shown to have a well-defined genotoxic effect in hepatocarcinogenesis. Consumption of food contaminated with aflatoxins, toxic metabolites of some species of Aspergillus fungi, is a specific mutagen. Aflatoxin is metabolized specifically in liver to aflatoxin B1-8,9-epoxide, a toxic product that induces a G to T mutation of the p53 gene at codon 249 [27-28]. Aflatoxin B1 exposure coexisting with HBV infection, increases the risk of HCC to a 5–10-fold compared with exposure to only one of these factors [29].

1.3 Genetic and epigenetic events in HCC

HCC is a multistep process going through rounds of hepatocyte turnover due to damage and regeneration because of the aetiological factors as stated earlier [5]. This multistep process includes chronic liver injury that produces inflammation, cell death, cirrhosis and regeneration, DNA damage, dysplasia, and finally well differentiated to poorly differentiated HCC (figure 1.1). Telomere shortening is accompanied starting with chronic liver disease and cirrhosis, followed by genomic instability and telomerase reactivation and occasionally structural aberrations in genes and chromosomes. During this multistep process, a number of molecular alterations must occur, but only a limited number of is known currently. These aberrations can be listed as tumor suppressor genes and oncogenes including TP53, β-catenin, ErbB receptor family members, MET and its ligand hepatocyte growth factor (HGF), p16(INK4a), E-cadherin. Alterations in microRNA expression may also be implicated in hepatocellular carcinogenesis [30-32]. The table showing the mutation types and rates of tumor suppressors and oncogenes are listed in the table 1.1.

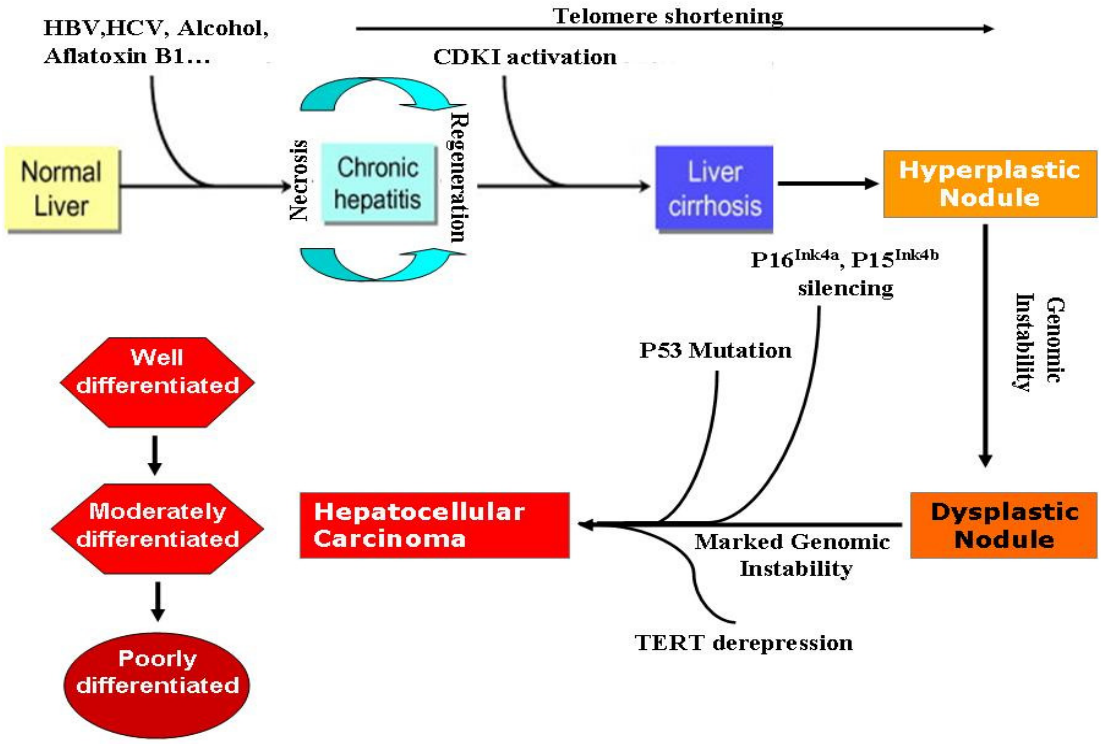

Figure 1.1: **Multistage processes of hepatocarcinogenesis [8, 13] (modified from ref. 8 and 13).**

Table 1.1: Mutations in tumor suppressor genes and oncogenes in HCC

Genes	Mutation Rates	References
p53	28-50%	[33-34]
M6P/IGF2R	25-55%	[35-36]
β-catenin	18-41%	[37-38]
p16	10%	[39]
Axin1&Axin2	5-10%	[40]
Smad2&Smad4	3-6%	[41]
BRCA2	5%	[42]
Rb	rare	[43]
Ras	rare	[44]

Recent advances showed that liver cancer cells harbor aberrant epigenetic abnormalities, suggesting that together with genetic events, epigenetics promote cancer progression. For instance, the CDKN2A gene encoding $p16^{Ink4a}$ and ARF proteins are not mutated whereas they are epigenetically silenced. More than 50% of HCCs display *de novo* methylation of the promoter of CDKN2A gene, resulting in loss of gene expression [13, 45]. Epigenetic mechanisms also contribute to strong expression of genes like TGF-α and IGF-2, promoting of growth of hepatocytes during hepatocarcinogenesis [46] .

Characterization of events involved in HCC dedifferentiation and invasiveness are ill known. Hepatocyte nuclear factors and E-cadherin of epithelial markers were downregulated in HCC [3, 47] and this is associated with tumor invasion and metastasis. In contrast, HCC invasiveness and/or metastasis are positive for mesenchymal markers such as snail [48], twist [49] and vimentin [50]. These changes represent the epithelial-mesenchymal transition (EMT) in HCC, as shown by *in vitro* studies [51-56]. Terminally differentiated hepatocytes express hepatocyte nuclear factor-4α (Hnf-4α) [57-58], and its expression is downregulated during HCC progression in mice [59]. This process is characterized by accumulation of genetic events like chromosomal gains and losses, as well as p53 mutations [6] and identified as dedifferentiation. A rare exception to this picture is the CTNNB1 gene that encodes β-catenin, a key component of the Wnt/β-catenin (canonical Wnt) signaling pathway.

1.4 Role of β-catenin In HCC

In the presence of wnt/canonical signaling ligands, these ligands binds to Frizzled receptor, disheveled is recruited to membrane and inhibits the GSK3b kinase and β-catenin is no longer phosphorylated and accumulated inside the cytoplasm and is translocated to nucleus, further activating several targets including MYC, cyclin-D1 and MMP7 (figure 1.2) [60].

β-catenin mutations were found to be associated with a subset of low grade (well-differentiated) HCCs with good prognosis and chromosome stability [40, 61-65]. Among 366 HCCs studied by Hsu et al., β-catenin mutations were associated with grade I histology. Another

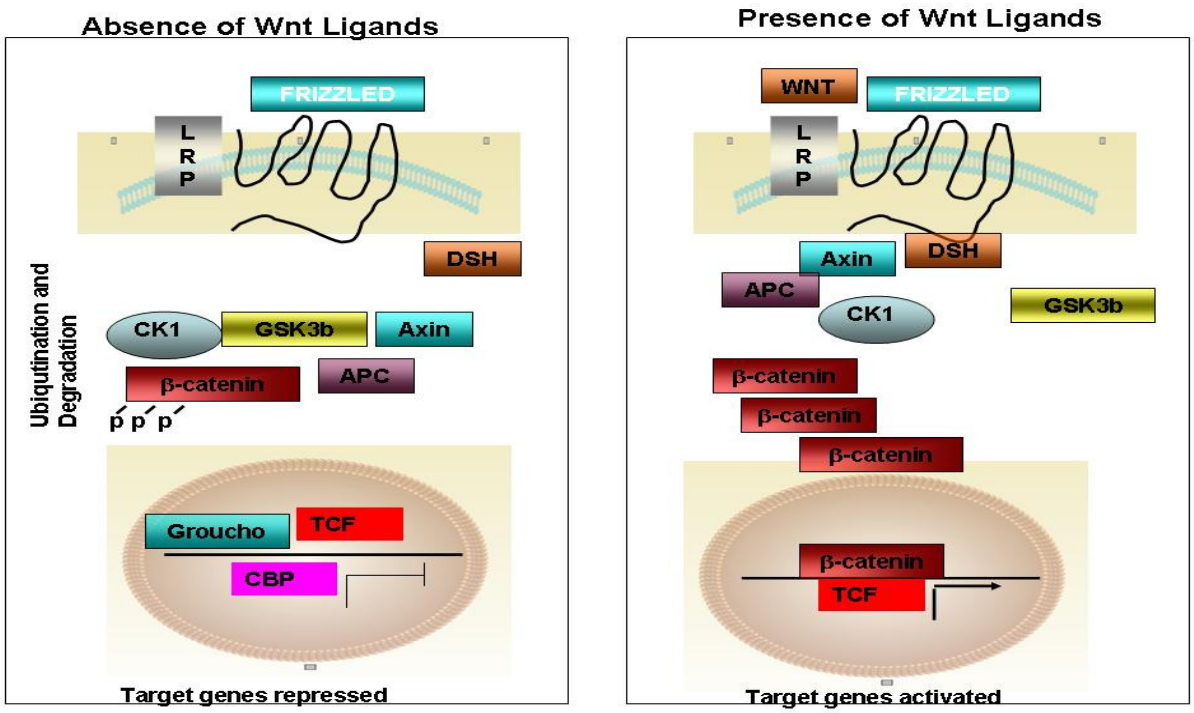

Figure 1.2: Overview of the canonical Wnt signaling pathway, (Modified from ref. 60) A) In the absence of Wnt ligands, the cytoplasmic β-catenin is degraded in the destruction complex, composed of APC, axin/conductin, and GSK-3β. First, β-catenin is phosphorylated on Ser 45 residue by CKIα (priming), primed β-catenin is further phosphorylated at Thr 41, Ser 37, and Ser 33 residues by GSK-3β. Phosphorylation of these amino acids triggers ubiquitination of β-catenin by β-TrCP and degradation in proteasomes. Therefore, the cytoplasmic level of β-catenin is kept low in the absence of Wnt. The LEF/TCFs cannot activate the target genes without β-catenin. The WIF-1, sFRP, and/or Dkk can inhibit the Wnt signaling by binding to Wnt ligands or LRP5/6. B) In the presence of Wnt, a) Wnt signaling triggers CKIε-dependent phosphorylation of Dvl (Dsh) and enhances the binding of Dvl (Dsh) to Frat-1. Frat-1 binds to GSK-3β in the Axin complex, resulting in a reduction of the phosphorylation of β-catenin by GSK-3β; or b) Wnt triggers the phosphorylation of LRP6 by CK1γ and GSK3β, which provides a docking site for Axin and recruits it to the plasma membrane. Wnt also enhances the binding of Dvl (Dsh) to Frizzled, and Dvl (Dsh) bound to Frizzled is necessary for the formation of a complex between Axin and LRP6, resulting in reduced phosphorylation of β-catenin and Axin by GSK3β. Therefore, β-catenin escapes from phosphorylation and subsequent ubiquitination, and accumulates in the cytoplasm. The accumulated cytoplasmic β-catenin goes into the nucleus, where it binds to LEF/TCFs and activates the transcription of target genes

study with similarly high number of tumors (n = 372) also showed that mutant nuclear β-catenin is associated with non-invasive tumor and but not with portal vein tumor thrombi [63]. In addition, β-catenin mutations were associated with good survival rates. Study of canonical Wnt

signaling activity in primary tumors is possible indirectly by using target genes [62]. For instance, using glutamine synthetase (encoded by canonical Wnt signaling target GLUL gene) as a marker for canonical Wnt signal activity, Audard et al. showed that 36% HCCs displayed canonical Wnt activation. These tumors are compatible with well-differentiated morphology. The association of β-catenin mutation and nuclear translocation with well-differentiated tumor grade was also reported using several transgenic mouse models of HCC [62, 66]. Liver tumors from c-myc and c-myc/TGF-β1 transgenic mice showed activated beta-catenin. However, it was very rare with faster growing and histologically more aggressive HCCs in the same model. Thus nuclear translocation of β-catenin and activation of canonical Wnt signaling are early events mostly affecting well-differentiated HCCs.

Mutations of β-catenin gene were initially identified in colorectal cancers, leading to aberrant β-catenin protein accumulation and constitutive activation of canonical Wnt signaling. APC gene mutations in colorectal cancer and AXIN1 in HCC also activate canonical Wnt signaling by β-catenin protein accumulation. Therefore, both β-catenin, APC or AXIN1 mutations are considered to display active or constitutive canonical Wnt signalling [67]. Only a subset of HCC is associated with activated of canonical Wnt signaling as opposed to colorectal cancers. Interestingly, oncogenic β-catenin expressing transgenic mice develop only hepatomegaly [68-69], in contrast to intestinal polyposis and microadenoma in intestinal cells [70].

Taken together, Wnt pathway and β-catenin mutations may play a dual role in HCC, both in the initiation of HCC by close association of β-catenin mutation with well differentiated HCC and later stages as well [5].

1.4.1 Structure of beta-catenin protein and interaction partners

The protein β-catenin has a dual role; one in the establishment and maintenance of cell–cell adhesion at adherens junctions, and the other in the regulation of gene expression through Wnt signaling [71-72]. Both of these roles are conserved throughout evolution [73]. The protein is composed of short N-terminal, C-terminal domains interrupted with central core domain consisting of 12 armadillo repeats (Figure 1.3). Both structural and signal regulatory roles are associated with all three domains [74]. β-catenin need partners to perform its function. α-catenin [75-76] and βTrCP [77] are the main partners binding at N-terminal domain. The α-catenin

binding, together with E-cadherin binding to the central core domain is required for adhesion role of β-catenin [78]. The BTrCP binding is necessary for its subsequent degradation of β-catenin after phosphorylation of specific sites at the same N-terminal domain by glycogen synthase kinase 3 beta (GSK-3β). This phosphorylation event is facilitated by a multiprotein complex including Axin which bind to β-catenin through armadillo repeat domain [74, 79], and (APC). The presence of Wnt ligands or active Wnt signalling efficiently decreases the destruction of β-catenin via inhibition of GSK-3β. LEF/TCF factors (TCF) bind to the armadillo repeat domain for its function in transcriptional activation of Wnt target genes. ICAT and Chibby proteins for inhibitory roles compete with TCF for binding to the same core domain [80-81].

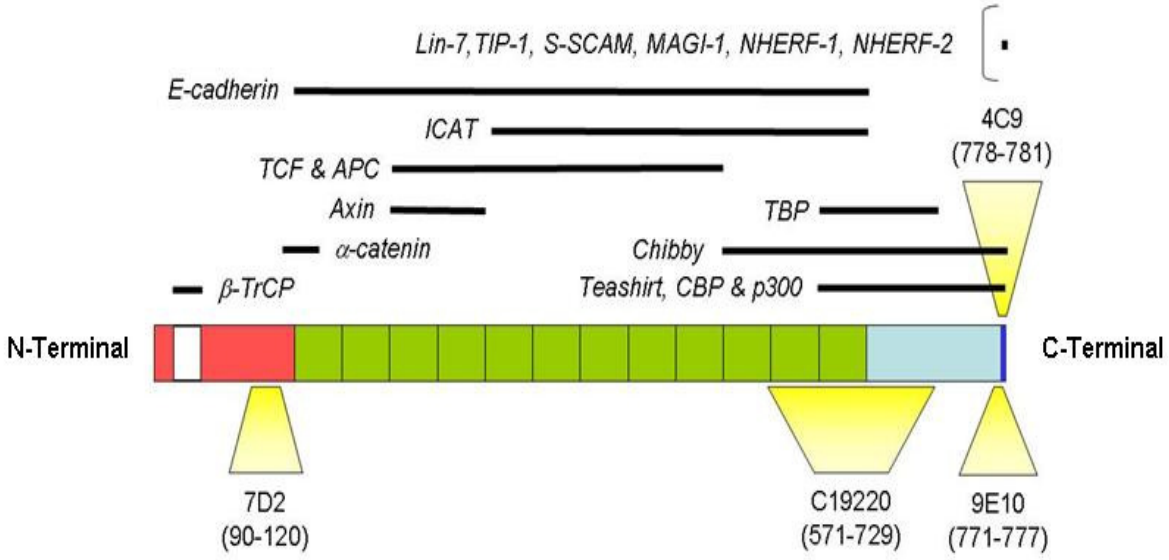

Figure 1.3 Schematic view of β-catenin protein domains, principal interacting proteins and monoclonal antibody epitopes [Yuzugullu et al, unpublished data].

The C-terminal domain of β-catenin has not been of great interest until recently. This acidic tail is the primary transactivation domain and TBP, CBP and p300 [82], as well as *Teashirt* [83], *Chibby* [80] are all associated through this domain. The C-terminal domain, together with the last three armadillo repeats of the core domain has been recently involved in nuclear import-export of the β-catenin protein [84]. Indeed the last 70 amino acids of β-catenin appear to play a crucial role in cytonuclear shuttling of β-catenin [85]. A relatively new and interesting aspect of the C-terminal domain of β-catenin is its interaction with a growing list of PSD95/DlgA/ZO-1

homology (PDZ)-interaction domain proteins. The PDZ domain is a specific protein-interaction module with an interaction 'pocket' that can be filled by a PDZ motif 'ligand'. The PDZ motifs are consensus sequences that usually located at the extreme intracellular carboxyl terminus. The last 4 amino acids of β-catenin (DTDL) which is highly conserved among all metezoans excluding C. elagans [73] is a consensus PDZ motif D(S/T)XL (X denotes any residue) [86]. Proteins bind to these PDZ motifs and thus can target directly or indirectly, cluster and cycle the receptors, ion channels as well as transporters. PDZ proteins can link the signaling pathways and different components. Such roles implicate their role in many diseases. They control the pre- and post synaptic proteins in neurotransmission and plasticity. At the synapse, PDZ proteins have a role in neurotransmitter vesicle docking and receptor cycling. Cell movements, migration, polarity, and neighbouring cell interactions, as well as cell phenotypes including morphology are controlled with PDZ machinery. Beta-catenin interacts with several PDZ proteins including synaptic scaffolding molecule (S-SCAM; [87-90], its non-neuronal isoform called membrane-associated guanylate kinase with inverted domain organization-1 (MAGI-1; [91], Na^+/H^+ exchanger regulatory factor-1/EBP50 (NHERF-1; [92-93] and NHERF-2; [94], Tax-1 interacting protein (TIP-1; [95-96], LIN-7 [97].

Cadherins and catenins play important roles in synapse assembly. The PDZ domain of β-catenin is involved in the localization of a reserved pool of synaptic vesicles [98]. If beta-catenin is lost in hippocampal pyramidal neurons, this leads to misregulation of response in response to prolonged repetitive stimulation and a corresponding decrease of vesicles. Beta-catenin modulation of vesicle localization is mediated by its PDZ binding domain [99]. Epithelial and neuronal beta-catenin interacts with LIN-7 PDZ proteins. This event is Ca^{2+} dependent and is mediated direct linking of LIN-7 to the C-terminal beta-catenin PDZ target sequence. Therefore it is ensured that LIN-7 is relocated to the junctions via beta-catenin and is a specific event. Moreover, when LIN-7 is present at the beta-catenin-containing junctions, it determines the accumulation of binding partners, thus suggesting the mechanism by which beta-catenin mediates the organization of the junctional domain [97]. Functional studies showed that in mouse embryonic fibroblasts, NHERF1 associates directly via PDZ2 domain with beta-catenin and is required for beta-catenin localization at the cell-cell junctions. NHERF1 inhibits cell motility and is required to suppress anchorage-independent growth. Thus, NHERF1 appears to be a cofactor with an essential role in the integrity of epithelial tissues by maintaining the proper localization

and complex assembly of β-catenin [93]. NHERF-2 links the N cadherin/catenin complex to the platelet-derived growth factor receptor to modulate the actin cytoskeleton and regulate cell motility [94]. In brain, being a multi-PDZ domain scaffolding protein, S-SCAM, binds and interacts with several different ligands including PTEN (phosphatase and tensin homolog), dendrin, axin, beta- and delta-catenin, dasm1 (dendrite arborization and synapse maturation 1), neuroligin, hyperpolarization-activated cation channels, beta1-adrenergic receptors, and NMDA receptors [100]. MAGI-1, presumably through its association with β-catenin, is required for Rap1 activation upon cell-cell contact and for enhancement of vascular endothelial cadherin-mediated cell adhesion [101]. TIP-1 binding to β-catenin inhibits its transcriptional activity and the overexpression of TIP-1 results in reduced proliferative capacity of colorectal cancer cells [95], suggesting an important role for TIP-1 interaction with the PDZ motif of β-catenin in the control of Wnt/β-catenin signaling. Interaction of the C-terminal domain of beta-catenin with PDZ domain-containing proteins is required to shape axon arbors of retinal ganglion cells [102].

1.5 Protein Kinase and Phosphatase Genes

In eukaryotic cells, signal transduction is mediated by protein kinases and phosphatases; by remodifying substrate activity. Protein kinases are among the largest families of genes in eukaryotes constituting about 2-2,5 % of the genome [103-104] and have been intensively studied. Cell metabolism, transcription, cell cycle progression, apoptosis, differentiation, cytoskeletal rearrangement, invasion and cell movement are controlled by protein kinases. Protein kinases are also implicated in critical regulation of cellular communication during development.

A total of 518 kinase genes are indentified so far [105] classified into 8 distinct classes, Table 1.2.

Table 1.2 Kinase distribution by major groups in human and model systems (modified from [105])

Group	Families	Subfamilies	Yeast kinases	Worm kinases	Fly kinases	Human kinases	Human pseudogenes	Novel human kinases
AGC	14	21	17	30	30	63	6	7

CAMK	17	33	21	46	32	74	39	10
CK1	3	5	4	85	10	12	5	2
CMGC	8	24	21	49	33	61	12	3
Other	37	39	38	67	45	83	21	23
STE	3	13	14	25	18	47	6	4
Tyrosine kinase	30	30	0	90	32	90	5	5
Tyrosine kinase-like	7	13	0	15	17	43	6	5
RGC	1	1	0	27	6	5	3	0
Atypical-PDHK	1	1	2	1	1	5	0	0
Atypical-Alpha	1	2	0	4	1	6	0	0
Atypical-RIO	1	3	2	3	3	3	1	2
Atypical-A6	1	1	1	2	1	2	2	0
Atypical-Other	7	7	2	1	2	9	0	4

Atypical-ABC1	1	1	3	3	3	5	0	5
Atypical-BRD	1	1	0	1	1	4	0	1
Atypical-PIKK	1	6	5	5	5	6	0	0
Total	134	201	130	454	240	518	106	71

Phosphatases act in reverse functions with kinases, remove the phosphate groups from phosphorylated proteins and thus phosphorylation and dephosphorylation depend on the highly regulated and opposing actions of kinases and phosphatases acting on the same substrate. Phosphatases are also classified into distinct classes depending on the substrate specificity (table 1.3).

Table 1.3. Phosphatase distribution by major groups in human and model systems(modified from [106-110])

Class	Substrate	Reference
Tyrosine-specific phosphatases	Phospho-Tyrosine	[106]
Serine/Threonine specific phosphatases	Phospho-Serine/Threonine	[107]
Dual Specificity Phosphatases	Phospho-Tyrosine/Serine/Threonine	[108]
Histidine Phosphatase	Phospho-Histidine	[109]
Lipid Phosphatase	Phosphatidyl-Inositol-3,4,5-Triphosphate	[110]

1.5.1 Role of Kinases and Phosphatases in cancer

Certain classes of signalling proteins and pathways are targeted much more frequently by oncogenic mutations than other genes [111]. Thus, as being enzymes governing extracellular growth, differentiation and developmental signals, mutations and dysregulation of protein kinases and phosphatases play causal roles in several human disease including cancer as well [112-113].

1.5.2 Role of Kinases and Phosphatases in liver cancer

Activation of phosphoinositide 3-kinases (PI3K)/Akt/mammalian target of rapamycin (mTOR) signaling pathway in HCC occurs between 30–50% of all cases and related to poor prognosis [114]. Active signalling is due to aberrant activation of tyrosine kinase receptor EGFR, IGF1R, MET, VEGFR, PDGFR or through constitutive activation of PI3K due to loss of function of PTEN. Loss of heterozygosity in PTEN locus (i.e. 10q) is frequent in HCC and mutation rates are fairly low in HCC, ranging from 0 to 11% [115]. Raf/Ras/Erk pathway is generally activated in advanced stages of liver cancer, due to upstream signalling from EGF, HGF or IGF signals [116]. These informations are incomplete and fragmentary. Indeed, a systematic analysis of protein kinases and phosphatases in HCC is lacking. There has also been no report of systematic analysis of the effects of systematic inactivation of kinases and phosphatases in these cancers.

1.6 Role of H19/IGF2 locus in HCC

The non-coding gene H19 and IGF2 genes are co-located in the same locus and are under the control of genomic imprinting, which leads to reciprocal monoallelic expression of H19 from the maternal allele and IGF2 from the paternal allele [117]. Loss of imprinting is observed for both H19 and IGF2. Moreover, H19 is highly expressed in liver cancer and has been shown to behave like an oncogene for liver cancer and it is essential for tumor cell growth [118]. Several studies showed that IGF-II is overexpressed in human HCCs and in some premalignant lesions [119-121] and this is correlated with loss of imprinting [122].

1.7 Senescence of hepatocytes and chronic liver disease

Liver cirrhosis, the irreversible terminal stage of chronic liver disease characterized by fibrous scarring, is a major cause of morbidity and mortality worldwide, with no effective therapy. Complications such as accumulation of ascites, bleeding, and portal hypertension are

frequent in patients with cirrhosis. The only effective therapy for cirrhosis is organ transplantation.

Normal hepatocytes in the adult liver are quiescent, they are renewed slowly, approximately once a year, as estimated by telomere loss which is 50–120 bp per year in healthy individuals [123-124]. However, as well as animal models chronic liver diseases showed that, liver has enormous regenerative capacity [125]. Exposure to viral and non viral damaging agents or as shown in partial hepatectomy, mature hepatocytes proliferates enormously and this process is so called regenerative capacity of liver. In addition, hepatocyte-progenitor cells are induced to restore liver hepatocyte populations [126]. However, hepatocytes, since they do not have telomerase activity, like other somatic cells, they cannot avoid telomere shortening during rounds of cell divisions. For this reason, liver cirrhosis is associated with decreased hepatoycte proliferation [127], is now considered to be a result of senescence arrest [13].

Cellular senescence is a permanent arrest of the cell cycle in response to diverse stress conditions such as dysfunctional telomeres, DNA damage, strong mitotic signals and disrupted chromatin (figure 1.4). Senescence, a strong anti-cancer mechanism is regulated by p53-retinoblastoma pathway and involves the activation of p21Cip1, p16Ink4a and p15Ink4b cyclin-dependent kinase (CDK) inhibitors [128]. Frequent inactivation of TP53 and CDKN2A genes, together with frequent upregulation of telomerase reverse transcriptase (TERT) strongly suggest that HCC tumor cells may bypass senescence to become immortalized [13]. Nevertheless, the detection of senescent cells in nearly 50% of HCC tumors provides evidence for the capacity of HCC cells to undergo senescence arrest under appropriate conditions [129]. Immortal HCC cell lines can spontaneously generate progeny that undergo replicative senescence [130]. Murine HCC tumors generated by the expression of a mutant Ras gene in p53-deficient hepatoblasts can be cleared by a massive senescence response upon reactivation of p53 expression [131-132]; and c-myc oncogene inactivation in murine HCCs results in senescence-mediated tumor regression

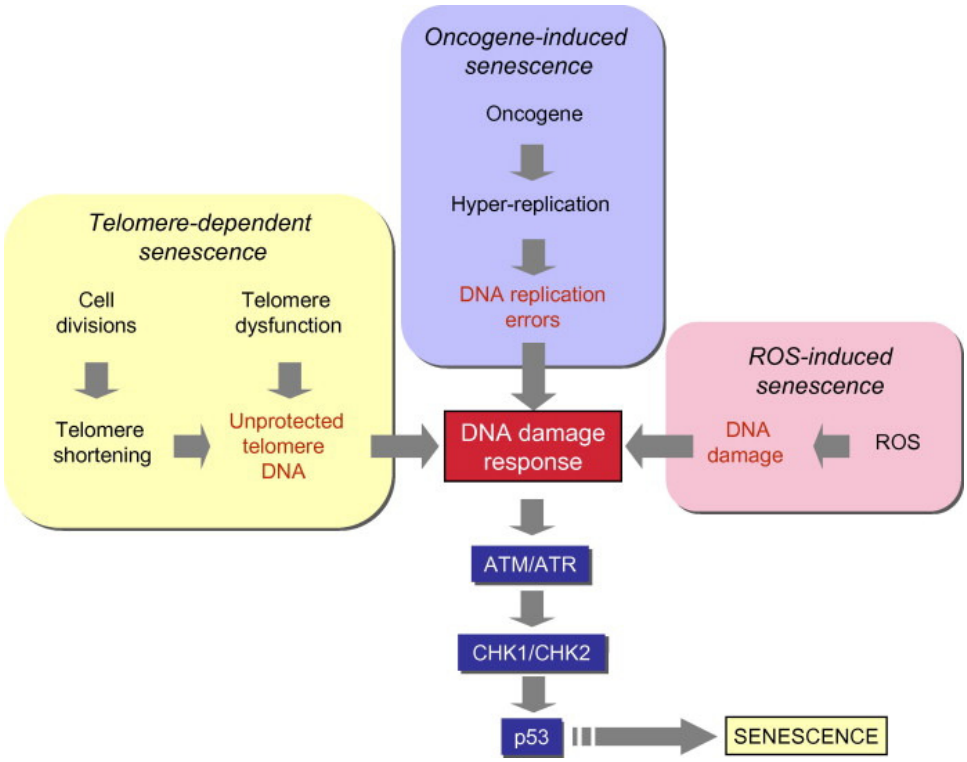

Fig. 1.4 DNA damage and p53 activation play a central role in different senescence pathways DNA damage (often in the form of double-strand breaks) activate upstream kinases (ATM and ATR) leading to p53 phosphorylation by CHK1 and CHK2 kinases. Phosphorylated p53 is released from MDM, and stabilized in order to induce senescence arrest or apoptosis (not shown here). (Modified from [13]).

1.8 Histone modifications

Major histone modifications include DNA methylation, covalent modifications of histones and repositioning of histones. Among these three, we started to understand the role of post-translational modifications of histones recently compared to DNA methylation.

Chromatin consists of repeating units of nucleosomes and the nucleosome consists of 146bp DNA wrapped to an octamer of four histone proteins (H3, H4, H2A and H2B). Basically, the protruding N-terminal ends of histone proteins are covalently modified by eight distinct types of mechanisms. Acetylations, methylation of lysines and arginines, phosphorylation, ubiquitylation, sumoylation, ADP ribosylation and proline isomeration are the eight major histone modifications and dictate the complexicity of regulation and biological roles. These covalent modifications work together to dictate and regulate the functioning of genome and change the local structure of the chromatin and in chromatin compaction, transcription regulation, DNA repair and replication, thus eventually contributes to genome to manifest itself as different phenotypes in differantiation

as well as diseases like cancer. To sum up, we can call these modifications as 'histone codes', a complicated code written by histone modifying enzymes and read by histone binding proteins. The complexity of code comes not only from different numbers of histone modifications reaching as high as 70 but also degree of modification (methylation at lysines or arginines may be one of three different forms: mono-, di-, or trimethyl for lysines and mono- or di- (asymmetric or symmetric) for arginines [133] and cross-talk between these codes [134]. The function of each code is difficult to understand and only recently we started to understand the biological functions. Modifications like lysine acetylation may affect the chromatin structure by neutralizing the basic negative charge of lysines and causing a permissive chromatin conformation for transcription to start. Phosphorylation is another way of changing the charge of chromatin thus leading to important consequences like mitosis and apoptosis [135-136]. Lysine methylation, in contrast to lysine acetylation has a different meaning depending on which lysine residues being methylated. This is because of the fact that histone methyl transferases have substrate specificity compared to histone acetyltransferases. The complexes in which enzymes are found [137], proteins associating with the enzymes of residue to modify [138], and the degree of methylation (mono-, di-, or tri-) [139] are the factors for residue specificity and thus biological roles. For instance, trimethylation of Histone 3 lysine 4 (H3K4Me3) on gene promoters means transcriptional activation, trimethylation of H3 lysine 36 (H3K36Me3) on gene coding region and histone 3 lysine 79 trimethylation (H3K79Me3) means transcriptional activation [140-141], whereas trimethylation of histone 3 lysine 9 (H3K9Me3) and lysine27 (H3K27Me3) on gene promoters means transcriptional repression [134]. After these codes are written by histone modifying enzymes, these codes are read by proteins that are recruited to these specific modifications and that have binding domains suitable for these histone marks. For example, methylation is recognized by chromo-like domains of the Royal family (chromo, tudor, MBT) and nonrelated PHD domains, acetylation is recognized by bromodomains, and phosphorylation is recognized by a domain within 14-3-3 proteins (figure 1.5).

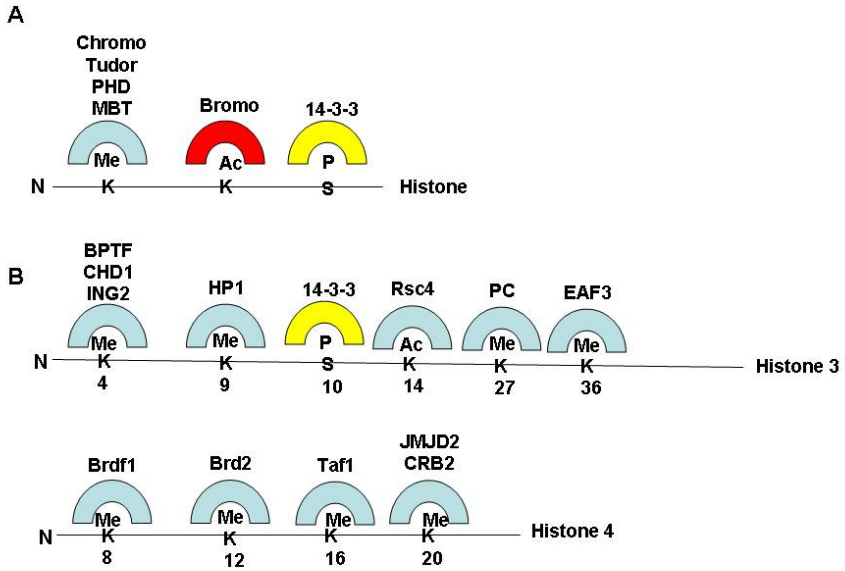

Figure 1.5 Recruitment of proteins to histones (modified from [134])

The dynamic and reversible modifications of each histone residue are regulated by specific enzymes. Histone acetyltransferases (HATs) add acetyl groups and histone deacetylases (HDACs) removes these and histone methyltransferases (HMTs) transfers methyl groups and histone demethylases (HDMs) reverses this [142-143]. The list of each type of enzymes is listed in table 1.4.

Table 1.4 Histone modifying enzymes and residues (modified from [134])

Enzymes that Modify Histones	**Residues Modified**		
Acetyltransferase		**Lysine Methyltransferase**	
HAT1	H4 (K5, K12)	SUV39H1	H3K9
CBP/P300	H3 (K14, K18) H4 (K5, K8) H2A (K5) H2B (K12, K15)	SUV39H2	H3K9
PCAF/GCN5	H3 (K9, K14, K18)	G9a	H3K9
TIP60	H4 (K5, K8, K12, K16) H3 K14	ESET/SETDB1	H3K9
HB01 (ScESA1, SpMST1)	H4 (K5, K8, K12)	EuHMTase/GLP	H3K9
ScSAS3	H3 (K14, K23)	CLL8	H3K9
ScSAS2 (SpMST2)	H4 K16	SpClr4	H3K9
ScRTT109	H3 K56	MLL1	H3K4
Deacetylases		MLL2	H3K4

SirT2 (ScSir2)	H4 K16	MLL3	H3K4
Lysine Demethylases		MLL4	H3K4
LSD1/BHC110	H3K4	MLL5	H3K4
JHDM1a	H3K36	SET1A	H3K4
JHDM1b	H3K36	SET1B	H3K4
JHDM2a	H3K9	ASH1	H3K4
JHDM2b	H3K9	Sc/Sp SET1	H3K4
JMJD2A/JHDM3A	H3K9, H3K36	SET2 (Sc/Sp SET2)	H3K36
JMJD2B	H3K9	NSD1	H3K36
JMJD2C/GASC1	H3K9, H3K36	SYMD2	H3K36
JMJD2D	H3K9	DOT1	H3K79
JMJD6	H3R2, H4R3	H3K9	H3K79
Arginine Methlytransferases	**Residues Modified**	Pr-SET 7/8	H4K20
CARM1	H3(R2,R17,R26)	SUV4 20H1	H4K20
PRMT4	H4R3	SUV420H2	H4K20
PRMT5	H3R8,H4R3	PRMT5	H4K20
Serine/Threonine Kinases	**Residues Modified**	EZH2	H3K27
Haspin	H3T3	RIZ1	H3K9
MSK1	H3S28	**Ubiquitilases**	
MSK2	H3S28	Bmi/Ring1A	H2AK119
CKII	H4S1	RNF20/RNF40	H2BK120
Mst1	H2BS14		

1.8.1 Histone modifications in HCC and other cancers

High-throughput sequencing technologies (Chip-seq) have enabled to elucidate the roles and characterization of histone modifications and aberrations in enzymes in diseases and tumorigenesis as well. Fraga et al, showed that global loss of acetylated H4-lysine 16 (H4K16Ac) and trimethylated H4-lysine 20 is a hallmark of human cancer including breast and liver cancer (H4K20Me3) [133]. HDACs are often overexpressed in various types of cancers including prostate and gastric tumors including liver cancer and there are drugs targeting HDACs under clinical trials [144-146]. Abnormal HAT activities are also observed in cancers, viral oncogene proteins such as E1A target CBP/P300 and disrupt their interaction with PCAF [147]. In leukemia, HAT and HAT related enzymes are reported to make fusion proteins [148]. Aberrant

alterations in methylation of H3K9 and H3K7 in cancer are also reported [149-150]. EZH2 is a histone methyl transferase acting on H3K27 residue is overexpressed in breast, prostate and liver cancers [149, 151]. Another histone methyltransferase acting on H3K9, G9a is associated with liver cancer [152]. MLL gene, acting on H3K4 is frequently makes fusion proteins with Hox genes and involves in leukemia [153]. Histone demethylases are also upregulated in prostate cancer and involved in tumorigenesis [142].

1.8.2 H3K4 methylation

Trithroax (Trx-G) group proteins are involved in H3K4 methylation and evolutionary conserved from flies to mammals. They are involved in epigenetic activation of homeodomain genes, whereas Polycomb repressor group (PcG) proteins mediate their silencing. These two antagonistic groups of proteins control important aspects of differentiation and proliferation [154].

1.8.2.1 MLL and SMYD3 – H3K4 methyltransferases

The mixed lineage leukemia (MLL) protein, SET domain containing H3K4 methyltransferase and activates of Hox gene expression during development. MLL and Hox genes frequently make fusion proteins, and involves in Leukemia [153]. SET- and MYND-domain-containing protein 3 (SMYD3), methyltransferase of H3K4, is found to be upregulated in colorectal and hepatocellular carcinoma cell lines and enhances cell growth and promotes transformation, whereas its inhibition represses cell growth in cancer cell lines [155].

1.8.3 H3K9 Methylation

Histone H3 lysine 9 (H3K9) methylation is recognized by HP1 and involves in heterochromatin formation and correlates with gene silencing in a variety of organisms. SUV39H1 and SUV39H2, mammalian homologues of Drosophila SU (VAR)3–9, are SET domain containing Histone methyltransferases acting on H3K9 residues.

1.8.3.1 SUV39H H3K9 methyltransferases

Single knockouts of SUV39H1-/- and SUV39H2 -/- mice are viable with no clear phenotype, however double knockout of both enzymes exhibit phenotypes. They show marked chromosomal instability, contributing to B-cell lymphoma, compromised viability. Correlating with their methyltransferase roles, reduction of H3K9Me2 and H3K9Me3 is observed with tumorigenic events that are: chromosomal abnormalities mainly mis-segregation, abnormally long telomeres and perturbration of Heterochromatin Protein 1 (HP1) binding at pericentric heterochromatin and telomeres [156]. SUV39H1 and HP1 interact with pRb to mediate gene silencing of Rb targets [157]. SUV39H1 also prevents Ras-induced tumorigenesis by promoting senescence [158]. No SUV39H1 mutations have been reported in human cancers yet.

1.8.4 H3K27 methylation

Polycomb group (PcG) proteins that are initially genetically defined in Drosophila melanogaster are the main complex acting on H3K27 methylation. There are two polycomb repressor complexes (PRC1 and PRC2). Consisting of BMI-1, Ring-1, HPH and HPC, PRC1 recognizes trimethylates H3K27 and mediates the maintenance of the silent state. PRC2, consists of enhancer of zeste homologue 2 (EZH2), suppressor of zeste 12 (SUV12) and embryonic ectoderm development (EED), instantiates gene repression with interacting partners like HDACs and DNA methyltransferases (DNMTs) [159].

1.8.4.1 EZH2 and JMJD3 enzymes

EZH2 is a histone methyl transferase acting on H3K27 residue is overexpressed in breast, prostate, colorectal carcinoma, bladder cancer, multiple myeloma and liver cancers [149, 151]. It plays essential roles in embryonic development and stem cell renewal [159]. EZH2 protein interacting with DNMTs to EZH2 target gene promoters suggests that EZH2 involves in silencing of tumor-suppressor genes during cancer cell evolution [160]. A Jumonji C family histone 3 lysine-27 (H3K27) demethylase, Jmjd3, plays a crucial role in development and macrophage plasticity and inflammation [161] The role of JMJD3 in human cancer is not clear yet.

1.8.5 H3K36 methylation

H3K36Me3 is found on the 3` end of elongated transcripts and implicated in transcription elongation. In budding yeast, it is found in at the 3` end of active genes and associated with RNA pol II, and found to have a role suppression of internal erroneous transcripts by recruiting complexes involving histone deactylase [162-163].

1.8.5.1 SETD2 methyltransferases

SETD2, histone methyltransferase gene acting on H3K36, is nonredundantly responsible for trimethylation of the histone mark H3K36. loss of H3K36me3 is found in 7 out of the 10 cleared renal cell carcinoma cell lines and missense mutations of SETD2 is found in 2 out of 10 primary cRCC [164]. SETD2 also associates with TP53 protein and Overexpression of SETD2 upregulated the expression levels of a subset of p53 targets including puma, noxa, p53AIP1, fas, p21, tsp1, huntingtin, but downregulated that of hdm2 [165].

1.8.5.2 FBXL11 Histone demethylases

The FBXL11, also named JHDM1A (CWYD domain-containing histone demethylase 1A) or KDM2A was discovered in 2006 as an enzyme catalyzing preferably in the demethylation of histone H3 lysine-dimethyl-36 in monomethyl-lysine [166]. In contrast to its orthologue (FBXL10/JHDM1B/KDM2B), the FBXL11 is apparently specific to the residue histone 3 lysine-36 (H3K36) [167]. Knockdown of its orthologue, FBXL10, in primary mouse embryonic fibroblasts inhibits cell proliferation and induces cellular senescence in a pRb- and p53 pathway-dependent manner [166].

1.8.6 H4K20 Methylation

Recent articles using mass spectrometry in human and in *Drosophila melanogaster* cells showed that the dimethylation of H4K20 is abundant, and H4K20me1 and H4K20me3 are relatively few in abundance. H4K20 methylation status also changes dynamically during the cell cycle and, notably, 98% of newly synthesized histone H4 becomes dimethylated within a few cell cycles [168]. Each methylation state for this residue has distinct functions. H4K20me2 involves in DNA repair and serves as a binding site for 53BP1 [169-170]. H4K20me1 has a role in

transcription and located on active genes [171-172]. H4K20Me3 is involved in pericentromeric heterochromatin formation and loss of trimethylation together with H4K16 acetylation is implicated in human cancer [133, 173]. Thus, there is a dynamic change in H4K20 methylation status. There has been no histone demethylation enzyme found acting on this residue.

1.8.6.1 Suv420H1 methyltransferase

Together with SUV39H1/2 and SUV420H1/2 enzymes have emerged as a hallmark of pericentric heterochromatin [174]. The loss of trimethylation of H4K20 in human cancer would suggest that the role of SUV420H1/H2 enzyme as a tumor suppressor role because controlled chromatin organization is crucial for gene expression regulation and genome stability.

1.9 DNA Methylation

DNMT3a and DNMT3b are de novo DNA methyltransferases responsible for methylation of 5` cytosine of CpG dinucleotides within the genome. DNMT1a is the other enzyme responsible for maintaining DNA methylation using the hemimethylated DNA as the substrate. These methylated DNAs are generally associated with silenced genes and condensed chromatin [175]. These methylation sites serve as docking site for silencing proteins.

One of the best examples of these silencing proteins is the DNA methyl binding protein, the MeCP2 (methyl-CpG binding protein) specifically recognize methylated cytosine residues. They recruit histone deacetylases (HDACS) to silence these genes. MeCP2 gene mutations are responsible for 95% of Rett syndrome [176].

1.9.1 DNA Methylation and cancer

CpG dinucleotides are generally methylated in a normal cell, except in front of many active genes. Cancer cells display global hypomethylation and a hypermethylation of CpG islands [177]. Loss of DNA methylation is associated with activation of proto-oncogenes like c-jun, c-MYC as well as H-Ras and also responsible for genomic instability. On the other hand, methylation of CpG dinucleotides is associated with silencing of tumor suppressor genes. APC, E-cadherin, p16Ink4a, SOCS-1, GSTP1, RASSF1A, Cox-2, CFTR, CCND2, and RIZ1 genes are found to be frequently methylated and thus silenced in HCC [178]. hTERT expression is also regulated by DNA methylation [179]. Some microRNAs including miRNA-1 is shown to be

silenced by DNA methylation and associated with liver cancer [180]. Reduced expression of T-cadherin via DNA methylation is also found to be associated with development of liver cancer [181].

The level of global DNA methylation and CpG hypermethylations are found to be associated with clinical outcome of several cancers including liver cancer [182].

1.10 Role of ATAD2 gene in cancer

ATAD2 is a gene of unknown function encoding a protein with a bromodomain and an ATPase domain of the AAA family suggesting functions related to genome regulation [183]. Reports from several independent groups established ATAD2 overexpression in a large set of tumors including breast, prostate, lung, and liver cancers [183,184,186]. The ATAD2 gene maps to 8q24.3 4.3 Mb distal to MYC, a well known oncogene. This chromosomal region is amplified frequently in different cancers, including HCC. Ciro et al. [184] have recently shown that ATAD2 gene is amplified in 17% of breast cancers and its overexpression correlates with tumor aggressivity in breast and lung cancers [183-184]. The exact mechanisms of ATAD2 overexpression in tumor cells and its cellular functions are presently unknown. However, recent studies indicate that ATAD2 is a direct target of E2F genes of the retinoblastoma pathway that is frequently deregulated in cancer cells [184]. Interestingly, ATAD2 was also identified as a critical co-activator of both E2Fs and c-MYC [184-185]. Downregulation of ATAD2 by siRNA or shRNA inhibits the entry of quiescent cells into S phase resulting in decreased colony-forming ability as well as inhibition of cell proliferation [184]. ATAD2 downregulation has also been associated with increased apoptotic response in some cell lines [183, 186]. Interestingly, some cell lines may not be responsive to ATAD2 inhibition [186]. Thus, ATAD2 overexpression in cancer cells could be due to either gene amplification or retinoblastoma pathway deregulation and that it may display oncogenic activity by its contribution to E2F- and c-MYC-mediated transcriptional activation.

CHAPTER 2. OBJECTIVES AND RATIONALE

As indicated previously, HCC kills nearly 600.000 people each year and the only effective therapy for this cancer is liver transplantation or tumor ablation when the tumor is small enough. These tumors are surprisingly resistant to conventional therapies such as chemotherapy and radiotherapy. Moreover, as HCC is almost always associated with cirrhosis, the treatment with cytotoxic agents is dangerous as they will also affect hepatic functions of the diseased liver. Therefore, there is urgent need to find novel therapeutic approaches against HCC in order to diminish death toll. One potentially useful approach is so called "targeted therapy", chemical or biological therapy based on targeting cancer-specific events (such oncogene activation, neoangiogenesis, and epigenetic alterations). However, this is a very difficult task for HCC, as only a few genetic and epigenetic targets are known, as reviewed in chapter 1.

Our overall goal is to discover "druggable target genes" in HCC. In other words, we wish to identify novel genes and novel mechanisms involved in these cancers in order to use them as potential therapeutic targets.

During my thesis work, I developed different approaches to find new mechanisms and novel targets:

1-Deciphering the role of canonical Wnt signaling in HCC: We hypothesized that canonical Wnt signaling is not only selectively activated in well-differentiated, but also repressed in poorly differentiated HCCs. To test this, we characterized and classified HCC cell lines according to their differentiation status and compared their expression of Wnt pathway genes, and activity of canonical Wnt signalling. In some cancers, due to mutations affecting APC, Axin and beta-catenin, wnt-beta-catenin pathway is abnormally activated in the absence of a Wnt ligand, and beta-catenin accumulating in cytoplasm and nucleus, activates Wnt target genes. For this aim, we identified monoclonal antibodies (Mabs) that selectively recognize membrane-bound, cytoplasmic and nuclear beta-catenin forms and test the clinical value of such Mabs in several human cancer types.

2. Systematic screening of protein kinases and phosphatases as potential therapeutic targets: There is evidence of aberrant activation of several signaling cascades in HCC, and a multikinase inhibitor, sorafenib, has shown survival benefits in patients with advanced HCC. We used siRNA

to screen a large number of kinases and phosphatases to identify related genes involved in HCC cell survival.

3-Screening of a set of selected epigenetic regulators as potential therapeutic targets: Genetic mutations are irreversible and some mutated genes such as TP53 can not be targeted for therapy. In contrast, epigenetic alterations in cancer cells are reversible in principle. Therefore, they may be ideal candidates for targeted therapy. Accordingly, histone acetylation and DNA methylation have been used as potential targets in the past. Among others, histone deacetylase inhibitors that stimulate histone acetylation and chemical analogs of methylated cytosine that induce DNA hypomethylation have been effectively used to inhibit the growth of tumor cells or to eliminate them by an apoptotic response [187]. Recent studies have indicated that senescence arrest or senescence escape could be regulated by epigenetic changes on chromatin. We wanted to identify key histone methylation and acetylation changes associated with senescence or senescence escape, and select key histone modifying enzymes, as potential targets for "pro-senescence" interventions (therapeutic interventions that allow senescence induction in cancer cells).

CHAPTER 3. MATERIALS AND METHODS

3.1 MATERIALS

3.1.1 Reagents

All laboratory chemicals were purchased from either Sigma (St. Louis, MO, U.S.A), Farmitalia Carlo Erba (Milano, Italy), Merck (Schucdarf, Germany), VWR company, (International S.A.S. Le Périgares, France).

Methanol: Sigma (St. Louis, MO, U.S.A)

Toluene: Sigma (St. Louis, MO, U.S.A)

Hydrochloric Acid 0,37 %: from Farmitalia Carlo Erba (Milano, Italy)

Formaldehyde 4 % : from VWR company, (International S.A.S.. Le Périgares, France)

DNA isolation kit: Flexigene DNA Kit with catalog number 51204 from Qiagen (Courtaboeuf –France)

Quick PCR purification kit with catalog number 28104 from Qiagen (Courtaboeuf – France)

Hispeed Plasmid Maxi kit with catalog number 12663 from Qiagen (Courtaboeuf – France)

QI Prep Spin Mini kit with catalog number 27106 from Qiagen (Courtaboeuf –France).

Sigma senescence cells kit: with catalog number CS0030 from Sigma (St. Louis, MO, U.S.A).

MN RNA isolation kit with catalog number 740955250 from MACHEREY-NAGEL GmbH & Co. KG (Düren · Germany)

Saponin from Quillaja bark : catalog number, S4521-25G from Sigma (St. Louis, MO, U.S.A)

Nuclear fast Red : catalog number N3020 form Sigma (St. Louis, MO, U.S.A)

Mayer's Haematoxylin: MHS16 from Sigma (St. Louis, MO, U.S.A)

Crystal Violet: catalog number C0775 from Sigma (St. Louis, MO, U.S.A)

Coomassie Brilliant Blue R: catalog number B8647-1EA from Sigma (St. Louis, MO, U.S.A)

Ponceau Stain Solution: catalog number PH70-1L from Sigma (St. Louis, MO, U.S.A)

Hexadimethrine Bromide: catalog number H9268-10G from Sigma (St. Louis, MO, U.S.A)

3.1.2 Bacterial Strains

The bacterial strain used in this work was: *E. coli*: DH5α and M15. Competent cells for Lentivirus studies Stbl3 Competent cells from Invitrogen Company and TAM1 ready competent cells from Active Motif (Rixensart, Belgium).

3.1.3 Enzymes

Restriction endonucleases used for gene cloning were purchased from either MBI Fermentas GmbH (Germany) or from Gibco Invitrogen SARL –France .

3.1.4 Nucleic Acids

DNA molecular weight standard and ultrapure deoxyribonucleotides were purchased from MBI Fermentas GmbH (Germany). pEGFP-N1 (Clontech, Palo Alto, CA), pcDNA3 (Invitrogen), pCI-Neo (Promega), pSuper, pSuperior.puro, pSuper.retro.gfp.neo (Oligoengine), and pGEX-4T1 (Amersham/Pharmacia, NJ, USA) were commercially obtained. pCDNA3-S33Y were prepared by inserting of S33Y cDNA from pCI-Neo-S33Y into pcDNA3. pAUCT-ΔN-β-catenin were prepared by inserting Xho I/Not I fragment of pCI-Neo-S33Y into pAUCT/CCW vector. pAUCT-C/EBPα was prepared by inserting BamHI-XhoI from pCDNA3.C/EBPα into pAUCT/CCW. The pShuttle-IRES-Wnt5a expression plasmid was constructed by subcloning of an EcoRI-cut Wnt5a cDNA fragment from plasmid pGEMTz-Wnt5a vector (a gift from R. Kemler) into BglII site of the pShuttle-IRES-hrGFP-1 vector (Stratagene, USA). pCI-Neo-mutant β-catenin (S33Y) expression plasmid, and pGL3-OT and pGL3-OF reporter plasmids were kindly provided by B. Vogelstein. The pAUCT-delta N-β-catenin plasmid expressing N-terminally truncated β-catenin (aa 98-781) under the control of Tet repressor was constructed using pAUCT-CCW vector (gift from Ali Fattaey, USA). A cDNA fragment of XhoI-NotI digestion from pCI-Neo-mutant β-catenin (S33Y) plasmid was inserted into XhoI-NotI site of pAUCT-CCW vector. PEGFP-Survivin vector is gift from Stephan Dimitrov team at Institute Albert Bonniot.

PEGFP-GW-Suv420H1 was a gift from Gunnar Schotta from Research Institute of Molecular Pathology(IMP), Vienna. PEGFP-BRDT plasmid was a gift from Saadi Kochbin team at Institue Albert Bonniot.

PGipz shRNAmir against gapdh with catalog numbers RHS4371, Scrambled with catalog number RHS4346, non-eukaryatic target RHS4480, FBXL11 with catalog numbers V2LHS_51035, V2LHS_51037, V2LHS_245727, JMJD2B with catalog numbers RHS4430-98713709, RHS4430-98714014, JMJD3 gene with catalog number RHS4430-98705669, SETD2 with RHS4430-99293307, RHS4430-98841349, RMM4431-99214758, SMYD2 with RHS4430-99149990, RHS4430-98896463 and Suv420H1 with RHS4430-99138317, RHS4430-99138820 were purchased from Openbiosystems (USA).

pTRIPz shRNAmir lentiviral vector targeting ATAD2 and shCTRL were purchased from open Biosystems company with catalog number RHS4696-99634057.

3.1.5 Oligonucleotides

The sequencing-primer used for cycle sequencing reactions oligonucleotides used in polymerase chain reactions (PCR), and 60 bp. HPLC grade oligos used for gene knock-down experiments were synthesized by either İONTEK (Istanbul, Turkey) or Eurofins MWG Operon (Roissy CDG, France).

3.1.6 Electrophoresis and gel imaging, luciferase assay, ELISA readings and spectrophotometer

Electrophoresis grade agarose was obtained from Sigma Biosciences Chemical Company Ltd. (St. Louis, MO, USA) and from Agarose D5 DNA grade from Euromedex (Souffelweyersheim-France). Horizontal electrophoresis apparatuses were from Stratagene (Heidelberg, Germany) and Mupid –ex company E-C Apparatus Corporation (Florida, USA). The power supply Power-PAC300 and Power-PAC200 was from Bio Rad Laboratories (CA, USA). GeneFlash SYNGENE Bioimaging is used to visualize DNA. The Molecular Analyst software used in agarose gel profile visualizing was from BioRad Laboratories (CA, USA). The Reporter Microplate Luminometer Reader was from Turner BioSystems Inc (Sunnyvale, CA, USA). ELISA reader and Spectrophotometer were from Beckman.

3.1.7 Tissue culture reagents

Dulbecco's modified Eagle's medium (DMEM), fetal calf serum was obtained from GIBCO Invitrogen company (Invitrogen SARL –France). L-glutamine, calcium and magnesium-free phosphate buffered saline (PBS), Penicillin/Streptomycin mixture was from Biological Industries, MEM Non essential aminoacids 10X and HBBS Hanks balanced salt sln and 0,5% trypsin-EDTA 10X were purchased from GIBCO Invitrogen company (Invitrogen SARL – France). Tissue culture flasks, petri dishes, 15 ml polycarbonate centrifuge tubes with lids and cryotubes were purchased from Costar Corp. VWR Company, (International S.A.S. Le Périgares, France). Geneticin-G418 sulfate was purchased GIBCO Invitrogen Company (Invitrogen SARL –France). Puromycin and Doxorubucin hydrochloride was purchased from Sigma (St. Louis, MO, USA).

3.1.8 Antibodies and chemiluminescence

The antibodies used in immunoblotting (western blotting) were obtained from different sources, and their working dilutions are given in Table 3.2.

ECL and ECL plus Western Blotting detection kit was purchased from Amersham Pharmacia Biotech Ltd. (Buckinghamshire, UK).

3.2 SOLUTIONS AND MEDIA

3.2.1 General Solutions

50X Tris-acetic acid-EDTA (TAE):	2 M Tris-acetate, 50 mM EDTA pH 8.5 Diluted to 1X for working solution purchased from Euromedex.
Ethidium bromide:	Uptime Interchim company 10 mg/ml in water (stock solution), 30 ng/ml (working solution)
4X Gel loading buffer:	Purchased from Invitrogen (SARL –France).

Bradford Stock Solution	purchased as ready sln from Sigma company with catalog number B6916

3.2.2 Microbiological media, reagents and antibiotics

Luria-Bertani medium (LB)	LB Medium : LB Broth 20g/L ROTH LB Agar: Lenox Agar from Invitrogen SARL – France
Glycerol stock solution	65% glycerol, 0.1 M $MgSO_4$, 0.025 M Tris.Cl, pH 8.0
Ampicillin	100 mg/ml solution in double-distilled water, sterilized by filtration and stored at -20°C (stock solution).100 µg/ml (working solution)
Kanamycin	300 mg/ml solution in double-distilled water sterilized by filtration and stored at -20°C (stock solution). Working solution was 30 µg/ml.
0.1 M IPTG	1.41 g IPTG in 50 ml double-distilled water, sterilized by filtration and stored at -20^{o}C.
SOB medium:	*Per liter:* 20 g tryptone (2%), 5 g yeast extract (0.5%), 0.584 gr NaCl (10 mM), 0.1864 g KCl (2.5 mM) autotclaved to sterilize. Then, 2.46 g MgSO4 and 2.03 g MgCl2 (10 mM) are added.
SOC medium:	was purchased from P/N 46/0700 Invitrogen company
Transformation Buffer (TB):	NuPage 20X Transfer buffer from Invitrogen company
Glycerol stock solution	65% glycerol, 0.1 M $MgSO_4$, 0.025 M Tris.Cl, pH 8.0. were mixed with 50% bacteria culture. Alternatively, 25% glycerol were added into bacteria culture.

3.2.3 Tissue culture solutions

DMEM/RPMI working medium	10% FBS, 1% penicillin/streptomycin, 1% Non-Essential Amino Acid were added and stored at 4°C.
10X Phosphate-buffered saline (PBS)	Purchased from Invitrogen Company Invitrogen SARL –France

3.2.4 BES Transfection solutions

2.5 M $CaCl_2$	3.675 g $CaCl_2$ in 10 ml double-distilled water. Sterilized by filtration through 0,2µm filter. Stored at -20°C
100 mM BES, pH 6.95	0.2132 g BES (N,N-bis(2-hydroxyethly) in double-distilled water. pH was adjusted to 6.95 with NaOH at room temperature. Stored at -20°C
2X BBS (BES buffer saline)	50 mM BES, pH 6.95, 280 mM NaCl, 1.5 mM Na_2HPO_4 in double-distilled water. Sterilized by filtration through 0,2µm filter. Stored at -20°C.

3.2.5 Antibiotics

Geneticin-G418 Sulfate)	500 mg/ml solution in double-distilled water. Sterilized by filtration and stored at -20°C (stock solution). 500 µg/ml (working solution for stable cell line selection), and 250 µg/ml (working solution for maintenance of stable cell lines).
Puromycin	2 mg/ml solution in double-distilled water, sterilized by filtration (0.2 um pores) and stored at -20°C (stock solution). 2 µg/ml (working solution for stable cell line selection), and 1 µg/ml (working solution for maintenance of stable cell lines).

Tetracycline	1 mg/ml solution in 70% Ethanol, sterilized by filtration (0.2 um pores) and stored at -20°C (stock solution). 5 µg/ml (working solution).

3.2.6 Immunoblotting solutions

10X Tris-buffer saline (TBS)	*Per liter:* 100 mM Tris-base, 1.5 M NaCl, pH 7.6 in double distilled water.
TBS-Tween (TBS-T)	0.1-0.5% Tween-20 solution in TBS. (Prepared freshly)
Blocking solution	3-5% (w/v) non-fat milk, 0.1-0.5% Tween-20 in TBS. 5 % BSA for histone antibodies (Prepared freshly).

3.2.7 RNA Study Solutions

DEPC-treated water	0.1% Diethylpyrocarbonate (DEPC) (v/v) in double-distilled water was stirred in loosely plugged bottle. Then autoclaved and stored at room temperature.

3.2.8 Immunofluorescence solutions

H33258 fluorochrome dye	1 mg/ml solution in double-distilled water and stored at -20 °C. Working solution was 1 µg/ml.
DAPI (4', 6-diamidino-2-phenylindole)	0.1-1 µg/ml (working solution in PBS).
4% paraformaldehyde	4 g paraformaldehyde, 5 mM NaOH in 100 ml. PBS, pH 7.4. Stable at 4°C for a week.
PBS-TritonX-100 (PBS-T)	0.1 TritonX-100 in PBS.

3.3 METHODS

3.3.1 General Methods

3.3.1.1 Long term storage of bacterial strains

To keep bacterial cells including plasmid in it or as empty for future experiments and to have a stock of strain in a laboratory is necessary. The most frequently used method is "Glycerol-Stock" method. A single colony picked from either an agar plate or a loop-full of bacterial stock was inoculated into 5 ml LB (with a selective agent if necessary) in 15 ml screw capped tubes. Tubes were incubated overnight at 37^{o}C and at 200 rpm. For glycerol stock, 700 µl of saturated culture was added into 700 ml of 65% glycerol v/v (32.5 ml glycerol, 5 ml $MgSO_4$, 1.25 ml Tris-Cl pH 8.0 completed to 50 ml with sterile water). This mix was frozen/stored at –70 or -80^{o}C

3.3.1.2 Purification of plasmid DNA using Qiagen miniprep kit

This method was preferred for isolation of plasmids in order to use in sequencing or cloning procedures. 5 ml of saturated culture was used for isolation of plasmid DNA by using "QI Prep spin miniprep plasmid DNA purification kit" (Qiagen- Courtaboeuf –France)) following manufacture's instructions.

3.3.1.3 Large-scale plasmid DNA purification

This method was used for isolation of plasmids in order to use in sequencing or mammalian cell transfection procedures by using "Hispeed Qiagen large-scale plasmid DNA purification kit" following manufacture's instructions.

3.3.1.4 Quantification and qualification of nucleic acids

Concentration and purity of the double stranded nucleic acids (plasmid and genomic DNAs), oligonucleotides and total RNAs were determined by using the Nanodrop from Thermoscientific Company.

3.3.1.5 Restriction enzyme digestion of DNA

Restriction enzyme digestions were routinely performed in 20 µl reaction volumes and typically 0.5-5 µg DNA was used. Reactions were carried out with the appropriate reaction buffer and conditions according to the manufacturer's recommendations.

Digestion of DNA with two different restriction enzymes was performed in the same reaction buffer to provide the optimal condition for both restriction enzymes. If no single reaction

buffer could be found to satisfy the buffer requirements of both enzymes, the reactions were carried out sequentially.

3.3.1.6 Gel electrophoresis of nucleic acids

3.3.1.6.1 Horizontal agarose gels of DNA samples

DNA fragments were fractionated by horizontal electrophoresis by using standard buffers and solutions. DNA fragments less than 1 kb were generally separated on 1.0% or 20 % agarose gel, those greater than 1 kb (up to 11 kb) were separated on 0.8 % agarose gels.

Agarose gels were completely dissolved in 1x TAE electrophoresis buffer to required percentage in microwave and ethidium bromide was added to final concentration of 30 µg/ml. The DNA samples were mixed with one volume loading buffer and loaded onto gels. The gel was run in 1x TAE at different voltage and time depending on the size of the fragments at room temperature.

3.3.2 Computer analyses

Restriction endonuclease maps of the plasmid DNAs were analyzed by using the WebCutter program (Max Heiman, 1995, maxwell@minerva.cis.yale.edu) available for free and public use at http://rna.lundberg.gu.se/cutter2/. Primers were designed by using web software provided by Steve Rozen and Whitehead Institute for Biomedical Research at http://frodo.wi.mit.edu/cgi-bin/primer3/primer3_www.cgi. Alignments of nucleic acids or protein sequence were performed by using web page at http://www.ncbi.nlm.nih.gov/BLAST/.

3.3.3 Characterization of Ig subtype of the anti-β-catenin antibodies

Subtypes of anti-β-catenin antibodies were identified by using "ImmmunoPure Monoclonal Antibody Isotyping Kit II" (Pierce) following kit instructions.

3.3.4 Tissue culture techniques

3.3.4.1 Cell Lines and stable clones

15 HCC derived cell lines (FLC4, Huh7, FOCUS, Mahlavu, Hep40, Hep3B, HepG2, PLC/PRF/5, SK-Hep1, Snu182, Snu387, Snu398, Snu423, Snu449 and Snu475) were used in this study, and cultured as described in previously [188]. Human colorectal carcinoma cell lines

SW480 (APC nonsense mutation at aa 446) and SW837 (APC nonsense mutation at aa 483) were grown in high glucose DMEM. Wnt3a expressing-mouse fibroblast NIH3T3-wnt3a cell line was obtained from R. Kemler.

Normal Lung Fibroblast cell line was MRC5 and MRC5-hTERT and hela (ATCC) cell lines were cultivated in DMEM. Huh7-, HepG2 and Hep3B-derived isogenic clones were obtained by either puromycin (1,5 μg/ml) selection after infection with pGIPz or pTRIPz (Invitrogen) or Geneticin (1500 μg/ml) for cells transfected with PEGFP-N1 and Suv420H1 enzyme expressing plasmid, and surviving expressing plasmid. Maintanance of stable cells were performed either using puromycin (0,25 μg/ml) or in the presence of 200 μg/ml geneticin G-418 sulfate depending on the plasmid selection markers.

3.3.4.2 Cryopreservation of cell lines

Exponentially growing cells (70% confluency) were harvested by trypsinization and neutralized with growth medium. The cells were counted and precipitated at 1500 rpm for 5 min. The pellet was suspended in a freezing solution (10% DMSO, 20% FCS and 70% DMEM for adherent cells; 10% DMSO, 90% FCS for special cells) at a concentration of $4x10^6$cells/ml. 1 ml of this solution was placed into 1 ml screw capped-cryotubes. The tubes were left at -70°C overnight in a shuttle containing isopropanol. The next day, the tubes were transferred into the liquid nitrogen storage tank.

3.3.4.3 Thawing cell lines

One vial of the frozen cell line from the liquid nitrogen tank was taken and immediately put into ice. The vial was left 1 minute on the bench to allow excess nitrogen to evaporate and then placed into 37^{o}C water bath until the external part of the cell solution was thawed (takes approximately 1-2 minutes). The cells were resuspended gently using a pipette and transferred immediately into a 15 ml. sterile tube containing 10 ml cold fresh medium. The cells were centrifuged at 1500 rpm at 4^{o}C for 5 minutes. Supernatant was discarded and the pellet was resuspended in 10 ml 37^{o}C culture medium to be plated into 100 mm dish. After overnight incubation in a humidified incubator at 37°supplied with 5% CO_2, culture mediums were replenished.

3.4 Growth conditions of cells

Dulbecco's modified Eagle's medium (DMEM) or RPMI 1640 supplemented with 10% FCS, 1 mM glutamine and penicillin and streptomycin (50 mg/ml), and 1% NEAA was used to culture the HCC cell lines. The cells were incubated in at 37°C in an incubator with an atmosphere of 5% CO_2 in air. Empty vector transfected stable clones were cultured in parental cell line's culture medium + 200 µg/ml geneticin G-418 sulfate, or 1 µg/ml puromycin. Doxycycline inducible cells were cultured in parental cell line's culture medium + 200 µg/ml geneticin G-418 sulfate + 3 - 5 µg/ml doxycycline.

The cells were passaged before reaching confluence. The growth medium was aspirated and the cells were washed once with calcium and phosphate-free PBS. Trypsin was added to the flask to remove the monolayer cells from the surface. The fresh medium was added and the suspension was pipetted gently to disperse the cells. The cells were transferred to either fresh petri dishes or fresh flasks using different dilutions (from 1:2 to 1:10) depending on requirements.

All media and solutions used for culture were kept at 4°C (except stock solutions) and warmed to 37°C before use.

3.5 Transfection and Virus Production

pGIPz and/or pTRIPz shRNAmir lentiviral and shCTRL were purchased from open Biosystems company. After transformation into STBL3 replication incompetent cells according to manufacturer`s recommendation, maxi prep isolation was performed. For transfection Trans-Lentiviral GIPz Packaging Mix with Hek-293TA cells and Arrest-in transfection reagents from Open-biosystems Company (Huntsville, USA) were used. All lentiviral studies were performed at Security level 2. 5.5 x 10^6 rapidly growing (split two days before) Hek293TA cells were plated into 10cm plates one day before. At the day of transfection, cell media were changed to serum free and antibiotic free media. 28,5 ug (26 ul) Trans-lentiviral packaging mix and 9ug of pGIPz or pTRIPz transfer vector was mixed into 1ml serum free media. Arrest-in transfection reagent (187,5 ul) was mixed into 1ml serum free media in a separate tube. The diluted DNA mix and transfection reagent is combined and mixed rapidly and incubated 20 minutes at room temperature. After this incubation 3ml of serum free media was added to transfection-DNA complexes and mixed gently and overlaid onto Hek293-TA cells containing plate and incubated 6 hours. Transfection mixture is replaced with 12 ml standard media, and 48-72 hours later media

containing virus particles were collected and filtered 0,45 uM PVDF filters and either directly used or kept at 4 C for up to 1 week.

3.6 Transduction of cells with viruses

The day before transduction cells were seeded into 24 well plates so that next day the confluency is about 30%-50%. The day of infection, media is aspirated and virus containing media is overlaid either using 6-8 μg/ml of Hexadimethrine Bromide in virus containing media 1mL for 6 well plates or 250 uL for 24 well plates. Cells were incubated with virus containing media for 4-6 hours and after incubation the media is removed and cells were cultured for 24 hours and selection with 1 μg/ml puromycin (Sigma) was started or continued for further experiments.

3.7 Transfection and Colony-forming ability assay

Cell survival was determined by assessing cell growth in 100 mm dishes after exposure to Trichostatin-A TSA(sigma). 100,000 HepG2, Hep3b, Hela and MRC5 (PDL 32) cells were seeded in 6-well plates and 24 hours later cells were transfected with ATAD2 siRNAs ordered from Eurogentec (France) (ATAD2 siRNA sequences: Atad2 siRNA1 ACUAACACUGCUGAAGCUG;Atad2 siRNA2 GGUUGUAGCUCCUCCAAAU, Atad2 siRNA3 GCUAAGGAUUUCGAGGUAG,Atad2 siRNA4 UCUUCUGCUGUCAGUGAUC,siCTRL GGCCUUUCACUACUCCUAC) using Oligofectamine transfection reagent using the protocol that Invitrogen recommends. 200 μM of siRNA and 4 μl of oligofectamine transfection reagent is used to transfect cells for 6 hours without serum and antibiotics. 3X serum containing media is added at the end of 6 hours and 3 days later cells are either treated with tricostatin-A (0,1 μM, 0,5 μM or 1 μM) for 24 hours or directly plated into 10 cm plates in triplicates. Equal volume of cells was plated into each plate. After 10 days of cell culture, colonies were fixed in cold methanol, stained with Crystal Violet (Sigma), and counted in triplicate experiments. Cell survival was calculated as the % ratio of cell numbers in treated versus untreated cells. Survival parameters were determined by plotting in excel.

3.8 Western immunoblotting

RIPA extracted or nuclear extracted proteins were subjected to electrophoresis using 10% or 4-12% Bis-Tris NuPAGE Novex or 3-8% Tris-Acetate Nupage mini gel systems (Invitrogen), according to the manufacturer's instructions. For detection whole cell lysates using RIPA extraction is used. For the detection of phosphorylated proteins, cell lysates were prepared according to the protocol provided by the supplier using the following lysis buffer: 20 mmol/L Tris (pH 7.5), 150 mmol/L NaCl, 1 mmol/L EDTA, 1 mmol/L EGTA, 1% Triton X-100, 1 mmol/L Na3VO4, 1 μg/ml leupeptin, 1 mmol/L phenylmethylsulfonyl fluoride. Following electrophoresis, proteins were transferred on to Immobilon-P PVDF membrane (Millipore, USA), and analyzed, using antibodies against target proteins.

3.9 Senescence-associated beta-galactosidase (SABG) assay

SABG activity was detected as described previously by dimri et al 1995, using senescent cell staining kit (Sigma).

3.10 Indirect immunofluorescence and confocal microscopy

Cells were fixed with 4% formaldehyde, and permeabilized with PBS supplemented with 0.5% saponine (Sigma) and 0.3% Triton X-100 (Sigma). After blocking for one hour, cells were incubated overnight at 4°C, with 1` antibodies, after washing with PBS-(0,03%) Triton-X, secondary antibodies conjugated to Alexa 568 or Alexa 488 (Invitrogen), counterstained with DAPI, and observed using Apotome (Zeiss) microscope. Images were captured with an Axiocam HRc color CCD camera (Zeiss) and digitally saved using Axio Imager software (Zeiss). Confocal microscopy analysis were examined under Zeiss LSM 510 Meta laser scanning confocal microscope (MPI Freibourg, Germany) using 488 nm and 543 nm laser excitation lines, and photographed.

3.11 Cell cycle analysis and bromodeoxyuridine (BrdU) incorporation assay

Cells were washed twice in PBS and fixed in ice-cold ethanol for 10 min. After two PBS washes, cells were incubated with 20 μg/ml of RNase A (Fermentas) at 37°C for 10 minutes and stained with propidium iodide (10 μg/ml in PBS; Sigma). Cell cycle distribution was determined by flow cytometry using FacScan and the CellQuest software (Becton Dickinson). Cell cycle

analysis combined with BrdU incorporation assay was done as described, except that cells were first labeled with 10 μmol/L BrdU (Sigma) for 2 hours prior to each testing time, and cells subjected to anti-BrdU staining after DNA denaturation with 4N HCl for 30 minutes using FITC-conjugated anti-BrdU antibody (BD Bioscience) at room temperature for 30 minutes in the dark.

3.12 Detection of Apoptosis using Annexin V staining

Cells were collected by centrifugation and resuspended by Annexin V binding buffer and stained with annexin V-cy3 dye and incubated 5 minutes at dark and further analyzed with FACS scan (Beckton Dickonson) with FL2 channel.

3.13 Detection of Histone acetylation levels using FACS

For detection of acetylation using FACS, we followed the protocol previously published by [189]. At day 3 of transfection, cells were collected and fixed for 15 minutes in 1% formaldehyde in PBS on ice and refixed using 70% EtOH. Cells were washed with 1XPBS containing 1% BSA and permeabilized with 0,1% Triton-X 100 for 10 minutes at room temperature and fixed with 10% normal goat serum and incubated with either H3PanAc (abcam ab47915) and H4PanAc (Upstate 06598) antibodies in 1%BSA-PBS solution and followed by Alexa488-conjugated secondary antibody (Invitrogen). After washes, cells were resuspended in PI (10 μg/ml in PBS; Sigma) and quantified by FACS scan (Beckton Dickonson) with FL1 and FL2 channel and imaged by FCS express V3 program.

3.14 Treatment of cell lines with TGF-beta and Doxorubucin

Purified recombinant human TGF-β1 (R&D Systems, Minneapolis, USA) was reconstituted in sterile 4 mM HCl containing 1 mg/ml bovine serum albumin (BSA, Sigma, St. Louis, MO, USA).Doxorubicine hydrochloride from Sigma, (St. Louis, MO, USA) were obtained commercially and solubilized as suggested by the manufacturers.

3.15 RNAi screening protocol

3.15.1 Optimization Protocol for RNAi

We ordered siRNAs targeting 126 kinase and 28 phosphatase genes form TRANSAT company in France. As a negative control against non eukaryotic sequences (scrambled) were

used. For positive control, we used a general positive control Polo like kinase (PLK) siRNA. This gene is implicated and essential for in cell division. We decided to look for inhibition of growth after knockdown of each gene. Inhibition of growth may be due to apoptosis, senescence and growth arrest so we used a sensitive method to quantify the viable cells after transfection. This method is originally developed in USA by NCI to screen for inhibitors against 60 cancer cell lines[190]. For the optimization studies, we used 96 well plates and plated 2000 and 5000 Huh7 cells in 0,2 mL media. 24 hours after plating, we transfected cells using 200nM PLK siRNA positive control using three different transfection reagents Oligofectamine (Invitrogen), Lipofectamine 2000 (Invitrogen, ref 11668), Fugene 6 (Roche).

Among these Fugene was eliminated because of toxicity and oligofectamine is chosen because of transfection efficiency. We optimized best amounts of reagent per amount of siRNAs. We used 200nM siRNA and 5000 cells per well of 96 well plate. After 6 hours of transfection, we added 50 µl of three times more serum containing media over the cells and after 72 hours, we performed Sulforhodamine B Staining protocol. We also included SCR siRNA and for each target we used 3 different siRNAs to eliminate off-target problem.

3.16 Sulforhodamine B staining protocol

Sulforhodamine B ($C_{27}H_{30}N_2O_7S_2$) is a fluorescent dye to quantify cellular proteins of cultured cells. The dye has absorbance at 585 nm light and fluorescence emission at 607 nm light. We fixed our cells using % 50 trichloroacetic acid for 1 hour at 4° C and stained with % 0.4% Sulforhodamine B solution for 30 minutes. After staining cells were washed four times with % 1 acetic acid solution and air dried. The dye is then dissolved in 10 µM TRIS base solution, and absorbance is read at 540 nm wavelength.

The results were obtained in triplicates and normalized to the negative SCR siRNA and Standard errors are also included.

3.17 In vivo Targeting and Screening

To optimize in vivo targeting and imaging, we obtained xenograft models of Huh7 cells and Alexa labelled RAFT-RGD and again Alexa dye labelled Transferrin were used.

3.18 Xenograft models

We injected 10 x 10^7 Huh7 cells in 100 µl PBS on the back of 10 NMRI-neo (Naval Medical Research Institute) immunodeficient mice. We observed the tumor of 8-10 mm diameter in size of all treated mice. Cells were injected s.c. into NMRI *nude* mice. Tumors and nontumorigenic cells at the injection sites were collected at day 37 and analyzed. These experiments have been approved by the Bilkent University Animal Ethics Committee.

3.19 Optical imaging of mice bearing tumors

After injection of day 25, we imaged mice using two different dyes. We used 200 µl of Alexa labelled RAFT-RGD and 100 µl of Alexa dye labelled Transferrin to image the mice. We anesthetized the mice and injected the dye, and start imaging process after 30 minutes, 1 hour, 2 hours, 3 hours and 24 hours later. Excitation wavelength was 630 nm and filtered emission wavelength was 665nm, and images were obtained either 100 ms or 200 ms using Hamamatsu digital camera (C4742-98-26LWGS, Hamamatsu Photonics K.K., Japan). Wasabi software was used to process images.

3.20 Transient transfection of eukaryotic cells using "Lipofectamine Reagent"

Transfection was performed with Lipofectamine 2000 reagent (Invitrogen) following manufacturer's instructions.

3.21 Extraction of total RNA from tissue culture cells and tissue samples

Total RNAs were isolated from cultured cells using the NucleoSpin RNA II Kit (MN Machete-Nagel, Duren, Germany) according to the manufacturer's protocol.

3.22 First strand cDNA synthesis

First strand cDNA synthesis from total RNA was performed using RevertAid First Strand cDNA synthesis kit (MBI Fermantas, Germany). The first strand reactions were primed with oligo(dT) primer to specifically amplified mRNA population with 3'-poly(A) tails.

1 to 5 µg total RNA was used to synthesize the first stand cDNA following the manufacturer's instruction. After 1:1 dilution of total reaction products in DNAse free water, 2 µl of diluted first strand cDNA was used for PCR.

3.23 Primer design for expression analysis by semi-quantitative PCR

The primer pairs that have been used in expression profile analyses were designed carefully. Forward and reverse primer were positioned on different exons of the gene of interest, so that the primer pair was either be able to produce a longer amplicon from genomic DNA or not be able to amplify from the covered genomic DNA region in a given PCR condition (critical parameter was extension time). Therefore the amplicon, which was amplified from cDNA, was not be longer than 1500 bp. Primers used for expression analysis have been designed strictly considering these criteria, and listed in Table 3.1.

3.24 Fidelity and DNA contamination control in first strand cDNAs

The fidelity and genomic DNA contamination of first strand cDNAs were checked before performing expression analyses. 2 µl of diluted first strand cDNA was used for cold-PCR amplification of the *glyceraldehyde-3-phosphate dehydrogenase (GAPDH)* transcript. *GAPDH* primer pair was designed to skip introns so that the products coming form gDNA have higher products.

3.25 Expression analysis of a gene by semi-quantitative PCR

10 x Invitrogen PCR supermixes were used to perform PCR according to manufacturer's recommendation.

3.26 Protocol for quantitative PCR

Quantitative PCR was performed using power Syber green (2X) PCR master mix (Stratagene company Massy- France) and (100 ng) cDNA as a template and 1 µl of 10 pmol forward and reverse primers. Stratagene Mx-3005 QPCR apparatus was used. The number of optimal PCR cycle was determined by an initial study for each gene by performing 45-cycle PCR. Agarose gels were analyzed by Densitometric Fluorescence-Chemiluminescence image analyzer and The Molecular Analyst software (BioRad).

Table 3.1: PCR primer list

Primer name	Sequence 5`-3`
hAES-Rev	CATCACATAGTGACGCTGCAT
hAES-For	ACCTACCCCAGCAACTCAAA
CtBP1-Rev	CCATCCGACAAGTAAGGG
CtBP1-For	CATCATCGTCCGGATTG
Chibby-Rev	AGCAGTGGACTCTGAAAGCA
Chibby-For	GGATCCCCGACTATGAACCT
AXIN2-Rev	TTTTTTGTGCTTTGGGCACTATG
AXIN2-For	CAGCGAGTATTACTGCTACTCGAAA
ICAT-Rev	TCTTCCGTCTCCGACCTGGA
ICAT-For	AAGAGTCCGGAGGAGATGTAC
Axin2-Rev	ATCTCCTCAAACACCGCTCCA
Axin2-For	CTGGCTCCAGAAGATCACAAAG
hTLE1-Rev	AGGCTTGCCGAGACCTGGACG
hTLE1-For	GGCAGTGCCGGCCTTCTTGCG
hTLE2-Rev	CGTTGAGAGTGCTGTGGGAGC
hTLE2-For	AGTGCTACGGGGCTGCTTGCT
hTLE3-Rev	TTTGGTCTTGGAGGAAGGTG
hTLE3-For	AAGGACAGCTTGAGCCGATA
hTLE4-Rev	CAGGTCCCAAATGGACAAAG
hTLE4-For	TCAAGGTCTGGGACATCAGC
SETD2_201_Rev	TAGGGAACACACATGCCAAG
SETD2_201_For	GGACAGTTTAAGTTCTCCTGCAA

SETD2_001_Rev	GTCGTCCCTGTTCTTCCAAA
SETD2_001_For	CGACCCCTGAAGAAGAAGAA
FBXL11_203_For	CGTGTTGCAATCTGGTTCCT
FBXL11_201_For	TGAGAATATCAGCTATCTTGAGAGAAA
FBXL11_201_203_Rev	CACCCCGCTGAATATACTCTACA
FBXL11_202_For	ATTGCTGGGAATGTCCAAAG
FBXL11_202_Rev	CAAAGTCTCTTGTCGCAGCA
Suv420h1F1	TGGAGATGGGTTCTTTGGAG
Rat-ATAD2-2-for	TTC ATG AGG AAA GGT GCT GA
Rat-ATAD2-2-rev	GAG ATC CGA TGC CCT CTT CT
ATAD2-rat-For	CCT CCC AGG TCA CAG ACA TT
ATAD2-rat-Rev	CAG CTG CTG CTG CTC TAC CT
H19-RsaI-for	CCA CCA CAT CAT CCC AGA GC
H19-RsaI-rev	GAA TGC TTG AAG GCT GCT CC
GapDH-For	GGC TGA GAA CGG GAA GCT TGT CAT
GapDH-Rev	CAG CCT TCT CCA TGG TGG TGA AGA
JMJD2B-201-202-For	ATC TCC ATG GAC GTG TTC GT
JMJD2B-201-Rev	GTA CCC TCC CCA GGG AAC T
JMJD2B-202-Rev	AGA TGC TTT GGC CTC TCC TC
Human ATAD2For	AGGCTCATTGGAAAAACCT
Human ATAD2Rev	CCTGCGGAAGATAATCGGTA

3.27 Crude total protein extraction

Adherent monolayer cells (both stable and parental cells) were grown to 70% confluency in growth medium without selective antibiotic. After removal of growth medium, cells were washed twice with ice-cold PBS to remove any serum residue. 400 µl of RIPA lysis-buffer (150

mM NaCl, 50 mM Tris-HCl pH 8.0, 0.5% sodium deoxycholate, 1 % NP-40, 0.1% SDS and 1X Complete Protein Inhibitor mix (Roche)) was added into 10 cm tissue culture petri dish, and cells were scraped with rubber scrapper. Complete lysis was achieved by pipetting of crude cell lysates several times and by incubating the lysates on ice for 30 min, and then centrifuged at 13.000 g for 30 minutes. Total cell protein was collected as supernatant.

3.28 Nuclear extract isolation protocol

Cells were lysed using a buffer containing 0,5 M KCL, 0,1% NP40, 0,5 mM DTT, 0,5 mM PMSF and TSA (50 ng/ml), 1x Protease inhibitor cocktail and 0,5 mL of pre-made buffer with 40% Glycerol and 6mM MgCl2 and 100 mM Hepes pH 7,9 and incubated on ice for 10 minutes. Cell were pelleted and resuspended equal amount of the same buffer and sonicated 5 minutes at high level with Bioraptor and further incubated on ice for 10 minutes and pelleted. Supernatant is containing chromatin proteins.

3.29 Quantification of proteins using Bradford Assay

The conventional Bradford protein assay was employed to quantity the protein in the lysates obtained from either crude total. After protein quantification, protein lysates were aliquoted into fresh tubes and, stored at –70°C.

Table 3.2 Antibodies used in this study and their dilution in various protocols

Antibody	Working Dilution (WB)	Working Dilution (IF)	Source/Clone/Cat #
β-catenin (MAb)	1:5000		Transduction Labs
β-catenin (MAb) 4C9	1:1		Home made 4C9
β-catenin (MAb) 9E10	1:1		Home made 9E10
vimentin		1:250	Becton Dickinson clone3B4
P15	1:2000		SantaCruz Sc612
Active Caspase 3	1:1000		Epitomics 1476-1
Cyclin D1	1:500		SantaCruz

p16	1:500		SantaCruz Sc468
Rb	1:1000		Becton Dickinson BD554136
Calnexin(Rabbit PAb)	1:10000		Sigma
Cyclin E	1:500		Transduction Labs
Cyclin A	1:500		Abcam
$p21^{Cip1}$	1:500		Santa Cruz
E-cadherin	1:2000		Santa Cruz 7870
PTEN	1:500		Cascade biosciences
P-ERK1/2	1:1500		Cell Signaling
ERK1/2	1:1500		Cell Signaling
phopho-AKT	1:750		Cell Signaling 9275
P44/p42	1:1500		Cell Signaling 9107
Pp44/pp42	1:1500		Cell Signaling 9106
NFKB	1:200		SantaCruz sc8414
HNF4	1:200		SantaCruz sc8987
HNF1a	1:200		SantaCruz sc8986
Z01			Transduction labs
Connexin43			SantaCruz sc9059
Total AKT	1:1000		Rabbit cell signaling
Bax rabbit	1:500		Upstate 06-499
Bak rabbit	1:500		Pharmingen 556396
Bad	1:1000		SantaCruz sc9292
P53-ser15			Cell signaling 9284
BCL-XL	1:500		SantaCruz sc7195
P21	1:500		Calbiochem OP24
tubulin			Calbiochem cp06
cyclinA	1:200		SantaCruz sc596
C-myc	1:200		SantaCruz sc42

E2F1	1:200		SantaCruz sc193
Albumin	1:1000		Abcam Ab10241
AFP1	1:500		Abcam Ab3980
Anti trypsin	1:1000		Abcam Ab9399
Bax rabbit	1:500		Upstate 06-499
H3K56Ac	1 :500		Gift from Arnauld (eq 2)
H3K23Ac	1:500		US biologicals
H3K18Ac	1:1000		Home made antibody
H4K5Ac	1:500	1:50	Home made antibody
ATAD2 antibody	1:500	1:200	Sigma (HPA019860)
H3PanAcetyl	1:500		Abcam 47915
H4PanAcetyl	1:500	1:250	Upstate 06598
HDAC1	1:200		SantaCruz Sc7872
HDAC2	1:200		SantaCruz Sc7899
HDAC4	1:200		SantaCruz Sc5245
HDAC5	1:500		Home made 605(U309)
P300	1:1000		SantaCruz Sc584
PCAF	1:200		SantaCruz Sc8999
HAT1	1:500		Sigma H7161
H3K4Me3	1:5000	1:1200	Abcam ab8580
H3K9Me1	1:2000	1:600	Abcam ab9045
H3 K9 Me3	1:5000	1:1200	Upstate 07-523
H3 K27 Me1	1:5000	1:1200	Upstate 07-448
H3 K27 Me3	1:5000	1:1200	Upstate 07-449
H3 K36 Me3	1:2000	1:600	Abcam ab 9050
H3 K79 Me3	1:2000	1:300	Abcam ab2621
H4K20Me3	1:2000	1:600	Upstate 07-463
H3 Pab	1:500		Abcam 1791

H4 Pab	1:500		Abcam10158
Phopho P38	1:1000		Cell Signaling 9211
P38 kinase	1:1000		Cell Signaling 9212
Akt			Cell Signaling 9272
Phospho SAPK/JNK	1:1000		Cell Signaling 9251
SAPK/JNK	1:1000		Cell Signaling 9252
H3K4Me1	1:2000	1:800	Upstate 07-436
H3K27Me2	0,5 µg/ml	1:600	Abcam Ab24684
H3K36Me1		1:600	Abcam Ab9048
H3K36Me2		1:500	Upstate 07-274
H4K20Me1	1:1000	1:600	Abcam Ab9051
H4K20Me2	1:2000	1:250	Abcam Ab9052
Setd2		1:100	Abcam Ab31358
EZH2	0,4 µg/ml	1:100	Abcam Ab3748
WHSC1		1:200	Abcam Abcam75359
H3R2Me2		1:600	Upstate Ups07585
H3R17Me2		1:900	Abcam Abcam 8284
H4R3Me2		1:600	Upstate Ups 07-213
Survivin	1 µg/ml	1:200	Abcam Ab469
Suv420H1(0032)	1:2000 (pure)		COVALABs
Connexin32			SantaCruz Sc7258
twist	1:1000	1:500	SantaCruz Sc81417
Bim	1:1000		Cell Signaling 2819
E6	1:500		SantaCruz Sc166689
E7	1:500		SantaCruz Sc6981

(WB: western blotting, IF: Immunofluorescence)

3.30 Luciferase assay

Endogenous TCF/LEF-dependent transcriptional activity was tested by using pGL3-OT and pGL3-OF reporter plasmids, as described previously [41], except that cells were transfected using Lipofectamine 2000 reagent (Invitrogen), following instructions provide by the supplier.

Mutant β-catenin-induced TCF/LEF-dependent transcriptional activity was tested after co-transfection of cells with pCI-Neo-mutant β-catenin (S33Y) expression plasmid (1.75 μg/well) together with the reporter plasmids. pCI-Neo (1.75 μg/well) was used as negative control. The effect of Wnt5a expression on TCF/LEF-dependent transcriptional activity was tested using Huh7 and HepG2 cell lines. Huh7 cell line was co-transfected with pCI-Neo-mutant β-catenin (S33Y) expression plasmid (1 μg/well) together with either pShuttle-IRES-Wnt5a (0.75 μg/well) or the empty vector pShuttle-IRES-hrGFP-1 (0.75 μg/well) and pGL3-OT/pGL3-OF reporter plasmids (0.75 μg/well for each). At 48 hour following transfection, luciferase assay was performed by using Luciferase Reporter Gene Assay, constant light signal kit (Roche Diagnostics GmbH., Mannheim, Germany). Luciferase activity was read with The Reporter® Microplate Luminometer (Turner BioSystems Inc., Sunnyvale, CA) and data was normalized according to transfection efficiency obtained with each transfection, as described previously [41]. HepG2 cell line was co-transfected with either pShuttle-IRES-Wnt5a (0.5 μg/well) or the empty vector pShuttle-IRES-hrGFP-1 (0.5 μg/well) and pGL3-OT/pGL3-OF reporter plasmids (0.5 μg/well for each), with an internal control (0.05 μg/well pRL-TK Renilla luciferase vector) in a 12-well plate, using Lipofectamine 2000 Transfection Reagent. Forty-eight hours post-transfection, the cells were washed with PBS, and lysed in passive lysis buffer (Dual Luciferase kit; Promega). The cell lysates were transferred into an OptiPlate 96-well plate (Perkin-Elmer) and assayed in a 1420-Multilabel counter luminometer, VICTOR3 (Perkin-Elmer) using the Dual-Luciferase kit (Promega). Relative TOP-FLASH luciferase units were measured and normalized against Renilla luciferase activity and further normalized luciferase activity against FOP-FLASH activity. All transfection experiments were performed in triplicate and data were expressed as mean of triplicate values (±S. D.) and p values were calculated. TCF/LEF activity was reported as the ratio of normalized luciferase activities obtained with pGL-OT and pGL-OF plasmids, respectively (mean ± S. D.).

3.31 Immunohistochemical studies for β-catenin Mabs

A total of 176 tumor samples including 54 colorectal cancer (48 adenocarcinoma, 2 signet ring cell carcinoma, 3 mucinous carcinoma, 1 villous adenocarcinoma), 32 hepatocellular carcinoma, 54 breast cancer (28 in situ ductal carcinoma and 26 invasive ductal carcinoma), and 42 endometrial cancer were tested for β-catenin immunoreactivity using 4C9 monoclonal

antibody. Three-micrometer-thick sections from the paraffin-embedded formalin-fixed blocks were used for hematoxylin-eosin staining and immunohistochemical studies. All sections for immunostaining were deparaffinized with xylene and alcohol and subject to antigen retrieval with microwave in Tris-EDTA buffer (pH 8.0) for 20 minutes. The endogenous peroxidase activity was blocked with 3 % hydrogen peroxide for 15 minutes at room temperature, and the sections were incubated with 1:5000 diluted anti-ß catenin antibody (4C9) for 1 hour at room temperature. After 3 washes in phosphate-buffered saline, the signals were detected by the Dako EnVision + Dual method, according to the manufacturer's instructions. After the third washing in phosphate-buffered saline, the specimens were incubated with diamino-benzidine at the appropriate concentration for development. The specimens were counterstained with hematoxylin. The intensity of β-catenin staining was graded as negative (0-4% positive cells), weakly positive (5-25% positive cells), moderately positive (26-75% positive cells), or strongly positive (76-100% positive cells).

3.32 Immunohistochemistry analysis of ATAD2 using tissue microarray

Tissue microarray containing 38 HCC with different TNM classification and 8 normal liver samples with catalog number LV-482 were purchased from Tebu-bio company (France). Tissues were deparrafinized using toluene and alcohol and subjected to antigen retrieval using citrate buffer pH 6.0 from Dia-Path (Italy) using water bath for 25 minutes. peroxidase activity was blocked with 3 % hydrogen peroxide for 15 minutes at room temperature, and the sections were incubated with 1:5000 diluted polyclonal Rabbit anti-ATAD2 antibody (Sigma) for 1 hour at room temperature. After 3 washes in phosphate-buffered saline, the signals were detected by the Dako EnVision + Dual method, according to the manufacturer's instructions. The specimens were counterstained with hematoxylin and eosin.

3.33 Statistical analysis

The statistical significance using was tested by using either Fisher Exact Probability Test ot paired t-test using an on-line tool http://faculty.vassar.edu/lowry/Vas sarStats.html.

CHAPTER 4. RESULTS

4.1 Canonical Wnt signaling is antagonized by noncanonical Wnt5a in hepatocellular carcinoma cells

This work was done in collaboration with other graduate students of Ozturk Lab. Therefore, some date reported here has been produced by other students. We present here all key experiments used for a recent publication (Yuzugullu et al., 2010) in order to keep the unity of the whole study.

We used a panel of HCC cell lines to characterize differentiation-dependent functions of Wnt pathway and canonical Wnt signaling in HCC.

4.1.1 Classification of hepatocellular carcinoma cell lines into "well-differentiated" and "poorly differentiated" subtypes

HCC cell lines were recently classified into "epithelial" and "mesenchymal" types based on E-cadherin and vimentin expression, sequentially [54]. Using 15 cell lines we checked the α-fetoprotein (AFP) expression (Figure 4.1.1). Positive expression were shown in six cell lines Huh7, Hep40, HepG2, Hep3B, Hep3B-TR, PLC/PRF/5; negative cell lines were SNU182, SNU387, SNU398, SNU423, SNU449, SK-Hep1, Mahlavu, FOCUS or weakly expressing cell lines were (SNU475). All AFP-positive (AFP+) cell lines also expressed E-cadherin, whereas only 3/9 (33%) of AFP- cell lines expressed this epithelial marker. AFP negative cell lines were also positive for mesenchymal cell markers including vimentin, slug, snail, twist-1 and twist-2. These markers also displayed weakly positive expression in some AFP positive cell lines. Immunocytochemical analysis of vimentin protein was performed in five AFP+ and five AFP- cell lines to confirm the results (Figure 4.1.2). Strong and homogenous immunostaining were detected with all five AFP- cell lines. In contrast, either negative or heterogeneous positivity were seen for AFP+ cells lines. These results showed that AFP+ HCC cell lines were epithelial-like, but they also expressed some of the mesenchymal cell markers at different degrees. In contrast, AFP- cell lines were strongly positive for mesenchymal markers but not with epithelial marker E-cadherin. Marked heterogeneity was obtained for mesenchymal markers. For example, SNU182

was positive for all five markers tested, whereas FOCUS was positive only for vimentin.

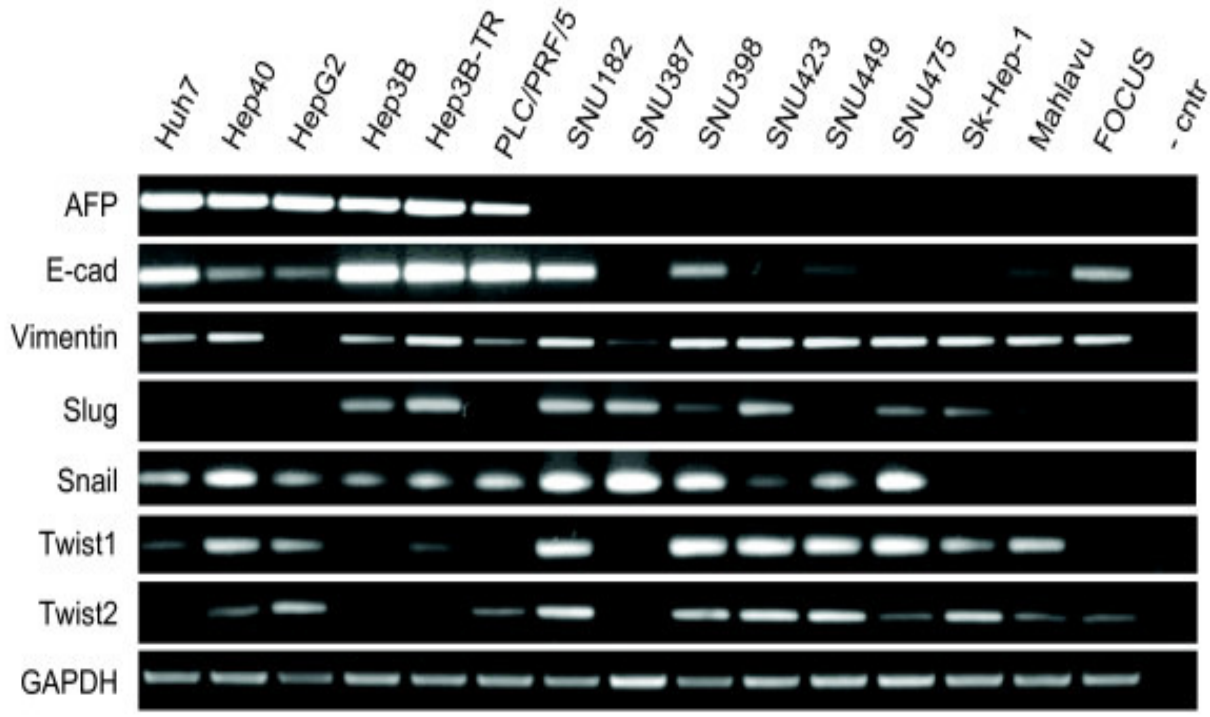

Figure 4.1.1 Expression analysis of a-fetoprotein (AFP), E-cadherin and five mesenchymal cell markers in HCC cell lines. Total RNAs were extracted from cell lines and used to detect gene expression by RT-PCR assay. GAPDH was used as a control for expression analyses.

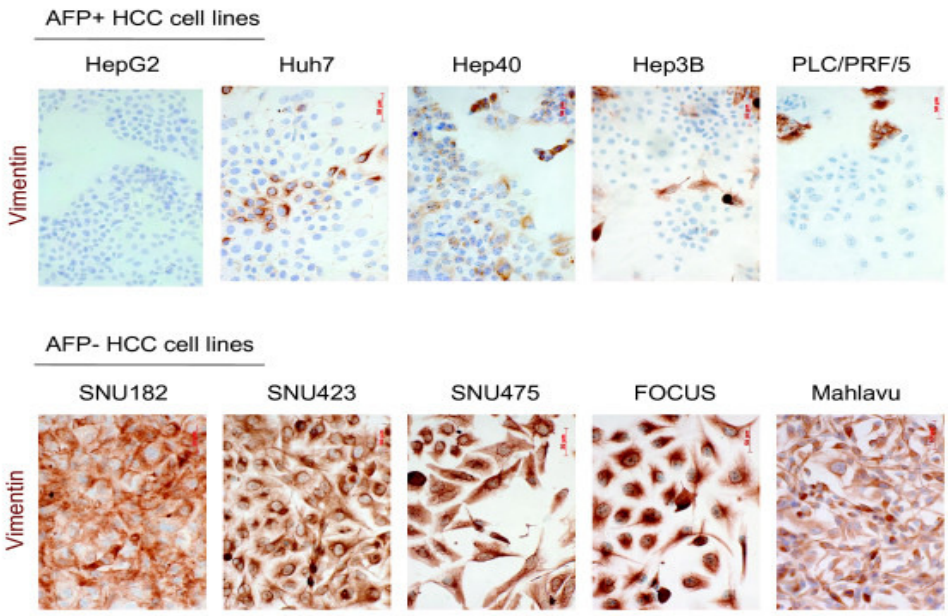

Figure 4.1.2 Immunocytochemical analysis of mesenchymal marker vimentin protein in AFP+ and AFP- HCC cell lines Cells grown on coverslips were subjected to immunoperoxidase assay using anti-vimentin antibody (brown), and counterstained with hematoxylin (blue).

HNF-4α and its downstream target HNF-1α are well characterized hepatocyte-associated epithelial cell markers [3]. Involved in liver development and hepatocyte specification, both are specific markers for well-differentiated function and morphology [191]. RT-PCR analysis in four AFP+, and seven AFP- cell lines showed that the expression of these HNFs displayed perfect correlation with the expression of AFP (Figure 4.1.3.a): four AFP+ cell lines Huh7, Hep3B, HepG2, Hep40 were also highly positive for both HNF-4α and HNF-1α. On the other hand, seven AFP- cell lines SNU398, SNU475, SNU449, SNU387, FOCUS, Mahlavu, SNU182 did not express these factors. Only weak HNF-4α expression was observed for SNU449, another AFP- cell line. Epithelial cells show low motility, whereas mesenchymal cells display high motility and invasive phenotypes. To test the epithelial and mesenchymal gene expression patterns of HCC cells correlated with their in vitro motility, we used wound-healing assay. After wounding, AFP- HCC cells (Mahlavu, SNU449, SNU475, SNU182) moved through the wound, whereas AFP+ HCC cells (Huh7, Hep3B, HepG2, Hep40) cells did not (Figure 4.1.3.b; Hep40 and SNU182 data not shown). These data showed that poorly differentiated cell lines display higher motility

(Figure 4.1.3.c). These data have been produced in the laboratory of N. Atabey (Dokuz Eylul University).

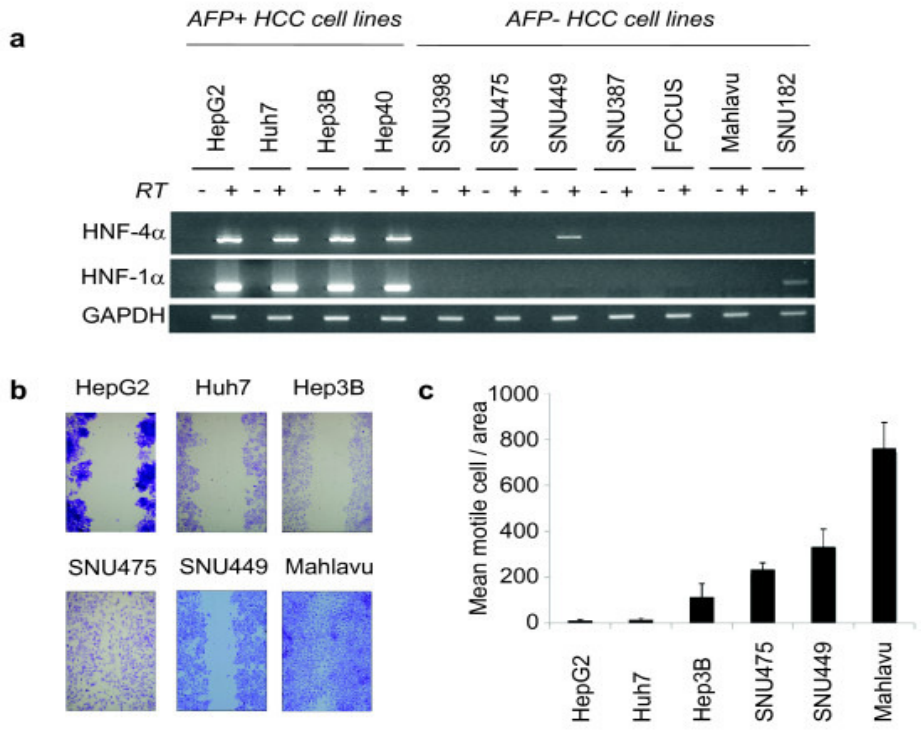

Figure 4.1.3 Expression of hepatocyte lineage markers HNF-4α and HNF-1α in HCC cell lines correlate with low motility. (a) Selective expression of HNF-4α and HNF-1α in AFP+ HCC cell lines. (b. c) Differential motility of AFP+ and AFP- HCC cell lines. Cells were cultured in six-well culture plates, and a single linear wound was made with a pipette tip in confluent monolayer cells. The distances between wound edges were measured at fixed points in each dish according to standardized template. After 24 hours migration, cell migration into the wound was visualized using phase contrast microscopy at ×20 magnification (b). The number of cells migrating beyond the wound edge was counted (c). Assays in six replicates, error bars; SD. SNU475 cells are larger cells giving rise to visual overestimation of migrating cell number in the picture shown in b.

Taken together, we classified our panel of HCC cell lines into two subtypes (Table 4.1.1). HepG2, Huh7, Hep3B and Hep40 cell lines were grouped into "well-differentiated" phenotype, because they express AFP, E-cadherin, HNF-4α and HNF-1α, and they display low motility and/or low invasiveness. Most of these features are confined to "well-differentiated" HCC tumors [2, 59, 192-193]. The remaining seven cell lines (SNU398, SNU475, SNU449, SNU387, FOCUS, Mahlavu, SNU182) were classified as "poorly-differentiated" HCC cell lines, because

of lack of expression of both hepatocyte lineage and epithelial cell markers. In addition, they shared many features with mesenchymal cells including the expression of mesenchymal markers (vimentin, slug, snail, twist-1, and twist-2), high motility and invasiveness. These expression and migratory features are associated with tumor dedifferentiation and confined to poorly differentiated HCCs [48-49, 55, 194].

Table 4.1.1: Well-differentiated and poorly differentiated HCC cell lines according to hepatocyte lineage, epithelial and mesenchymal markers, and in vitro motility and invasiveness assays

Cell Lines	Fetal Hepatocyte Marker	Epithelial & Hepatocyte Markers			Mesenchymal markers					Motility	Invasiveness
	AFP	HNF4a	HNF1a	E-cadherin	Vimentin	Slug	Snail	Twist-1	Twist-2		
Well-differentiated											
HepG2	High	High	High	Low	(-)	Low	Low	Low	High	Low	Low [55]
Huh7	High	High	High	High	Low	(±)	Low	Low	(-)	Low	Low [55]
Hep3B	High	High	High	High	Low	High	Low	(-)	(-)	Low	Low ([195]
Hep40	High	High	High	Low	High	(-)	High	High	Low	Low	n.t.
Poorly differentiated											
SNU398	(-)	(-)	(-)	Low	High	Low	High	High	High	Low	n.t.
SNU475	(±)	(-)	(-)	(-)	High	High	High	High	Low	High	n.t.
SNU449	(-)	Low	(-)	(±)	High	Low	Low	High	High	High	n.t.
SNU387	(-)	(-)	(-)	(-)	Low	High	High	(-)	(±)	n.t.	n.t.
FOCUS	(-)	(-)	(-)	Low	High	Low	(-)	(-)	Low	n.t.	n.t.
Mahlavu	(-)	(-)	(-)	(±)	High	Low	(-)	High	Low	High	High [195]
SNU182	(-)	(-)	(±)	High	high	High	High	High	High	High	n.t.

(-); not detected; ±; traces; n.t.; not tested.

4.1.2 Expression TCF/LEF family of transcription factors

Using the same panel of HCC cell lines, we analyzed the expression of 45 Wnt pathway genes by RT-PCR assay for TCF/LEF factors. The TCF-1 and TCF-4 were highly expressed in all HCC cell lines, while TCF-3 expression was limited to a subset of cell lines (Figure 4.1.4). LEF-1 expression was negative or weak, except for SNU398 cells. These findings indicated that all HCC cells were equipped with at least two nuclear factors mediating canonical Wnt signaling. These experiments have been performed by K.Benhaj [5].

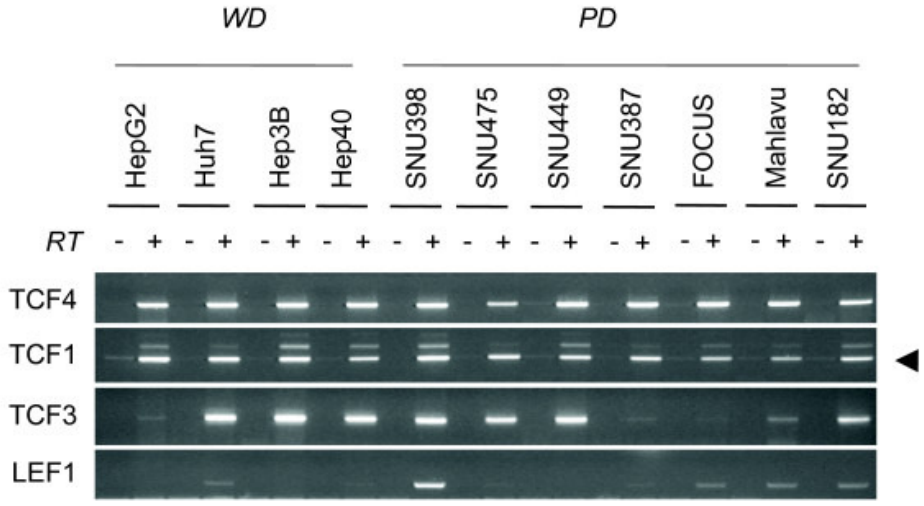

Figure 4.1.4 Comparative analysis of TCF/LEF transcription factors in hepatocellular carcinoma cell lines. Total RNAs were extracted from cell lines and used to detect gene expression by RT-PCR assay of four members of TCF/LEF family. See Figure 4.1.3 for GAPDH loading control.

4.1.3 Expression of Frizzled receptors and LRP co-receptors

Next, 10 Frizzled receptors and their two co-receptors were analyzed. Two canonical (FZD1, FZD5) and three noncanonical (FZD3, FZD4, FZD6) Frizzled receptors were positive in all cell lines tested. Also, most of the cell lines expressed FZD2, FZD7 and FZD8 (Figure 4.1.5-top). All cell lines also expressed LRP-5 and LRP-6 co-receptors (Figure 4.1.5-bottom). HCC cell lines were equipped with canonical and noncanonial Wnt signaling receptors, so that each HCC cell line was likely to respond to both canonical and noncanonical Wnt signals. These experiments have been performed by K.Benhaj.

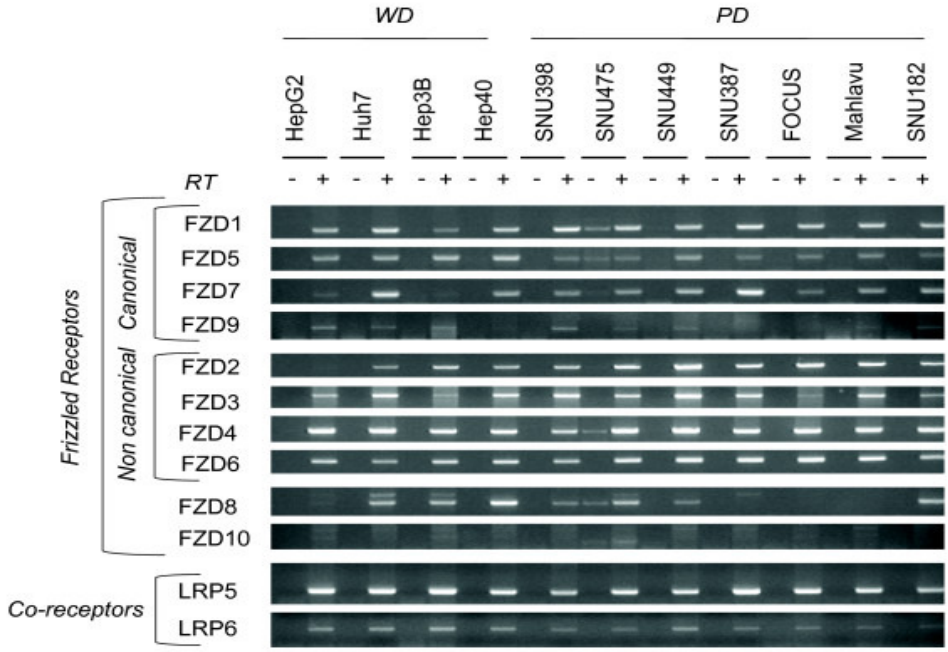

Figure 4.1.5 Comparative analysis of Frizzled receptors and LRP co-receptors in hepatocellular carcinoma cell lines (Modified from [5])**.** Frizzled receptors involved in canonical and noncanonical Wnt signaling were tested for expression by RT-PCR assay (Top). The expression of LRP co-receptors was analyzed similarly (bottom). Total RNAs were extracted from cell lines and used to detect gene expression by RT-PCR assay. See Figure 4.1.3 for GAPDH loading control.

4.1.4 Differential expression of canonical and noncanonical Wnt ligands

In humans, 19 known genes encoding canonical and noncanonical Wnt ligands were identified [196]. Among eight known canonical Wnt ligands, only Wnt3 was strongly and uniformly expressed in all cell lines tested. Most of the cell lines also expressed Wnt10b strongly (Figure 4.1.6). Four out of seven noncanonical Wnt ligands, Wnt4, Wnt5a, Wnt5b and Wnt 7b were expressed in most of the poorly differentiated cell lines tested. Well differentiated cell lines did not express these ligands. Wnt4, Wnt5a and Wnt5b transcripts were not detectable in three cell lines, and Wnt7b in two of this group of cell lines (Figure 4.1.7-top). Other Wnt ligands were not characterized in terms of their specificity [196]. Among these ligands, Wnt9a expression was detectable in nearly all cell lines tested. In contrast, Wnt9b and Wnt2b expressions were associated to well differentiated and poorly differentiated cell lines, respectively (Figure 4.1.7-bottom).

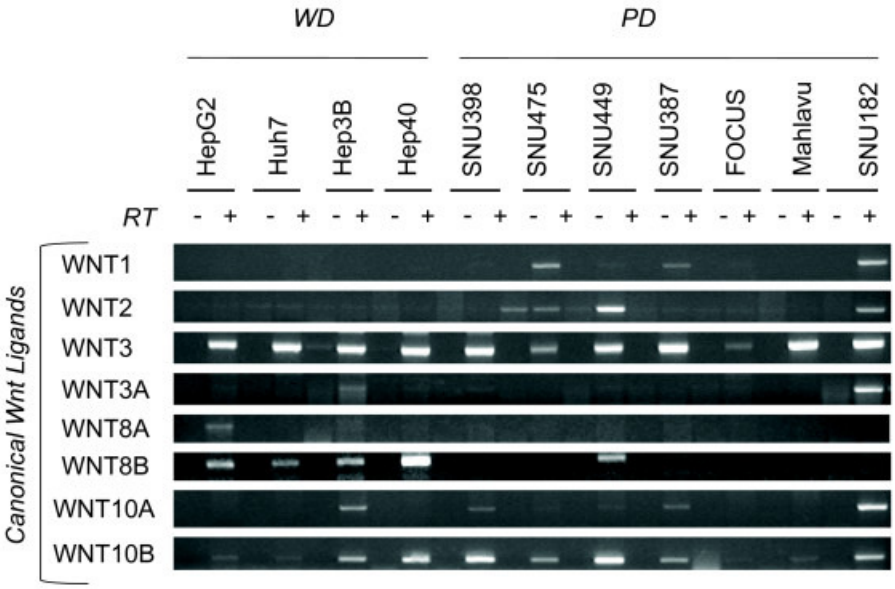

Figure 4.1.6 Comparative analysis of canonical Wnt ligands in hepatocellular carcinoma cell lines (Modified from [5]). Canonical Wnt ligands were tested for expression by RT-PCR assay. Total RNAs were extracted from cell lines and used to detect gene expression by RT-PCR assay. See Figure 4.1.3 for GAPDH loading control.

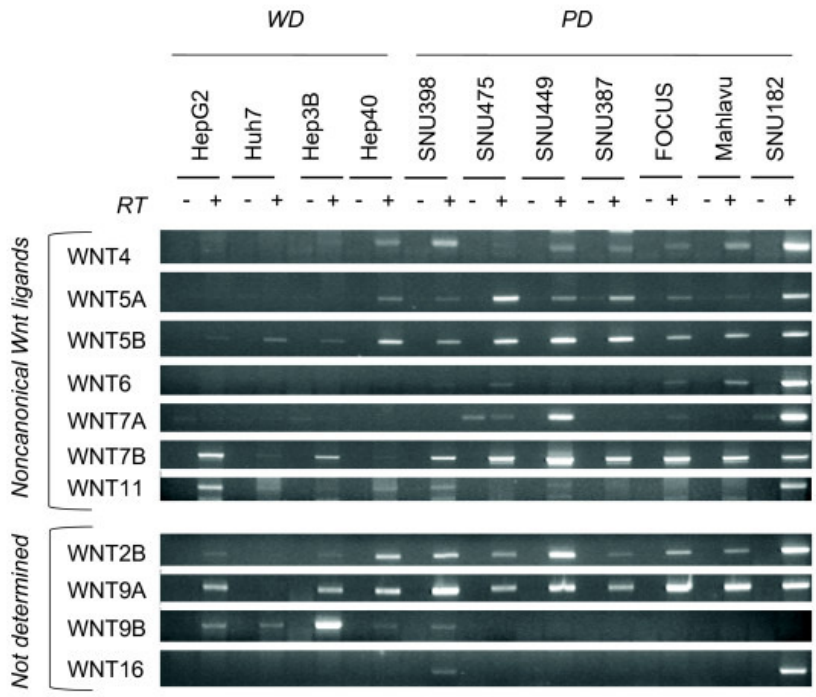

Figure 4.1.7 Comparative analysis of noncanonical (top) and unclassified (bottom) Wnt ligands in hepatocellular carcinoma cell lines (Modified from [5]). Noncanonical and unclassified Wnt ligands were tested for expression by RT-PCR assay. Total RNAs were extracted from cell lines and used to detect gene expression by RT-PCR assay. See Figure 4.1.3 for GAPDH loading control.

HCC cell lines, independent of their differentiation status, were equipped with major components of Wnt signaling pathway with the exception of noncanonical Wnt ligands. In contrast, Wnt ligand expression displayed two types of selectivity. First, among known canonical ligands, only Wnt3 and Wnt10b displayed strong expression in most cell lines showing no specificity at all. Second, four noncanonical Wnt ligands were expressed in HCC cell lines with a high selectivity for poorly differentiated ones. These findings may have several implications. Most, most HCC cell lines were equipped with an canonical Wnt ligands, as reported previously for breast and ovarian cancer cell lines [197]. In contrast, selective expression of noncanonical Wnt ligands in only poorly differentiated cell lines could be due to autrocrine noncanonical Wnt signaling system in these cells. Paracrine mechanism is another possibility also. Noncanonical Wnt ligands including Wnt 5a might inhibit canonical Wnt signaling in HCC cells, as previously reported in other cell types [198-200]. These experiments have been performed by K.Benhaj [5].

4.1.5 Autocrine canonical Wnt signaling in well differentiated hepatocellular carcinoma cell lines

Activated TCF/LEF-dependent transcription by canonical signalling activity can be quantified by reporters containing TCF/LEF-responsive elements [67, 201]. We surveyed canonical Wnt signaling in HCC cell lines using TCF/LEF reporter pGL3-OT plasmid, as described previously [202]. First, we compared TCF/LEF (TCF) activity in three cell lines with known mutations in canonical Wnt signaling pathway (Figure 4.1.8.a). Hepatoblastoma-derived well-differentiated HepG2 cell line displays β-catenin mutation. Poorly-differentiated SNU398 and SNU475 cell lines display β-catenin and AXIN1 mutations, respectively [188, 203]. We obtained the highest normalized TCF activity with HepG2 cells. Compared to HepG2, SNU398 cells displayed 50% less TCF activity. SNU475 cells despite having Axin1 deletion (data not shown; [188, 203], no TCF activity is detected in SNU475 cells. On the other hand, another AXIN1 mutant cell line PLC/PRF/5 also being a well differentiated cell line, showed high TCF activity [203].

We also screened the TCF activity of other cell lines that displayed wild-type β-catenin and AXIN1 status [188, 202-203]. (3-4 fold) TCF activity was detected in well-differentiated Huh7 and Hep3B cell lines; this is low but found to be significant. Whereas, all five poorly differentiated cell lines SNU449, SNU387, FOCUS, Mahlavu and SNU182 and well differentiated Hep40 cell line showed no detectable TCF activity (Figure 4.1.8.b). Hep40 cells, being a well differentiated cell line was included in this group although it shows a missense AXIN1 mutation/polymorphism (R454H). This is because functional significance of this mutation is not fully characterised [202].

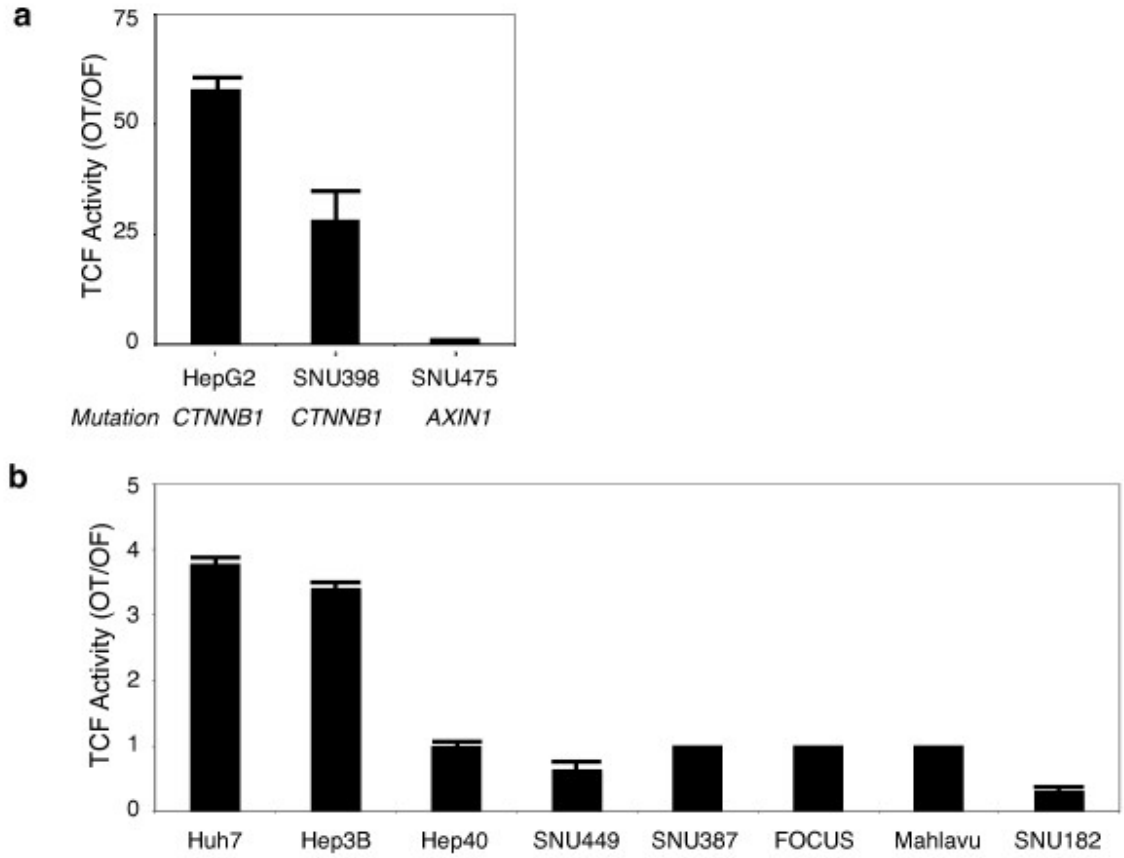

Figure 4.1.8 Frequent constitutive activation of canonical Wnt signaling in well-differentiated, but not in poorly differentiated hepatocellular carcinoma cell lines (modified from[5]). (a) Comparative analysis of the canonical Wnt signaling in hepatoma cell lines with known mutations of β-catenin or Axin-1 genes. TCF reporter assay shows that well-differentiated HepG2 cells display high signaling activity. In contrast, canonical Wnt signaling is attenuated in poorly differentiated SNU398, and undetectable in poorly differentiated SNU475 cell line. Assays in triplicate, error bars; SD. (b) Comparative analysis of the canonical Wnt signaling in HCC cell lines with wild-type β-catenin and Axin-1 genes. Huh7 and Hep3B cell lines (both well-differentiated) display weak but significantly

increased TCF reporter activity. Other cell lines (all poorly differentiated, except Hep40) display no detectable TCF reporter activity. TCF activity denotes the ratio of signals detected with pGL3-OT (OT) and pGL3-OF (OF) plasmids, respectively. Assays in triplicate, error bars; S. D. Cells were transfected with the reporter gene pGL3-OT (OT) harboring LEF-1/TCF binding sites for β-catenin and the corresponding pGL3-OF (OF) without these sites.

Taken together, 12 hepatoma cell lines were tested for TCF activity. Independent of β-catenin or AXIN1 status, TCF activity was detected in four out of five (80%) well-differentiated cell lines, whereas only one out of seven (14%) poorly differentiated cell lines had constitutive TCF activity. First, this data correlated with the hypothesis that well-differentiated HCC cell lines display in general an autocrine/paracrine canonical Wnt signaling. Second, the great majority of poorly differentiated cell lines lack such autocrine/paracrine activity despite the expression of canonical Wnt3 ligand.

4.1.6 Canonical Wnt signaling is repressed in poorly differentiated hepatocellular carcinoma cells

The lack of canonical Wnt activity in poorly differentiated cells could be due to either lack of significant signaling activity, or alternatively to an active repression. Axin2, HTLE family, hAES, Chibby, CTBP and ICAT downstream to β-catenin display inhibitory activity on canonical Wnt signalling [204]. We checked the expression of these genes, but failed to detect any correlation with TCF activity or differentiation state (Figure 4.1.9).

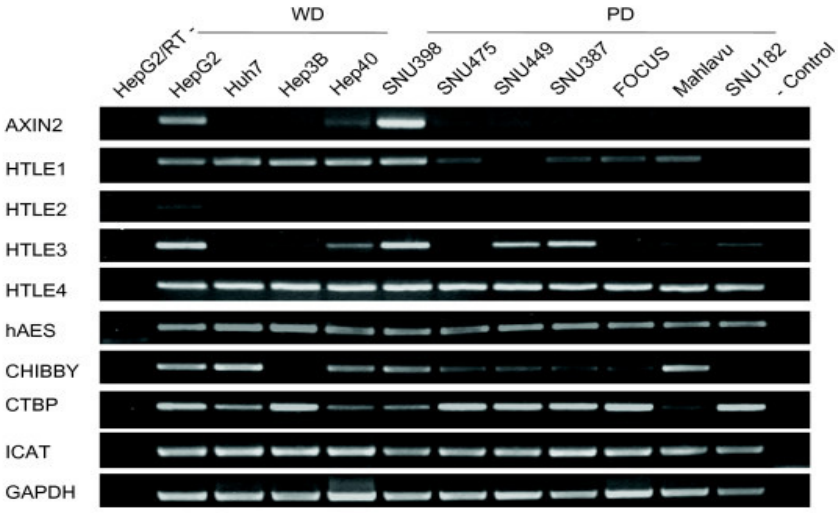

Figure 4.1.9 Expression analysis of genes inhibiting canonical Wnt signaling downstream to β-catenin in HCC cells. Total RNAs were extracted from cell lines and used to detect gene expression by RT-PCR assay. GAPDH RT-PCR was used as a loading control.

Next, we compared TCF activity in Huh7, SNU449 and SNU182 cell lines ectopically expressing a mutant (S33Y)-β-catenin (Figure 4.1.10). Total β-catenin protein in Huh7 and SNU449 but not that strong with SNU182 cells was detected after transient transfection (Figure 4.1.10a). Well-differentiated Huh7 cells responded to mutant β-catenin expression by a strong activation of TCF/LEF reporter (130 folds). Under the same experimental conditions, only 5 folds activity was detected in SNU449 cells. SNU182 cells were totally unresponsive (Figure 4.1.10b) [5]. These important differences between well-differentiated and two different poorly differentiated cell lines are apparently not due because of transient transfection efficiencies, the measured activities have been normalized by dual luciferase assay (see material and methods section).

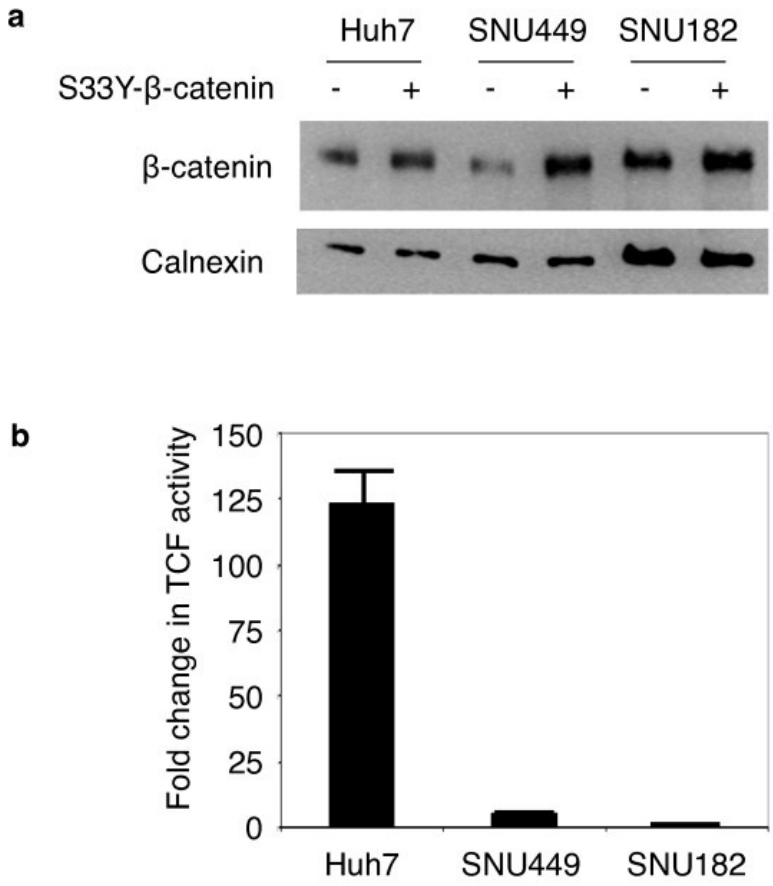

Figure 4.1.10 Ectopic expression of mutant β-catenin induces high canonical Wnt activity in well-differentiated, but not in poorly differentiated hepatocellular carcinoma cells (modified from [5]). (a) Well-differentiated Huh7, and poorly differentiated SNU449 and SNU182 cell lines were co-transfected with either pCI-neo-mutant β-catenin (S33Y) plasmid (S33Y-β-catenin +) or empty pCI-neo plasmid (S33Y-β-catenin -), and cellular β-catenin levels at post-transfection 48 h were tested by immunoblotting. Calnexin was used as a loading control. (b) Cell lines were treated as described, then pCI-neo-mutant β-catenin (S33Y)-transfected cells were subjected to TCF reporter assay. TCF activity denotes the ratio of signals detected with pGL3-OT (OT) and pGL3-OF (OF) plasmids, respectively. Assays in triplicate, error bars; SD. Co-transfections included pGL-OT or pGL-OF, in addition to pCI-neo plasmids in both (a) and (b).

Next, we generated a clone from SNU449 cells (SNU449-cl8) with Tet repressor controlled expression of N-terminally truncated β-catenin (aa 98-781) in order to confirm this data. These forms of mutant β-catenin are frequently detected in cancer cells including HCC. The lack of Ser/Thr phosphorylation sites (aa Ser23, Ser29, Ser33, Ser37, Thr41, Ser45) that are critically involved in its ubiquitin-mediated degradation, leads to oncogenic activation canonical Wnt signaling [67]. As shown in figure 4.11a, SNU449-cl8 cells expressed only wild-type β–catenin in the presence of tetracycline (Tet-on conditions), while expressing both wild-type and truncated β-catenin at comparable levels in Tet-off conditions. Only a weak activation (3-4 folds) of TCF reporter activity was obtained, similar to data obtained by transient transfection experiments (Figure 4.1.11b). This low level of activation was similar to that seen in well-differentiated HCC cells in the absence of β-catenin or Axin-1 mutation (Fig. 4.1.8b), and confirmed that Wnt signaling is actively repressed in this poorly differentiated HCC cell line. For comparison, well-differentiated HepG2 cells expressing wild-type and a similar N-terminally truncated β-catenin (D25-140aa) activated TCF reporter gene by more than 60-fold (Figure 4.1.8a). In other words, although both Tet-off SNU449-cl8 and HepG2 cells displayed a heterozygous truncating β-catenin mutation, TCF activation was 15-fold less in poorly differentiated SNU449 background. We performed immunofluorescence detection to see accumulation of truncated β-catenin using confocal microscopy (Figure 4.1.11c). The induction of truncated β-catenin in Tet-off SNU449-cl8 cells did not change membrane form of β-catenin distribution significantly. Only a weak cytoplasmic accumulation with slight increases in both membrane and nuclear localization were observed. Whereas in colorectal cancer cells (APC-

mutated), used as a positive control [205], we detected strong nuclear accumulation of β-catenin by the same technique.

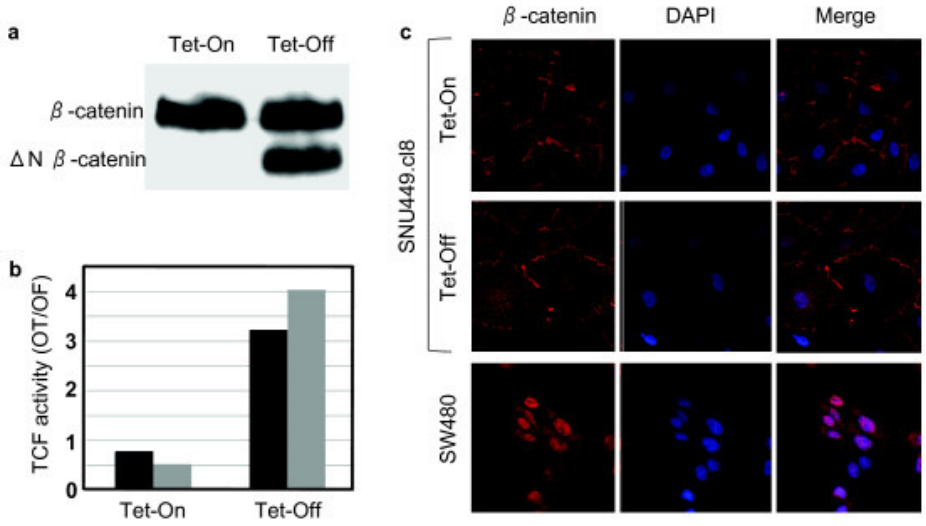

Figure 4.1.11 Minimal TCF reporter activity and lack of nuclear accumulation of mutant β-catenin in poorly differentiated SNU449.cl8 cells (modified from [5]). SNU449 cells were stably transfected with Tet-responsive ΔN-β-catenin expression vector to obtain SNU448.cl8 cells. (a) Induced expression of N-terminally truncated ΔN-β-catenin protein in the Tet-Off conditions, as tested by western blot assay. Total cell lysates were extracted from cells and subjected to western blot assay using anti-β-catenin antibody. (b) TCF activity is only weakly induced in Tet-off conditions, as tested by duplicate experiments. (c) SNU449.cl8 cells at Tet-On state express wild-type endogenous β-catenin protein principally located at cell membrane. Under Tet-Off conditions the staining pattern remains almost identical despite ΔN-β-catenin expression. Note lack of nuclear accumulation. SW480 cells used as positive control displayed strong nuclear β-catenin staining. Cells were grown on coverslips, subjected to indirect immunofluorescence assay using anti-β-catenin antibody (red), counterstained with DAPI (blue) and examined by confocal microscopy.

4.1.7 WNT5A inhibits canonical Wnt signaling in HCC cells

Wnt5a is best known for its antagonistic effect on canonical Wnt signaling [206]. Therefore, we ectopically expressed Wnt5a and checked its effect on mutant-β-catenin-induced TCF activity in Huh7 cell line. In the absence of Wnt5a, TCF activity was measured more than 160-fold by mutant β-catenin in this cell line. Co-expression of Wnt5a resulted in three-fold repression of TCF activity (Figure 4.1.12a). To confirm our observations, we also tested the effects of Wnt5a on TCF activity induced by endogenous mutant β-catenin using HepG2 cell line. The expression of Wnt5a in this cell line caused a significant inhibition of TCF activation

mediated by endogenous β-catenin ($P < 0.05$; Figure 4.1.12b). We concluded that Wnt5a that is selectively expressed in poorly differentiated HCC cell lines, and probably similarly acting selectively in the repression of canonical Wnt signaling in these cells.

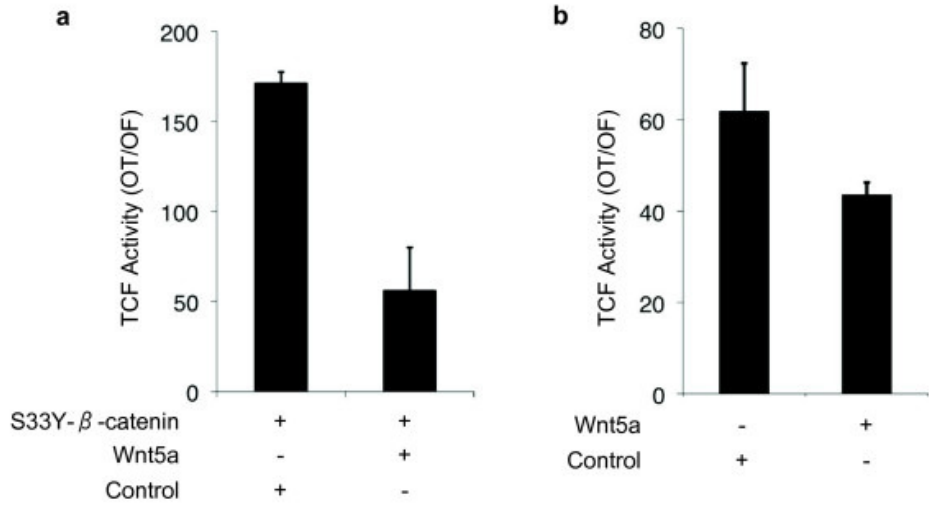

Figure 4.1.12 Wnt5a inhibits canonical Wnt signaling activity in Huh7 and HepG2 cells. (a) Huh7 cells were co-transfected with either pCI-neo-mutant β-catenin (S33Y) plasmid (S33Y-β-catenin +) along with pShuttle-IRES-WNT5a or empty pShuttle-IRES vector. 48 hours post transfection; cells were subjected to TCF reporter assay. TCF activity denotes the ratio of signals detected with pGL3-OT (OT) and pGL3-OF (OF) plasmids, respectively. Assays in triplicate, error bars; SD. Co-transfections included pGL-OT or pGL-OF, in addition to pCI-neo-S33Y-β-catenin and pIRES plasmids. (b) HepG2 experiments were performed under similar conditions, except that pCI-neo-mutant β-catenin (S33Y) plasmid was omitted.

4.2 Selective monoclonal antibodies directed against C-terminal domain of β–Catenin

We aimed to develop monoclonal antibodies (Mabs) that selectively recognize membrane-bound, cytoplasmic and nuclear beta-catenin forms and to test their clinical value using immunohistochemical staining of several tumor samples. For this purpose a former PhD student Nuri Ozturk obtained several home–made monoclonal antibodies and characterized the epitopes of each antibody. The details of immunization and hybridoma procedure and epitope mapping can be found at thesis of Dr. Nuri Ozturk (Ozturk, 2006). Here we will discuss further characterization of these monoclonal antibodies (Mabs). The two Mabs (9E10 and 4C9) with selective recognition ability were identified. These Mabs recognized partially overlapping epitopes located at the last 10 amino acid residues of β-catenin. 9E10 was directed against a

seven amino acid epitope (771-SNQLAWF-777), the 4C9 was directed against the last four amino acids (DTDL) that is a binding site for PDZ-domain proteins (Ozturk N. unpublished data).

4.2.1 Antibody Isotyping

4C9 and 9E10 was classified as IgG1(κ) by a mouse monoclonal antibody isotyping kit (Pierce ELISA Mouse Antibody Isotyping Kit, US).

4.2.2 Selective immunoreactivity of 4C9 and 9E10 antibodies against cellular β-Catenin

Among all known anti-β-catenin antibodies, our 4C9 and 9E10 antibodies occupy a particular position because together they are directed against the last 10 carboxy-terminal amino acids. This end of β-catenin is implicated in interactions with a handful of different proteins displaying PDZ domains, such β-catenin complexes are expected to be retained in specific locations where such PDZ domain proteins are located. For example, several of these proteins are known to anchor their binding partners in close proximity of plasma membrane. On the other hand, β-catenin has also known to be found in the cytoplasm as well as in the nucleus particularly when it is not involved in cadherin-mediated cellular adhesion and/or transducing wnt signaling into gene regulation at nuclear level. It is unknown whether such cytoplasmic and nuclear forms of β-catenin are also complexed with PDZ-domain proteins. We hypothesized that our antibodies could react selectively with different, presumably PDZ-bound and PDZ-free forms of β-catenin in different cellular locations; we tested in situ immunoreactivity of our antibodies with cellular β-catenin using immunoperoxidase, immunofluorescence and confocal microscopy techniques. To explore selective immunoreactivity of 4C9 and 9E10 antibodies, we performed detailed analyses on different cell lines using confocal microscopy techniques. It is known that activating mutations in the Wnt/β-Catenin pathway lead to accumulation of β-Catenin in the cytoplasm as well as in the nucleus where it interacts with TCF/LEF family of transcription factors and activates transcription of the Wnt responsive genes. Based on this model we have used immunofluorescence staining to study the effect of the mutations identified in the APC mutant colorectal carcinoma cell lines SW480, SW837 and β-Catenin mutant HCC cell line Snu398-i and ΔN-β-Catenin expressing inducible clone of another HCC cell line Snu449-c8. SW480 colorectal carcinoma cells containing a truncated APC were intensely stained in the nucleus and

cytoplasm by both 4C9 and 9E10 whereas commercial anti-β-Catenin antibody (Transduction Labs) stained in the nucleus weakly. SW480 was not stained in the membrane with any of these antibodies (Figure 4.2.1.A). Another APC mutant colorectal carcinoma cell line, SW837 was stained positively in the nucleus, with a very weak membrane staining by 4C9 and 9E10 whereas membrane was stained continuously by commercial anti-β-Catenin antibody and nucleus was negative (Figure 4.2.1.B). Snu398-i which has a missense β-Catenin mutation, showed that both antibodies showed a intense nuclear staining, while 4C9 and 9E10 have weak membrane staining when compared to commercial anti- β-Catenin antibody (Figure 4.2.1.C). These findings confirm that mutations in the Wnt/ β-Catenin pathway elements were activating and β-Catenin accumulates in the nucleus as mentioned above. Also extensive analysis of an inducible clone which stably expressed mutant β-Catenin (ΔN-β-Catenin) and a mouse fibroblast cell line which expresses Wnt3a ligand stably confirmed this statement. Snu449.c8 with a tetracycline regulatable expression of mutant β-Catenin (ΔN-β-Catenin) showed a 16 fold induction of Axin2 which is a direct target of β-Catenin (Yuzugullu et al., unpublished data). This clone expresses ΔN- β-Catenin in the absence of tetracycline. Snu449.c8 cells were stained intensely more in the nucleus and cytoplasm when compared to non-induced state. Commercial anti-β-Catenin antibody stained the membrane uniformly whereas 4C9 and 9E10 has an intense nuclear staining like APC mutant colorectal carcinoma cell lines (Figure 4.2.2.A and 4.2.2.B). Further experiments with Nih3T3 cells stably expressing wnt3a ligand also showed consistent data with the previous results. Cells cultured with the wnt3a conditioned media checked for the autocrine activity. Cells were stained in the nucleus intensely with 9E10 whereas membrane was not stained. Commercial anti-β-Catenin antibody had a uniform membrane staining (Figure 4.2.1.D). These results showed that as in colon cancer models, β-catenin and APC mutations led to accumulation of β-Catenin both in the cytoplasm and nucleus. Also our hybridomas successfully reacted against β-catenin in the nucleus and cytoplasm whereas membrane staining was more intense with commercial anti- β-Catenin antibody as shown with various cell types with different mutation status.

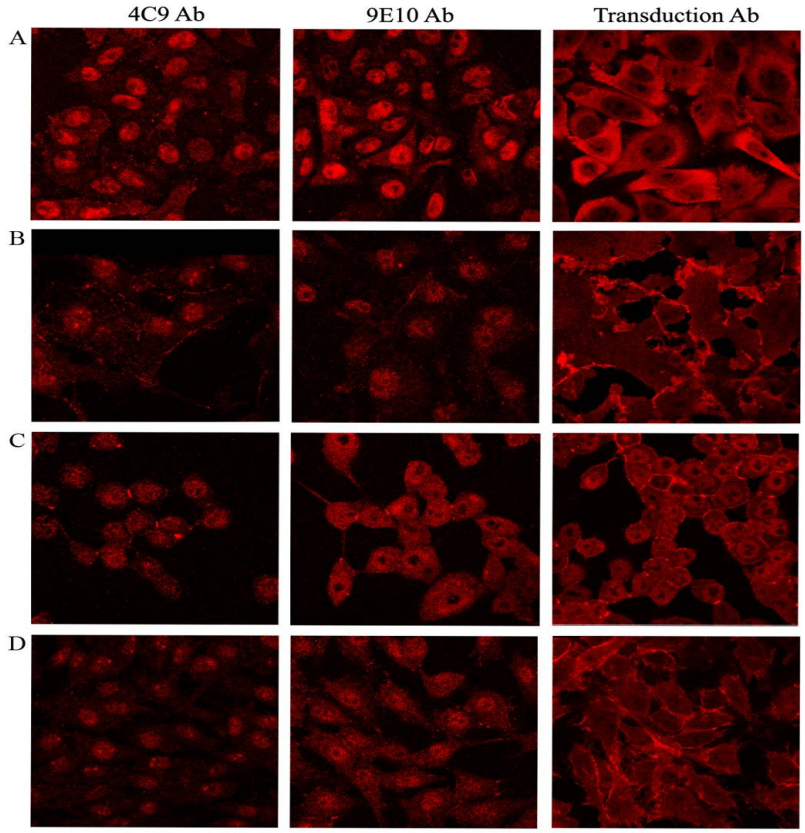

Figure 4.2.1 Confocal microscopy of 4C9, 9E10 and commercial β-catenin antibodies in β-catenin mutant cell lines. Strong nuclear staining with 4C9 and 9E10 antibodies but not with commercial antibody in APC mutant colorectal carcinoma cell lines in (a) SW480 cell line, (b) in SW837, (c) in beta-catenin mutant HCC cell line Snu398-i and (d) wnt3a induced Nih3T3 cells. Note that commercial β-catenin antibody reacted to membrane beta-catenin forms. Cells were grown on coverslips, subjected to indirect immunofluorescence assay using anti-β-catenin antibody (red), counterstained with DAPI (blue) and examined by confocal microscopy.

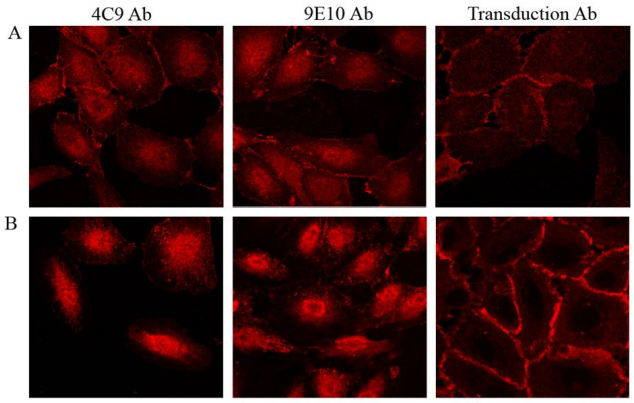

Figure 4.2.2 Confocal microscopy of 4C9, 9E10 and commercial β-catenin antibodies in poorly differentiated SNU449.cl8 cells. (a) SNU449.cl8 cells at Tet-On state express wild-type endogenous β-catenin protein principally located at cell membrane. (b) Under Tet-Off conditions, ΔN-β-catenin accumulated in the nucleus detected by 4C9 and 9E10 Mabs but not with commercial antibody. Cells were grown on coverslips, subjected to indirect immunofluorescence assay using anti-β-catenin antibody (red), counterstained with DAPI (blue) and examined by confocal microscopy.

4.2.3 9E10 Mab immunoreactivity with primary tissue and tumor samples:

In order to show the selective immunoreactivity of these Mabs, we used immunohistochemistry staining of β-catenin in several types of paraffin embedded normal and carcinoma specimens. We first performed a comparative staining between the two antibodies using a total of 28 in situ ductal carcinoma and 26 invasive ductal carcinoma specimens. Staining in normal breast areas showed that both antibodies showed the same pattern of immunoreactivity specific to membrane with incomplete pattern with no nuclear staining (Figure 4.2.3.A and 4.2.3.C). For the two different types of breast cancer tissues, both 4C9 and 9E10, showed heterogenous membrane staining, while nuclear and/or cytoplasmic stainings were not observed (Figure 4.2.3.B and 4.2.3.D).

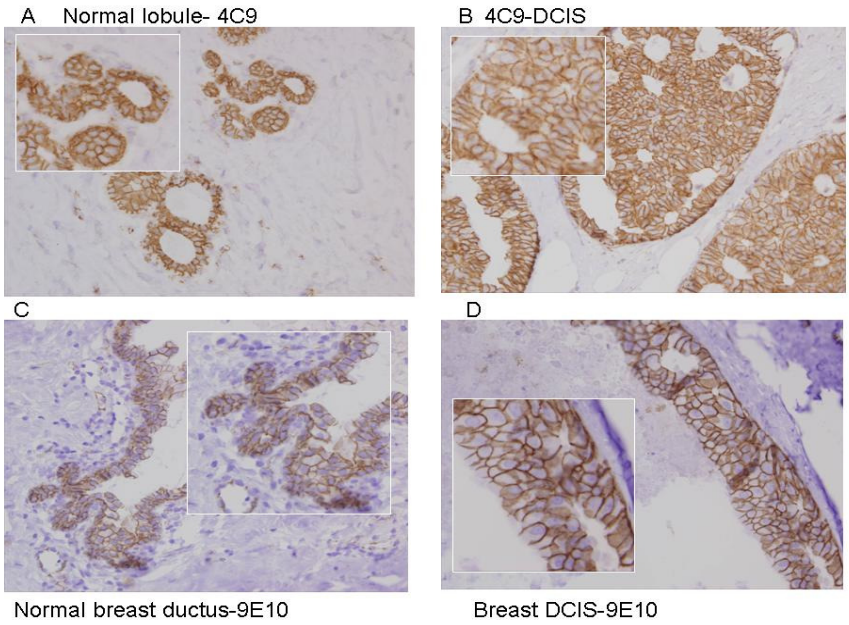

Figure 4.2.3 Immunohistochemistry analysis of 4C9 and 9E10 in paraffin embedded normal and breast cancer samples. DAB Staining in normal breast areas showed that both antibodies showed the same pattern of immunoreactivity specific to membrane with incomplete pattern with no nuclear staining in (A) and (C), heterogenous membrane staining, while nuclear and/or cytoplasmic stainings were not observed in (B) and D).
Based on these stainings, our antibodies showed specific immunoreactivity to membrane form of β–catenin in 35 of 54 breast tumors (65 %) with 61% of in situ ductal carcinoma and 69% of invasive ductal carcinoma showing mostly weakly or moderately heterogeneous membrane staining (Table 4.2.1)

Since both antibodies showed similar staining pattern in breast cancer samples, we continued analyzing a panel of carcinoma tissues with only clone 9E10. A total of 32 hepatocellular carcinoma, 43 endometrial carcinomas and 62 colon carcinoma samples were stained with 9E10 Mab.

Table 4.2.1 Distribution of membrane form of β-catenin expression in the tumor samples

Tumor Type (n)	**Negative[1] (%)**	**Weakly Positive[2] (%)**	**Moderately Positive[3] (%)**	**Highly Positive[4] (%)**	**Total Positive (%)**
Colorectal carcinoma (54)	2 (3.5)	2 (3.5)	9 (17.0)	41 (76.0)	51 (94.5)
Hepatocellular carcinoma (32)	20 (62.5)	3 (9.5)	5 (15.5)	4 (12.5)	12 (37.5)
Endometrial carcinoma (42)	30 (71.5)	2 (5.0)	4 (9.5)	6 (14.0)	12 (28.5)

Breast carcinoma (54)	19 (35.0)	14 (30.0)	18 (33.0)	3 (6.0)	35 (65.0)
In situ ductal carcinoma (28)	11 (39.5)	6 (21.5)	9 (32.0)	2 (7.0)	17 (61.0)
Invasive ductal carcinoma (26)	8 (31.0)	8 (31.0)	9 (35.0)	1 (4.0)	18 (69.0)

1=0-4%; 2=5-25%; 3=26-75%; 4=76-100%

We performed immunohistochemistry staining in 33 hyperplastic and 42 endometrium tumor samples. In hyperplastic lesions of endometrium samples, heterogeneous β-catenin membrane staining was observed in 17 of (51,5%) 33 samples. Only one sample showed cytoplasmic staining, while nuclear staining was not observed in any elements of hyperplastic lesions. Membrane β-catenin staining patterns were observed in 12 of (28,5%) 42 of endometrial carcinomas, ranging from strong membrane (14%) staining to weak (5%) staining (Figure 4.2.4). Cytoplasmic immunostaining was observed only in 3 samples (< 1%). In one case with coexistence of carcinoma and atypical hyperplasia lesions, membrane immunoreactivity was found to be decreased in the former as compared to the latter, while nuclear immunoreactivity was not found in both lesions in all samples.

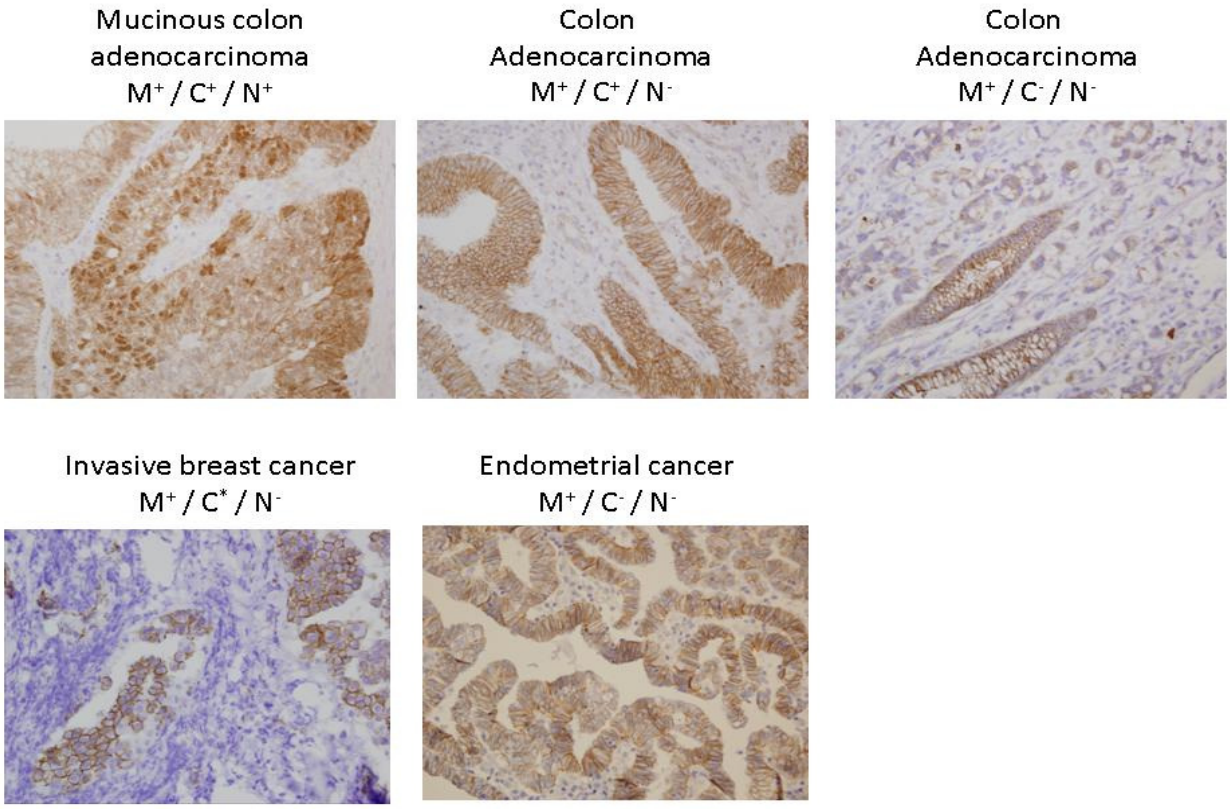

Figure 4.2.4 Immunohistochemistry analysis of 9E10 in paraffin embedded carcinoma samples. DAB Staining in nuclear positive mucinous colon carcinoma, nucleus negative, cytoplasm and membrane positive colon adenocarcinoma, only membrane positive colon adenocarcinoma and membrane and cytoplasm positive invasive breast cancer and only membrane positive endometrial cancer samples.

We also stained 32 Hepatocellular carcinoma samples using the same technique. 12 of (37,5%) 35 samples exhibited membrane staining with different levels of staining. Nuclear and/or cytoplasmic staining was not observed in these samples.

Previous reports showed that nuclear β catenin expression was highly associated with progression of colorectal tissue from normal epithelial tissue, polyps, adenomas, to carcinomas. Therefore we analyzed immunoreactivity of our antibody using a total of 54 patients with colorectal carcinoma samples, namely: 48 colorectal adenocarcinoma, 2 colorectal signet ring cell carcinomas, 3 mucinous carcinomas and 1 villous adenocarcinoma. Among these, two of the colorectal signet ring cell carcinoma samples were found to be negative. For the remaining colon carcinoma samples, 50 of (96,2%) 54 showed moderately or strong membrane staining with a

percentage of 17% versus % 76 respectively . Weakly and moderately nuclear, with or without cytoplasmic, immunostaining was apparent in 11 (20.5%) of 54 carcinomas. Weakly stained cytoplasmic β-catenin was found in 15 of (28%) of all samples (Figure 4.2.4). Table 4.2.2.

Table 4.2.2 Distribution of different forms of ß-catenin expression in 54 colorectal cancer samples using 9E10 antibody.

Cellular localization	**Negative[1] (%)**	**Weakly Positive[2] (%)**	**Moderately Positive[3] (%)**	**Highly Positive[4] (%)**	**Total Positive (%)**
Nucleus	43 (79.5)	9 (16.5)	2 (4.0)	0 (0.0)	11 (20.5)
Cytoplasm	39 (72.0)	15 (28.0)	0 (0.0)	0 (0.0)	15 (28.0)
Membrane	2 (3.5)	2 (3.5)	9 (17.0)	41 (76.0)	51 (94.5)

4.3 Targeting human kinome and phosphatome in hepatocellular carcinoma cells using RNAi

Our aim was to identify and inhibit human kinase and phosphatase genes that are contributing to escape from senescence. We started this project using our unique in vitro model of immortality/senescence. This model is composed of isogenic clones of liver cancer cell line Huh7. One isogenic clone was immortal and the other is senescence programmed. In 2006, our laboratory showed that this immortal clone of huh7 cell line is immortal and have the capacity to form tumor in nude mice whereas the other have reverted from immortality, and have a limited lifespan just like hepatocytes, and do not have the capacity to form tumors in vivo [130]. Using these two isogenic clones, we performed microarray analysis and more than 54000 probes were analyzed. We mapped 518 kinase and 223 phosphatases in this array and searched for kinases and

phosphatases that are upregulated more than 1 fold in immortal isogenic clones with respect to either early passages of senescent clones or in senescencent clone. We obtained 126 kinase genes and 28 phosphatase genes that are upregulated more than 1 fold in immortal clone. We further qualified and listed these genes using Pubmed and online databases like Oncomine and publicly annotated cancer genes lists and finally ordered these genes and called this list as "the priority list".

We further validated these genes using microarray expression results of cirrhotic and HCC samples performed in our laboratory. After siRNA screening of these target genes, we used automated system to check the efficiency of knockdown using the method that National Cancer Institute (NCI) is using.

4.3.1 Validation of kinase and phosphatase target genes

We validated our priority ordered genes using differentially expressed gene lists of *in vivo* microarray results performed in our group using HCC and cirrhotic samples. As a total 22 cirrhotic and 17 HCC samples were used in this experiment and 6017 differentially expressed genes with p value ≤ 0,05 (Bagislar et al., unpublished data). We searched for the genes that are listed in 6017 differentially expressed genes. The values are listed in table 4.3.1 for kinases and Table 4.3.2. for phosphatases.

Table 4.3.1 Validation of kinases obtained *in vitro* and *in vivo*

Gene Symbol	Probe Number	Average Normal Log.	Average tumor Log.	Tumor-normal Log	Tumor-normal fold change
CDC2	**203213_at**	5.63	7.13	1.5	2.8
CDC2	**210559_s_at**	4.88	6.27	1.4	2.6
PBK	**219148_at**	4.22	5.52	1.3	2.5
BUB1	**209642_at**	3.89	5.14	1.25	2.4
CDC2	**203214_x_at**	5.21	6.2	0.99	2.0
NEK3	**239539_at**	4.78	5.46	0.68	1.6
CDK6	**224851_at**	8.25	8.93	0.68	1.6
CASK	**211208_s_at**	8	8.63	0.63	1.5
IRAK1	**201587_s_at**	8.32	8.94	0.62	1.5
CASK	**207620_s_at**	6.18	6.76	0.59	1.5

PLK4	**204887_s_at**	5.21	5.79	0.58	1.5
PAK1	**230100_x_at**	6.04	6.51	0.47	1.4
PAK2	**208877_at**	8.19	8.65	0.47	1.4
PLK1	**202240_at**	5.26	5.71	0.45	1.4
PLK4	**204886_at**	2.83	3.28	0.45	1.4
MASTL	**228468_at**	5.39	5.84	0.45	1.4
HIPK2	**225116_at**	8.73	9.14	0.41	1.3
BUB1	**215509_s_at**	4.05	4.46	0.4	1.3
TRRAP	**202642_s_at**	7.73	8.1	0.37	1.3
MAP3K7	**206854_s_at**	7.97	8.33	0.36	1.3
MAP2K2	**202424_at**	8.62	8.98	0.36	1.3
NEK3	**213116_at**	7.08	7.41	0.33	1.3
HIPK2	**225097_at**	9.01	9.34	0.33	1.3
TLK1	**210379_s_at**	4.68	5	0.32	1.2
PAK2	**236283_x_at**	6.88	7.18	0.3	1.2
MAP3K7	**206853_s_at**	6.82	7.1	0.28	1.2
MAPKAPK2	**201460_at**	8.3	8.57	0.27	1.2
PLK4	**211088_s_at**	2.95	3.14	0.18	1.1
BUB1	**216277_at**	3.32	3.46	0.14	1.1

Table 4.3.2 Validation of phosphatase genes obtained *in vitro* and *in vivo*

Gene Symbol	Probe Number	Average Normal Log.	Average tumor Log.	Tumor-normal Log	Tumor-normal fold change
CDKN3	1555758_a_at	5.04	6.49	1.45	2.73
CDKN3	209714_s_at	5.33	6.51	1.18	2.27
PSPH	205194_at	5.57	6.29	0.72	1.65
PPP3CB	209817_at	7.18	7.66	0.48	1.39
PTPN11	212610_at	10.23	10.67	0.44	1.36
PTPRM	1555579_s_at	8.51	8.93	0.42	1.34
CDC25C	217010_s_at	3.66	4.03	0.37	1.29
PTPRM	203329_at	8.04	8.38	0.34	1.27
PTPN18	1569552_at	3.21	3.54	0.33	1.26
PPP4R1	201594_s_at	8.8	9.09	0.29	1.22
PNKP	218961_s_at	6.76	7.01	0.25	1.19
PTPN18	203555_at	7.5	7.7	0.2	1.15

4.3.2 *In vitro* screening

We screened a total of 378 siRNAs targeting 126 kinase genes and 84 siRNAs targeting 28 phosphatases in vitro using Huh7 cells. We obtained and quantified the viable cells left in the plates after 72 hours of transfection. We calculated normalized values and inhibition rates of each transfection and listed them as in table 4.3.3. In table 4.3.3 and figure 4.3.1, we showed the kinase genes showing 70% or more inhibition. In table 4.3.4. and figure 4.3.2 we showed the phosphatases whose knock down induced growth inhibition of 50% or more. As a total of all siRNAs, 6% of kinases and 17% of phosphatase genes were found to be effective.

Table 4.3.3 *in vitro* screening results of kinases

Group name	Gene Name	Repeat 1	Repeat 2	Repeat 3	Mean	STDV	Normalized survival %
OTH22_1071	PLK1_1071	0.296	0.383	0.525	0.401	0.116	55.7
OTH22_1316	PLK1_1316	0.142	0.244	0.521	0.302	0.196	41.9
OTH22_881	**PLK1_881**	**0.128**	**0.180**	**0.299**	**0.202**	**0.088**	**28.1**
CAM13_287	CHK1_287	0.276	0.258	0.193	0.242	0.044	33.6
CAM13_758	**CHK1_758**	**0.241**	**0.203**	**0.221**	**0.222**	**0.019**	**30.7**
CAM13_908	CHK1_908	0.228	0.395	0.356	0.326	0.087	45.3
CAM2_182	**CaMK1a_182**	**0.112**	**0.148**	**0.151**	**0.137**	**0.022**	**19.0**
CAM2_192	**CaMK1a_192**	**0.134**	**0.147**	**0.144**	**0.142**	**0.007**	**19.6**
CAM2_426	**CaMK1a_426**	**0.136**	**0.127**	**0.112**	**0.125**	**0.012**	**17.3**
CAM47_000	**smMLCK_000**	**0.130**	**0.127**	**0.229**	**0.162**	**0.058**	**22.5**
CAM47_001	**smMLCK_001**	**0.186**	**0.118**	**0.200**	**0.168**	**0.044**	**23.3**
CAM47_002	smMLCK_002	0.128	0.175	0.374	0.226	0.131	31.3
CAM59_1664	PKD3_1664	0.472	0.393	0.444	0.436	0.040	60.5
CAM59_550	**PKD3_550**	**0.287**	**0.169**	**0.201**	**0.219**	**0.061**	**30.4**
CAM59_603	**PKD3_603**	**0.216**	**0.259**	**0.180**	**0.218**	**0.040**	**30.3**
CAM9_1002	CaMK2d_1002	0.356	0.392	0.217	0.322	0.092	44.6
CAM9_1063	**CaMK2d_1063**	**0.302**	**0.125**	**0.178**	**0.202**	**0.091**	**28.0**
CAM9_981	CaMK2d_981	0.367	0.214	0.181	0.254	0.099	35.2
CMG11_1253	PCTAIRE2_1253	0.133	0.198	0.564	0.298	0.232	41.4
CMG11_1333	PCTAIRE2_1333	0.233	0.441	0.287	0.320	0.108	44.4
CMG11_943	**PCTAIRE2_943**	**0.223**	**0.187**	**0.237**	**0.216**	**0.026**	**29.9**
CMG2_213	**CDC2_213**	**0.144**	**0.241**	**0.275**	**0.220**	**0.068**	**30.5**
CMG2_322	CDC2_322	0.203	0.211	0.271	0.228	0.037	31.7
CMG2_69	**CDC2_69**	**0.180**	**0.241**	**0.219**	**0.213**	**0.031**	**29.6**

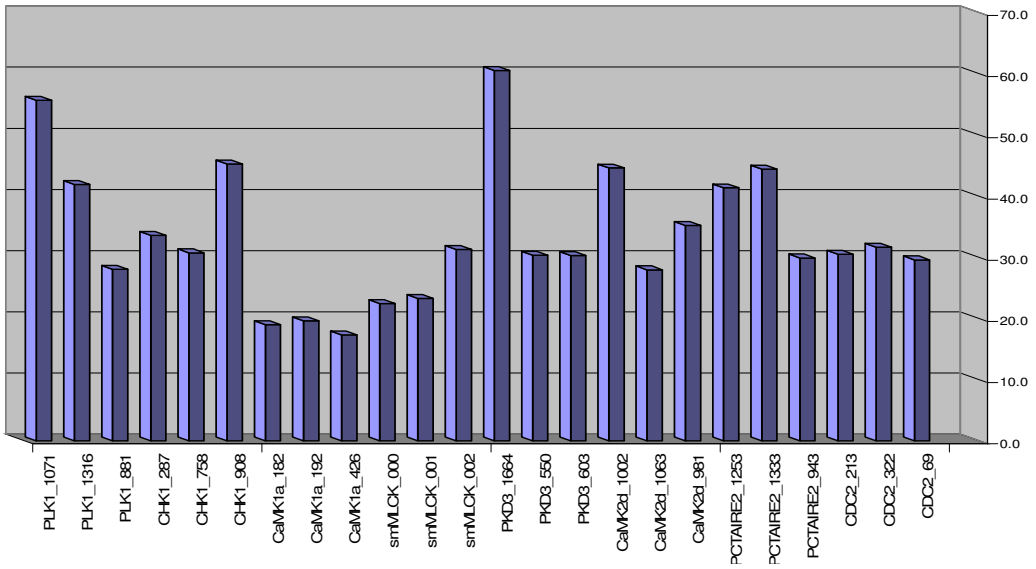

Figure 4.3.1. Normalized survival percentage of kinase genes

Table 4.3.4 *in vitro* screening results of phosphatases

Group name	Gene Name	Repeat 1	Repeat 2	Repeat 3	Mean	STDV	Normalized survival %
PTP030-1824	PTPN11-1824	0.952	0.853	1.106	0.970	0.127	134.6
PTP030-5015	**PTPN11-5015**	**0.217**	**0.218**	**0.302**	**0.246**	**0.049**	**34.1**
PTP030-5849	PTPN11-5849	0.479	0.567	0.615	0.554	0.069	76.8
OTHER2-014-241	INPP4A-241	1.251	1.285	1.341	1.292	0.045	179.2
OTHER2-014-2463	**INPP4A-2463**	**0.274**	**0.299**	**0.404**	**0.326**	**0.069**	**45.2**
OTHER2-014-550	INPP4A-550	0.212	0.359	0.879	0.483	0.350	67.0
PTP001-2273	PTPRA-2273	0.743	1.063	1.069	0.958	0.187	132.9
PTP001-2836	PTPRA-2836	0.390	0.402	0.411	0.401	0.011	55.6
PTP001-333	**PTPRA-333**	**0.297**	**0.365**	**0.391**	**0.351**	**0.049**	**48.7**
OTHER3-10-513	PNKP-513	0.525	0.482	0.723	0.577	0.129	80.0
OTHER3-10-514	**PNKP-514**	**0.327**	**0.330**	**0.434**	**0.364**	**0.061**	**50.4**
OTHER3-10-550	PNKP-550	1.329	1.201	1.287	1.272	0.065	176.5
PTP001-2273	PTPRA-2273	0.743	1.063	1.069	0.958	0.187	132.9
PTP001-2836	PTPRA-2836	0.390	0.402	0.411	0.401	0.011	55.6
PTP001-333	**PTPRA-333**	**0.297**	**0.365**	**0.391**	**0.351**	**0.049**	**48.7**

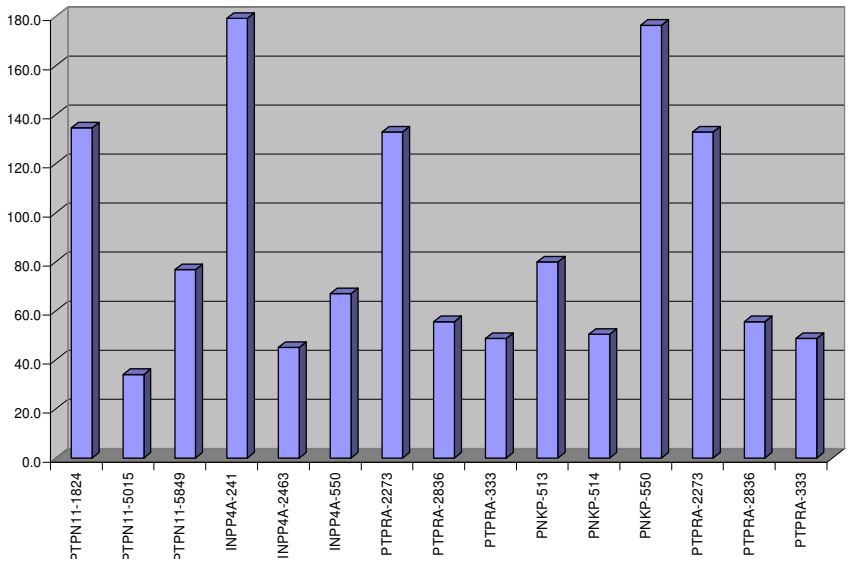

Figure 4.3.2 Normalized survival percentage of phosphatase genes

We also showed the map of effective kinases on the human kinome tree as in figure 4.3.3.

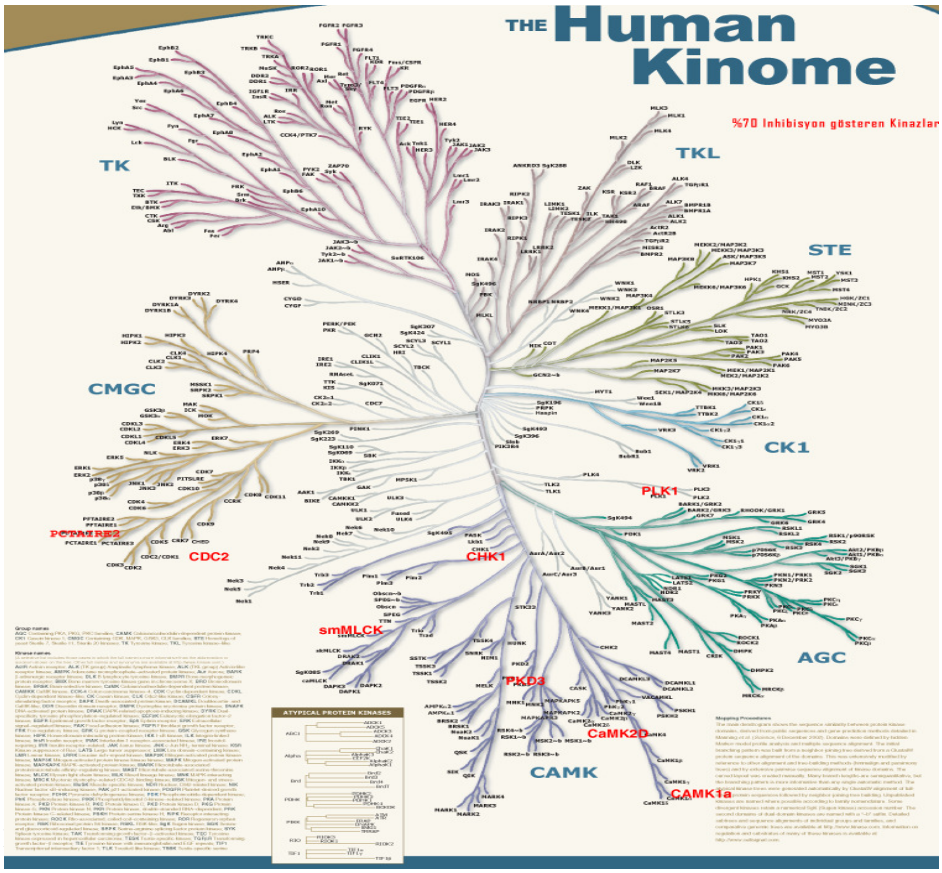

4.3.3 Development of *in vivo* screening method

In order to validate the effect of knockdowns of kinases and phosphatases we developed xenograft models using Huh7 cell line. $10x10^{7}$ cells were injected on the back of the nude mice and after xenograft models are obtained, using Alexa-RAFT-RGD and Alexa Transferrin dyes targeting only tumor cells, we tried to image implanted tumor cells using fluorescent imagers. Although we obtained images of xenograft tumors under white light both imaging and targeting methods were negative (figure 4.3.4.A) Since Alexa labelled RAFT-RGD molecules are targeting αV-β3 integrin molecules on the membrane surface of Huh7 cells, it seems that these cells are negative for this type of receptor. These results also showed that Huh7 cells are transferrin receptor negative as well (figure 4.3.4.B). All the Alexa RAFT-RGD dyes are observed in kidneys if the animal rather than the tumor as observed in the pictures. Positive control cells of TSA cell line were imaged nicely (figure 4.3.4.C)

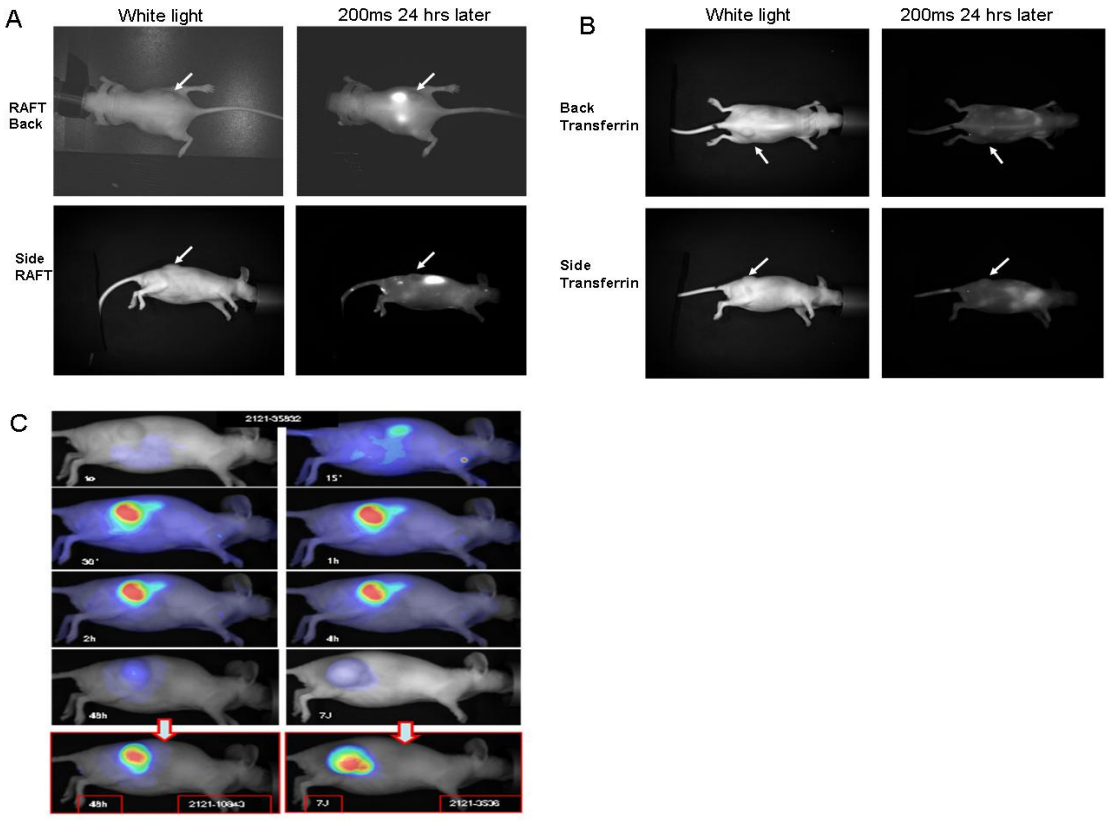

Figure 4.3.4 in vivo imaging of Alexa-RAFT RGD targeted Huh7 xenograft tumors in A. in vivo imaging of Alexa-transferrin targeted Huh7 xenograft tumors in B. Positive control cells (TSA cells) imaged with RAFT molecule in C.

4.4 Epigenetic targets in liver cancer

In order to identify novel epigenetic marks associated with immortality and senescence, we have characterized the histone methylation patterns *in vitro* and *in vivo*. We analyzed isogenic senescent and immortal HCC cells, as well as cirrhosis and HCC tissues. (Bagislar S. & Yuzugullu H. unpublished data). To test this hypothesis, we performed immunoblotting and immunostaining of each histone methylation pattern. Immunoblotting results in vitro and in vivo are already discussed in the PhD dissertation of Sevgi Bagislar (Bagislar, 2010). To confirm the results using a second *in vitro* method, we have stained isolated normal hepatocytes, immortal Huh7 cells and as a senescence model, we have treated Huh7 cells 3 days with low dose Doxorubucin (50 ng/mL). We showed that senescence is induced more than 90% for both Huh7 cells and HepG2 with 3 days and persisted up to 6 days (figure 4.4.1)(Gursoy-Yuzugullu et al unpublished data).

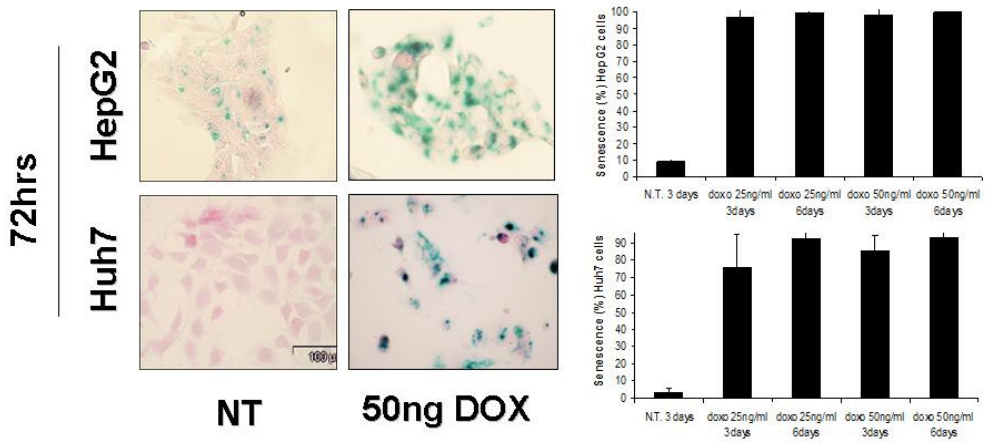

Figure 4.4.1 SABG staining of HepG2 and Huh-7 cells and the rate of SABG-positive cells reached as high as %90 percent after LD DOX treatment for 3 days and persisted up to day 6 as well.

Immunoblotting with H3K4Me1 showed that both normal hepatocytes and Huh7 cells and senescent cells were homogenously weak positive, and for H3K4Me3 remained strong positive for all cell types (figure 4.4.2.A top). For H3K9me1 and H3K9me3, cells were stained strongly positive. These residues were also found to be all same for all the conditions tested. For H3K27 residues, normal hepatocytes were stained strong positive for mono and tri methyl antibodies and a weak staining of dimethyl K27. Doxorubucin treated Huh7 cells and immortal cells for all

methylation status of H3K27 were same. Dimethylation of H3K27 is found to be increased in Huh7 with respect to normal hepatocytes (figure 4.4.2.A bottom). Mono and trimethylation of H3K36 was strong for normal hepatocytes and remained the same for Huh7 immortal and senescence conditions, with a low staining pattern for monomethyl H3K36 in normal hepatocytes and a strong positivity for immortal huh7 cells (figure 4.4.2.B top).

Only H4K20me3 is strong positive for normal hepatocytes, with monomethylation negative and dimethylation heterogenous positive. Monomethylation of H4K20 in Huh7 cells and senescence condition was scattered but strong positive. As confirmed here, H4K20me3 is decreased in Huh7 cells and became strong positive in Huh7 senescence conditions (figure 4.4.2.B bottom).

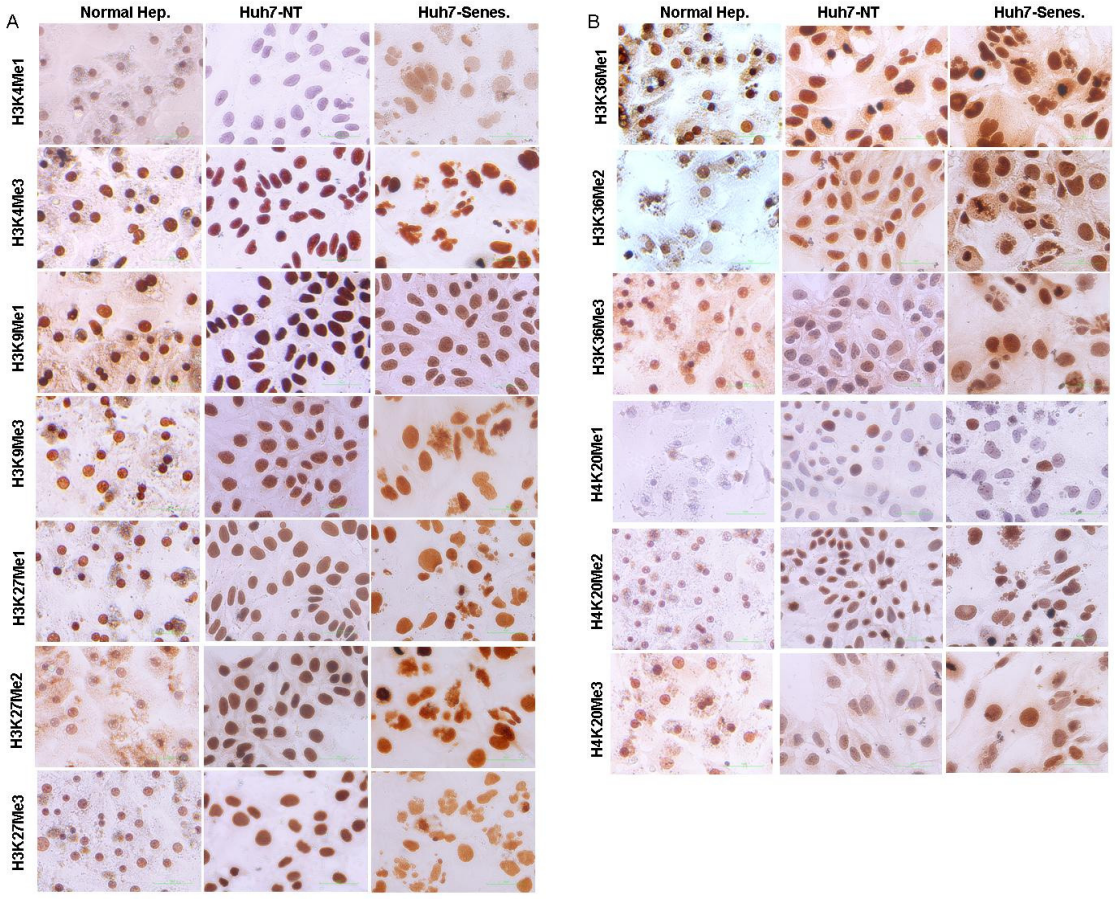

Figure 4.4.2 Immunostaining of Normal hepatocytes, Huh7 and LD-Doxorubucin treated Huh7 cells with methylation specific histone lysine antibodies.

For arginine residues of three conditions, H3R2Me2, H3R17Me2 and H4R3Me2 remained unchanged with a strong nuclear positivity.

Lastly we also checked Pan Acetyl staining of H4 and H4K5Acetylation in the three cell types. We found that all three conditions H4Pan Acetyl levels and H4K5Acetylation were strong positive and remained unchanged.

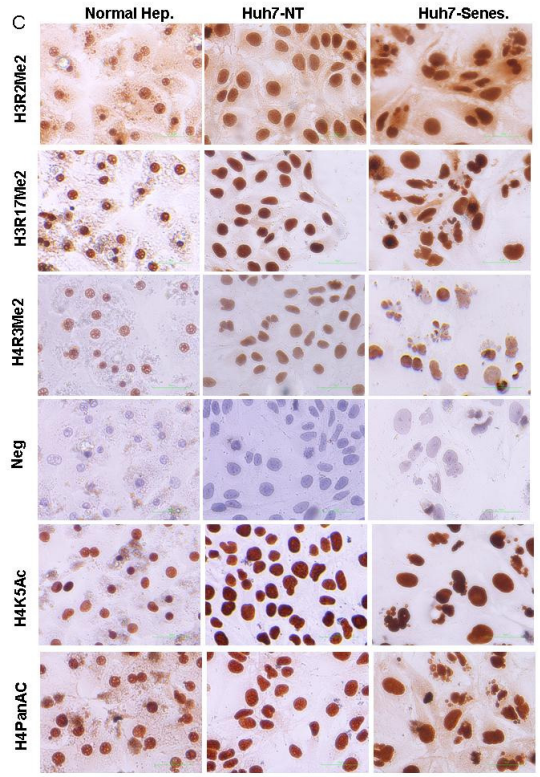

Figure 4.4.2.C Immunostaining of Normal hepatocytes, Huh7 and LD-Doxorubucin treated Huh7 cells with arginine methylation and acetylation specific histone antibodies.

4.4.1 Immunostaining of Histone modifying Enzymes in normal hepatocytes and immortal Huh7 cells and DNA damage induced senescence model

After we have the levels of methylation of each histone mark in vitro, using the same conditions and models we also stained the histone modifying enzymes that we previously identified from differentially expressed gene list (unpublished data). These enzymes might be responsible for the decrease of global histone methylation in HCC. We stained EZH2 HMT enzyme acting on H3K27Me residue and it is clear from the staining that this enzyme is weakly expressed in normal hepatocytes and became strong positive in Huh7 cells and remained same in

our DNA damage senescence model (figure 4.4.3 top). We stained three enzymes acting on H3K36 residue, one demetylase FBXL11 and two histone methyltransferase SetD2 and WHSC1. Among these FBXL11 is studied extensively in this thesis. FBXL11 remained strong positive for the three

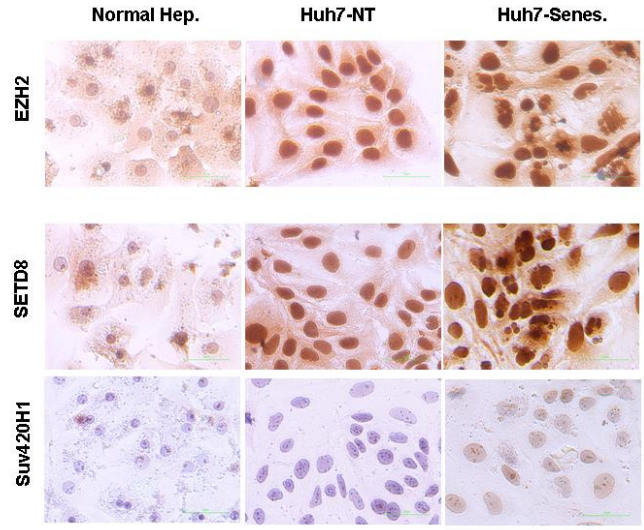

Figure 4.4.3 Immunostaining of normal hepatocytes, Huh7 and LD-Doxorubucin treated Huh7 cells with EZH2, SETD8 and Suv420H1 enzyme antibodies.

Conditions (figure 4.4.4 bottom). SetD2 a histone methyltransferase is stained weakly nuclear and some cytoplasmic staining in normal hepatocytes and correlating with H3K36me3 staining it is strongly positive in nucleus of huh7 cells and remained the same in senescence model as well (figure 4.4.4.top). Very interestingly WHSC1 gene a methyl transferase is negatively stained in normal hepatocytes and became very strongly nuclear positive for huh7 cells and remained strong in its senescence model (figure 4.4.4 middle).

For the H4K20 methylation, we checked the status of two histone methyltransferase one SETD8 and the other our home made antibody Suv420H1 (0032). For SetD8, we obtained weak positivity in normal hepatocytes and a strong staining in Huh7 cells and senescence model, confirmed the increase in positivity of H4K20Me2 in huh7 and senescence cells. Lastly Suv420H1 enzyme is found negative for all the conditions tested.

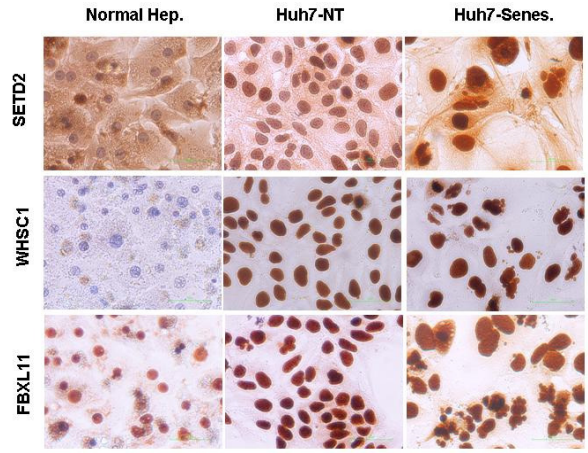

Figure 4.4.4 Immunostaining of normal hepatocytes, Huh7 and LD-Doxorubucin treated Huh7 cells with SETD2, WHSC1 and FBXL11 enzyme antibodies.

4.4.2 Histones are hypomethylated in HCC compared to cirrhosis and normal hepatocytes in vivo

To check the in vivo relevance of these in vitro findings, we performed immunohistochemistry analysis with the antibodies of residues which were validated to be altered in-vitro using immunostaining and western blotting. We have collaborated with Dr. Funda Yılmaz in Ege University Department of Pathology for the staining of selected histone residues. She performed staining of formalin fixed paraffin-embedded normal liver, cirrhosis, and HCC tissue samples with H3K27me3, H4K20me3, H3K36me3, H3R17me2a, H4R3me2a residues. (Bağışlar and Yuzugullu et al., unpublished data).

These data were also stated in the PhD dissertation of Dr. Sevgi Bagislar (Bagislar, 2010). During this part of my thesis, we performed many experiments together with her and in order to keep the unity, harmony and to keep the integrity of this part, I included the in vivo data as follows:

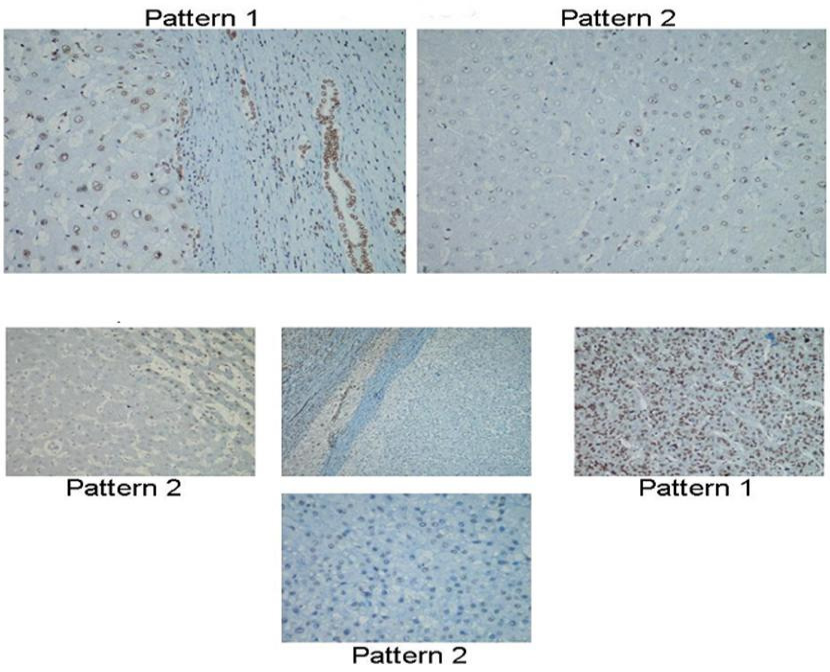

Figure 4.4.5 Histone methylation in in-vivo Images of Pattern 1 and 2 staining. Homogenously and strongly stained areas were named as "Pattern 1", on the other hand heterogeneous and weak staining, partial or local loss of nuclear positivity was called "Pattern 2". Top, and middle panel images were examples of H3K36me3 staining, bottom panel from H3R17me2a straining.

All normal livers stained showed a homogenous and ubiquitous nuclear positivity pattern in 10 samples. This kind of staining pattern will be named as pattern 1 (Figure 4.4.5). Local or dispersed loss of nuclear positivity in a heterogeneous fashion (pattern 2) is obtained for all (n=10) HCCs for all residues, and in cirrhosis for H4K20me3 and H3R17me2 (Figure 4.4.5). A significant decrease in macro regenerative nodules but not with micro-regenerative nodules was obtained for H3K36me3 and H3R17me2 residues. Loss of trimethylation of H3K27 residue was 10% for cirrhotic samples (n=13) with a corresponding significantly higher decrease reaching to 33% of HCC (n=10) was observed (Figure 4.4.6). Ubiquitous and homogeneous H4K20me3 nuclear staining in normal livers decreased 33% for cirrhotic samples, and decreased more prominently, 75%, for HCC. The same decrease was observed with trimethylation of H3K36me3. H3K36Me3 staining decreased 33% for HCC samples. Partial loss was observed in 25% and 66% of cirrhosis and HCC samples, respectively. For H4R3me2a, staining decreased 12% for cirrhotic samples and 66% for HCC samples. These global hypomethylation of H3K27me3, H4K20me3, H3K36me3 and H4R3me2a in HCC positively correlated with in-vitro stainings performed with

immortal and senescent Huh7 clones. These residues may be involved in aberrant misregulation of oncogenes and tumor suppressors in HCC.

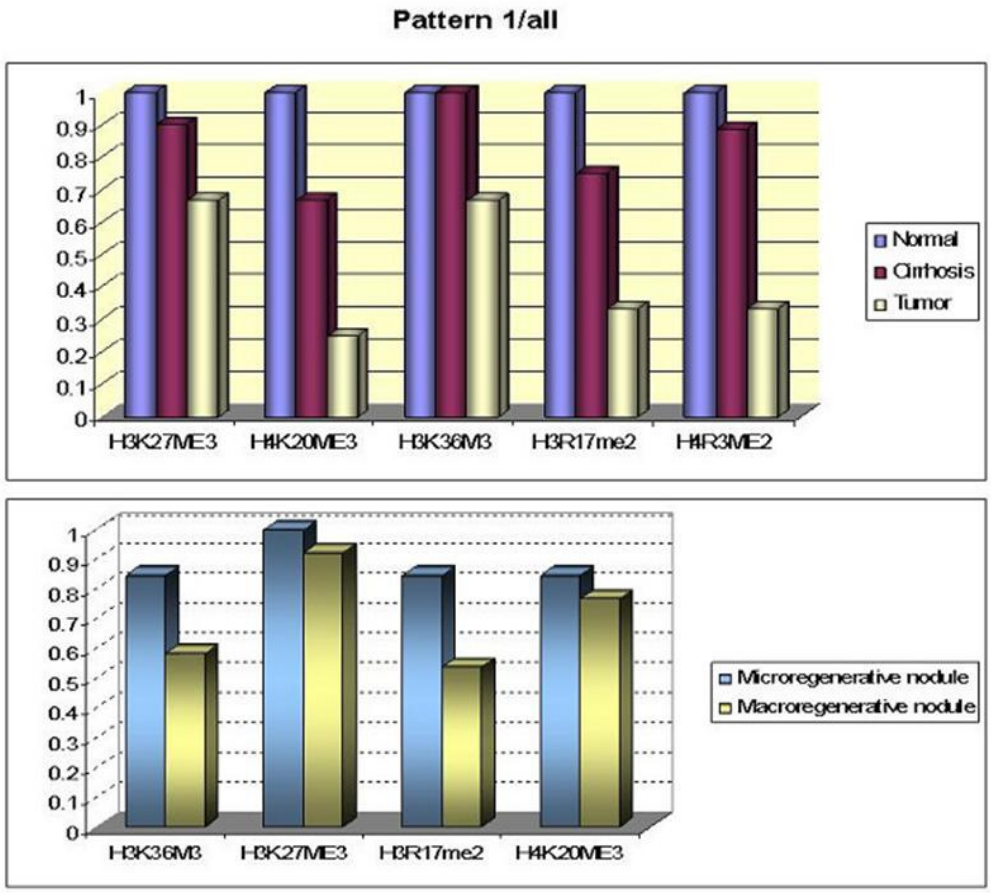

Figure 4.4.6 Bar-chart representations of the results of immunohistochemistry counts of indicated histone residues. Y-axis values were calculated by dividing the number of pattern 1tissue samples to number of all tissue samples for a given histone residue and tissue type. A partial loss of the 5 residues tested in HCC samples was observed. Bottom chart represents the same counts comparing macro- and micro-regenerative nodules. H3K36me3 and H3R17me2a residues were observed to loss ubiquitous staining pattern in macro-regenerative nodules compared to micro-regenerative nodules.

4.4.3 Validation and targeting of histone modifying enzymes responsible for aberrant histone codes

To search for these aberrant histone modifying enzymes playing a role during hepatocarcinogenesis, we have selected 5 enzymes acting on these validated methylated residues and further characterized their role in HCC.

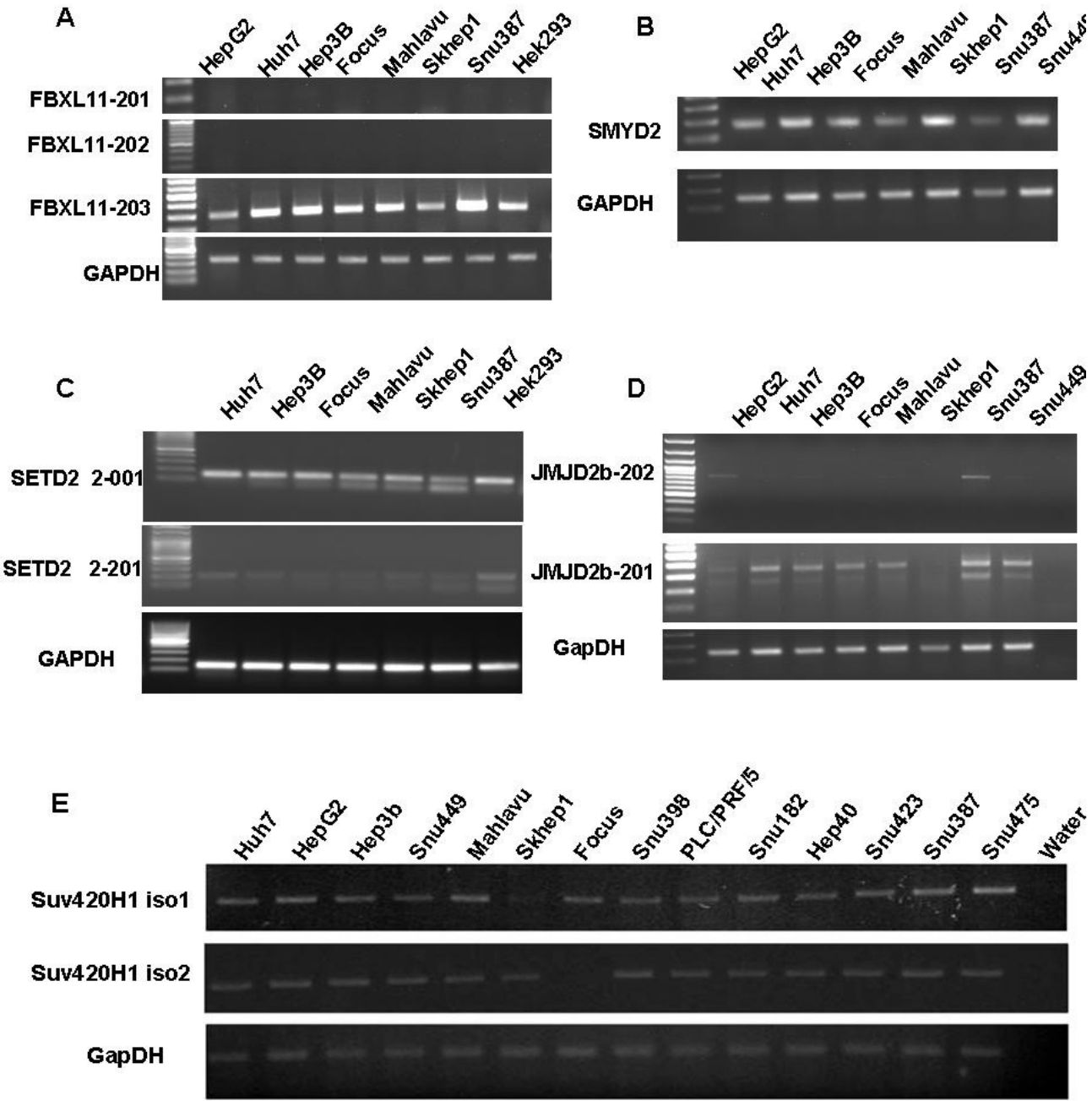

Figure 4.4.7 RT-PCR analysis of histone modifying enzymes in HCC cell lines. A) FBXL11 isoforms B.) SMYD2 gene C.) SETD2 gene isoforms and D.) JMJD2b isoforms.

We selected enzymes acting on H3K9, H3K27, H3K36 and H4K20 residues. JHDM1a/FBXL11 and JMJD2b demetylase enzymes works on H3K36 residues, JMJD3

demetylase work on H3K27 residue and SETD2 and SMYD2 histone methyltransferases work on H3K36 residues and Suv420H1 histone methyl transferase enzyme works on H4K20 residue. We first checked the isoforms of each enzyme using databases and their expression levels in HCC cell lines using semi quantitative RT-PCR. We ordered specific primers to each isoforms of enzymes using different sequences and skipping introns as well. As shown in figure 4.4.7.A, we showed that FBXL11 demetylase enzyme isoform 203 is ubiquitiously expressed in all HCC cell lines tested, whereas isoform 201 and 202 do not exist. Another histone methyltransferase SMYD2 gene acting on the same residue with a single isoform is also ubiquitously expressed in HCC cell lines (figure 4.4.7.B). SetD2 histone methyltransferase also acting on H3K36Me residue have also two isoforms and isoform number 2-001 is also highly expressed in these cell lines tested (figure 4.4.7. C). JMJD2b enzyme acting on H3K9 and H3K27 with an isoform number 201 is highly expressed in 6 of 8 HCC cell lines tested (figure 4.4.7.D). Lastly, H4K20 methyltransferase Suv420H1 has two isoforms and both isoforms are homogenously expressed in 13 out of 14 HCC cell lines (figure 4.4.7.E).

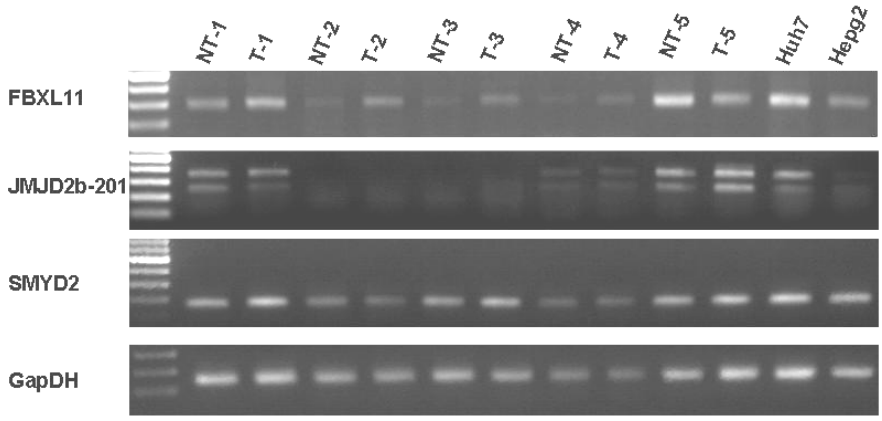

Figure 4.4.8 RT-PCR analysis of histone modifying enzymes in tumor and non-tumor pairs. FBXL11 isoforms SMYD2 gene and JMJD2 is shown. (NT: normal tissue, T: tumor sample)

Further characterization of these selected enzymes, have a role in tumorigenesis process, we also checked their expression status in tumor and non tumor samples using semi quantitative RT-PCR method (figure 4.4.8). We selected FBXL11, JMJD2b and SMYD2 enzymes in the first place. Among these three residues FBXL11 enzyme is shown to be upregulated in 4 out 5 tumor samples with respect to non-tumor pairs. SMYD2 enzyme is found to be slightly increased in two

tumor samples with a homogenous expression in all the samples. JMJD2b is also positive in 3 samples with no change between tumor and non tumor pairs. After confirmation to further characterize their roles in HCC, we selected minimum 2 shRNA lentiviral vectors to perform knockdown studies of these enzymes in HCC and screened all the enzymes listed above.

Using two different shRNAmir expressing lentiviral vectors to knockdown the target enzymes; we covered nearly all the residues we validated. We also used one lentiviral vector targeting GapDH, two control lentiviral vectors targeting non-eukaryotic sequences and scrambled sequences. Bicistronic expression of GFP protein together with shRNA targeting each ezyme allowed us to follow the efficiency and effect of knockdown. We infected HepG2 cell line because of the fact that this cell line has a functional p53 and RB signaling pathway and Huh7 cell line because we have the preliminary results of aberrant activation of these enzymes in this cell line (Bagislar et al, unpublished data). We infected the cells in 24 well plates in duplicates so that with one copy of each infection we screened phenotypic changes like apoptosis, growth arrest and senescence. The other copy of the infected cells were subjected to puromycin selection for 5 days till all the cells died in the control non-infected wells and we obtained stable clones of each infection. We ensured that infection was not toxic to cells using light microscopy.

4.4.4 Validation of Knock-down of enzymes in HCC cells

To ensure that we have successfully targeted HCC cells with shRNA constructs, we selected FBXL11 enzyme and further characterized because of easy access of Antibodies against FBXL11 and its aberrant upregulation in tumor cells. First we showed that our antibody is working, using immunoblotting of RIPA extracted total lysates of HCC cell lines, we confirmed the expression of FBXL11 enzyme in cell lines tested (figure 4.4.9.A). We showed that all cell lines expressed FBXL11 and there is not much difference between immortal Huh7 cell line and its isogenic early senescent and senescent clones.

Using two cell lines, Huh7 and HepG2 cell line, we took the infected cells and took pictures of shRNAs targeting all the cells using DAPI staining and GFP color (figure 4.4.10.B). We isolated nuclear extracts and confirmed that FBXL11 is knocked down. We showed that FBXL11 is decreased significantly but not completely in huh7 and hepG2 cells (figure 4.4.10.C). Among the three shRNAs targeting FBXL11-sh35 was the most efficiently working lentivirus. We also find its role in liver cancer cells using H3K36 mono, di and tri methyl specific

antibodies. We showed that H3K36 trimethyl is slightly increased in all shRNAs targeting FBXL11 but not with shRNA control. We did not observe change in the corresponding dimethyl and monomethyl residues.

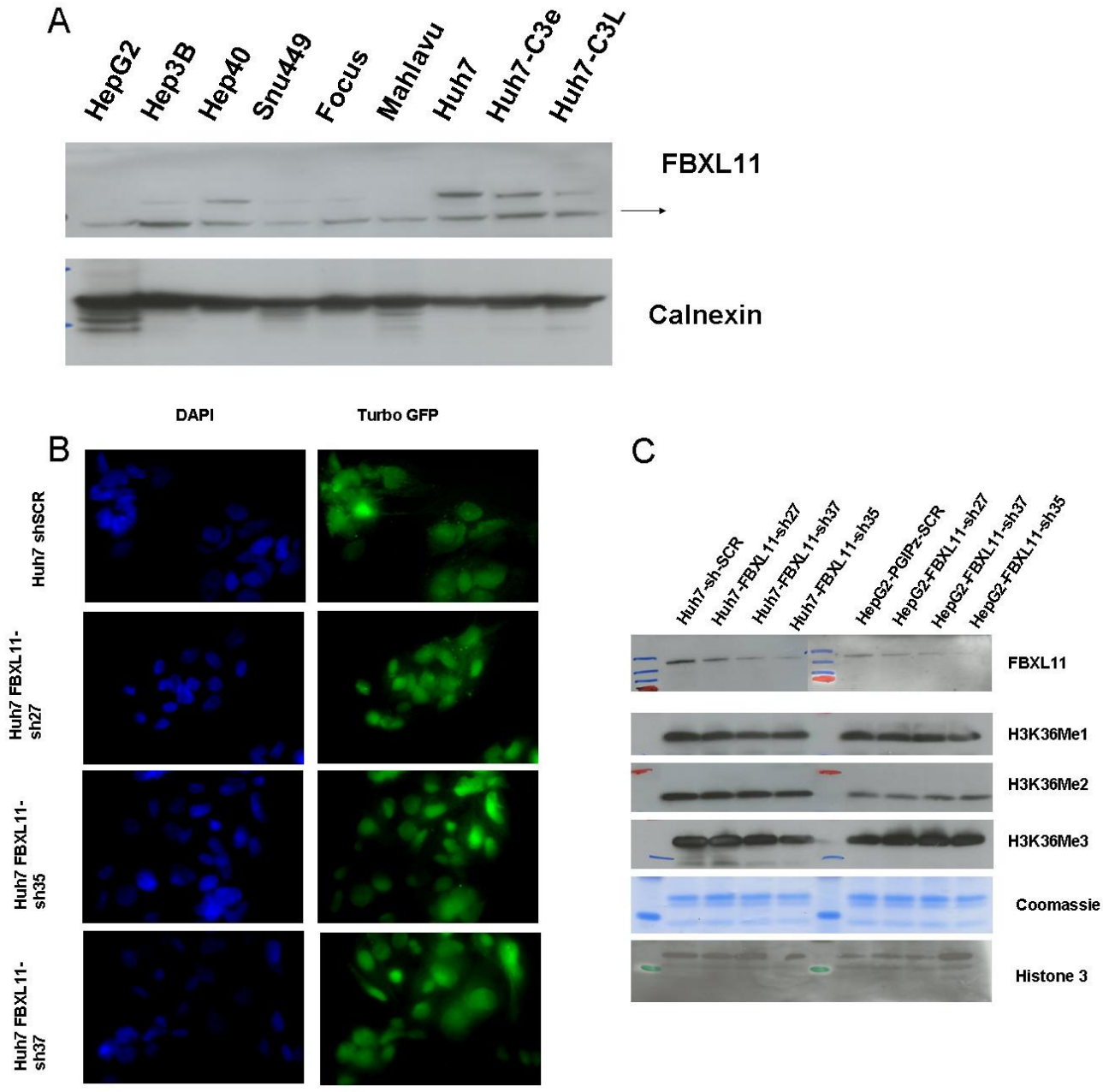

Figure 4.4.9 FBXL11 knockdown in HepG2 and Huh7 cell lines. A. expression status of FBXL11 enzyme in cell lines B. GFP expressing shRNAmir targeting FBZL11 in infected Huh7 cells, C. Knockdown of FBXL11 as shown by FBXL11 antibody (sh-SCR stands for scrambled shRNA).

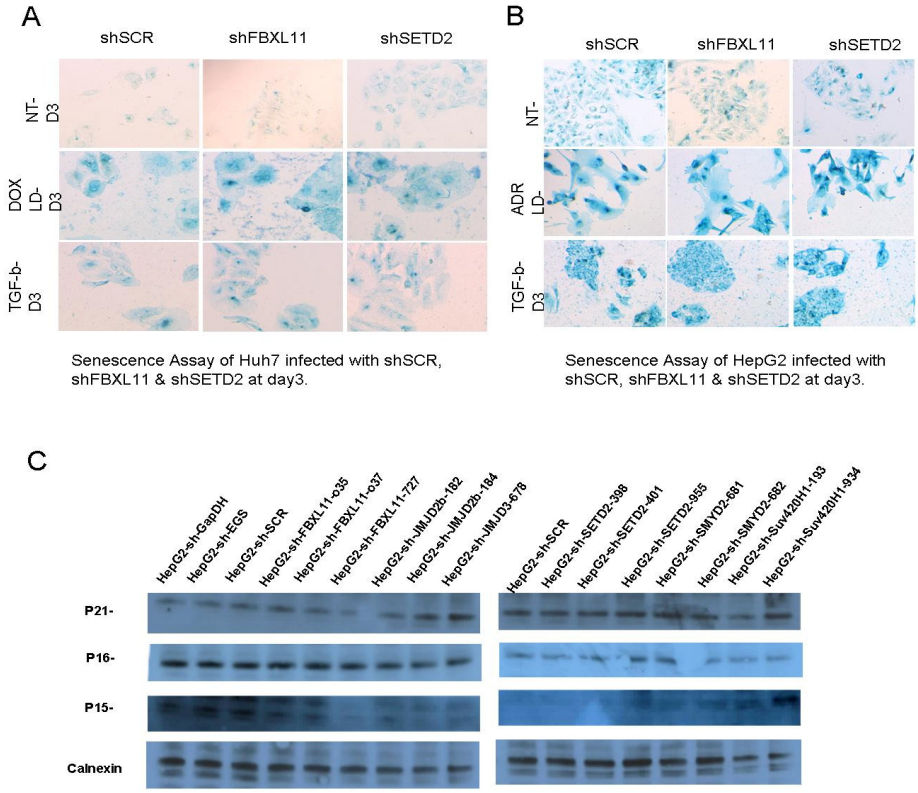

Figure 4.4.10 Knockdown of enzymes failed to induce apoptosis and induce tumor suppressors, A. Knockdown of SetD2 enzyme in Huh7 cells and HepG2 cells (B) failed to induce senescence and failed to induce tumor suppressors (C)

4.4.5 Knockdown of enzymes failed to induce apoptosis, senescence and inhibition of growth of cells

Short term (3 days) and long term (7 days) light microscopy observations, together with SA-beta galactosidase staining showed that neither of the cell lines showed significant change in growth characteristics and cell phenotypes of cells with respect to control cells infected with either shRNA targeting GapDH or scrambled vectors. We asked the response of these cells to DNA damage induced and TGF-beta induced senescence responses. We treated cells with Low dose Doxorubucin and TGF-beta treatment for 3 days and checked their senescence responses. Results showed that knock-down of enzymes did not make significant change in their response to DNA damage induced senescence (figure 4.4.10 A and B).

4.4.6 Knockdown of enzymes failed to affect main p53 and Rb pathways

Form all the infections of HepG2 cells, we extracted total protein lysates and checked whether the knockdown of these enzymes caused any change on major tumor suppressors like p21(Cip1), p16(Ink4a) and p15(Ink4b) were up-regulated (figure 4.4.10.C). We failed to observe any significant upregulation of all proteins confirming the result of the phenotypic observations and SA-beta-galactosidase results. This may be explained by the redundancy of histone methyltransferase and demethylase enzymes working in the same residue. For instance FBXL11, FBXL10 and JMJD2a and JMJD2c enzymes are demethylases working on H3K36 residue and methyltransferases NSD1, SETD2 and SMYD2 are also acting on the same residue.

4.4.7 Role of Histone 4 K20 methylation and Suv420H1 enzyme in liver cancer

We and others showed that there is a global loss of histone4K20 methylation in liver cancer [207] . We also isolated cells from 12 tumor and 12 cirrhotic livers and performed H4K20 trimethyl western. Results showed that generally non tumor samples have high levels of trimethyl H4K20 with respect to HCC cells (figure 4.4.11.A).

To understand the hypomethylation of histone 4 Lysine 20 residue in HCC cells, we checked the mono, di and tri methylation of HCC cell lines using immunoblotting (figure4.4.11 B). To search for the enzyme responsible for this, we also checked the mRNA levels of Suv420H1 enzyme in these cell lines using quantitative RT-PCR (figure 4.4.11.C). We found a positive correlation of mRNA levels of the suv420H1 enzyme and H4K20 trimethyl levels. For instance Huh7 and Snu475 cell lines expressed the high levels of Suv40H1 enzymes on the other hand Snu398 and Snu423 cell lines showed the lowest levels of H4K20Me3 and Suv40H1 transcripts. We saw that H4K20Me2 is ubiquitously expressed and monomethyl K20 is almost negative except Snu398 cells (figure4.4.11 B).

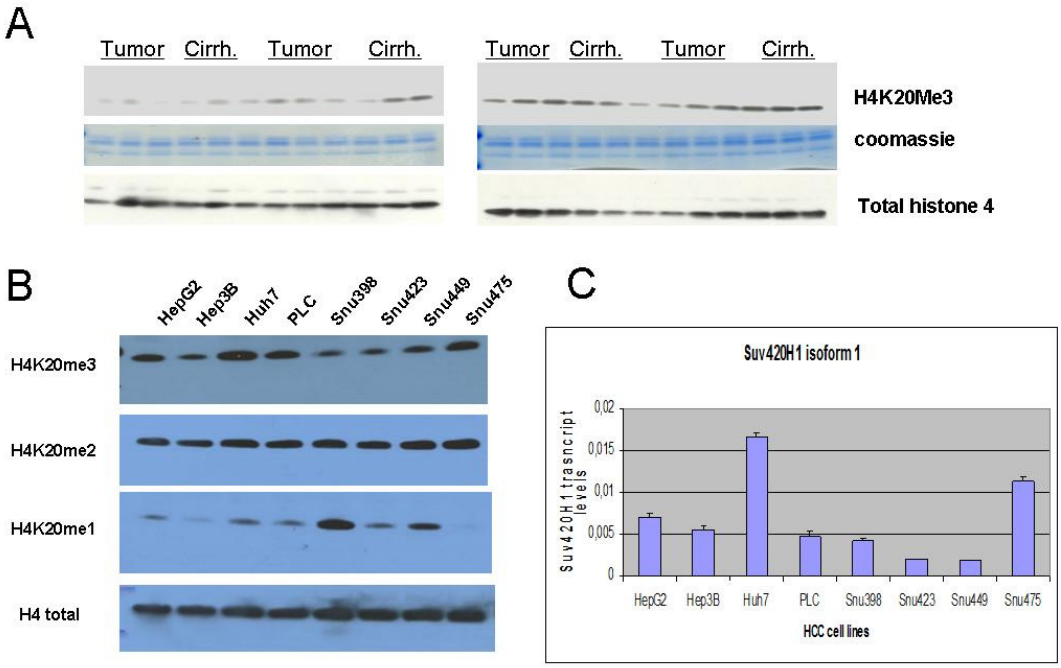

Figure 4.4.11 H4K20 methylation in HCC cells and tumor and non-tumor pairs, A. H4K20Me3 status in tumor and non-tumor samples (B) H4K20 mono, di and trimethylation status in HCC cell lines (C) Suv420H1 enzyme responsible for trimethylation of H4K20Me3.

4.4.8 H4K20 trimethylation is upregulated in replicative senescence and DNA Damage induced senescence models

To further understand the role of loss of trimethylation of Histone 4 K20, we checked the levels of H4K20Me3 in isogenic immortal and senescent clones of Huh7 and MRC5 cell lines.

Both early senescencent and senescent clones of Huh7 and MRC5 increased the levels of H4K20Me3 as shown by immunostaining (figure 4.4.12 A and B). We also took HepG2 cells and Huh7 cells, used DNA damage induced senescence assay to check the levels of H4K20Methylation. Immunofluorescence, western blotting, immunostaining and SA-beta gal results were used to check the levels of methylation. After LD doxorubucin treatment for 3 days, we induced senescence using LD-DOX in HepG2 and Huh7 cells and costaining showed that 4K20Me3 levels increased after treatment with a corresponding decrease in H4K20Me1 but not with H4K20Me2 residues. Immunoflurescence data confirmed these results as well.
(figure 4.4.13 A and C).

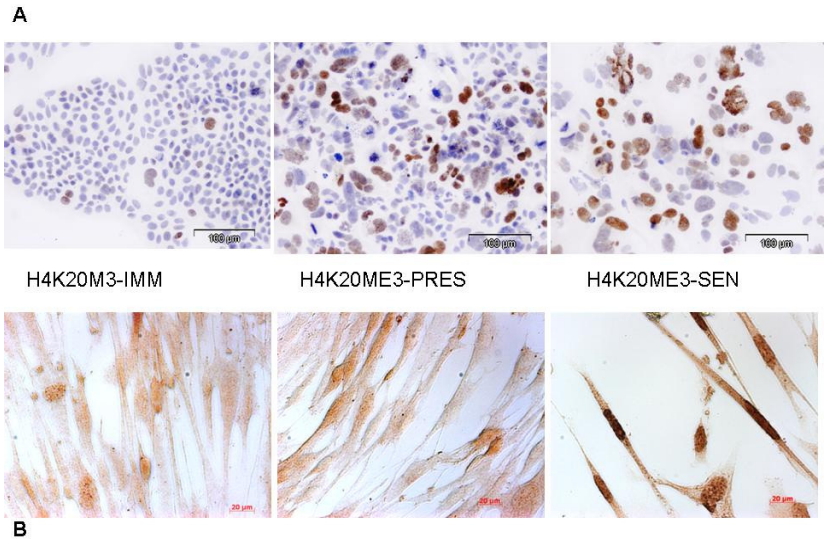

Figure 4.4.12 H4K20Me3 levels in Huh7 cells and MRC5 cell lines A. immortal, early senescencent and senescent clones of Huh7 cells B. In immortal, early senescencent and senescent clones of MRC5 cells.

To find the enzyme responsible for the increase of H4K20Me3 upregulation in normal cells and after Doxorubucin induced DNA damage models we checked the expression status of Suv420H1 using quantitative Real-time PCR. We took 8 cell lines and Low dose Doxorubucin is used to treat these cells for 3 days. And figure 4.4.13.D showed that 6 out of 8 cell lines tested Suv420H1 enzyme transcripts are increased. We confirmed this using immunostaining of Suv420H1 using a home made antibody, as shown in figure 4.4.3 bottom panel there is a slight increase in Suv420H1 levels in Huh7 cells treated with LD-Doxorubucin.

4.4.9 Suv420H1 enzyme is the responsible enzyme for trimethylation of H4K20

At that time, there were no working suv420H1 antibody (till we ordered an antibody from a company) so we continued characterizing the role of Suv420H1 in HCC using Mouse GFP tagged Suv420H1 expressing vector. We used Huh7 cell line to transiently overexpress mouse form of Suv420H1 enzyme, since this enzyme is fused to GFP tag, we could follow the transfected cells as well. As a control we used one GFP expressing vector, and a GFP fused

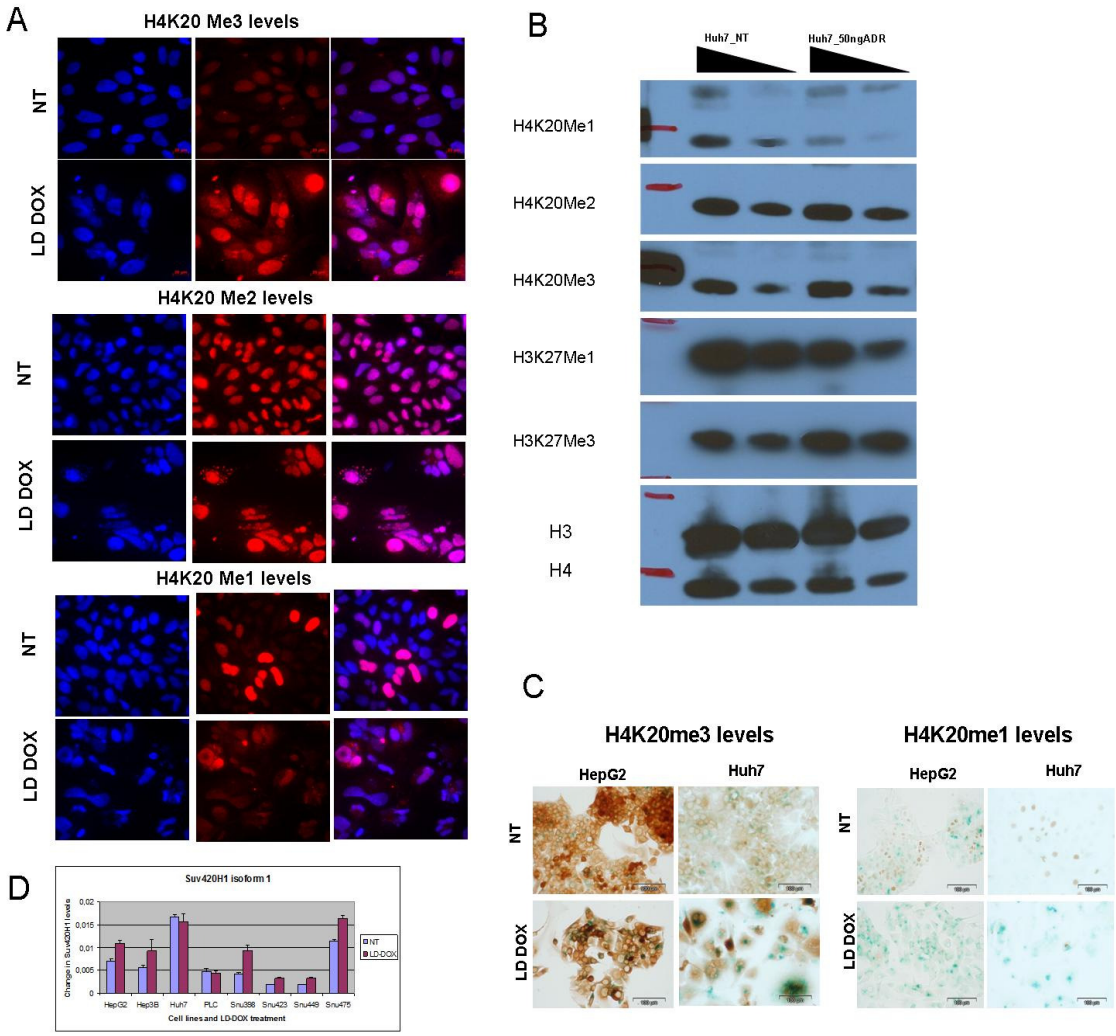

Figure 4.4.13 H4K20 methylation status in Huh7 cells after LD-Dox treatment A. H4K20 methylation is increased after DNA Damage senescence models (A) and (C), or using immunoblotting results in (B) and Suv420H1 is responsible for this increase in liver cancer cells (D).

BRDT, is a non functional enyzme expressing vector. BRDT is an acetyl binding protein and this vector codes for a non-functional form of BRDT protein. After 48 hours of transient transfection, we used immunofluorescence to check the levels of H4K20Me1, H420Me3, and H3K4Me3 is also used as a control (Figure 4.4.14). Results showed that mouse Suv420H1 is capable of increasing H4K20Me3 and since basal levels of H4K20me1 is already low; it was difficult to see the compensating decrease. GFP and BRDT-GFP expressing cells did not show these phenotypes. H3K4Me3 levels remained unchanged (Figure 4.4.14).

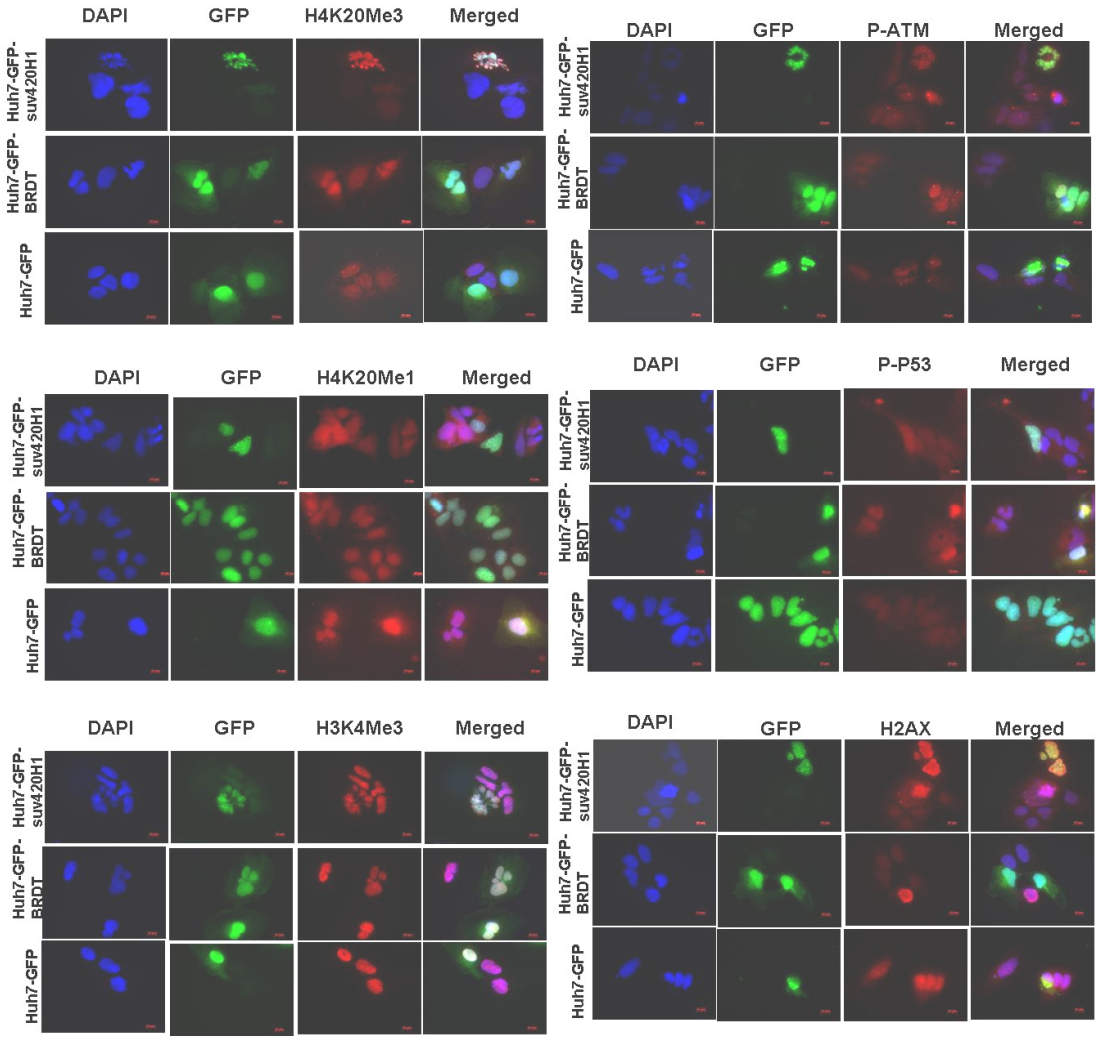

Figure 4.4.14 Effect of Suv420H1 overexpression in HCC cells

Phenotypic observations showed us that transfected cells became multinucleated and looked like mitotic catastrophe (Figure 4.4.14). These phenotypic changes were not observed with control vector transfected cells. Mitotic catastrophic cells occur due of the abnormal mitosis events. Cells cannot divide, generally look like multinucleated with abnormal shape of nuclei. So to test our hypothesis, we tried to make stable clones of Suv420H1. But unfortunately, we could not succeed this using HCC cell lines. We tried Huh7, HepG2 and Hep40 cell lines but we failed to get stable clones, although we could get colonies with GFP and BRDT-GFP vectors.

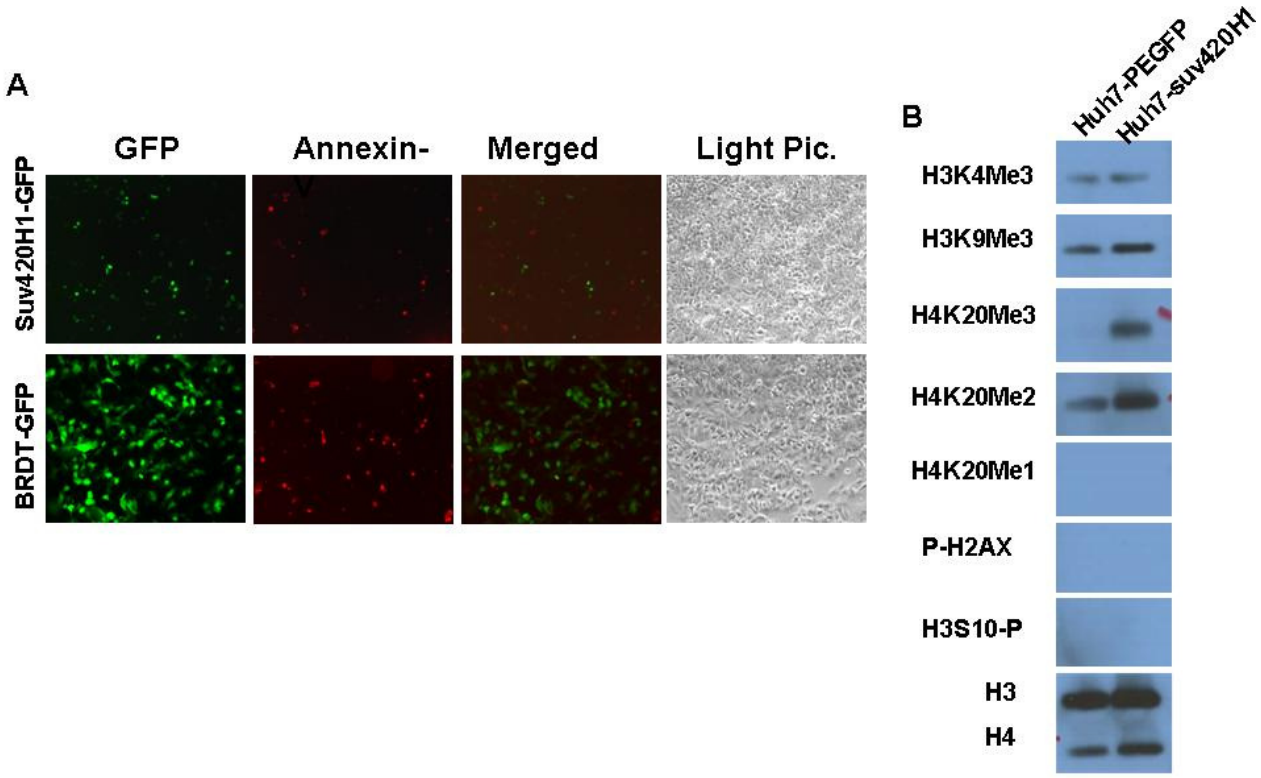

Figure 4.4.15 Suv420H1 did not induce apoptosis in HCC cells, A. Ectopic Suv420H1 overexpression did not induce apoptosis in Huh7 cells B. Histone methylation pattern after Suv420H1 overexpression.

We tested if these cells are apoptotic or senescent using Annexin-V staining and SA-Beta-gal subsequently (figure 4.4.15.A). We could not find a correlation of GFP positive and Annexin-V stained apoptotic cells. We also could not observe senescent cells in Suv420H1-GFP transfected cells (data not shown). Using the immunofluorescence, we also checked Damage markers like p-p53 Ser20, phospho-ATM and H2AX. Neither of these markers showed significantly positive results with neither Suv420H1-GFP or BRDT-GFP or only GFP transfected cells (Figure 4.4.14). We confirmed these finding using another technique. After 48 hours of transfection in Huh7 cells, we isolated histones and we checked H4K20Me3 and H4K20Me2 and H3K9Me3 and H3K4Me3 residues and also H2AX as a damage marker. Upon transfection we observed a strong increase in H4K20Me3 and H4K20Me2 residues. H3K4Me3 remained unchanged and we could not detect H2AX and H4K20Me1 (figure 4.4.15.B). To test mitotic catastrophe, we also checked H3S10-p, and we could not detect this protein either.

Thus we decided to change our model to non HCC cell line; we used hek293T cells for easy transfection. We obtained 4 stable clones for Suv420H1-GFP and 3 clones for GFP vector and 4 clones for BRDT-GFP vector. We did not observe unusual phenotype with any of these clones. We confirmed the function of ectopically expressed Suv420H1 enzyme as an increase in H4K20Me3 and a compensating decrease in H4K20Me1 and no change of H4K20Me2, and H3K9Me3 residues (figure 4.4.15.A).

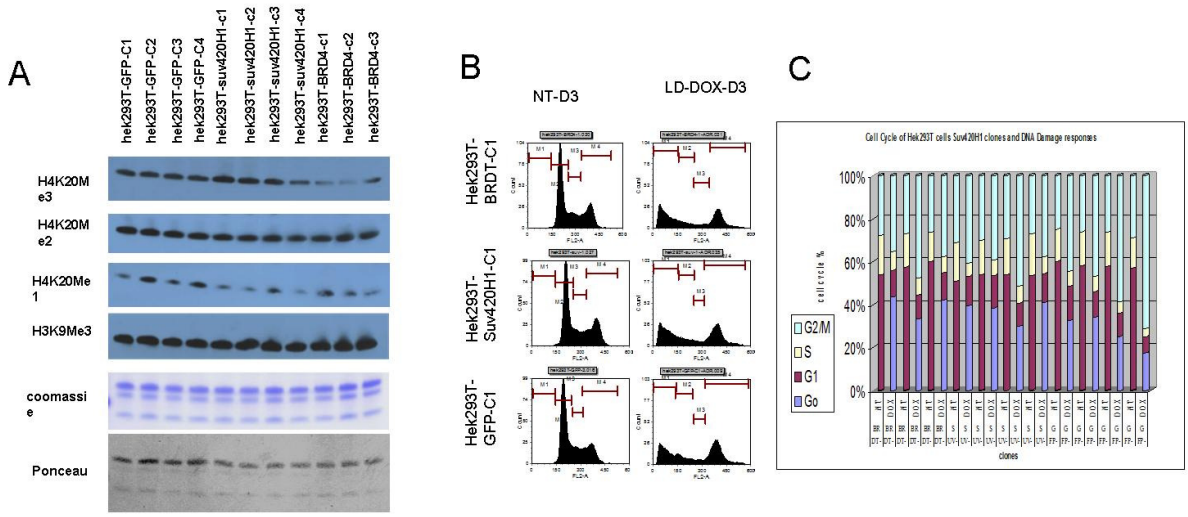

Figure 4.4.16 Effect of Suv420H1 ectopic expression in Hek293T cells and DNA damage response of cells did not change. A. Histone methylation status of suv420H1 overexpressing Hek293T stable clones and B. cell cycle response of these stable clones

4.4.10 Suv420H1 failed to change the DNA Damage response of cells to Doxorubucin treatment

We wanted to check whether Suv420H1 enyzme is involved in DNA damage response of cells. We already used Doxorubucin treatment to induce DNA damage, apoptosis and/or senescence. We treated Hek293T stable clones with doxorubucin for 3 days and using PI stain we checked cell cycle distribution in the presence or absence of Doxorubucin. As shown in figure 4.4.16.B as a representative cell cycle pattern in the absence or presence of Doxorubucin, the response of Suv420H1-GFP clones, GFP clones and BRDT-GFP clones did not change.

In order to study the endogenous and human Suv420H1, we ordered Rabbit polyclonal antibody to COVALAB Company in France. They made one polyclonal antibody and using the small isoform of human Suv420H1 enzyme expressing vector, we transiently transfected small isoform of Suv420H1 enzyme in hek293T cells. Immunoblotting both affinity purified and non purified westerns showed that we could detect the by using this antibody. Before and after immunopurification we performed western blotting and optimized the dilution of the human Suv420H1 antibody. As can be observed at figure 4.4.17 we can detect small isoform of human Suv420H1 protein.

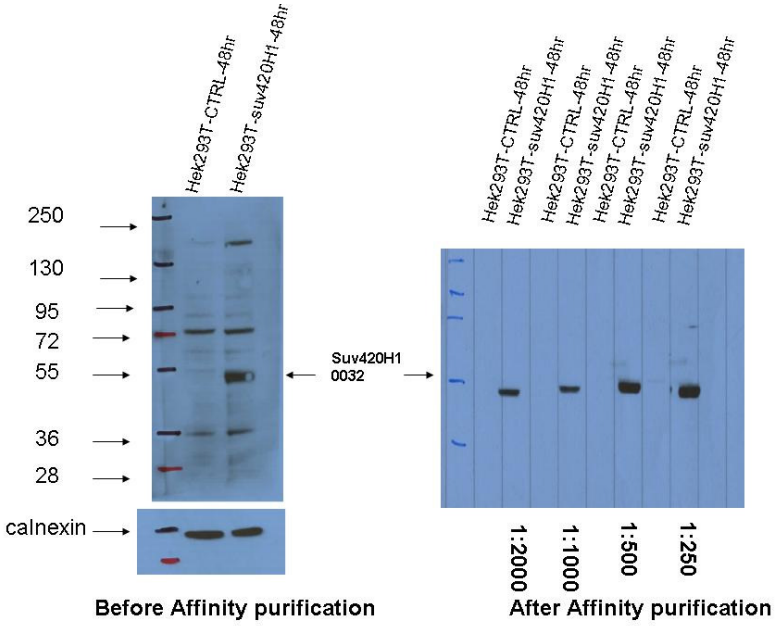

Figure 4.4.17 new polyclonal Suv420H1 antibody (suv0032) recognized ectopically expressed small isoform of human Suv420H1 protein.

4.4.11 Suv420H1 failed to regulate the imprinting of H19 gene inHCC cells

H19 is normally a maternally imprinted non-coding gene and expressed only during embryonal development. Although its expression is shut off in most tissues postnatally, it is reactivated during adult tissue regeneration and also observed in Wilms tumor, lung cancer as well. Moreover, H19 is highly expressed in liver and has been shown to behave like an oncogene for liver cancer and it is essential for tumor cell growth[118]. Imprinting is regulated by DNA methylation on Imprinting Control Regions (ICR). Recently it is found that DNA methylation at

these ICR are associated with of Histone methylation especially with H3K9 and H4K20 [208] It is found that liver cells at the imprinted allele highly associated with H4K20me3 for H19 gene. So we hypothesized that overexpression of H4K20Me3 via Suv420H1 enzyme could change biallelic expression of H19 to monoallelic expression and inhibit HCC cells growth.

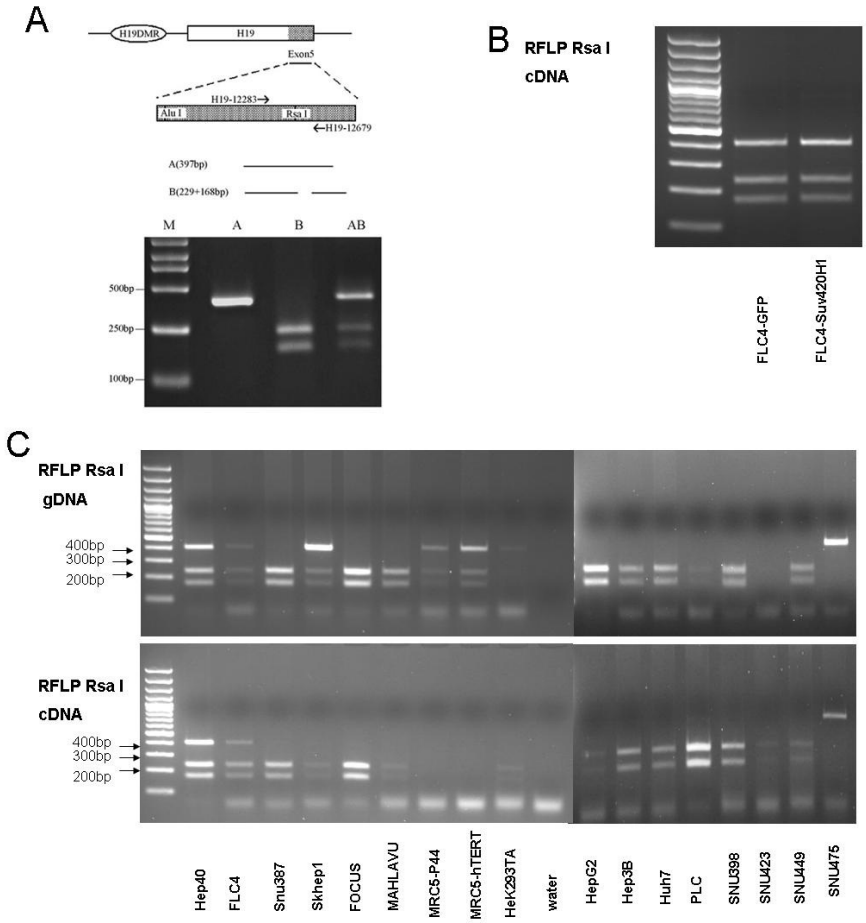

Figure 4.4.18 The polymorphism analysis in H19 gene exon 5 (RsaI at bp 12511); H19 bases are numbered as found in GenBank Accession No. AF125183 (gi: 4731323). IGF2-758, IGF2-993, H19-12283, and H19-12679 represent PCR primers for amplification of IGF2 and H19. (A)Predicted products for the A and B alleles of each polymorphism are drawn below the schematic. (C) Actual products of genotype analysis of HCC cell lines top. Actual products of cDNA RFLP in HCC cell lines showed monoallelic or biallelic expression of H19 gene. B. transient Suv420H1 overexpression did not change biallelic expression of H19 gene polymorphism.

To assess our hypothesis we characterized HCC cell lines for loss of imprinting for H19 gene using genomic and cDNA RFLP. The polymorphism was analyzed in H19 exon5 (RsaI at bp 12511). Non-imprinted allele (397 bp) is cut into 229 bp and 168 bp (figure 4.4.18.A). The

PCR was performed both from genomic DNA of cell lines and cDNAs. After RsaI digestion and RFLP is load to gels. Among the tested 14 HCC cell lines, only FLC4 and Hep40 cell lines showed loss of imprinting. (figure 4.4.18. C). Therefore to test our hypothesis we tried to get stable clones of FLC4 and Hep40 cell line using Suv420H1-GFP plasmid. We could not obtain stable clones due to the problems mentioned above. We tried multiple (3X times) transient transfection of FLC4 cell lines with GFP expressing control vector and Suv420H1-GFP expression vector. We ensured that cells are all GFP positive under fluorescence microscope and isolated cDNA from these clones. We performed RFLP analysis using the same enzyme. We failed to change the allelic pattern of FLC4 cell line (figure 4.4.18.B).

4.5 Role of ATAD2 gene in Liver Cancer

4.5.1 Identification of ATAD2

By combining gene expression profiles performed in our lab using isogenic senescent and immortal HCC cells, as well as cirrhosis and HCC tissues, we identified ATAD2 gene, predicted to be overexpressed in liver cancer and associated with immortality related genes network (figure 4.5.1.A). Recently two groups showed that ATAD2 is highly expressed in several human solid tumors including lung, breast, and prostate and is a strong predictor of mortality in lung and breast cancers [184, 186]. ATAD2 is significantly amplified 2.4 fold in immortal huh7 cell line with respect to its senescent isogenic clone and also 4.2 fold in liver cancer with respect to cirrhotic samples (figure 4.5.1.B). ATAD2 gene is found in 8q24 chromosome region, a region frequently amplified and found near to MYC oncogene and is of 1,391 aminoacids long. In this locus ATAD2 is overexpressed together with other genes (figure 4.5.1.C). It has a conserved region of two AAA (ATPases Associated with diverse cellular Activities) domains [209] and a bromodomain for binding acetylated histones [210].

A

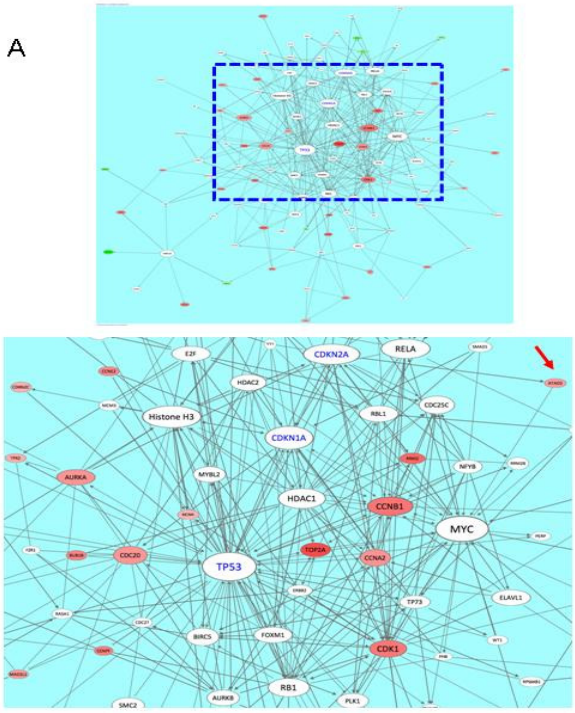

B

Gene	Function	Fold-Change (Imm./Sen. Huh7)	Fold-change (HCC/Cirrhosis)
EZH2	Polycomb-group (PcG) family member	3.5	2.8
MLF1IP	Centromere assembly	2.5	3.7
ATAD2	Bromodomain protein, unknown func.	2.4	4.2
FAM83D	Chromokinesis	2.1	5.7
CCNE2	Cell cycle G1/S transition	2.0	4.5
PUS7	PRNA isomerization	1.9	2.1
BUB3	Spindle-checkpoint	1.9	1.7
RRM2	Deoxyribonucleotide synthesis	1.8	4.6
ZNF251	Unknown	1.7	1.8
SMYD3	Histone methyltransferase	1.7	2.4
RMI1	Repression of DNA crossover	1.6	2.2
XPOT	Nuclear export of tRNA	1.6	1.8
SAC3D1	JAK/STAT pathway	1.5	2.4
IGFBP3	Plasmatic IGF-binding protein	-1.5	-4.0
CFTR	Chloride channel	-1.6	-7.6
GNA14	Alpha q G protein	-1.7	-2.5
FOS	Transcription factor	-2.0	-5.8
LIFR	LIF receptor	-2.3	-2.1
CYP39A1	Cholesterol -> bile acids.	-2.4	-7.6
MUM1L1	Unknown	-2.6	-3.5
GPR128	Unknown	-2.9	-4.5
NAT2	N-acetyltransferase	-3.3	-6.6
TACSTD1	Adhesion molecule, stem-cell marker	-3.9	-20.5
VIPR1	Vvasoactive intestinal peptide receptor	-4.0	-2.0
TFPI2	Protease inhibitor	-5.8	-5.0
FAM134B	Unknown	-6.6	-5.6
TMEM27	Amino acid transporter	-42.3	-10.5

S Bagislar, M. Ozturk et al.
(manuscript in preparation)

C

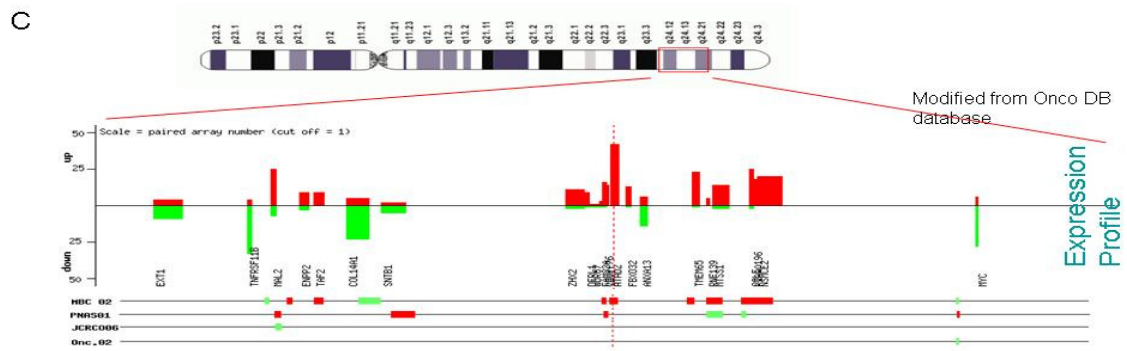

Figure 4.5.1 Identification of ATAD2, A. IPA analysis network showing ATAD2 in immortality related genes network, B. ATAD2 Fold change of differentially expressed genes including other histone related genes C. ATAD2 gene and overexpression status of ATAD2 in 8q24 gene locus near Myc oncogene.

4.5.2 ATAD2 is highly expressed in immortal HCC cells

Further searches in databases showed that ATAD2 gene is overexpressed at least two fold in 76% of paired HCC arrays [211] (Figure 4.5.1.C). We checked the levels of ATAD2 transcripts in liver cancer cell lines using quantitative RT-PCR. Normal liver was used to normalize the expression of ATAD2 gene; we also included human normal lung fibroblast cell

line to compare to see if ATAD2 is up in immortal cells. We showed that 9 out of 14 liver cancer cell lines showed more than 5 fold expression of ATAD2 whereas both normal human liver and lung cell line showed the least expression (figure 4.5.2.A). We performed immunoblot analysis of ATAD2 to determine the protein expression in HCC cells and normal human liver tissue. We showed that the ATAD2 protein was readily detectable in all HCC cells, with Huh7, Hep40, HepG2, Hep3B and FLC4 cells displaying the highest protein levels (Fig.4.5.2. B), and that the ATAD2 protein is undetectable in normal human liver tissue. We used Hep3b cells transfected with siRNA1 to show the specificity of ATAD2 antibody.

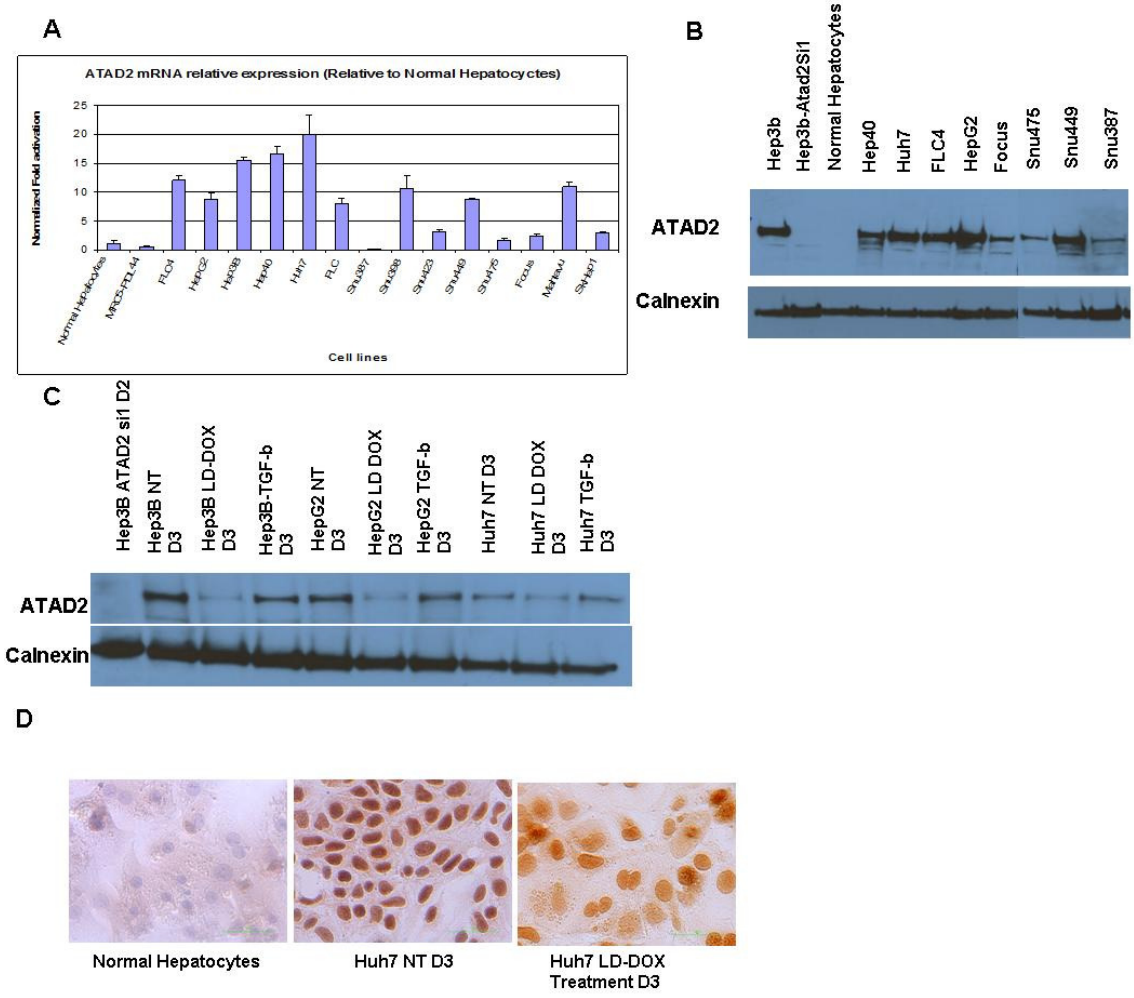

Figure 4.5.2 ATAD2 expression is up in HCC cells, A. relative mRNA levels using Q-PCR B. Immunoblotting of ATAD2 in HCC cell lines and C. ATAD2 protein levels in senescence models of HCC D. ATAD2 is stained strongly in HCC cells.

Very recently, we showed that TGF-β is a potential senescence inducer in HCC cells and low-dose Doxorubucin treatment of HCC cells also induces senescence (Senturk, Mumcuoglu et al. 2010)(Gursoy-Yuzugullu, unpublished data). Using these two models, we checked the expression status of ATAD2 protein in HCC cells using immunoblotting. Hep3b, HepG2 and Huh7 cells showed a significant decrease of ATAD2 protein expression upon low-dose Doxorubucin treatment and a slight decrease of in Hep3b cells was observed in TGF-b treated Hep3b cells (Figure 4.5.2.C). Both assays showed that ATAD2 is up in immortal HCC cells but not in normal cells. To confirm this finding, we performed immunostaining of normal hepatocytes and compared the levels of protein expression with Huh7 cells either in the absence or presence of LD-Doxorubucin. Correlated with Q-PCR and western data, isolated normal human hepatocytes were ATAD2 negative and Huh7 cells were strongly stained, and LD-Doxorubucin treatment decreased ATAD2 levels in Huh7 cells after 3 days (figure 4.5.2.D).

4.5.3 ATAD2 expression is associated with high grade and increased risk of lymph node invasion of tumor cells

To confirm the upregulation of ATAD2 in HCC in vivo, we checked ATAD2 expression in tumor and non-tumor pairs using both Quantitative RT-PCR and western blot techniques. Atad2 mRNA levels are higher in 5 out of 7 tumor tissues compared to non-tumor tissues (Figure 4.5.C). Western blot analysis also showed that expression of ATAD2 in normal liver is down regulated. 4 normal liver samples were tested and 3 of them did not express ATAD2 protein (figure 4.5.3 A and B). Of 15 tumor non-tumor pairs were tested, 8 pairs have higher expression of ATAD2 in tumors and 5 in cirrhotic samples. And 3 of the cases showed unchanged (figure 4.5.3. B). We also tested 24 separate cirrhotic samples and detected ATAD2 protein in 18 of the cases (figure 4.5.3.A). Thus, while we barely detected ATAD2 protein in normal livers, ATAD2 expression was high in malignant livers.

We performed immunohistochemical staining in HCC and normal liver tissue arrays to visualize the localization and expression status of ATAD2. 38 HCC samples with different grades and 8 normal liver samples were stained. ATAD2 staining was markedly nuclear positive in 16 out of 38 HCC samples, with highly correlated with grades and TNM classification. 3 out of 18 samples (16%) with T2N0 were positive and the positivity increased to 50% (9 out of 18) in T3NO samples. 2 of the T3N1 samples were positive. All of the normal livers (8/8) were ATAD2

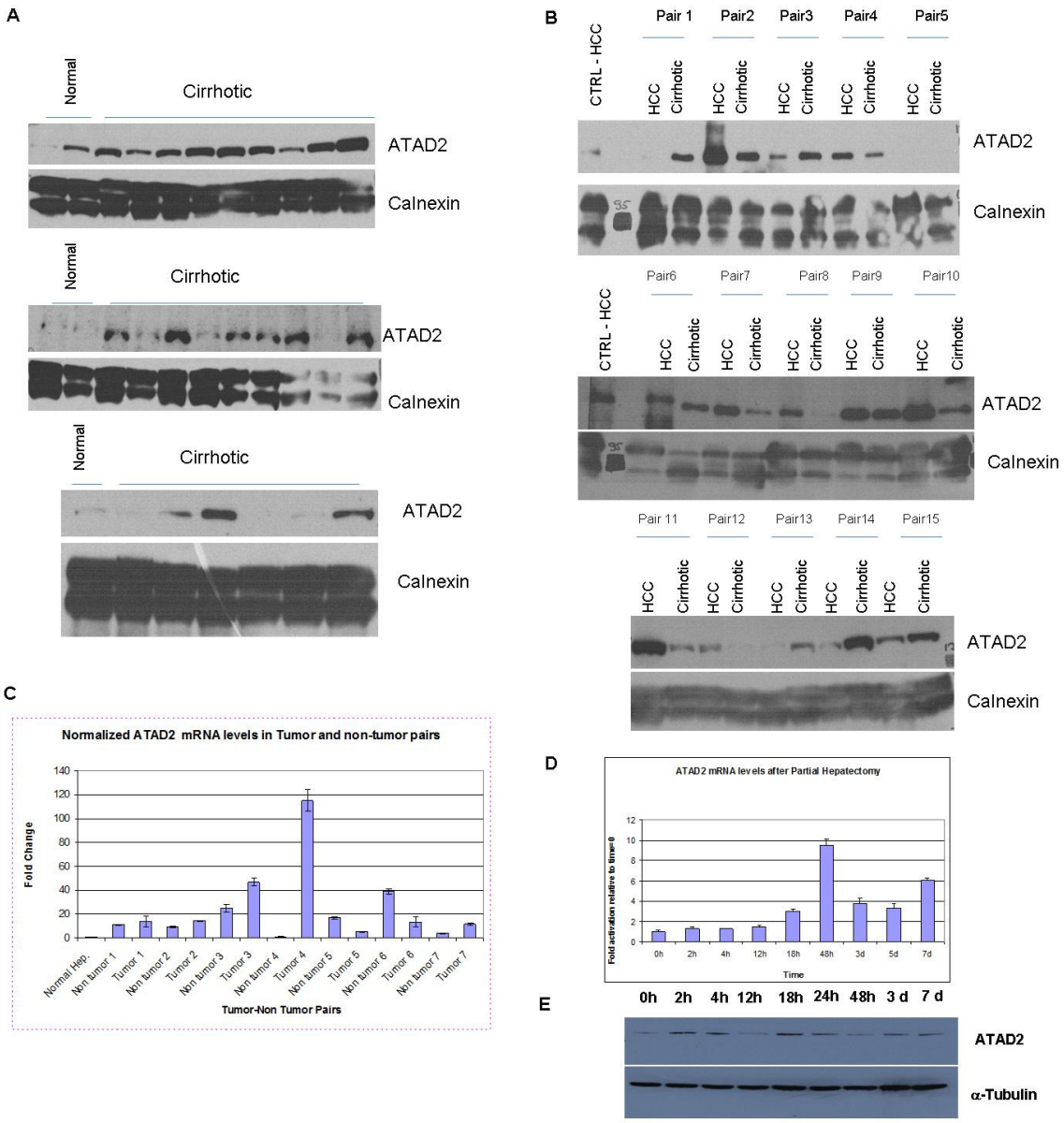

Figure 4.5.3 ATAD2 expression status in malignant and normal cells A. in Cirrhotic tissues B. in tumor-non-tumor pairs C. QPCR analysis in Tumor non-tumor pairs D. QPCR analysis of ATAD2 after rat liver regeneration models E. immunoblotting of QPCR of ATAD2

Negative (Table 4.5.1). Representative Stainings of positive tumor samples and negative normal livers were shown in figure 4.5.4. Taken together these results showed that ATAD2 expression is associated with high grade tumors and there is an increased risk of lymph node invasion of tumor cells.

(Table 4.5.1). Immunohistochemistry analysis of ATAD2 protein in HCC samples

Pathologic Stage	No of samples	Positive	Percentage%
T2NO	18	3	17%
T3NO	18	9	50%
T3N1	2	2	100%
Normal Liver	8	0	0%

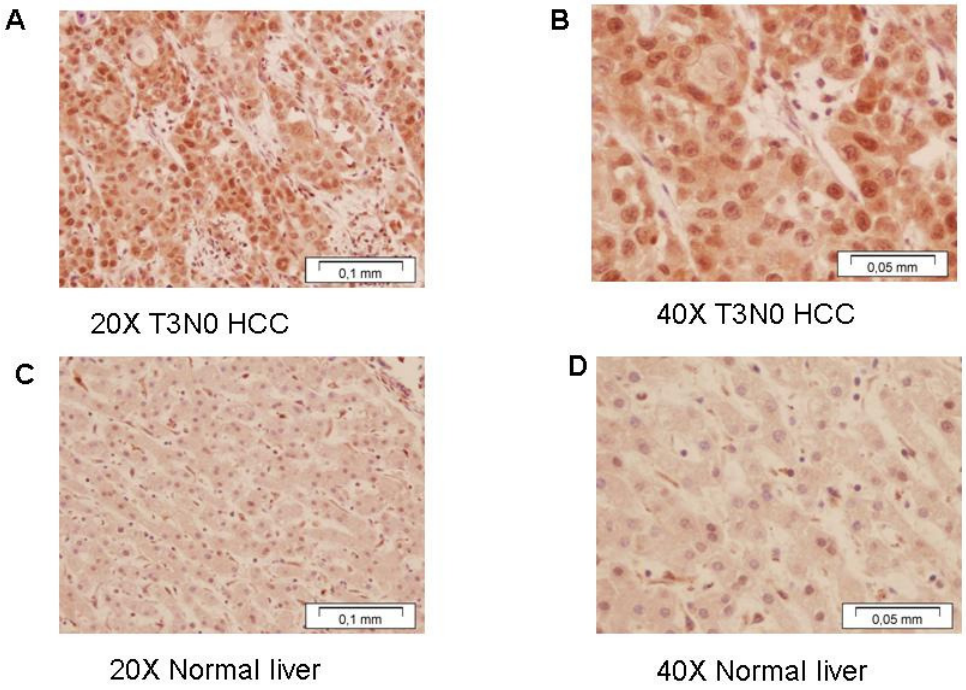

Figure 4.5.4 immunohistochemistry images of HCC samples (A and B) stained with ATAD2 whereas negative staining is observed in normal samples (C and D).

To characterize the role of ATAD2 in hepatocyte growth, we checked the expression of ATAD2 after rat liver regeneration samples using both quantitative RT-PCR and western blot. ATAD2 mRNA levels reached to two fold after 18th hour peaking at 48th hour, and stayed more than 4 fold up to one week (figure 4.5.3.D). Immunoblotting data showed that the increase of ATAD2 peaked at 18th hour and also for day 3 and day 7 with different translation dynamics than the transcript expression (figure 4.5.3.E).

4.5.4 Inhibition of ATAD2 expression induces apoptosis in liver cancer cells and affects the growth of normal cells

To investigate the role of ATAD2 in liver cancer, a panel of HCC cell lines was transfected with 4 different siRNAs targeting different sequences ATAD2 transcript and cell growth was checked compared to control siRNA using coomassie staining after 96 hours of transfection. 4 HCC cell lines, Hep3b, HepG2, FLC4 and Snu449 showed a higher growth inhibition at least two different siRNAs but not with control scrambled siRNA. ATAD2 knockdown did not effect the growth of Huh7, PLC/PRF/5, Hep40 and Skhep1 cell lines (Figure 4.5.5). We confirmed this data with colony formation experiment for Hep3b and HepG2 cells. We transfected these two cell lines with siRNA1, siRNA3 and control siRNA and after 72 hours of transfection, we plated equal volume of cells and checked colony formation capacities after 10 days. Knockdown of ATAD2 significantly decreased the colony numbers in both HepG2 and Hep3b cells (figure 4.5.6.A and C). ATAD2 knockdown decreased the average colony numbers from 356 with control siRNA to 156 with siRNA1 and 192 with siRNA3. HepG2 cells formed 771 colonies with control siRNA and 464 and 597 colonies in average with siRNA1 and siRNA3 subsequentially. (Figure 4.5.6. B and D).

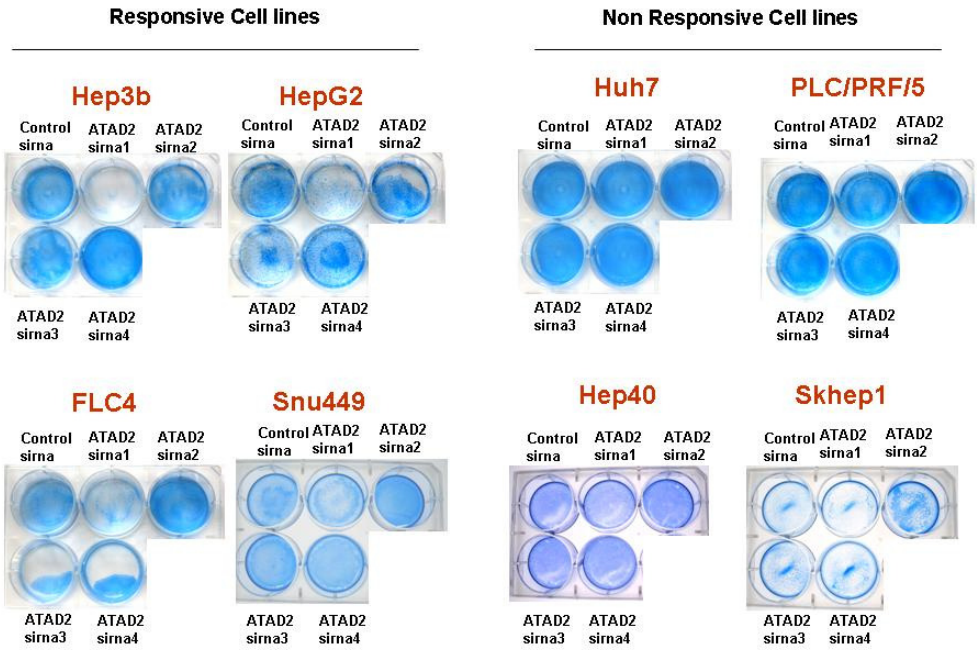

Figure 4.5.5 ATAD2 knockdown inhibited cell growth of HCC cells as stained by coomassies staining after transfection with 4 different siRNA targeting ATAD2 and controlsiRNA at day 4.

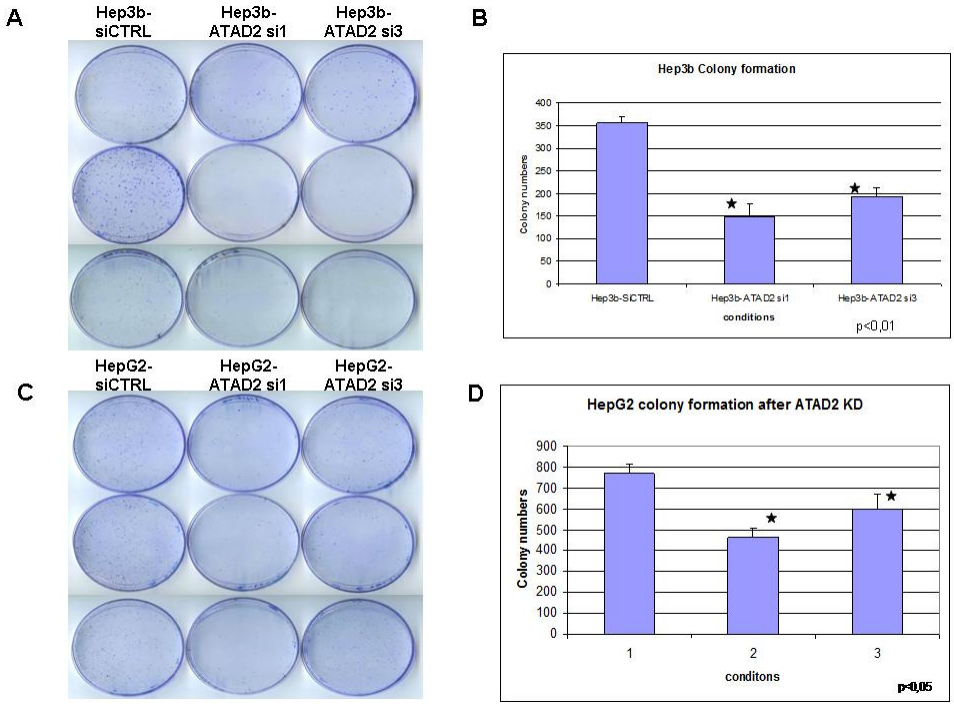

Figure 4.5.6 Colony formation experiment of Hep3b and HepG2 cell lines after transfection of ATAD2 siRNAs. A. Hep3b cells colony pictures in riplicates at day 13 and crystal violet stained and quantified colonies in B, C. HepG2 cells colony formation pictures in triplicates at day 13 and crystal violet stained and quantified colonies in D.

To understand the mechanism of growth inhibition, we performed cell cycle analysis using FACS. Propidium Iodide (PI) staining of Hep3b and HepG2 cells after transfection with siRNA1 and siRNA3 at day 2 and day 3 showed that apoptosis is induced after ATAD2 knockdown. G0 cells were quantified as 37% at day 2 and 61% at day 3 for Hep3b cells using siRNA1 and 7% and 13 % using siRNA3 for day 2 and day 3. The level of apoptosis in hepG2 cells reached up to 40% with siRNA1 and 31% siRNA3 at day 3 (Figure 4.5.7 A and B). Huh7 and Hep40 cells were found to be resistant to apoptosis after ATAD2 knockdown (Figure 4.5.7.C). Apoptotic cells in Hep3b, HepG2, PLC/PRF/5 and FLC4 cell lines detached and rounded up, as shown in (figure 4.5.7.D). Further confirmation of apoptosis in these cells was made by Annexin-V FACS staining of cells at day 2. As expected, induction of apoptosis in Hep3b and HepG2 cells shifted Annexin-V positive cells to right as shown in the figure 4.5.7.E

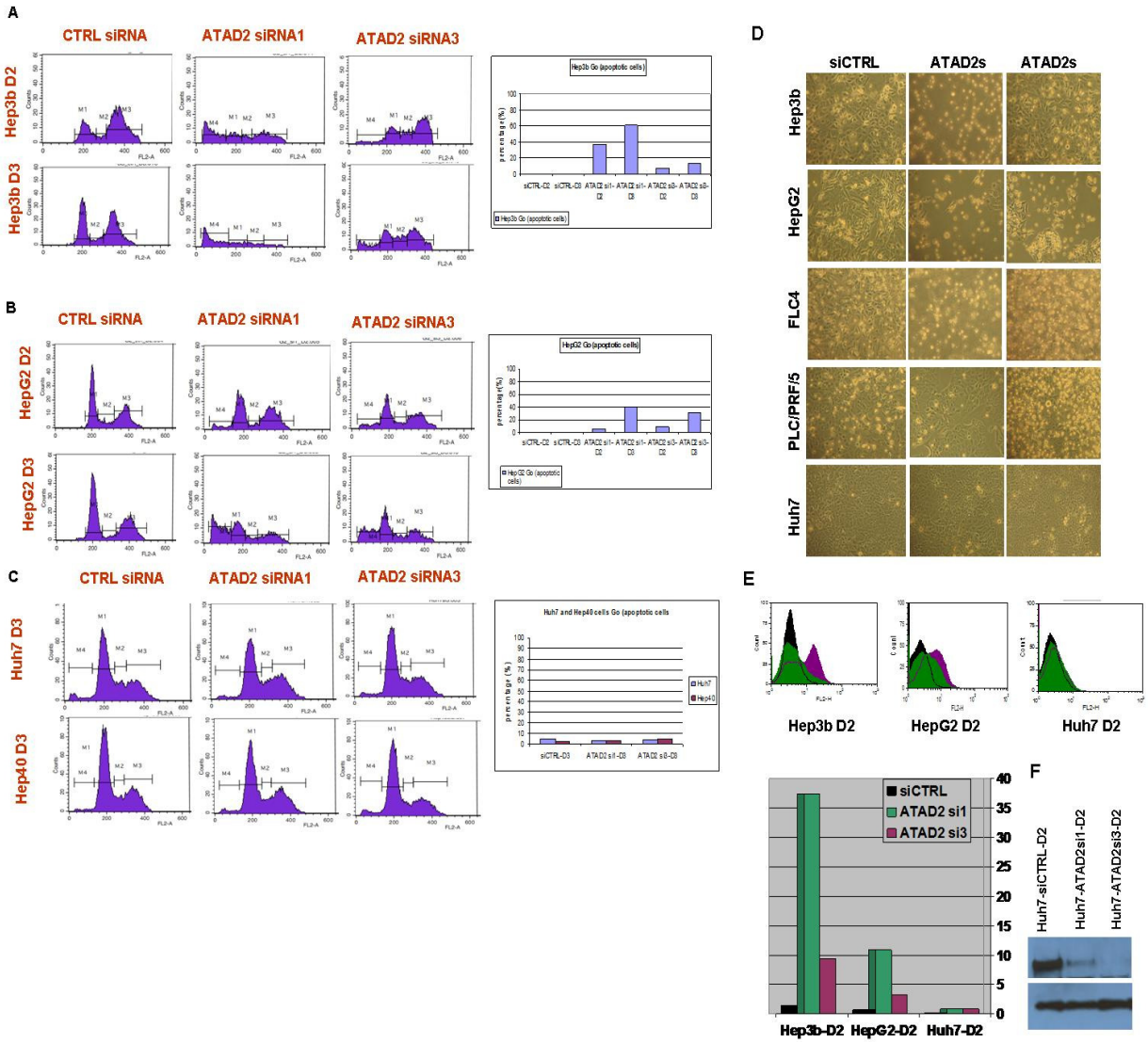

Figure 4.5.7 Apoptosis was detected in Hep3b and HepG2 cells but not Huh7 and Hep40 cells. A. PI staining and further cell cycle analysis showed Go accumulation of A. Hep3b B. HepG2 but not D. Huh7 and Hep40 cells. D. Apoptotic cells detached and round up from all the cell lines except Huh7 E. Apoptosis was confirmed using Annexin-V FACS analysis F. Huh7 ATAD2 KD

and quantified as in the graph (figure 4.5.7 Bottom). We did not observed the shift for Huh7 cells and to test the efficiency of knockdown in Huh7, we showed that knockdown of ATAD2 in Huh7 was enough to induce apoptosis (figure 4.5.7.F).

Knockdown of ATAD2 was quantified using quantitative RT-PCR in Hep3b and HepG2 cells. Two different experiments using siRNA1 and control siRNA in triplicates showed that

ATAD2 transcripts were decreased significantly both in Hep3b and HepG2 cells (figure 4.5.8 A.). Results were confirmed with western blotting as shown in figure 4.5.8.B.

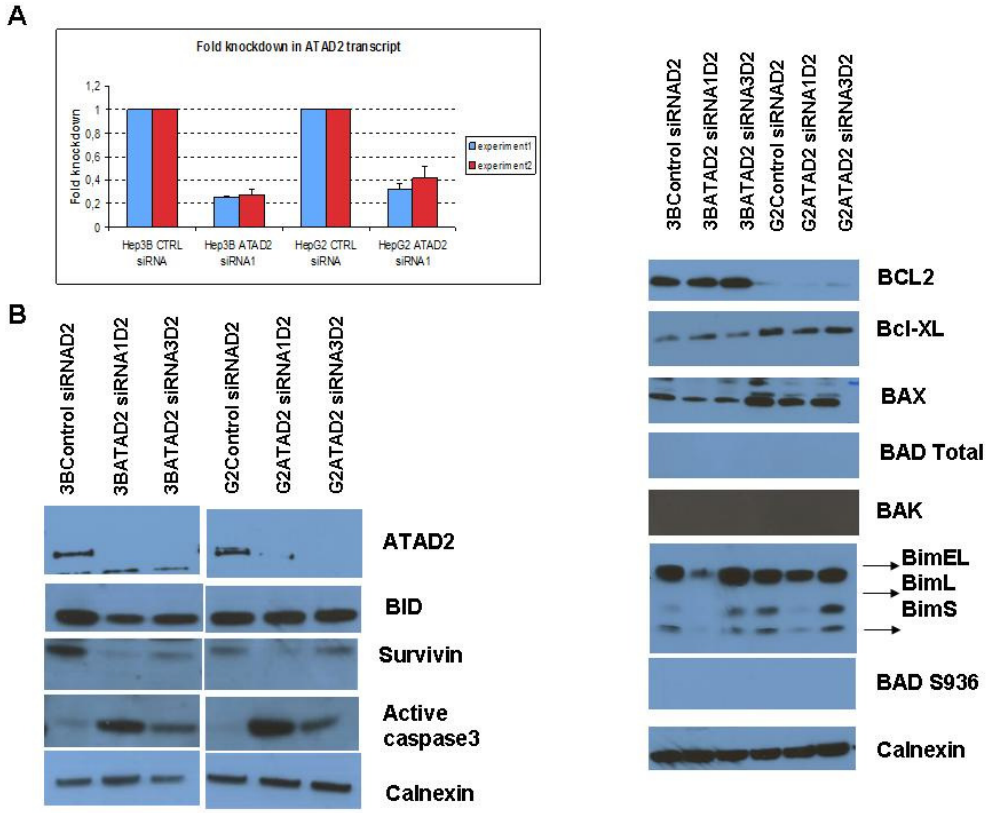

Figure 4.5.8 ATAD2 Knockdown is shown in Hep3b and HepG2 cells A. by QPCR B. western and pro and anti apoptotic genes were checked by western.

4.5.5 Mechanism of Apoptosis in liver cancer cells

We next investigated the molecular mechanism of apoptosis after ATAD2 knockdown in Hep3b and HepG2 cells. ATAD2 binds to acetylated histones with bromodomains and through its ATPase domain it may regulate DNA-Protein or other complexes on transcriptional regulation of apoptotic and non-apoptotic genes. To test this hypothesis we first determined the type of apoptosis and searched for molecular mechanism of apoptosis.

Using activated caspase 3 antibody and western blotting, we confirmed that apoptosis is caspase 3 dependent (fig 4.5.8.B). To search for additional regulators of apoptosis, we screened a number of bcl-2 family members and other apoptosis executers as well. Pro-survival genes such as Bcl-2 and Bcl-xL and pro-apoptosis genes such as bax, bid and bim proteins were found to be not changing. (fig 4.5.8. B). Survivin a member of inhibitor of Apoptosis (IOA) family of

antiapoptotic protein and has a dual role for cancer; anti-apoptosis and cell division [212-214]. We showed that survivin expression is downregulated with both ATAD2 siRNA1 and SiRNA3 transfection in Hep3b and HepG2 cells.

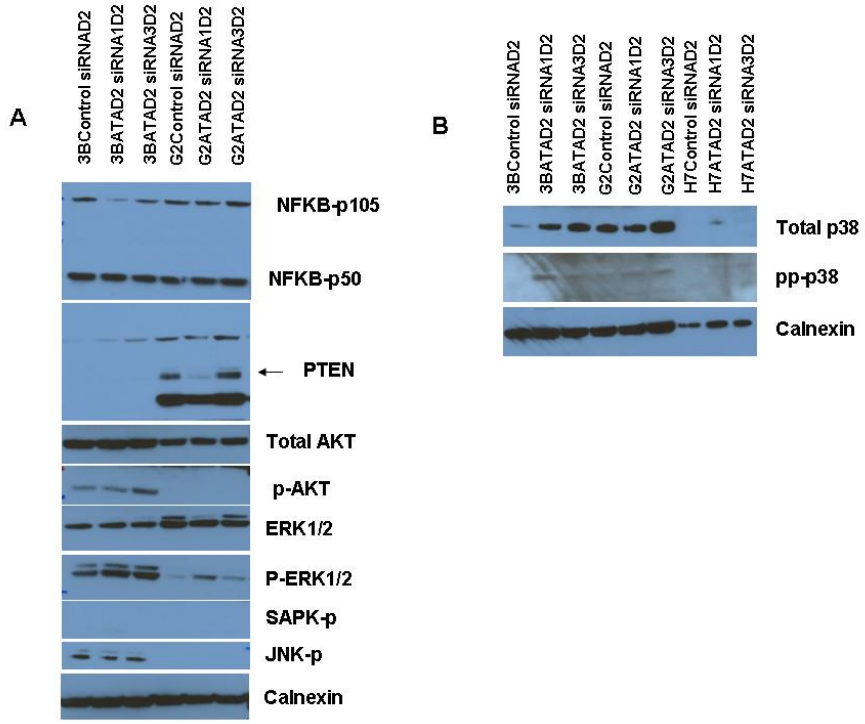

Figure 4.5.9 Expression levels of Survival kinases after ATAD2 KD in Hep3b and HepG2 cells in A. p38 stress kinases in B.

We also checked key apoptosis and survival pathway genes such as AKT, JNK, ERK, p38 and NFK-B genes. We failed to find a significant change in neither total AKT nor phosphorylated form of AKT and total ERK1/2 kinase and phospho ERK1/2 kinases. These kinases are generally involved in survival of cells. JNK kinase and NFK-B were not changing as well (figure 4.5.9 A). On the other hand, we showed total levels of p38 kinase and its active phosphorylated forms are upregulated after ATAD2 knockdown in Hep3b, HepG2 and Huh7 cells (figure 4.5.9 B). These results showed us that ATAD2 is upstream of p38 kinase.

Apoptosis is a part of a differentiation process, and occurs in vivo as well. To test the hypothesis that liver cancer cells are forced to differentiate after ATAD2 knockdown and thus may eventually lead cells to go to apoptosis, we checked a panel of markers of liver cell differentiation. We previously described the markers for the expression of hepatocyte lineage markers, epithelial and mesenchymal markers. We checked the expression of these markers and

unfortunately neither the hepatocyte lineage markers HNF-1α, HNF-4α, anti-trypsin1 and ZO-1 nor E-cadherin and vimentin being epithelial-mesenchymal markers, did not change after ATAD2 knockdown at the conditions that we see apoptosis (Figure 4.5.10 A).

We also checked the expression of main tumor suppressors to explore the role of ATAD2 in liver cancer cells. After ATAD2 knockdown, we did not see any significant change of p15Ink4b, p16Ink4a and p21Cip1 and also phosphorylated serine15 p53 and BP53 protein using western blot. Neither of these tumor suppressors nor damage markers was found to be changed (Figure 4.5.10. B).

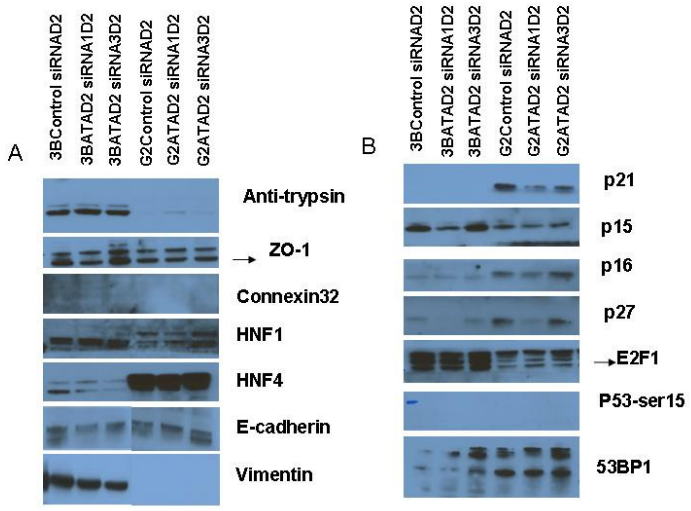

Figure 4.5.10 Epithelial and Liver specific markers after ATAD2 knockdown in A. and tumor suppressor genes in B.

4.5.6 Survivin did not rescue loss of ATAD2 induced apoptosis in liver cancer cells

As stated earlier, survivin has a dual role; it may act as an anti-apoptotic protein and has a role in cell division. In the conditions that we see apoptosis, there is a decrease of expression of survivin protein. So to dissect the role of survivin protein for liver cancer, we made recombinant GFP-fused survivin overexpressing stable colonies in Hep3b cells and also GFP overexpressing colonies as control. We confirmed the overexpression of survivin using western blot (figure 4.5.11.A). Then we performed ATAD2 knockdown in these clones to see whether survivin can rescue cells from loss of ATAD2 induced apoptosis. Unfortunately survivin did not rescue cells from apoptosis, to show the result, only one of the colonies was given as a figure here (figure

4.5.11. B).

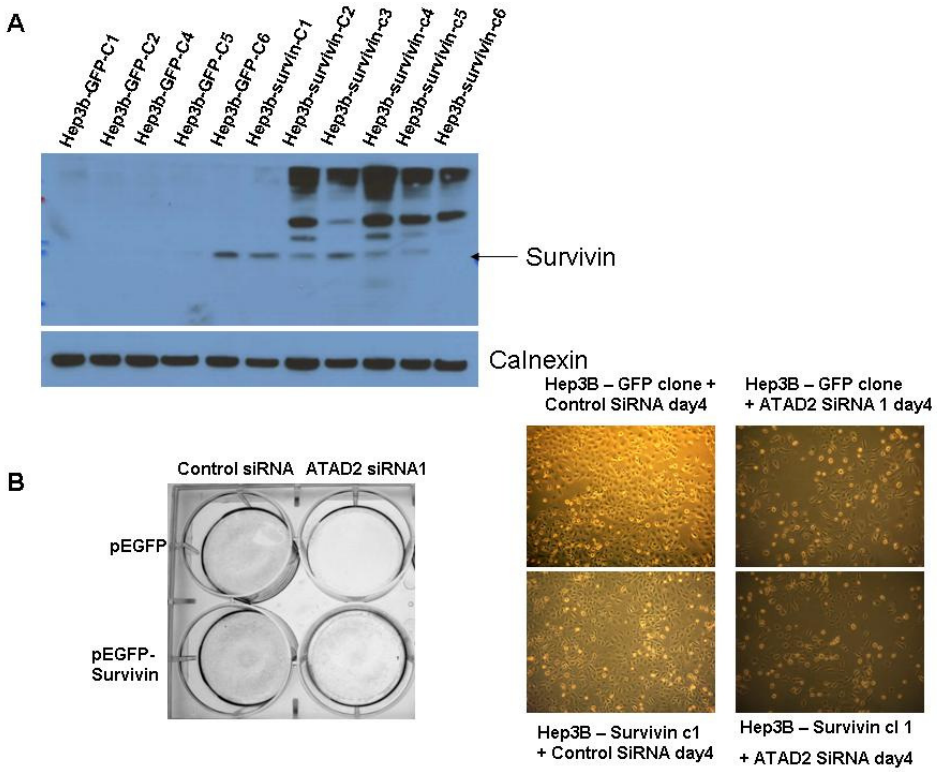

Figure 4.5.11 Survivin failed to rescue loss of ATAD2 induced apoptosis in Hep3b cells. A, Survivin western showing overexpression of surviving in Hep3b clones B. Survivin overexpressing Hep3b cells still going to apoptosis.

4.5.7 RNAi targeting of ATAD2 inhibited cell proliferation and colony formation of non-liver cells

To evaluate the effect of ATAD2 depletion on the proliferation of hela cells, we used BrdU labeling and colony formation assays of Hela cells and MRC5 cells. Hela cells were transfected with 4 different siRNAs and the decrease of ATAD2 protein was shown by western blotting (figure 4.5.13.B). After transfection cells were subjected to short term BrdU staining using FACS analysis. We detected significant decrease of BrdU incorporation specifically with siRNA1 transfection. BrdU incorporation is robustly decreased from 22% for siCTRL to 5% at day 3 with G1 arrest reaching as high as 70% of cells for siRNA1 with respect to 58% for control siRNA transfected cells (figure 4.5.12.A). We confirmed this finding via colony formation experiment. siRNA1 and siRNA3 transfection reduced colony numbers significantly with respect

to siCTRL and treatment of cells with low dose 0,1uM, medium dose 0,5uM or high dose 1uM TSA synergized with knockdown and decreased significantly colony number($p < 0,01$). Figure 4.5.12 B and C showed the decrease of colony formation either alone or together with TSA treatment. These data showed that ATAD2 knockdown decreased the cell growth and the colony formation capacity non-liver cancer cells as well.

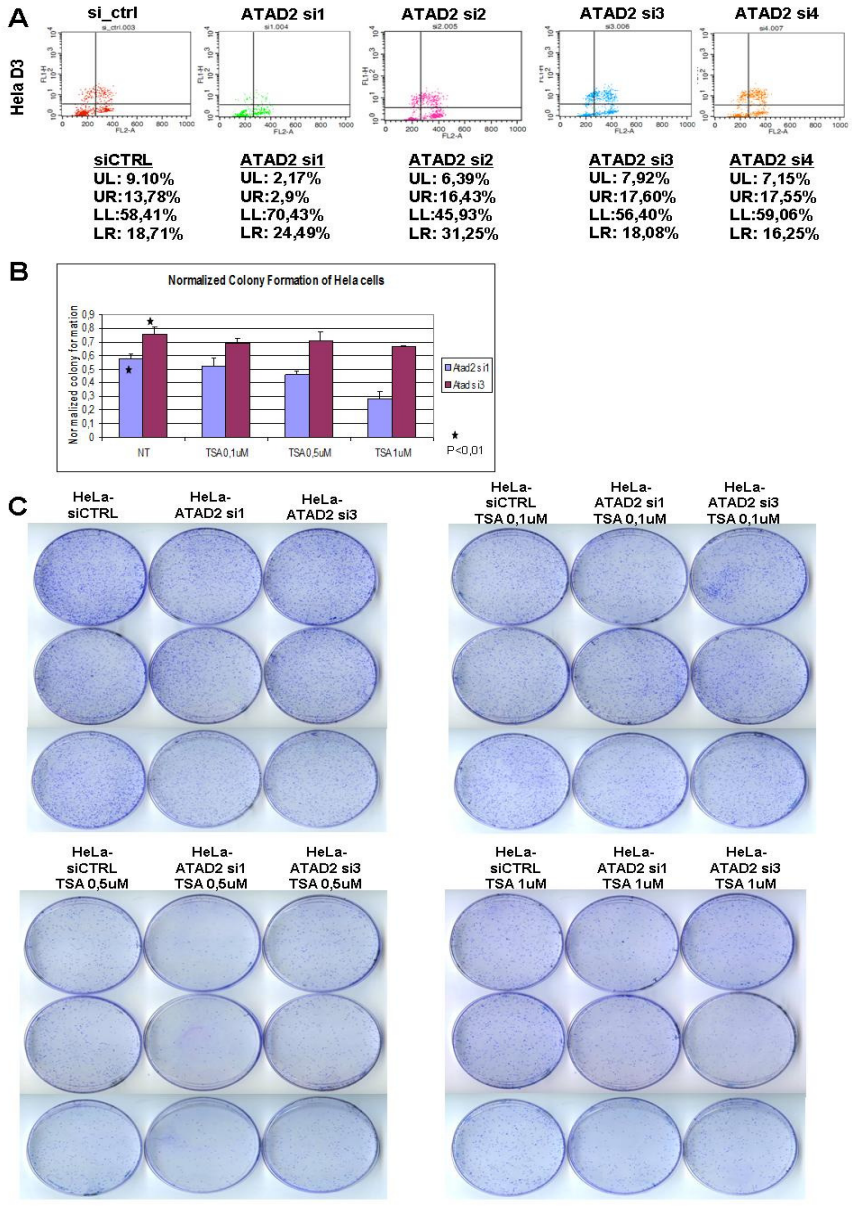

Figure 4.5.12 ATAD2 knockdown inhibited growth and colony formation of Hela cells. A. BrdU FACS analysis of Hela cells after ATAD2 KD. B. and C. Colony formation assay performed after ATAD2 KD and TSA treatment of HCC cells potentiates the effect of KD.

We checked key regulators of Rb and p53 pathways to understand the mechanism of decreased the cell proliferation in Hela cells. Loss of ATAD2 protein in Hela cells increased p53 protein levels and its main target p21Cip1 protein levels with 3 of the ATAD2 siRNAs (Figure 4.5.13A and B). To our surprise, this was not expected. Because hela cells were infected with Human papilloma virus and p53 and Rb pathways were shown to be inactive. To explain the increase of p53 protein levels after ATAD2 loss, we hypothesized that ATAD2 may bind to E6 and E7 oncoproteins and regulate their expression as well. We checked E6 and E7 protein levels

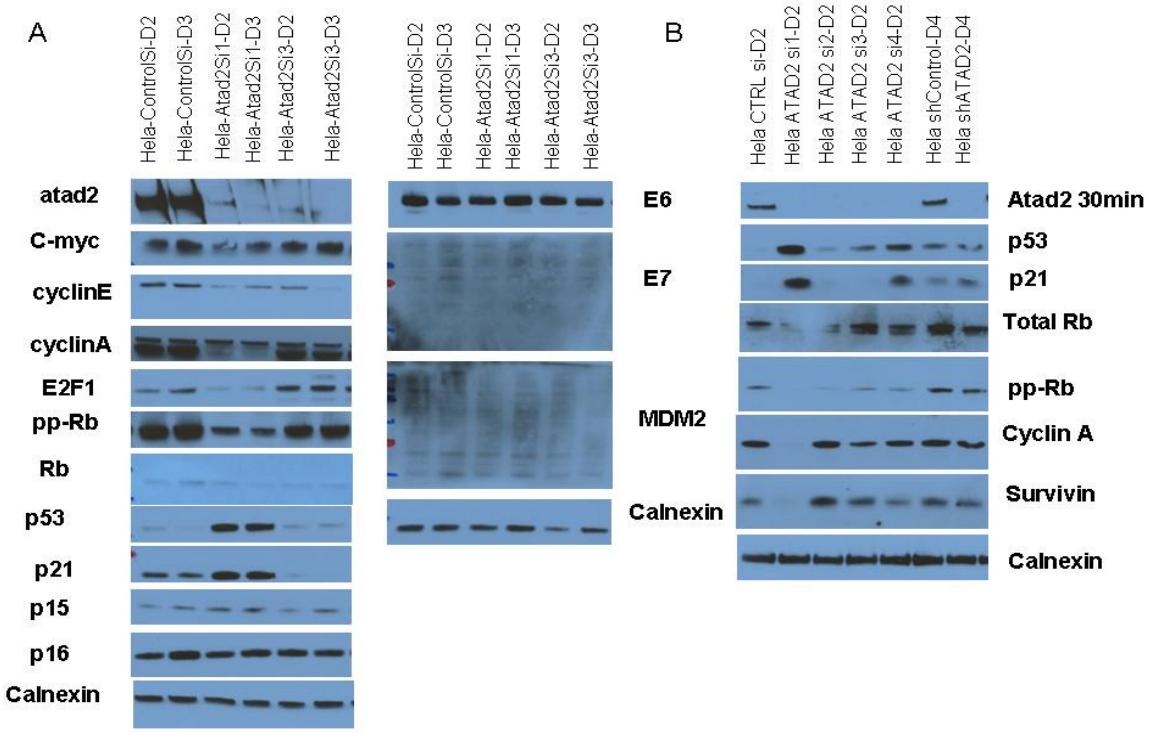

Figure 4.5.13 Key cell cycle regulatory protein expression after ATAD2 KD in Hela cells

using western blotting. As shown in the figure E6 levels did not change significantly and E7 antibody was not good enough or undetectable. Downstream of p53/ p21Cip1 pathway is Rb protein. We detected a decrease in phosphorylated levels of Rb but not with total levels of Rb protein. E2F protein levels were also decreased and this lead to decrease of cylin E and Cyclin A protein levels (figure 4.5.13.middle panel). ATAD2 was shown to be co-activator with C-myc oncogene protein. So we checked c-myc protein levels with the same lysates and c-myc was decreased. To repeat the experiments and to see the effect of other siRNAs as well, we repeated the westerns with all siRNAs (figure 4.5.13.B).

4.5.8 Loss of ATAD2 induced senescence in MRC5 cells

ATAD2 gene was down in senescence associated gene list therefore we expected loss of ATAD2 would induce senescence in liver cells. To see the effect of ATAD2 loss in normal cells we changed our model to MRC5, human normal lung fibroblast cells. MRC5 cells reached to full senescence at around population doubling 70, so we do not expect these cells to show significant senescence rates at PDL 30. Successful knockdown of ATAD2 protein in MRC5 PDL 30 was shown by western blotting (figure 4.5.14.B). We performed senescence assay after transfection and showed that loss of ATAD2 induced senescence with siRNA1 and siRNA4 at day 3 (figure 4.5.14.A). We repeated these experiments with immortal MRC5 cells and obtained the same results as shown in figure 4.5.14.A lower panel. Not only normal MRC5 cells but also immortal MRC5 cells showed senescence after loss of ATAD2 protein showing that it is inducing premature senescence. Short term BRDU analysis together with PI staining showed that after ATAD2 loss, BrdU incorporation did not change for presenescent MRC5 (PDL 32) most probably because the cells arrested at G2/M phase of the cell cycle at day 3 for all the siRNA1 and siRNA 4 tested (figure 4.5.14.D and E). To confirm these results we performed colony formation experiment in presenescent MRC5 cells. Colony numbers significantly decreased for both siRNA1 and siRNA3 (figure 4.5.14. C). We also performed p53 western to see if senescence is p53 dependent whereas only siRNA2 increased p53 protein levels slightly (figure 4.5.14.B). These results showed that ATAD2 protein did not induce apoptosis but senescence in these cells.

4.5.9 RNAi knockdown of ATAD2 using tet-inducible lentivirus system

To determine the tumor suppression effect of ATAD2 loss by RNAi and to image in vivo, we developed a tetracycline regulatable lentiviral vector expressing shRNA cassette against ATAD2 transcript (figure 4.5.15.A). Using this vector we infected Hep3b, Huh7 and Hela cells. We also used a control vector expressing scrambled sequence. When induced by doxocycline, shRNA is expressed and cells started to express RFP protein, therefore we could trace the cells in vitro and in vivo. We induced the Huh7, Hep3b and Hela cells stably expressing ATAD2 shRNA and shCTRL and preparing RIPA lysates we showed the knockdown of ATAD2 protein (figure 4.5.15.B). Increasing dose of Doxocycline showed the efficient knockdown of ATAD2 in Huh7 and Hep3b cells (Figure 4.5.15. C). Indirect immunofluorescence was also used to follow knock-

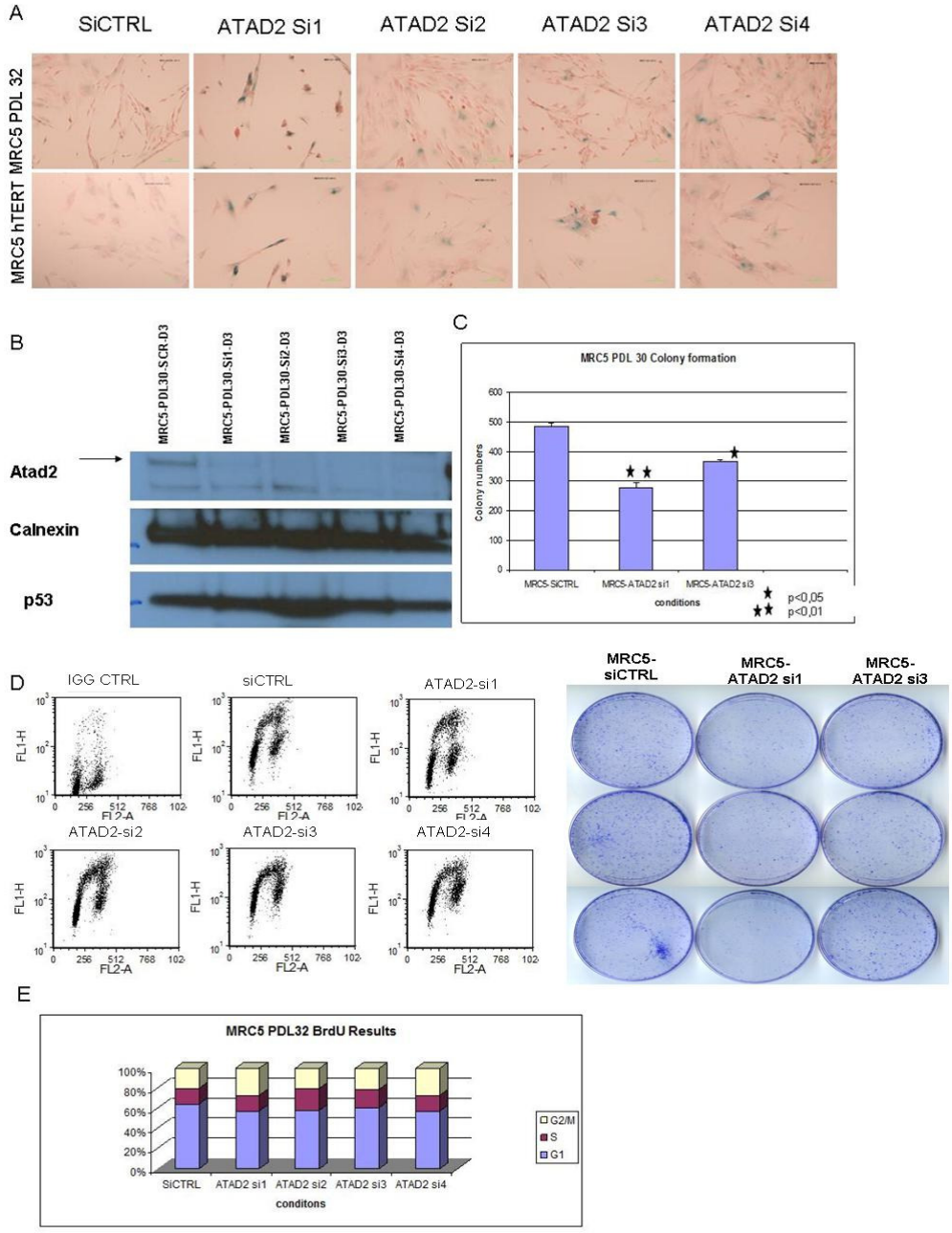

Figure 4.5.14 ATAD2 KD in MRC5 cells induce senescence in MRC5 mortal and immortal cells in A. B. ATAD2 KD showed in MRC5 cells C. Colony formation capacity decreased D. and E. BrdU incorporation did not change significantly.

down of ATAD2 protein in Huh7 cells (figure 4.5.15.D). Huh7 cells were heterogenous in terms of efficiency of knock-down. Almost half of the cells were successfully downregulated ATAD2 protein, whereas control shRNA expressing cells were homogenously positive. ATAD2

knockdown is showed using staining of ATAD2 with green color and loss of ATAD2 is observed in red fluorescence protein and thus ShRNA expressing ATAD2 cells (figure 4.5.15.D). Caron et al showed that ATAD2 is binding to H4K5Ac histones, to see if ATAD2 knockdown destabilizing or havening any effect on levels of H4K5Ac, we stained cells with H4K5Ac antibody. Costaining did not show any effect on H4K5Ac levels with knockdown of ATAD2 (figure 4.5.15.E).

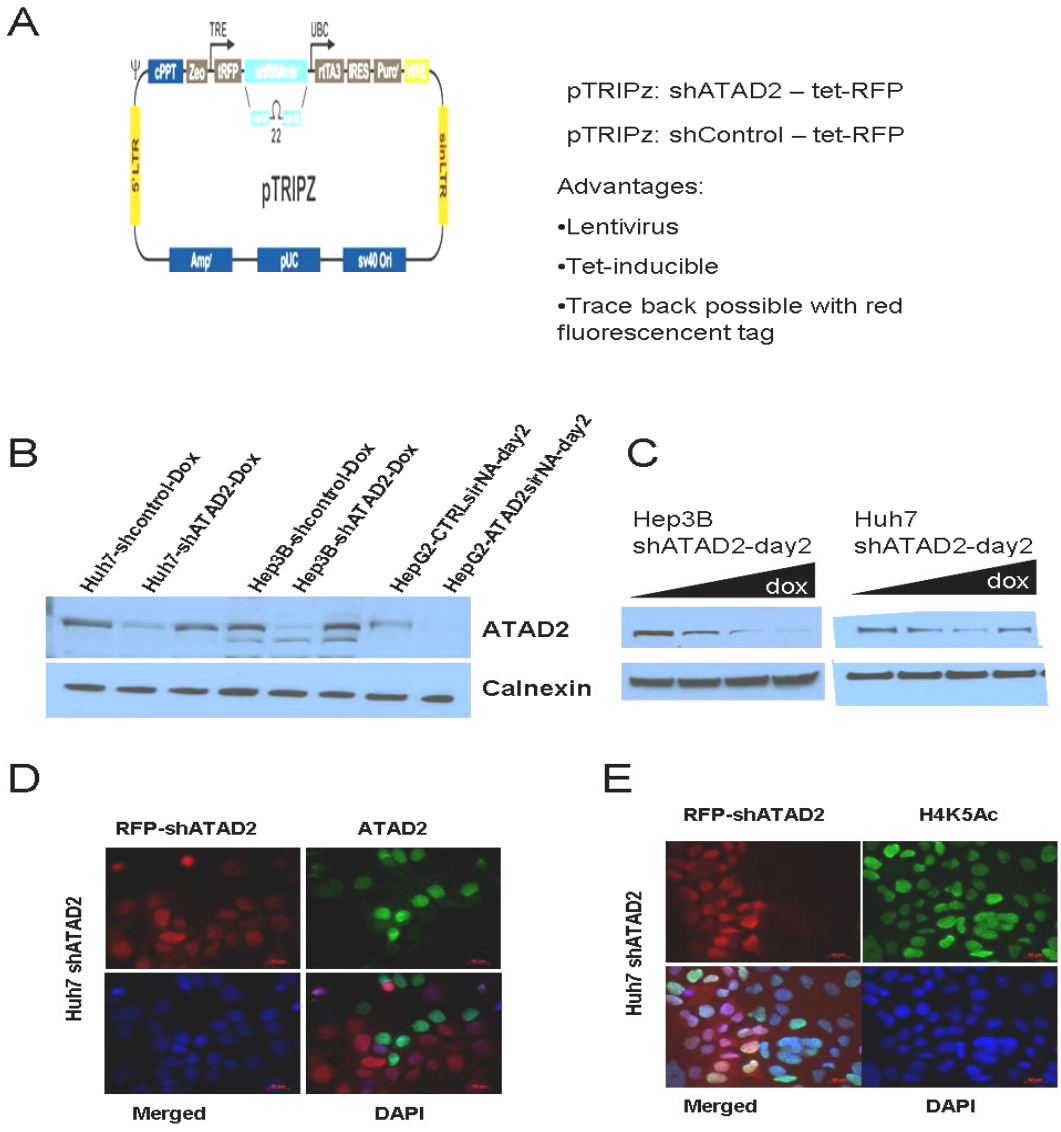

Figure 4.5.15 shRNA lentiviral vectors downregulated ATAD2 levels when induced by doxycycline. A. Lentiviral vector and advantages B. and C. ATAD2 KD after infection and induction D. and E. ATAD2 KD and H4K5Acetyl staining after induction and loss of ATAD2.

4.5.10 Downregulation of ATAD2 expression by tet-inducible RNAi suppressed tumorigenecity of HCC cells in vivo

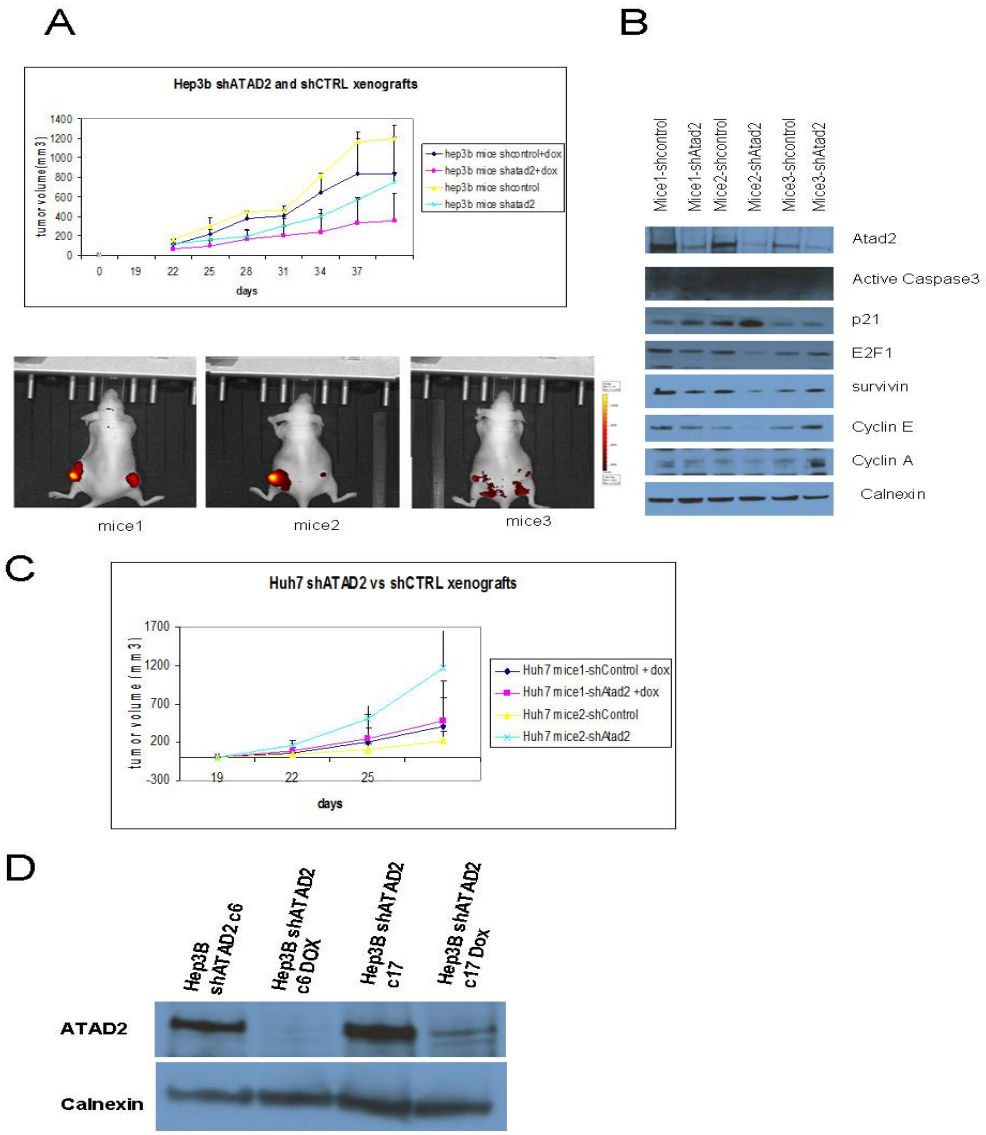

Figure 4.5.16 Xenograft models and imagining of shATAD2 and ShCTRL hep3b and huh7 cells in A and C sequentially B. cell cycle regulating genes in shATAD2 tumors and D. New subclones of Hep3b shATAD2 cells.

Using this system, we injected $10x10^6$ shCTRL and shATAD2 cells into the right and left side of the 6 mice for both Huh7 and Hep3b cells. We fed 3 mice with doxycycline in drinking water to induce the expression of shATAD2 and shCTRL. We measured size of tumors every 3 or 4 days, and plotted the graph as in the figure 4.5.16.A. and C. Results clearly showed that

Huh7 injected tumors were not responsive to knockdown of ATAD2 (figure4.5.16.C). Whereas we detected a suppression of tumorigenecity of hep3b cells expressing shATAD2 with respect to shCTRL when induced with doxycycline. Before mice were executed, we performed in vivo imaging of xenografts using Xenogen Ivis Kinetics in vivo imaging system. RFP expressing tumors were visualized and photographs were taken as red color (figure 4.5.16.B). We executed the mice and extracted the tumors and performed western analysis to see the specificity of the knockdown and mechanism of tumor shrinkage. Westernblot analysis was performed to see ATAD2 protein levels between shATAD2 and ShCTRL tumors. ATAD2 protein levels were significantly decreased for mice 1 and 2. For the three mice, we also checked apoptosis via caspase3 and key tumor suppressors. We showed that caspase 3 was not activated but p21 levels were significantly increased with a corresponding decrease in E2F1 and cyclin E and A proteins. Survivin protein is also found to be decreased for these tumors (figure 4.5.16.B).

We increased the number of mice from 4 to 10 animals, however during that time these cells somehow lost the expression of shATAD2 as followed by RFP and ATAD2 western. We then subcloned Hep3b cells and obtained two subclones that downregulated the expression of ATAD2 protein when induced. We named these clones Hep3b shATAD2 clone 6 and shATAD2 clone 17. We plan to increase animal numbers to 10 using these two subclones (figure 4.5.16.D).

4.5.11 Loss of ATAD2 increased histone acetylation and increased p300 histone acetyltransferase levels

There is fine balance between activity of histone deacytylases (HDACs) and histone acetyltransferases (HATs) in cells. Today we know that HDAC are overexpressed in several cancer and HDAC inhibitors like trichostatin (TSA) and sodium butyrate inhibits histone deactylation and increases histone acetylation levels. HDAC inhibitors are also used to treat cancer. Several articles showed that this leads to growth arrest and/or apoptosis. Therefore we investigated whether ATAD2 loss increased histone acetylation. We used nuclear extract preparation to check the levels of global histone acetylation after loss of ATAD2 protein. Using both pan Acetyl H3 and pan Acetyl H4 antibodies, and further using specisific residues we showed that global H3 levels but not H4 acetylation were significantly increased after loss of ATAD2 in Hep3b cells but not with Huh7 cells (figure4.5.17. A and B). We also used TSA treatment as a positive control. Levels of histone 3 and histone 4 acetylations reached to

maximum levels after TSA treatment. We checked specifically a few acetylated residues and showed that H3K18 Acetyl and H4K5Ac are upregulated for Hep3b and HepG2 cells but not with Huh7 cells (figure 4.5.17.A).

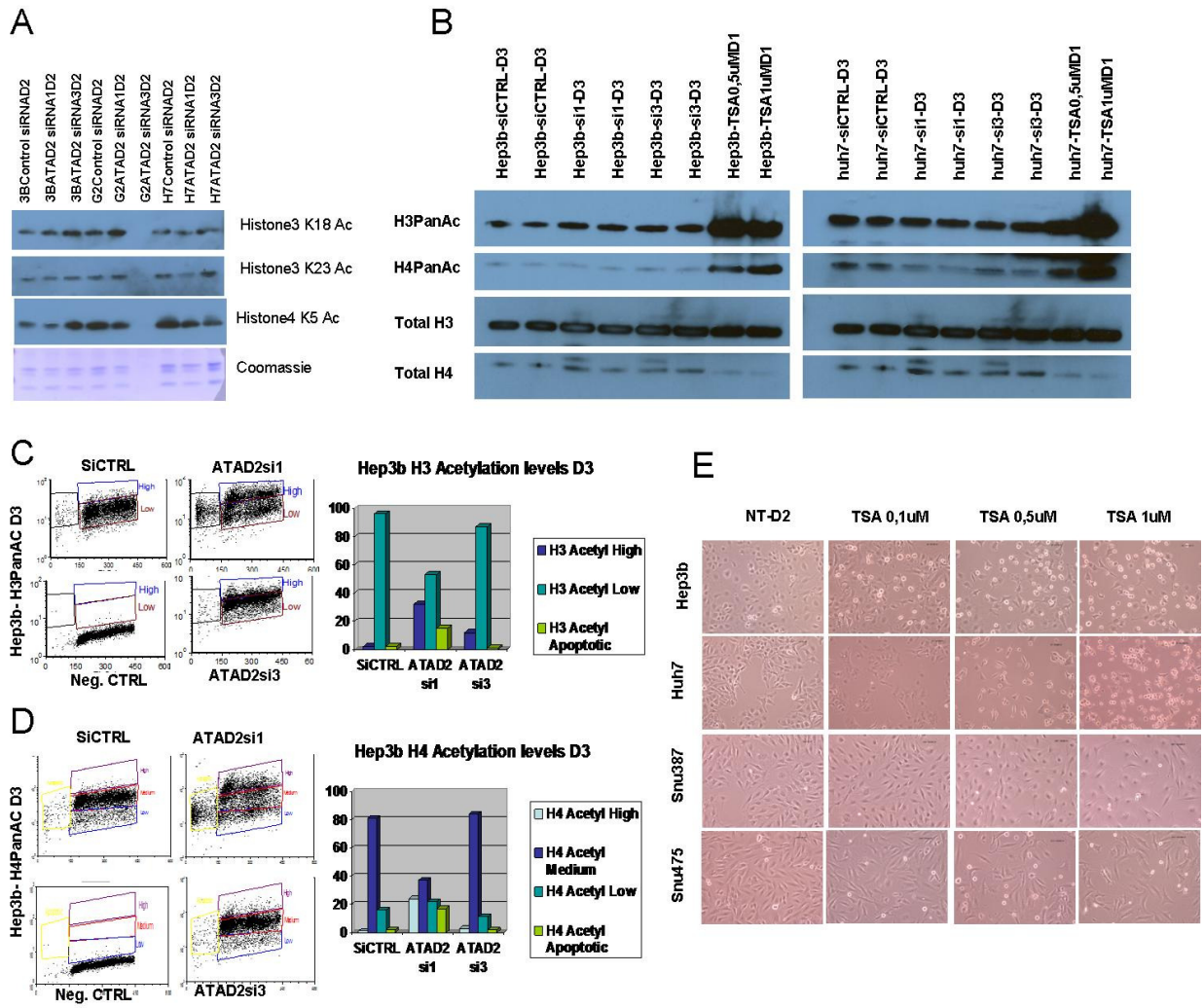

Figure 4.5.17 ATAD2 KD leads to increase in global histone acetylation increase A. specific histone acetylation western and B. total H4 and H3 acetylation levels and C. and D. confirmation of global H3 and H4 acetylation increase as shown by FACS E. TSA treatment of Hep3b and Huh7 induced apoptosis but not with snu387 and snu475 cell lines.

We further confirmed the results with FACS analysis using the same antibodies. This experiment showed that cells are at low H3 acetylation levels and significantly reached to high acetylation levels after siRNA1 and SiRNA3 transfection (figure 4.5.17. C). Apoptotic cells were

also acetylated as shown in figure 4.5.17.C. H4 acetylation was also increased from low and medium level to high levels after transfection with siRNA1 and SiRNA3 (figure 4.5.17. D).

Since histone acetylation increase can induce apoptosis, as a proof to ATAD2 induced histone acetylation increase, we treated Hep3b and Huh7 cells with TSA and observed their phenotypes. Hep3b and Huh7 cells but not Snu387 and Snu475 cells induced apoptosis. Using FACS analysis we quantified the apoptosis rates of cells (figure 4.5.17.E).

4.5.12 ATAD2 knockdown induced HAT expression in Liver Cancer cells

To search for the responsible enzyme increase in acetylation for ATAD2, using differentially expressed HATs and HDACs in our microarray data, and we searched HATs downregulated in HCC or HDACs upregulated in HCC. We find 7 targets and using immunoblotting we stained p300, HAT1, PCAF and HDAC1, 2, 4 and 5 enzymes. Among these enzymes, only P300 correlated with our data (Figure 4.5.18).

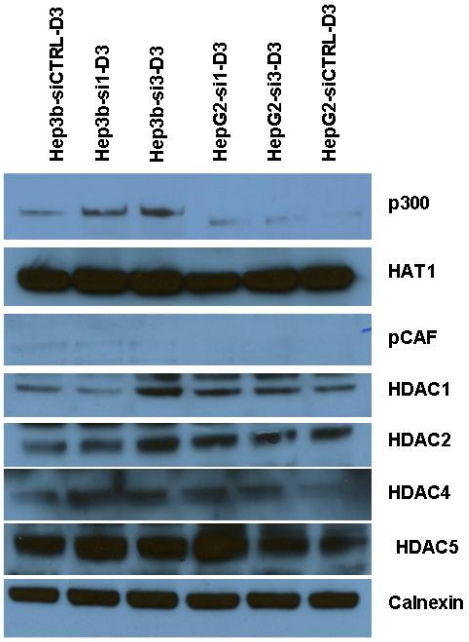

Figure 4.5.18 Key histone acetyltransferase and deacytylases expression after ATAD2 Knockdown

CHAPTER 5. DISCUSSION

5.1 Canonical Wnt signaling is antagonized by noncanonical Wnt5a in hepatocellular carcinoma cells

Most of the Wnt ligands and receptors are involved in different cellular processes by initiating canonical or noncanonical Wnt signals [196]. Canonical and noncanonical Wnt pathways function antagonistically [198-199, 206]. Thereby this information links β-catenin in extremely complex cellular processes some of which are only mediated by canonical Wnt pathway. Liver development and adult liver homeostatasis can be accounted in these complex events and canonical Wnt signaling cascade contributes to both liver regeneration and liver "zonation" by regulating certain liver-specific metabolic programs [215]. Besides, it is important for the activation of liver stem or progenitor cells, as well as HCC-initiating cells [216-219].

Canonical Wnt signaling is not frequently mutationally activated in HCC, except in hepatoblastoma [220]. It is highly limited in a cluster of HCCs with different etiological background including low p53 mutation rate, negative HBV status and chromosomal stability, as mentioned earlier along with lower histological grade and better patient survival. Surprisingly, β-catenin mutations are infrequent in more advanced and poorly differentiated HCCs, suggesting the association with poor prognosis [61, 63]. These data suggests that although known as an active player in HCC malignancy, canonical Wnt signaling is not required and also repressed for advanced HCCs. To sum up, constitutive activate canonical Wnt pathway by β-catenin mutation may be required HCC induction and development implicated with differentiation-dependent events. HCC-derived cell lines were used to show this role for further experiments.

Firstly, classification of 11 HCC cell lines into "well-differentiated" and "poorly differentiated" subtypes using hepatocyte lineage, epithelial and mesenchymal cell markers, and in vitro migration assays.

While well-differentiated HCC cell lines possess many common features with hepatocytes including expression and E-cadherin, and epithelial morphology, poorly differentiated cell lines express different mesenchymal markers strongly and generally lack the expression of hepatocyte lineage and epithelial markers. Their in vitro behaviors were discriminative as well. Poorly differentiated cell lines were found to be moving more in the wounding assay compared to well-differentiated cell lines, they were more motile (Table 4.1.1). Previously, a global expression

profiling study categorized HCC cell lines in Group I and Group II [219]. Group I was perfectly correlated with well-differentiated cells and Group II with poorly differentiated cells. Induction of oncofetal promoters with increased expression of AFP and IGF-II were affliated to Group I, whereas invasion and metastac genes were affiliated to Group II. Our classification of cells into well differentiated and poorly differentiation was also positively correlated with epithelial and mesenchymal HCC cells respectively. [54]. As a result of EMT process, mesenchymal cancer cells are produced with high invasive and metastatic capabilities [221]. This is also correlated with the data we obtained with higher motility of poorly differentiated subtype reported here. Thus, when considered these two types of cell lines are alike well-differentiated and poorly differentiated HCC tumors, respectively. The mutual relationship between the status of Wnt pathway and HCC differentiation status is showed here using this.

The same type of expression analysis of Wnt ligands and Frizzled receptors were reported for mouse hepatocytes, but analysis of Wnt signaling components in liver or hepatocytes was ill known [222]. Canonical receptors Fzd7 and Fzd9, as well as noncanonical Fzd2, Fzd3, Fzd4 and Fzd6 were found to be expressed for mouse hepatocytes. For HCC cell lines, we reproduced the same analysis with the exception of Fzd9 with weak expression. Additionally, we observed increased expression of canonical Fzd1 and Fzd5 in most HCC cell lines. The expression frequency of these receptors was not linked to HCC cell differentiation status. Canonical Wnt1 and Wnt2, and noncanonical Wnt4, Wnt5a, Wnt5b and Wnt11 were expressed for mouse hepatocytes. All or the most of the HCC cells were equipped with canonical Wnt3 and wnt10b ligands but they lost the expression of canonical Wnt1 and Wnt2. Wnt8b was expressed only in well-differentiated cell lines. Noncanonical Wnt4, Wnt5a and Wnt5b ligands were expressed mutually exclusively in the poorly differentiated cell lines, but not in well-differentiated cell lines. Most of the poorly differentiated cell lines also expressed noncanonical Wnt7b. Wnt3, Wnt4, Wnt5a, Fzd3, Fzd6 and Fzd7 have been previously implicated in HCC tumors [223-225]. Overexpression of Wnt10b in HCC [226] and increased levels of Wnt5a transcripts in chronic hepatitis, cirrhosis and HCC [227] was announced previously. C-terminally mutated HBV X protein upregulating Wnt5a expression in HCC cells [227] suggests the role of wnt5a in the clinical relevance of HBV at least in HBV-related liver diseases. Thus noncanonical Wnts may be used as to predict HCC prognosis.

In this study we also showed that well-differentiated cell lines showed active canonical Wnt signaling at variable degrees with high signaling activity was associated with β-catenin and Axin1 mutations in two well differentiated cell lines. For the other two well differentiated cell lines we also showed some activity but the functional significance is not known [5].

Stem cell and cancer cell self-renewal in other cancer types has been shown to have canonical Wnt signaling activity and thus the presence of canonical wnt signalling activity in well-differentiated-HCC cell lines such as HepG2, Huh7 and PLC/PRF/5 may be linked with HCC stem cells [228].

Our third observation was poorly differentiated cell lines do not have canonical Wnt signaling activity in six out of seven poorly differentiated cell lines. Even a poorly differentiated cell 475 cell line with deleterious Axin1 mutation (SNU475) lacked canonical activity. Thus this suggests the presence of an active repression of activity in these cells. Transient or Tet-regulated expression of mutant β-catenin failed to induce canonical Wnt signaling activity in two different poorly differentiated cell lines. Using confocal imaging we linked this weak activity to poor nuclear accumulation of β-catenin in SNU449.cl8 cell line.

Wnt5a act as an antagonist and regulator of β-catenin levels in other cell types [216-217]. Hereby we also showed that Wnt5a-expressing plasmid can significantly inhibit canonical Wnt signaling in HCC cells. The mechanism of Wnt5a antagonism is not known yet. In breast cancer cells, nuclear beta-catenin and expression of target genes were observed when wnt5a is lost [229]. The results that ectopically and endogenously expressed N-terminally truncated forms of β-catenin suggest that Wnt5a is acting downstream to β-catenin. Wnt5a can inhibit canonical Wnt signaling either by proteasomal degradation [230], or, by downregulating TCF activity without influencing β-catenin levels [198] in kidney epithelial cells. such models can very well be applied to our findings. Knockdown of noncanonical Wnt ligands in poorly differentiated HCC cell lines may help to elucidate the mechanisms of lack of canonical wnt signalling in liver cancer.

Wnt5a can be a tumor suppressor or oncogenic depending on cellular context. Wnt5a plays an oncogenic role in melanoma, gastric, pancreas, prostate cancer, but as a tumor suppressor role in HCC, neuroblastoma, leukemia, colon, and thyroid cancers [206]. It may have a role in tumor progression by inducing EMT. Furthermore, the Wnt5A/Protein kinase C pathway was shown to activate invasion in melanoma cells via of an EMT [68]. Similarly pancreas cancer

cells expressed CUTL1 that also upregulates Wnt5a and induced migration, proliferation and invasiveness [231].

To sum up we showed that canonical Wnt activity is active in well-differentiated, but repressed in poorly differentiated HCC cell lines may also implicate the association of β-catenin mutations with well-differentiated, but not in poorly differentiated tumors and that a dual function of Wnt signaling cancer initiation and tumor progression.

5.2 Selective monoclonal antibodies directed against C-terminal domain of β–Catenin

We used immunofluorescence and immunohistochemistry studies using a panel of tumor cells to further characterize the antibodies that we have developed in our laboratory and their selective affinity to the different cellular and functional forms of beta-catenin. When we consider the fact that beta-catenin protein can be found in three different subcellular localizations with different modes of regulation in complex with several different types of proteins and interaction partners, the use of antibodies showing selective affinity to dissect different subcellular localizations and functionally active beta-catenin gains a significant amount of importance. This complexity of beta-catenin is partially due to the different interaction partners which also depend on the presence of beta-catenin in different subcellular portions of the cells. In figure 1.3, we mapped the sites of interaction of several different β-Catenin binding proteins along the beta-catenin protein. Our Mabs, 4C9 and 9E10 clones were directed on the very C-terminal end, partially overlapping on the last 10 aminoasid residues of the β-catenin protein. We were able to find 10 different proteins which can localize this part of β-catenin in the literature. Together with well known interactors of β-catenin such as TBP, Chibby, Theashirt, CBP/p300, 6 different PDZ domain proteins (Lin-7, TIP1, S-SCAM, MAGI-1, NHERF-1, NHERF-2) can also bind this region (figure 1.3). Thus there is a competition for binding this region. In order for 4C9 and 9E10 Mabs to bind their epitopes, this part of the protein should be free of PDZ proteins and be conformationally available. Compared to commercial antibody, confocal microscopy analysis showed that our hybridomas successfully reacted against β-catenin in the nucleus and cytoplasm whereas membrane staining was more intense with commercial anti-β-Catenin antibody in APC mutated colorectal carcinoma cell lines; SW480 and SW837 and beta-catenin mutant cell line Snu398 cell lines. As a result the selective immunoreactivity of our hybridomas towards cytoplasmic and nuclear β-Catenin but not to membrane bound form of β-Catenin can be

explained due to the availability of the last 10 aminoasid residues of β-Catenin in cytoplasmic and nuclear pools of β-Catenin protein. For example, PDZ binding proteins are known to anchor their binding partners in close proximity of plasma membrane and are expected to interact with membrane bound form of beta-catenin but not with the nuclear pool of beta-catenin. This data explains why we can detect nuclear and cytoplasmic beta-catenin with our hybridomas directed against this PDZ domain but not with commercial antibody. The strong selective immunoreactivity of our antibodies is also proven by ΔN-β-Catenin expressing inducible clone of HCC cell line Snu449-c8. In the presence accumulating mutant β-Catenin, both antibodies showed the increased immunoreactivity only to cytoplasmic and nuclear β-Catenin whereas commercial antibody failed to show such specific increased immunoreactivity.

Unfortunately, we failed to show such specific immunoreactivity in tumor samples of different organs. In most of the cases except colon carcinoma samples, our antibodies reacted well against membrane bound form of β-Catenin. We can explain such a discrepancy by the lack of deparaffinization procedure in immunofluorescence techniques. The denaturation protocol for paraffin embedded tissue samples may help the membrane bound β-Catenin protein readily available compared to cytoplasmic and nuclear form of β-Catenin.

Activating mutations (APC and beta-catenin mutations and/or constitutive activation by Wnt ligands) in the Wnt/β-Catenin pathway elements lead to accumulation of β-Catenin in the cytoplasm as well as in the nucleus where it interacts with TCF/LEF family of transcription factors and activates transcription of the Wnt responsive genes. The specific immunoreactivity of active beta-catenin staining by these antibodies makes them more valuable due to their recognition of β-Catenin with diverse functions. Our tissue staining data showed that these antibodies have the capacity to detect β-Catenin pools which has oncogenic roles in different cancer types. 9E10 antibody staining in different types of tumor tissues showed that only a subset of colon carcinoma tissues are nuclear positive. In the literature similar findings were associated with a subset of tumors harboring APC or beta-catenin mutations leading to accumulation of oncogenic beta-catenin. In correlation with this data, breast and endometrium cancer tissue samples which are known to be APC and beta-catenin mutation negative were found to be nuclear negative. Nuclear positivity detected by these antibodies (4C9 and 9E10) would be an indicative of presence of APC and activating beta-catenin mutations in the tissue samples. In

conclusion, these anti β-catenin antibodies not only showed a great potential to detect different cellular functions, as well as tumor-associated aberrations of β-catenin protein in the clinical studies but also they may serve as an important tool to decipher several interacting partners of beta-catenin to decipher their role in contribution to carcinogenesis.

5.3 Screening of human kinome and Phosphatome

In order to identify novel pro-senescence targets, we performed siRNA screening for kinases and phosphatases. We determined a set of kinases and phosphatases for siRNA screening using differentially expressed genes obtained from microarray data with isogenic senescent and immortal HCC cells, as well as cirrhosis and HCC tissues. From a list of 518 kinase and 223 phosphatases, we identified126 kinase genes and 28 phosphatase genes that are upregulated in immortal HCC cells. Using a sensitive method to quantify cell viability after transfection, we screened all kinase and phosphatase genes. Thus we have identified kinases or phosphatases that might have significant role in HCC cell survival. Genes showing least viability after sulphordamine-B assay identified as essential kinases or phosphatases whose knock-down induced cellular senescence, apoptosis and growth arrest.

Three different siRNA sequences were used to eliminate the off-target effect; therefore our assay is specific to identify the role of each gene.

Among all the kinases tested, 6% of all kinases (8/126) and 17% (5/28) were found to be essential for cell survival. Among these kinases, CDK1, CDK2, PcTaire2, CHK2, and PLK1 were already implicated in cell cycle and mitosis. MYLK, CAMK2d, and CAMK1a are also implicated in cell signaling and survival.

The effect of knock-down of phosphatases could be investigated under two different groups, one group of phosphatases whose knock-down decreased the cell survival and the other group whose knock-down help cells to increase cell survival. The knock-down of these phosphatases might derepress the oncogenic enzymes or pathways, thus activate survival of cells. The second group could be explained by their antagonistic role against kinases which are oncogenic and upstream of these kinases in the same pathway or cross-talk of pathways which are quite common for kinase signaling pathways.

We also developed in vivo screening method using xenograft models in nude mice. Using the same sequences against kinases validated in vitro we can test the effect of knock-down using

this xenograft models. We failed to image these tumors in vivo using Alexa labelled RAFT-RGD and Alexa- labelled Transferrin dyes. This might be cell type dependent, because liver cells express transferrin receptors. Therefore other cell lines can be tested for transferrin receptor expression.

5.4 Histone methylation and Role of histone modifying enzymes in liver cancer

In this study, for the first time, we showed and mapped the global methylation status of each histone methylation residues for immortal and senescent liver cells. These marks are good candidates to predict disease prognosis and reveals potential therapeutic targets for HCC. We also characterized histone modifying enzymes that play a significant role and aberrantly expressed in liver cancer cells. By using knock-down and overexpression studies, we tried to dissect the role of these histone modifying enzymes in liver cancer. We made a preliminary screen using lentiviruses targeting 6 different histone modifying enzymes, but we failed to show any phenotype after knock-down using RNAi.

Among these enzymes, we further screened these enzymes whose inhibition would induce cell senescence in liver cancer and investigate their role in senescence. On the transcriptional level, we failed to show any affect on expression of tumor suppressor proteins such as p21, p16 and p15 in two different cell lines. This may be explained by the redundancy of enzymes working in the same residues and dynamic regulation of these modifications.

We further characterized the role of suv420H1 gene in liver cancer. By ectopic overexpression studies, we showed that suv420H1 enzyme is responsible for trimethylation of H4K20 residue and aberrant nuclei containing cells are formed after transient transfection. We checked the DNA damage after transient overexpression but we failed to show a role of suv420H1 in induction of DNA damage. Since H4K20me3 is involved in gene silencing, we asked whether induction of SUV420H1 enzyme in liver cancer would restore the imprinting of H19 gene. Overexpression of SUV420H1 did not restore the imprinting of H19 gene in liver cancer cells. However the restore of monoallelic expression might require combinatory involvement of epigenetic changes like histone methylation and DNA methylation on the promoter and imprinting control center of H19 gene.

5.5 Role of ATAD2 in hepatocellular carcinoma

ATAD2 has been suggested as a driver gene for genomic amplification at chromosome 8q23 in HCC many years ago, based on comparative genomic expression analysis [232]. Despite this provocative observation published eight years ago, the role of ATAD2 in HCC remains totally unknown. We performed preliminary experiments in relation with its potential role in senescence bypass and HCC malignancy. Firstly, we showed that ATAD2 protein expression is low or undetectable in normal liver as well as in isolated human hepatocytes. In contrast, its expression was upregulated in HCC cell lines. Similarly, experiments with tumor tissue arrays indicated that it was frequently overexpressed in a subset of advanced HCC tumors. We also showed that ATAD2 protein is overexpressed in liver cancer samples with an increased of positivity of advanced tumors. Downregulation of ATAD2 expression by specific siRNAs in normal fibroblasts (MRC5) and HeLa cells was associated with an increased in senescence-associated beta-galactosidase (SABG) activity and decreased BrdU incorporation into cellular DNA (Fig. 2A). In addition, both cell lines displayed decreased colony forming ability following ATAD2 inactivation (Fig. 2B). These effects were accompanied with both p53 and $p21^{Cip1}$ accumulation in HeLa cells (Fig, 2C), strongly suggesting that ATAD2 may help cancer cells to bypass senescence arrest by neutralizing $p21^{Cip1}$-mediated inhibition of pRb phosphorylation. Interestingly, ATAD2 downregulation in p53- and pRb-deficient Hep3B cells resulted in massive apoptotic response (Fig. 2D), strongly suggesting that it may participate to several tumor survival mechanisms. Our preliminary findings provide proof-of-principle that the inhibition of ATAD2 may represent a promising approach for HCC therapy. Based on our preliminary data, our goal is to substantiate the potential oncogenic role of ATAD2 gene in HCC.

We also showed that ATAD2 knockdown increased global histone acetylation levels significantly contributing to activation of apoptosis related genes. Correlated with this finding p300 histone acetyltransferase levels were upregulated in two cell lines tested. Further support came from the treatment of these cell lines with TSA. TSA treatment of HCC cells induced apoptosis with increased levels of global acetylation.

As ATAD2 is an acetylated histone-binding protein, we also tested the combinatory anti-tumor effects of histone deacetylase inhibitors together with ATAD2 inactivation by RNA interference. Treatment of Hela cells with different doses of TSA after ATAD2 siRNA transfection, decreased the colony formation capacity of these cells.

CHAPTER 6. FUTURE PERSPECTIVES

Histone modifying enzymes acting on the same residues can be targeted at the same time to eliminate the redundancy problem. As performed for protein kinases, histone methylation enzymes can be screened or targeted with small molecule inhibitors acting on a family of enzymes having the same active region.

In relation with a potential oncogenic role of ATAD2 in HCC, we need to elucidate the oncogenic role of ATAD2 by testing the potential role of ATAD2 in senescence bypass. Overexpression of ATAD2 in mortal cells like MRC5 cells may be performed and cells will then be challenged to replicative senescence by in vitro passaging or to oncogene-induced senescence by retroviral expression of H-Ras^{V12} or DNA Damage models.

To identify the ATAD2 regulated genes in liver cancer, global gene expression analysis or high throughput sequencing (CHIP-seq) can be performed. The testing of ATAD2 protein as a potential tumor marker can be performed, the number of sections of several numbers of cirrhotic and cancer samples can be stained and prognostic potential of ATAD2 protein can be shown.

For kinase and phosphatases identified in vitro using siRNA screening should be validated in vivo and the specific role of each enzyme should be also investigated using overexpression and knock-down studies. The pathways in which these kinases are acting can also be targeted with specific inhibitors.

REFERENCES

1. Bruix, J., et al., *Focus on hepatocellular carcinoma.* Cancer Cell, 2004. **5**: p. 215 - 219.
2. Kojiro, M., *Histopathology of liver cancers.* Best Pract Res Clin Gastroenterol, 2005. **19**: p. 39 - 62.
3. Abelev, G. and N. Lazarevich, *Control of differentiation in progression of epithelial tumors.* Adv Cancer Res, 2006. **95**: p. 61 - 113.
4. Hsu, H., et al., *Tumor invasiveness and prognosis in resected hepatocellular carcinoma. Clinical and pathogenetic implications.* Cancer, 1988. **61**: p. 2095 - 2099.
5. Yuzugullu, H., et al., *Canonical Wnt signaling is antagonized by noncanonical Wnt5a in hepatocellular carcinoma cells.* Molecular Cancer, 2009. **8**(1): p. 90.
6. Thorgeirsson, S. and J. Grisham, *Molecular pathogenesis of human hepatocellular carcinoma.* Nat Genet, 2002. **31**: p. 339 - 346.
7. Bosch, F.X., J. Ribes, and J. Borras, *Epidemiology of primary liver cancer.* Semin Liver Dis, 1999. **19**(3): p. 271-85.
8. Farazi, P.A. and R.A. DePinho, *Hepatocellular carcinoma pathogenesis: from genes to environment.* Nat Rev Cancer, 2006. **6**(9): p. 674-87.
9. Limdi, J.K. and J.R. Crampton, *Hereditary haemochromatosis.* QJM, 2004. **97**(6): p. 315-24.
10. El-Serag, H.B., T. Tran, and J.E. Everhart, *Diabetes increases the risk of chronic liver disease and hepatocellular carcinoma.* Gastroenterology, 2004. **126**(2): p. 460-8.
11. Farrell, G.C. and C.Z. Larter, *Nonalcoholic fatty liver disease: from steatosis to cirrhosis.* Hepatology, 2006. **43**(2 Suppl 1): p. S99-S112.
12. Tannapfel, A. and C. Wittekind, *Genes involved in hepatocellular carcinoma: deregulation in cell cycling and apoptosis.* Virchows Arch, 2002. **440**(4): p. 345-52.
13. Ozturk, M., et al., *Senescence and immortality in hepatocellular carcinoma.* Cancer Lett, 2009. **286**(1): p. 103-13.
14. Lavanchy, D., *Hepatitis B virus epidemiology, disease burden, treatment, and current and emerging prevention and control measures.* J Viral Hepat, 2004. **11**(2): p. 97-107.
15. Lavanchy, D., *Worldwide epidemiology of HBV infection, disease burden, and vaccine prevention.* J Clin Virol, 2005. **34 Suppl 1**: p. S1-3.
16. Block, T.M., et al., *Molecular viral oncology of hepatocellular carcinoma.* Oncogene, 2003. **22**(33): p. 5093-107.
17. Tokino, T., et al., *Chromosome deletions associated with hepatitis B virus integration.* Virology, 1991. **185**(2): p. 879-82.
18. Nijhara, R., et al., *An internal segment (residues 58-119) of the hepatitis B virus X protein is sufficient to activate MAP kinase pathways in mouse liver.* FEBS Lett, 2001. **504**(1-2): p. 59-64.
19. Feitelson, M.A., et al., *Genetic mechanisms of hepatocarcinogenesis.* Oncogene, 2002. **21**(16): p. 2593-604.
20. Ueda, H., et al., *Functional inactivation but not structural mutation of p53 causes liver cancer.* Nat Genet, 1995. **9**(1): p. 41-7.
21. Rehermann, B. and M. Nascimbeni, *Immunology of hepatitis B virus and hepatitis C virus infection.* Nat Rev Immunol, 2005. **5**(3): p. 215-29.

22. Rehermann, B., *Immune responses in hepatitis B virus infection.* Semin Liver Dis, 2003. **23**(1): p. 21-38.
23. Park, K.J., et al., *1Hepatitis C virus NS5A protein modulates c-Jun N-terminal kinase through interaction with tumor necrosis factor receptor-associated factor 2.* J Biol Chem, 2003. **278**(33): p. 30711-8.
24. Majumder, M., et al., *Hepatitis C virus NS5A protein impairs TNF-mediated hepatic apoptosis, but not by an anti-FAS antibody, in transgenic mice.* Virology, 2002. **294**(1): p. 94-105.
25. Melen, K., et al., *Expression of hepatitis C virus core protein inhibits interferon-induced nuclear import of STATs.* J Med Virol, 2004. **73**(4): p. 536-47.
26. McKillop, I.H. and L.W. Schrum, *Alcohol and liver cancer.* Alcohol, 2005. **35**(3): p. 195-203.
27. Bressac, B., et al., *Selective G to T mutations of p53 gene in hepatocellular carcinoma from southern Africa.* Nature, 1991. **350**(6317): p. 429-31.
28. Hsu, I.C., et al., *Mutational hotspot in the p53 gene in human hepatocellular carcinomas.* Nature, 1991. **350**(6317): p. 427-8.
29. Kew, M.C., *Synergistic interaction between aflatoxin B1 and hepatitis B virus in hepatocarcinogenesis.* Liver Int, 2003. **23**(6): p. 405-9.
30. Gramantieri, L., et al., *Cyclin G1 is a target of miR-122a, a microRNA frequently down-regulated in human hepatocellular carcinoma.* Cancer Res, 2007. **67**(13): p. 6092-9.
31. Ladeiro, Y., et al., *MicroRNA profiling in hepatocellular tumors is associated with clinical features and oncogene/tumor suppressor gene mutations.* Hepatology, 2008. **47**(6): p. 1955-63.
32. Kota, J., et al., *Therapeutic microRNA delivery suppresses tumorigenesis in a murine liver cancer model.* Cell, 2009. **137**(6): p. 1005-17.
33. Oda, T., et al., *p53 gene mutation spectrum in hepatocellular carcinoma.* Cancer Res, 1992. **52**(22): p. 6358-64.
34. Puisieux, A. and M. Ozturk, *TP53 and hepatocellular carcinoma.* Pathol Biol (Paris), 1997. **45**(10): p. 864-70.
35. De Souza, A.T., et al., *M6P/IGF2R gene is mutated in human hepatocellular carcinomas with loss of heterozygosity.* Nat Genet, 1995. **11**(4): p. 447-9.
36. Yamada, T., et al., *Loss of the gene encoding mannose 6-phosphate/insulin-like growth factor II receptor is an early event in liver carcinogenesis.* Proc Natl Acad Sci U S A, 1997. **94**(19): p. 10351-5.
37. Terris, B., et al., *Close correlation between beta-catenin gene alterations and nuclear accumulation of the protein in human hepatocellular carcinomas.* Oncogene, 1999. **18**(47): p. 6583-8.
38. Nhieu, J.T., et al., *Nuclear accumulation of mutated beta-catenin in hepatocellular carcinoma is associated with increased cell proliferation.* Am J Pathol, 1999. **155**(3): p. 703-10.
39. Liew, C.T., et al., *High frequency of p16INK4A gene alterations in hepatocellular carcinoma.* Oncogene, 1999. **18**(3): p. 789-95.
40. Taniguchi, K., et al., *Mutational spectrum of beta-catenin, AXIN1, and AXIN2 in hepatocellular carcinomas and hepatoblastomas.* Oncogene, 2002. **21**: p. 4863 - 4871.
41. Yakicier, M.C., et al., *Smad2 and Smad4 gene mutations in hepatocellular carcinoma.* Oncogene, 1999. **18**(34): p. 4879-83.

42. Katagiri, T., Y. Nakamura, and Y. Miki, *Mutations in the BRCA2 gene in hepatocellular carcinomas.* Cancer Res, 1996. **56**(20): p. 4575-7.
43. Zhang, D.E., et al., *Function of PU.1 (Spi-1), C/EBP, and AML1 in early myelopoiesis: regulation of multiple myeloid CSF receptor promoters.* Curr Top Microbiol Immunol, 1996. **211**: p. 137-47.
44. Shen, H.M. and C.N. Ong, *Mutations of the p53 tumor suppressor gene and ras oncogenes in aflatoxin hepatocarcinogenesis.* Mutat Res, 1996. **366**(1): p. 23-44.
45. Verdun, R.E. and J. Karlseder, *Replication and protection of telomeres.* Nature, 2007. **447**(7147): p. 924-31.
46. Grisham, J.W., *Hepatocyte lineages: of clones, streams, patches, and nodules in the liver.* Hepatology, 1997. **25**(1): p. 250-2.
47. Osada, T., et al., *E-cadherin is involved in the intrahepatic metastasis of hepatocellular carcinoma.* Hepatology, 1996. **24**: p. 1460 - 1467.
48. Sugimachi, K., et al., *Transcriptional repressor snail and progression of human hepatocellular carcinoma.* Clin Cancer Res, 2003. **9**: p. 2657 - 2664.
49. Lee, T., et al., *Twist overexpression correlates with hepatocellular carcinoma metastasis through induction of epithelial-mesenchymal transition.* Clin Cancer Res, 2006. **12**: p. 5369 - 5376.
50. Hu, L., et al., *Association of Vimentin overexpression and hepatocellular carcinoma metastasis.* Oncogene, 2004. **23**: p. 298 - 302.
51. Cicchini, C., et al., *Snail controls differentiation of hepatocytes by repressing HNF4alpha expression.* J Cell Physiol, 2006. **209**: p. 230 - 238.
52. Giannelli, G., et al., *Laminin-5 with transforming growth factor-beta1 induces epithelial to mesenchymal transition in hepatocellular carcinoma.* Gastroenterology, 2005. **129**: p. 1375 - 1383.
53. Lee, H., et al., *Loss of Raf kinase inhibitor protein promotes cell proliferation and migration of human hepatoma cells.* Gastroenterology, 2006. **131**: p. 1208 - 1217.
54. Fuchs, B., et al., *Epithelial-to-mesenchymal transition and integrin-linked kinase mediate sensitivity to epidermal growth factor receptor inhibition in human hepatoma cells.* Cancer Res, 2008. **68**: p. 2391 - 2399.
55. Matsuo, N., et al., *Twist expression promotes migration and invasion in hepatocellular carcinoma.* BMC Cancer, 2009. **9**: p. 240.
56. Miyoshi, A., et al., *Snail and SIP1 increase cancer invasion by upregulating MMP family in hepatocellular carcinoma cells.* Br J Cancer, 2004. **90**: p. 1265 - 1273.
57. Parviz, F., et al., *Hepatocyte nuclear factor 4alpha controls the development of a hepatic epithelium and liver morphogenesis.* Nat Genet, 2003. **34**: p. 292 - 296.
58. Battle, M., et al., *Hepatocyte nuclear factor 4alpha orchestrates expression of cell adhesion proteins during the epithelial transformation of the developing liver.* Proc Natl Acad Sci USA, 2006. **103**: p. 8419 - 8424.
59. Lazarevich, N., et al., *Progression of HCC in mice is associated with a downregulation in the expression of hepatocyte nuclear factors.* Hepatology, 2004. **39**: p. 1038 - 1047.
60. Gregorieff, A. and H. Clevers, *Wnt signaling in the intestinal epithelium: from endoderm to cancer.* Genes Dev, 2005. **19**(8): p. 877-90.
61. Hsu, H., et al., *Beta-catenin mutations are associated with a subset of low-stage hepatocellular carcinoma negative for hepatitis B virus and with favorable prognosis.* Am J Pathol, 2000. **157**: p. 763 - 770.

62. Audard, V., et al., *Cholestasis is a marker for hepatocellular carcinomas displaying beta-catenin mutations.* J Pathol, 2007. **212**: p. 345 - 352.
63. Mao, T., et al., *Expression of mutant nuclear beta-catenin correlates with non-invasive hepatocellular carcinoma, absence of portal vein spread, and good prognosis.* J Pathol, 2001. **193**: p. 95 - 101.
64. Wong, C., S. Fan, and I. Ng, *beta-Catenin mutation and overexpression in hepatocellular carcinoma: clinicopathologic and prognostic significance.* Cancer, 2001. **92**: p. 136 - 145.
65. Laurent-Puig, P. and J. Zucman-Rossi, *Genetics of hepatocellular tumors.* Oncogene, 2006. **25**: p. 3778 - 3786.
66. Calvisi, D., et al., *Activation of beta-catenin during hepatocarcinogenesis in transgenic mouse models: relationship to phenotype and tumor grade.* Cancer Res, 2001. **61**: p. 2085 - 2091.
67. Barker, N. and H. Clevers, *Mining the Wnt pathway for cancer therapeutics.* Nat Rev Drug Discov, 2006. **5**: p. 997 - 1014.
68. Cadoret, A., et al., *New targets of beta-catenin signaling in the liver are involved in the glutamine metabolism.* Oncogene, 2002. **21**: p. 8293 - 8301.
69. Harada, N., et al., *Lack of tumorigenesis in the mouse liver after adenovirus-mediated expression of a dominant stable mutant of beta-catenin.* Cancer Res, 2002. **62**: p. 1971 - 1977.
70. Harada, N., et al., *Intestinal polyposis in mice with a dominant stable mutation of the beta-catenin gene.* EMBO J, 1999. **18**: p. 5931 - 5942.
71. Nelson, W.J. and R. Nusse, *Convergence of Wnt, beta-catenin, and cadherin pathways.* Science, 2004. **303**(5663): p. 1483-7.
72. Reya, T. and H. Clevers, *Wnt signalling in stem cells and cancer.* Nature, 2005. **434**: p. 843 - 850.
73. Schneider, S.Q., J.R. Finnerty, and M.Q. Martindale, *Protein evolution: structure-function relationships of the oncogene beta-catenin in the evolution of multicellular animals.* J Exp Zool B Mol Dev Evol, 2003. **295**(1): p. 25-44.
74. Daniels, D.L., K. Eklof Spink, and W.I. Weis, *beta-catenin: molecular plasticity and drug design.* Trends Biochem Sci, 2001. **26**(11): p. 672-8.
75. Aberle, H., et al., *Assembly of the cadherin-catenin complex in vitro with recombinant proteins.* J Cell Sci, 1994. **107 (Pt 12)**: p. 3655-63.
76. Pokutta, S. and W.I. Weis, *Structure of the dimerization and beta-catenin-binding region of alpha-catenin.* Mol Cell, 2000. **5**(3): p. 533-43.
77. Wu, G., et al., *Structure of a beta-TrCP1-Skp1-beta-catenin complex: destruction motif binding and lysine specificity of the SCF(beta-TrCP1) ubiquitin ligase.* Mol Cell, 2003. **11**(6): p. 1445-56.
78. Choi, H.J., A.H. Huber, and W.I. Weis, *Thermodynamics of beta-catenin-ligand interactions: the roles of the N- and C-terminal tails in modulating binding affinity.* J Biol Chem, 2006. **281**(2): p. 1027-38.
79. Xing, Y., et al., *Crystal structure of a beta-catenin/axin complex suggests a mechanism for the beta-catenin destruction complex.* Genes Dev, 2003. **17**(22): p. 2753-64.
80. Takemaru, K., et al., *Chibby, a nuclear beta-catenin-associated antagonist of the Wnt/Wingless pathway.* Nature, 2003. **422**(6934): p. 905-9.
81. Graham, T.A., et al., *The crystal structure of the beta-catenin/ICAT complex reveals the inhibitory mechanism of ICAT.* Mol Cell, 2002. **10**(3): p. 563-71.

82. Hecht, A., et al., *The p300/CBP acetyltransferases function as transcriptional coactivators of beta-catenin in vertebrates.* EMBO J, 2000. **19**(8): p. 1839-50.
83. Gallet, A., et al., *The C-terminal domain of armadillo binds to hypophosphorylated teashirt to modulate wingless signalling in Drosophila.* EMBO J, 1999. **18**(8): p. 2208-17.
84. Koike, M., et al., *beta-Catenin shows an overlapping sequence requirement but distinct molecular interactions for its bidirectional passage through nuclear pores.* J Biol Chem, 2004. **279**(32): p. 34038-47.
85. Krieghoff, E., J. Behrens, and B. Mayr, *Nucleo-cytoplasmic distribution of beta-catenin is regulated by retention.* J Cell Sci, 2006. **119**(Pt 7): p. 1453-63.
86. Hall, R.A., et al., *A C-terminal motif found in the beta2-adrenergic receptor, P2Y1 receptor and cystic fibrosis transmembrane conductance regulator determines binding to the Na+/H+ exchanger regulatory factor family of PDZ proteins.* Proc Natl Acad Sci U S A, 1998. **95**(15): p. 8496-501.
87. Nishimura, W., et al., *Interaction of synaptic scaffolding molecule and Beta -catenin.* J Neurosci, 2002. **22**(3): p. 757-65.
88. Yamada, H., et al., *Reconstructed beta-catenin/TCF4 signaling in yeast applicable to functional evaluation of APC mutations.* Am J Pathol, 2003. **163**(6): p. 2201-9.
89. Hirabayashi, Y., et al., *The Wnt/beta-catenin pathway directs neuronal differentiation of cortical neural precursor cells.* Development, 2004. **131**(12): p. 2791-801.
90. Sumita, K., et al., *Synaptic scaffolding molecule (S-SCAM) membrane-associated guanylate kinase with inverted organization (MAGI)-2 is associated with cell adhesion molecules at inhibitory synapses in rat hippocampal neurons.* J Neurochem, 2007. **100**(1): p. 154-66.
91. Dobrosotskaya, I.Y. and G.L. James, *MAGI-1 interacts with beta-catenin and is associated with cell-cell adhesion structures.* Biochem Biophys Res Commun, 2000. **270**(3): p. 903-9.
92. Shibata, T., et al., *EBP50, a beta-catenin-associating protein, enhances Wnt signaling and is over-expressed in hepatocellular carcinoma.* Hepatology, 2003. **38**(1): p. 178-86.
93. Kreimann, E.L., et al., *Cortical stabilization of beta-catenin contributes to NHERF1/EBP50 tumor suppressor function.* Oncogene, 2007. **26**(36): p. 5290-9.
94. Theisen, C.S., et al., *NHERF links the N-cadherin/catenin complex to the platelet-derived growth factor receptor to modulate the actin cytoskeleton and regulate cell motility.* Mol Biol Cell, 2007. **18**(4): p. 1220-32.
95. Kanamori, M., et al., *The PDZ protein tax-interacting protein-1 inhibits beta-catenin transcriptional activity and growth of colorectal cancer cells.* J Biol Chem, 2003. **278**(40): p. 38758-64.
96. Besser, J., et al., *Tip-1 induces filopodia growth and is important for gastrulation movements during zebrafish development.* Dev Growth Differ, 2007. **49**(3): p. 205-14.
97. Perego, C., et al., *Mammalian LIN-7 PDZ proteins associate with beta-catenin at the cell-cell junctions of epithelia and neurons.* EMBO J, 2000. **19**(15): p. 3978-89.
98. Salinas, P.C. and S.R. Price, *Cadherins and catenins in synapse development.* Curr Opin Neurobiol, 2005. **15**(1): p. 73-80.
99. Bamji, S.X., et al., *Role of beta-catenin in synaptic vesicle localization and presynaptic assembly.* Neuron, 2003. **40**(4): p. 719-31.
100. Deng, F., et al., *Stargazin and other transmembrane AMPA receptor regulating proteins interact with synaptic scaffolding protein MAGI-2 in brain.* J Neurosci, 2006. **26**(30): p. 7875-84.

101. Sakurai, A., et al., *MAGI-1 is required for Rap1 activation upon cell-cell contact and for enhancement of vascular endothelial cadherin-mediated cell adhesion.* Mol Biol Cell, 2006. **17**(2): p. 966-76.
102. Elul, T.M., et al., *N- and C-terminal domains of beta-catenin, respectively, are required to initiate and shape axon arbors of retinal ganglion cells in vivo.* J Neurosci, 2003. **23**(16): p. 6567-75.
103. Rubin, G.M., et al., *Comparative genomics of the eukaryotes.* Science, 2000. **287**(5461): p. 2204-15.
104. Lander, E.S., et al., *Initial sequencing and analysis of the human genome.* Nature, 2001. **409**(6822): p. 860-921.
105. Manning, G., *Genomic overview of protein kinases.* WormBook, 2005: p. 1-19.
106. Zhang, Z.Y., B. Zhou, and L. Xie, *Modulation of protein kinase signaling by protein phosphatases and inhibitors.* Pharmacol Ther, 2002. **93**(2-3): p. 307-17.
107. Mumby, M.C. and G. Walter, *Protein serine/threonine phosphatases: structure, regulation, and functions in cell growth.* Physiol Rev, 1993. **73**(4): p. 673-99.
108. Camps, M., A. Nichols, and S. Arkinstall, *Dual specificity phosphatases: a gene family for control of MAP kinase function.* FASEB J, 2000. **14**(1): p. 6-16.
109. Baumer, N., et al., *Expression of protein histidine phosphatase in Escherichia coli, purification, and determination of enzyme activity.* Methods Mol Biol, 2007. **365**: p. 247-60.
110. Maehama, T., F. Okahara, and Y. Kanaho, *The tumour suppressor PTEN: involvement of a tumour suppressor candidate protein in PTEN turnover.* Biochem Soc Trans, 2004. **32**(Pt 2): p. 343-7.
111. Hanahan, D. and R.A. Weinberg, *The hallmarks of cancer.* Cell, 2000. **100**(1): p. 57-70.
112. Blume-Jensen, P. and T. Hunter, *Oncogenic kinase signalling.* Nature, 2001. **411**(6835): p. 355-65.
113. Cohen, P., *Protein kinases--the major drug targets of the twenty-first century?* Nat Rev Drug Discov, 2002. **1**(4): p. 309-15.
114. Schmitz, K.J., et al., *Activation of the ERK and AKT signalling pathway predicts poor prognosis in hepatocellular carcinoma and ERK activation in cancer tissue is associated with hepatitis C virus infection.* J Hepatol, 2008. **48**(1): p. 83-90.
115. Villanueva, A., et al., *Pivotal role of mTOR signaling in hepatocellular carcinoma.* Gastroenterology, 2008. **135**(6): p. 1972-83, 1983 e1-11.
116. Calvisi, D.F., et al., *Ubiquitous activation of Ras and Jak/Stat pathways in human HCC.* Gastroenterology, 2006. **130**(4): p. 1117-28.
117. Reik, W. and J. Walter, *Genomic imprinting: parental influence on the genome.* Nat Rev Genet, 2001. **2**(1): p. 21-32.
118. Matouk, I.J., et al., *The H19 non-coding RNA is essential for human tumor growth.* PLoS One, 2007. **2**(9): p. e845.
119. Cariani, E., et al., *Differential expression of insulin-like growth factor II mRNA in human primary liver cancers, benign liver tumors, and liver cirrhosis.* Cancer Res, 1988. **48**(23): p. 6844-9.
120. Ng, I.O., et al., *Expression of insulin-like growth factor II mRNA in hepatocellular carcinoma.* J Gastroenterol Hepatol, 1998. **13**(2): p. 152-7.
121. Aihara, T., et al., *Clonal analysis of precancerous lesion of hepatocellular carcinoma.* Gastroenterology, 1996. **111**(2): p. 455-61.

122. Li, X., et al., *Disrupted IGF2 promoter control by silencing of promoter P1 in human hepatocellular carcinoma.* Cancer Res, 1997. **57**(10): p. 2048-54.
123. Takubo, K., et al., *Telomere lengths are characteristic in each human individual.* Exp Gerontol, 2002. **37**(4): p. 523-31.
124. Aikata, H., et al., *Telomere reduction in human liver tissues with age and chronic inflammation.* Exp Cell Res, 2000. **256**(2): p. 578-82.
125. Michalopoulos, G.K., *Liver regeneration.* J Cell Physiol, 2007. **213**(2): p. 286-300.
126. Utoh, R., et al., *Susceptibility of chimeric mice with livers repopulated by serially subcultured human hepatocytes to hepatitis B virus.* Hepatology, 2008. **47**(2): p. 435-46.
127. Delhaye, M., et al., *Relationship between hepatocyte proliferative activity and liver functional reserve in human cirrhosis.* Hepatology, 1996. **23**(5): p. 1003-11.
128. Campisi, J. and F. d'Adda di Fagagna, *Cellular senescence: when bad things happen to good cells.* Nat Rev Mol Cell Biol, 2007. **8**(9): p. 729-40.
129. Paradis, V., et al., *Replicative senescence in normal liver, chronic hepatitis C, and hepatocellular carcinomas.* Hum Pathol, 2001. **32**(3): p. 327-32.
130. Ozturk, N., et al., *Reprogramming of replicative senescence in hepatocellular carcinoma-derived cells.* Proc Natl Acad Sci U S A, 2006. **103**(7): p. 2178-83.
131. Xue, W., et al., *Senescence and tumour clearance is triggered by p53 restoration in murine liver carcinomas.* Nature, 2007. **445**(7128): p. 656-60.
132. Wu, C.H., et al., *Cellular senescence is an important mechanism of tumor regression upon c-Myc inactivation.* Proc Natl Acad Sci U S A, 2007. **104**(32): p. 13028-33.
133. Fraga, M.F., et al., *Loss of acetylation at Lys16 and trimethylation at Lys20 of histone H4 is a common hallmark of human cancer.* Nat Genet, 2005. **37**(4): p. 391-400.
134. Kouzarides, T., *Chromatin modifications and their function.* Cell, 2007. **128**(4): p. 693-705.
135. Liu, C.L., et al., *Single-nucleosome mapping of histone modifications in S. cerevisiae.* PLoS Biol, 2005. **3**(10): p. e328.
136. Pokholok, D.K., et al., *Genome-wide map of nucleosome acetylation and methylation in yeast.* Cell, 2005. **122**(4): p. 517-27.
137. Lee, M.G., et al., *An essential role for CoREST in nucleosomal histone 3 lysine 4 demethylation.* Nature, 2005. **437**(7057): p. 432-5.
138. Metzger, E., et al., *LSD1 demethylates repressive histone marks to promote androgen-receptor-dependent transcription.* Nature, 2005. **437**(7057): p. 436-9.
139. Steward, M.M., et al., *Molecular regulation of H3K4 trimethylation by ASH2L, a shared subunit of MLL complexes.* Nat Struct Mol Biol, 2006. **13**(9): p. 852-4.
140. Liang, G., et al., *Distinct localization of histone H3 acetylation and H3-K4 methylation to the transcription start sites in the human genome.* Proc Natl Acad Sci U S A, 2004. **101**(19): p. 7357-62.
141. Bernstein, B.E., et al., *Genomic maps and comparative analysis of histone modifications in human and mouse.* Cell, 2005. **120**(2): p. 169-81.
142. Shi, Y., *Histone lysine demethylases: emerging roles in development, physiology and disease.* Nat Rev Genet, 2007. **8**(11): p. 829-33.
143. Haberland, M., R.L. Montgomery, and E.N. Olson, *The many roles of histone deacetylases in development and physiology: implications for disease and therapy.* Nat Rev Genet, 2009. **10**(1): p. 32-42.
144. Rikimaru, T., et al., *Clinical significance of histone deacetylase 1 expression in patients with hepatocellular carcinoma.* Oncology, 2007. **72**(1-2): p. 69-74.

145. Halkidou, K., et al., *Upregulation and nuclear recruitment of HDAC1 in hormone refractory prostate cancer.* Prostate, 2004. **59**(2): p. 177-89.
146. Song, J., et al., *Increased expression of histone deacetylase 2 is found in human gastric cancer.* APMIS, 2005. **113**(4): p. 264-8.
147. Yang, X.J., et al., *A p300/CBP-associated factor that competes with the adenoviral oncoprotein E1A.* Nature, 1996. **382**(6589): p. 319-24.
148. Yang, X.J., *The diverse superfamily of lysine acetyltransferases and their roles in leukemia and other diseases.* Nucleic Acids Res, 2004. **32**(3): p. 959-76.
149. Valk-Lingbeek, M.E., S.W. Bruggeman, and M. van Lohuizen, *Stem cells and cancer; the polycomb connection.* Cell, 2004. **118**(4): p. 409-18.
150. Nguyen, C.T., et al., *Histone H3-lysine 9 methylation is associated with aberrant gene silencing in cancer cells and is rapidly reversed by 5-aza-2'-deoxycytidine.* Cancer Res, 2002. **62**(22): p. 6456-61.
151. Kirmizis, A., S.M. Bartley, and P.J. Farnham, *Identification of the polycomb group protein SU(Z)12 as a potential molecular target for human cancer therapy.* Mol Cancer Ther, 2003. **2**(1): p. 113-21.
152. Kondo, Y., et al., *Alterations of DNA methylation and histone modifications contribute to gene silencing in hepatocellular carcinomas.* Hepatol Res, 2007. **37**(11): p. 974-83.
153. Krivtsov, A.V. and S.A. Armstrong, *MLL translocations, histone modifications and leukaemia stem-cell development.* Nat Rev Cancer, 2007. **7**(11): p. 823-33.
154. Wang, G.G., C.D. Allis, and P. Chi, *Chromatin remodeling and cancer, Part I: Covalent histone modifications.* Trends Mol Med, 2007. **13**(9): p. 363-72.
155. Hamamoto, R., et al., *SMYD3 encodes a histone methyltransferase involved in the proliferation of cancer cells.* Nat Cell Biol, 2004. **6**(8): p. 731-40.
156. Peters, A.H., et al., *Loss of the Suv39h histone methyltransferases impairs mammalian heterochromatin and genome stability.* Cell, 2001. **107**(3): p. 323-37.
157. Ait-Si-Ali, S., et al., *A Suv39h-dependent mechanism for silencing S-phase genes in differentiating but not in cycling cells.* EMBO J, 2004. **23**(3): p. 605-15.
158. Braig, M., et al., *Oncogene-induced senescence as an initial barrier in lymphoma development.* Nature, 2005. **436**(7051): p. 660-5.
159. Sparmann, A. and M. van Lohuizen, *Polycomb silencers control cell fate, development and cancer.* Nat Rev Cancer, 2006. **6**(11): p. 846-56.
160. Croonquist, P.A. and B. Van Ness, *The polycomb group protein enhancer of zeste homolog 2 (EZH 2) is an oncogene that influences myeloma cell growth and the mutant ras phenotype.* Oncogene, 2005. **24**(41): p. 6269-80.
161. Das, N.D., K.H. Jung, and Y.G. Chai, *The role of NF-kappaB and H3K27me3 demethylase, Jmjd3, on the anthrax lethal toxin tolerance of RAW 264.7 cells.* PLoS One, 2010. **5**(3): p. e9913.
162. Joshi, A.A. and K. Struhl, *Eaf3 chromodomain interaction with methylated H3-K36 links histone deacetylation to Pol II elongation.* Mol Cell, 2005. **20**(6): p. 971-8.
163. Carrozza, M.J., et al., *Histone H3 methylation by Set2 directs deacetylation of coding regions by Rpd3S to suppress spurious intragenic transcription.* Cell, 2005. **123**(4): p. 581-92.
164. Duns, G., et al., *Histone methyltransferase gene SETD2 is a novel tumor suppressor gene in clear cell renal cell carcinoma.* Cancer Res, 2010. **70**(11): p. 4287-91.
165. Xie, P., et al., *Histone methyltransferase protein SETD2 interacts with p53 and selectively regulates its downstream genes.* Cell Signal, 2008. **20**(9): p. 1671-8.

166. Tsukada, Y., et al., *Histone demethylation by a family of JmjC domain-containing proteins.* Nature, 2006. **439**(7078): p. 811-6.
167. Agger, K., et al., *The emerging functions of histone demethylases.* Curr Opin Genet Dev, 2008. **18**(2): p. 159-68.
168. Pesavento, J.J., et al., *Certain and progressive methylation of histone H4 at lysine 20 during the cell cycle.* Mol Cell Biol, 2008. **28**(1): p. 468-86.
169. Sanders, S.L., et al., *Methylation of histone H4 lysine 20 controls recruitment of Crb2 to sites of DNA damage.* Cell, 2004. **119**(5): p. 603-14.
170. Botuyan, M.V., et al., *Structural basis for the methylation state-specific recognition of histone H4-K20 by 53BP1 and Crb2 in DNA repair.* Cell, 2006. **127**(7): p. 1361-73.
171. Vakoc, C.R., et al., *Profile of histone lysine methylation across transcribed mammalian chromatin.* Mol Cell Biol, 2006. **26**(24): p. 9185-95.
172. Barski, A., et al., *High-resolution profiling of histone methylations in the human genome.* Cell, 2007. **129**(4): p. 823-37.
173. Kohlmaier, A., et al., *A chromosomal memory triggered by Xist regulates histone methylation in X inactivation.* PLoS Biol, 2004. **2**(7): p. E171.
174. Souza, P.P., et al., *The histone methyltransferase SUV420H2 and Heterochromatin Proteins HP1 interact but show different dynamic behaviours.* BMC Cell Biol, 2009. **10**: p. 41.
175. Moss, T.J. and L.L. Wallrath, *Connections between epigenetic gene silencing and human disease.* Mutat Res, 2007. **618**(1-2): p. 163-74.
176. Li, E., *Chromatin modification and epigenetic reprogramming in mammalian development.* Nat Rev Genet, 2002. **3**(9): p. 662-73.
177. Lund, A.H. and M. van Lohuizen, *Epigenetics and cancer.* Genes Dev, 2004. **18**(19): p. 2315-35.
178. Moribe, T., et al., *Methylation of multiple genes as molecular markers for diagnosis of a small, well-differentiated hepatocellular carcinoma.* Int J Cancer, 2009. **125**(2): p. 388-97.
179. Iliopoulos, D., et al., *Epigenetic regulation of hTERT promoter in hepatocellular carcinomas.* Int J Oncol, 2009. **34**(2): p. 391-9.
180. Datta, J., et al., *Methylation mediated silencing of MicroRNA-1 gene and its role in hepatocellular carcinogenesis.* Cancer Res, 2008. **68**(13): p. 5049-58.
181. Yan, Q., et al., *Reduced T-cadherin expression and promoter methylation are associated with the development and progression of hepatocellular carcinoma.* Int J Oncol, 2008. **32**(5): p. 1057-63.
182. Calvisi, D.F., R.M. Pascale, and F. Feo, *Dissection of signal transduction pathways as a tool for the development of targeted therapies of hepatocellular carcinoma.* Rev Recent Clin Trials, 2007. **2**(3): p. 217-36.
183. Caron, C., et al., *Functional characterization of ATAD2 as a new cancer/testis factor and a predictor of poor prognosis in breast and lung cancers.* Oncogene, 2010.
184. Ciro, M., et al., *ATAD2 is a novel cofactor for MYC, overexpressed and amplified in aggressive tumors.* Cancer Res, 2009. **69**(21): p. 8491-8.
185. Zou, C., et al., *Lack of Fas antagonism by Met in human fatty liver disease.* Nat Med, 2007. **13**(9): p. 1078-85.
186. Zou, J.X., et al., *Androgen-induced coactivator ANCCA mediates specific androgen receptor signaling in prostate cancer.* Cancer Res, 2009. **69**(8): p. 3339-46.

187. Issa, J.P., *DNA methylation as a therapeutic target in cancer.* Clin Cancer Res, 2007. **13**(6): p. 1634-7.
188. Cagatay, T. and M. Ozturk, *P53 mutation as a source of aberrant beta-catenin accumulation in cancer cells.* Oncogene, 2002. **21**: p. 7971 - 7980.
189. Ronzoni, S., et al., *New method to detect histone acetylation levels by flow cytometry.* Cytometry A, 2005. **66**(1): p. 52-61.
190. Alley, M.C., et al., *Feasibility of drug screening with panels of human tumor cell lines using a microculture tetrazolium assay.* Cancer Res, 1988. **48**(3): p. 589-601.
191. Ishiyama, T., et al., *Expression of HNFs and C/EBP alpha is correlated with immunocytochemical differentiation of cell lines derived from human hepatocellular carcinomas, hepatoblastomas and immortalized hepatocytes.* Cancer Sci, 2003. **94**: p. 757 - 763.
192. Du, G., et al., *Expression of P-aPKC-iota, E-cadherin, and beta-catenin related to invasion and metastasis in hepatocellular carcinoma.* Ann Surg Oncol, 2009. **16**: p. 1578 - 1586.
193. Wang, W., et al., *Expression of HNF-1 alpha and HNF-1 beta in various histological differentiations of hepatocellular carcinoma.* J Pathol, 1998. **184**: p. 272 - 278.
194. Niu, R., et al., *Up-regulation of Twist induces angiogenesis and correlates with metastasis in hepatocellular carcinoma.* J Exp Clin Cancer Res, 2007. **26**: p. 385 - 394.
195. Riou, P., et al., *Expression of T-cadherin in tumor cells influences invasive potential of human hepatocellular carcinoma.* FASEB J, 2006. **20**: p. 2291 - 2301.
196. Staal, F., T. Luis, and M. Tiemessen, *WNT signalling in the immune system: WNT is spreading its wings.* Nat Rev Immunol, 2008. **8**: p. 581 - 593.
197. Bafico, A., et al., *An autocrine mechanism for constitutive Wnt pathway activation in human cancer cells.* Cancer Cell, 2004. **6**: p. 497 - 506.
198. Mikels, A. and R. Nusse, *Purified Wnt5a protein activates or inhibits beta-catenin-TCF signaling depending on receptor context.* PLoS Biol, 2006. **4**: p. e115.
199. Nemeth, M., et al., *Wnt5a inhibits canonical Wnt signaling in hematopoietic stem cells and enhances repopulation.* Proc Natl Acad Sci USA, 2007. **104**: p. 15436 - 15441.
200. Ishitani, T., et al., *The TAK1-NLK mitogen-activated protein kinase cascade functions in the Wnt-5a/Ca(2+) pathway to antagonize Wnt/beta-catenin signaling.* Mol Cell Biol, 2003. **23**: p. 131 - 139.
201. Morin, P., et al., *Activation of beta-catenin-Tcf signaling in colon cancer by mutations in beta-catenin or APC.* Science, 1997. **275**: p. 1787 - 1790.
202. Erdal, E., et al., *Lithium-mediated downregulation of PKB/Akt and cyclin E with growth inhibition in hepatocellular carcinoma cells.* Int J Cancer, 2005. **115**: p. 903 - 910.
203. Satoh, S., et al., *AXIN1 mutations in hepatocellular carcinomas, and growth suppression in cancer cells by virus-mediated transfer of AXIN1.* Nat Genet, 2000. **24**: p. 245 - 250.
204. Brantjes, H., et al., *All Tcf HMG box transcription factors interact with Groucho-related co-repressors.* Nucleic Acids Res, 2001. **29**: p. 1410 - 1419.
205. Munemitsu, S., et al., *Regulation of intracellular beta-catenin levels by the adenomatous polyposis coli (APC) tumor-suppressor protein.* Proc Natl Acad Sci USA, 1995. **92**: p. 3046 - 3050.
206. McDonald, S. and A. Silver, *The opposing roles of Wnt-5a in cancer.* Br J Cancer, 2009. **101**: p. 209 - 214.
207. Gonzalo, S. and M.A. Blasco, *Role of Rb family in the epigenetic definition of chromatin.* Cell Cycle, 2005. **4**(6): p. 752-5.

208. Delaval, K., et al., *Differential histone modifications mark mouse imprinting control regions during spermatogenesis.* EMBO J, 2007. **26**(3): p. 720-9.
209. Neuwald, A.F., et al., *AAA+: A class of chaperone-like ATPases associated with the assembly, operation, and disassembly of protein complexes.* Genome Res, 1999. **9**(1): p. 27-43.
210. Zeng, L. and M.M. Zhou, *Bromodomain: an acetyl-lysine binding domain.* FEBS Lett, 2002. **513**(1): p. 124-8.
211. Chen, X., et al., *Gene expression patterns in human liver cancers.* Mol Biol Cell, 2002. **13**(6): p. 1929-39.
212. Ambrosini, G., C. Adida, and D.C. Altieri, *A novel anti-apoptosis gene, survivin, expressed in cancer and lymphoma.* Nat Med, 1997. **3**(8): p. 917-21.
213. Ambrosini, G., et al., *Induction of apoptosis and inhibition of cell proliferation by survivin gene targeting.* J Biol Chem, 1998. **273**(18): p. 11177-82.
214. Li, F., et al., *Control of apoptosis and mitotic spindle checkpoint by survivin.* Nature, 1998. **396**(6711): p. 580-4.
215. Nejak-Bowen, K. and S. Monga, *Wnt/beta-catenin signaling in hepatic organogenesis.* Organogenesis, 2008. **4**: p. 92 - 99.
216. Hu, M., et al., *Wnt/beta-catenin signaling in murine hepatic transit amplifying progenitor cells.* Gastroenterology, 2007. **133**: p. 1579 - 1591.
217. Apte, U., et al., *Wnt/beta-catenin signaling mediates oval cell response in rodents.* Hepatology, 2008. **47**: p. 288 - 295.
218. Yang, W., et al., *Wnt/beta-catenin signaling contributes to activation of normal and tumorigenic liver progenitor cells.* Cancer Res, 2008. **68**: p. 4287 - 4295.
219. Lee, J. and S. Thorgeirsson, *Functional and genomic implications of global gene expression profiles in cell lines from human hepatocellular cancer.* Hepatology, 2002. **35**: p. 1134 - 1143.
220. Armengol, C., et al., *Wnt signaling and hepatocarcinogenesis: The hepatoblastoma model.* Int J Biochem Cell Biol, 2009.
221. Kalluri, R. and R. Weinberg, *The basics of epithelial-mesenchymal transition.* J Clin Invest, 2009. **119**: p. 1420 - 1428.
222. Zeng, G., et al., *Wnt'er in liver: expression of Wnt and frizzled genes in mouse.* Hepatology, 2007. **45**: p. 195 - 204.
223. Merle, P., et al., *Oncogenic role of the frizzled-7/beta-catenin pathway in hepatocellular carcinoma.* J Hepatol, 2005. **43**: p. 854 - 862.
224. Kim, M., et al., *Functional interaction between Wnt3 and Frizzled-7 leads to activation of the Wnt/beta-catenin signaling pathway in hepatocellular carcinoma cells.* J Hepatol, 2008. **48**: p. 780 - 791.
225. Bengochea, A., et al., *Common dysregulation of Wnt/Frizzled receptor elements in human hepatocellular carcinoma.* Br J Cancer, 2008. **99**: p. 143 - 150.
226. Yoshikawa, H., et al., *WNT10B functional dualism: beta-catenin/Tcf-dependent growth promotion or independent suppression with deregulated expression in cancer.* Mol Biol Cell, 2007. **18**: p. 4292 - 4303.
227. Liu, X., et al., *Expression of Wnt-5a and its clinicopathological significance in hepatocellular carcinoma.* Dig Liver Dis, 2008. **40**: p. 560 - 567.
228. Chiba, T., et al., *Side population purified from hepatocellular carcinoma cells harbors cancer stem cell-like properties.* Hepatology, 2006. **44**: p. 240 - 251.

229. Roarty, K., et al., *Loss of TGF-beta or Wnt5a results in an increase in Wnt/beta-catenin activity and redirects mammary tumour phenotype.* Breast Cancer Res, 2009. **11**: p. R19.
230. Topol, L., et al., *Wnt-5a inhibits the canonical Wnt pathway by promoting GSK-3-independent beta-catenin degradation.* J Cell Biol, 2003. **162**: p. 899 - 908.
231. Ripka, S., et al., *WNT5A--target of CUTL1 and potent modulator of tumor cell migration and invasion in pancreatic cancer.* Carcinogenesis, 2007. **28**: p. 1178 - 1187.
232. Crawley, J.J. and K.A. Furge, *Identification of frequent cytogenetic aberrations in hepatocellular carcinoma using gene-expression microarray data.* Genome Biol, 2002. **3**(12): p. RESEARCH0075.

This is the permission letter of Molecular Cancer journal, for my thesis entitled as 'Genetic and Epigenetic Targets in Liver Cancer'.

With this permission I have rights to use the text and figures of my article published in Molecular Cancer journal with the following citation: **Yuzugullu H,** Benhaj B, Ozturk N, Senturk S, Celik E, Toylu A, Tasdemir N, Yilmaz M, Erdal E, Akcali KC, Atabey N and Ozturk M. Canonical Wnt signaling is antagonized by noncanonical Wnt5a in hepatocellular carcinoma cells. **Molecular Cancer** 8: e90, 2009.

The permission is for all the figures starting with 4.1.1 to 4.1.12 and all the text within introduction, Methodology and Results and discussion.

BioMed Central Open Access Charter

Every peer-reviewed research article appearing in any journal published by BioMed Central is 'open access', meaning that:

1. The article is universally and freely accessible via the Internet, in an easily readable format and deposited immediately upon publication, without embargo, in an agreed format - current preference is XML with a declared DTD - in at least one widely and internationally recognized open access repository (such as PubMed Central).
2. The author(s) or copyright owner(s) irrevocably grant(s) to any third party, in advance and in perpetuity, the right to use, reproduce or disseminate the research article in its entirety or in part, in any format or medium, provided that no substantive errors are introduced in the process, proper attribution of authorship and correct citation details are given, and that the bibliographic details are not changed. If the article is reproduced or disseminated in part, this must be clearly and unequivocally indicated.

BioMed Central is committed permanently to maintaining this open access publishing policy, retrospectively and prospectively, in all eventualities, including any future changes in ownership.

BioMed Central has established an independent Board of Trustees. If and when a change of ownership should be considered, the Board of Trustees will be asked to judge and advise whether sufficient guarantees to continue a policy of unconditional open access for research articles are being offered and agreed by any prospective new owner. BioMed Central will not enter into a change of ownership agreement unless the Board of Trustees accepts these

guarantees.

Any change in the composition of the Board of Trustees will be subject to approval by a majority of the existing members of the Board of Trustees.

The Board of Trustees consists of the following members:

Open access articles in BioMed Central's journals are identified by this logo:

ELSEVIER LICENSE
TERMS AND CONDITIONS

Aug 05, 2010

This is a License Agreement between haluk yuzugullu ("You") and Elsevier ("Elsevier") provided by Copyright Clearance Center ("CCC"). The license consists of your order details, the terms and conditions provided by Elsevier, and the payment terms and conditions.

All payments must be made in full to CCC. For payment instructions, please see information listed at the bottom of this form.

Supplier	Elsevier Limited The Boulevard,Langford Lane Kidlington,Oxford,OX5 1GB,UK
Registered Company Number	1982084
Customer name	haluk yuzugullu
Customer address	bilkent universitesi fen fakultesi ankara, other 06800
License number	2482430761106
License date	Aug 05, 2010
Licensed content publisher	Elsevier
Licensed content publication	Cancer Letters
Licensed content title	Senescence and immortality in hepatocellular carcinoma
Licensed content author	Mehmet Ozturk, Ayca Arslan-Ergul, Sevgi Bagislar, Serif Senturk, Haluk Yuzugullu
Licensed content date	1 December 2009
Licensed content volume number	286
Licensed content issue number	1
Number of pages	11
Type of Use	reuse in a thesis/dissertation
Requestor type	Not specified
Intended publisher of new work	n/a
Portion	full article
Format	both print and electronic
Are you the author of this Elsevier article?	Yes
Will you be translating?	No
Order reference number	
Title of your thesis/dissertation	Genetic and Epigenetic Targets in liver cancer
Expected completion date	Aug 2010

Estimated size (number of pages)	144
Elsevier VAT number	GB 494 6272 12

Terms and Conditions

INTRODUCTION

1. The publisher for this copyrighted material is Elsevier. By clicking "accept" in connection with completing this licensing transaction, you agree that the following terms and conditions apply to this transaction (along with the Billing and Payment terms and conditions established by Copyright Clearance Center, Inc. ("CCC"), at the time that you opened your Rightslink account and that are available at any time at http://myaccount.copyright.com).

GENERAL TERMS

2. Elsevier hereby grants you permission to reproduce the aforementioned material subject to the terms and conditions indicated.

3. Acknowledgement: If any part of the material to be used (for example, figures) has appeared in our publication with credit or acknowledgement to another source, permission must also be sought from that source. If such permission is not obtained then that material may not be included in your publication/copies. Suitable acknowledgement to the source must be made, either as a footnote or in a reference list at the end of your publication, as follows:

"Reprinted from Publication title, Vol /edition number, Author(s), Title of article / title of chapter, Pages No., Copyright (Year), with permission from Elsevier [OR APPLICABLE SOCIETY COPYRIGHT OWNER]." Also Lancet special credit - "Reprinted from The Lancet, Vol. number, Author(s), Title of article, Pages No., Copyright (Year), with permission from Elsevier."

4. Reproduction of this material is confined to the purpose and/or media for which permission is hereby given.

5. Altering/Modifying Material: Not Permitted. However figures and illustrations may be altered/adapted minimally to serve your work. Any other abbreviations, additions, deletions and/or any other alterations shall be made only with prior written authorization of Elsevier Ltd. (Please contact Elsevier at permissions@elsevier.com)

6. If the permission fee for the requested use of our material is waived in this instance, please be advised that your future requests for Elsevier materials may attract a fee.

7. Reservation of Rights: Publisher reserves all rights not specifically granted in the combination of (i) the license details provided by you and accepted in the course of this licensing transaction, (ii) these terms and conditions and (iii) CCC's Billing and Payment terms and conditions.

8. License Contingent Upon Payment: While you may exercise the rights licensed immediately upon issuance of the license at the end of the licensing process for the transaction, provided that you have disclosed complete and accurate details of your proposed use, no license is finally effective unless and until full payment is received from you (either by publisher or by CCC) as provided in CCC's Billing and Payment terms and conditions. If full payment is not received on a timely basis, then any license preliminarily granted shall be deemed automatically revoked and shall be void as if never granted. Further, in the event that you breach any of these terms and conditions or any of CCC's Billing and Payment terms and conditions, the license is automatically revoked and shall be void as

if never granted. Use of materials as described in a revoked license, as well as any use of the materials beyond the scope of an unrevoked license, may constitute copyright infringement and publisher reserves the right to take any and all action to protect its copyright in the materials.

9. Warranties: Publisher makes no representations or warranties with respect to the licensed material.

10. Indemnity: You hereby indemnify and agree to hold harmless publisher and CCC, and their respective officers, directors, employees and agents, from and against any and all claims arising out of your use of the licensed material other than as specifically authorized pursuant to this license.

11. No Transfer of License: This license is personal to you and may not be sublicensed, assigned, or transferred by you to any other person without publisher's written permission.

12. No Amendment Except in Writing: This license may not be amended except in a writing signed by both parties (or, in the case of publisher, by CCC on publisher's behalf).

13. Objection to Contrary Terms: Publisher hereby objects to any terms contained in any purchase order, acknowledgment, check endorsement or other writing prepared by you, which terms are inconsistent with these terms and conditions or CCC's Billing and Payment terms and conditions. These terms and conditions, together with CCC's Billing and Payment terms and conditions (which are incorporated herein), comprise the entire agreement between you and publisher (and CCC) concerning this licensing transaction. In the event of any conflict between your obligations established by these terms and conditions and those established by CCC's Billing and Payment terms and conditions, these terms and conditions shall control.

14. Revocation: Elsevier or Copyright Clearance Center may deny the permissions described in this License at their sole discretion, for any reason or no reason, with a full refund payable to you. Notice of such denial will be made using the contact information provided by you. Failure to receive such notice will not alter or invalidate the denial. In no event will Elsevier or Copyright Clearance Center be responsible or liable for any costs, expenses or damage incurred by you as a result of a denial of your permission request, other than a refund of the amount(s) paid by you to Elsevier and/or Copyright Clearance Center for denied permissions.

LIMITED LICENSE

The following terms and conditions apply only to specific license types:

15. **Translation**: This permission is granted for non-exclusive world **English** rights only unless your license was granted for translation rights. If you licensed translation rights you may only translate this content into the languages you requested. A professional translator must perform all translations and reproduce the content word for word preserving the integrity of the article. If this license is to re-use 1 or 2 figures then permission is granted for non-exclusive world rights in all languages.

16. **Website**: The following terms and conditions apply to electronic reserve and author websites:
Electronic reserve: If licensed material is to be posted to website, the web site is to be password-protected and made available only to bona fide students registered on a relevant course if:
This license was made in connection with a course,
This permission is granted for 1 year only. You may obtain a license for future website posting,

All content posted to the web site must maintain the copyright information line on the bottom of each image,
A hyper-text must be included to the Homepage of the journal from which you are licensing at http://www.sciencedirect.com/science/journal/xxxxx or the Elsevier homepage for books at http://www.elsevier.com , and
Central Storage: This license does not include permission for a scanned version of the material to be stored in a central repository such as that provided by Heron/XanEdu.

17. **Author website** for journals with the following additional clauses:

All content posted to the web site must maintain the copyright information line on the bottom of each image, and
he permission granted is limited to the personal version of your paper. You are not allowed to download and post the published electronic version of your article (whether PDF or HTML, proof or final version), nor may you scan the printed edition to create an electronic version,
A hyper-text must be included to the Homepage of the journal from which you are licensing at http://www.sciencedirect.com/science/journal/xxxxx , As part of our normal production process, you will receive an e-mail notice when your article appears on Elsevier's online service ScienceDirect (www.sciencedirect.com). That e-mail will include the article's Digital Object Identifier (DOI). This number provides the electronic link to the published article and should be included in the posting of your personal version. We ask that you wait until you receive this e-mail and have the DOI to do any posting.
Central Storage: This license does not include permission for a scanned version of the material to be stored in a central repository such as that provided by Heron/XanEdu.

18. **Author website** for books with the following additional clauses:
Authors are permitted to place a brief summary of their work online only.
A hyper-text must be included to the Elsevier homepage at http://www.elsevier.com

All content posted to the web site must maintain the copyright information line on the bottom of each image
You are not allowed to download and post the published electronic version of your chapter, nor may you scan the printed edition to create an electronic version.
Central Storage: This license does not include permission for a scanned version of the material to be stored in a central repository such as that provided by Heron/XanEdu.

19. **Website** (regular and for author): A hyper-text must be included to the Homepage of the journal from which you are licensing at http://www.sciencedirect.com/science/journal/xxxxx. or for books to the Elsevier homepage at http://www.elsevier.com

20. **Thesis/Dissertation**: If your license is for use in a thesis/dissertation your thesis may be submitted to your institution in either print or electronic form. Should your thesis be published commercially, please reapply for permission. These requirements include permission for the Library and Archives of Canada to supply single copies, on demand, of the complete thesis and include permission for UMI to supply single copies, on demand, of the complete thesis. Should your thesis be published commercially, please reapply for permission.

21. **Other Conditions**:

v1.6

Gratis licenses (referencing $0 in the Total field) are free. Please retain this printable license for your reference. No payment is required.

If you would like to pay for this license now, please remit this license along with your payment made payable to "COPYRIGHT CLEARANCE CENTER" otherwise you will be invoiced within 48 hours of the license date. Payment should be in the form of a check or money order referencing your account number and this invoice number RLNK10826519. Once you receive your invoice for this order, you may pay your invoice by credit card. Please follow instructions provided at that time.

Make Payment To:
Copyright Clearance Center
Dept 001
P.O. Box 843006
Boston, MA 02284-3006

If you find copyrighted material related to this license will not be used and wish to cancel, please contact us referencing this license number 2482430761106 and noting the reason for cancellation.

Questions? customercare@copyright.com or +1-877-622-5543 (toll free in the US) or +1-978-646-2777.

Molecular Cancer

BioMed Central

Research

Open Access

Canonical Wnt signaling is antagonized by noncanonical Wnt5a in hepatocellular carcinoma cells

Haluk Yuzugullu†[1,2], Khemais Benhaj†[1,3], Nuri Ozturk[1], Serif Senturk[1], Emine Celik[4], Asli Toylu[4], Nilgun Tasdemir[1], Mustafa Yilmaz[1], Esra Erdal[1,4], Kamil Can Akcali[1], Nese Atabey[4] and Mehmet Ozturk*[1,2]

Address: [1]Department of Molecular Biology and Genetics, Faculty of Science, Bilkent University, 06800, Ankara, Turkey, [2]Centre de Recherche INSERM-Université Joseph Fourrier U823, Institut Albert Bonniot, 38706 La Tronche Cedex, France, [3]Centre de Biotechnologie de Sfax, B.P "1177", 3038 Sfax, Tunisia and [4]Department of Medical Biology and Genetics, Dokuz Eylul University School of Medicine, Izmir, 35340 Turkey

Email: Haluk Yuzugullu - yuzugulh@ujf-grenoble.fr; Khemais Benhaj - bilhaj@alumni.bilkent.edu.tr; Nuri Ozturk - nuri_ozturk@med.unc.edu; Serif Senturk - serif@bilkent.edu.tr; Emine Celik - emine.celik@gmail.com; Asli Toylu - asli.toylu@deu.edu.tr; Nilgun Tasdemir - tasdemir@cshl.edu; Mustafa Yilmaz - myilmaz@ug.bilkent.edu.tr; Esra Erdal - esra.erdal@deu.edu.tr; Kamil Can Akcali - akcali@fen.bilkent.edu.tr; Nese Atabey - nese.atabey@deu.edu.tr; Mehmet Ozturk* - ozturkm@ujf-grenoble.fr

* Corresponding author †Equal contributors

Published: 22 October 2009

Molecular Cancer 2009, **8**:90 doi:10.1186/1476-4598-8-90

Received: 4 March 2009
Accepted: 22 October 2009

This article is available from: http://www.molecular-cancer.com/content/8/1/90

Abstract

Background: β-catenin mutations that constitutively activate the canonical Wnt signaling have been observed in a subset of hepatocellular carcinomas (HCCs). These mutations are associated with chromosomal stability, low histological grade, low tumor invasion and better patient survival. We hypothesized that canonical Wnt signaling is selectively activated in well-differentiated, but repressed in poorly differentiated HCCs. To this aim, we characterized differentiation status of HCC cell lines and compared their expression status of Wnt pathway genes, and explored their activity of canonical Wnt signaling.

Results: We classified human HCC cell lines into "well-differentiated" and "poorly differentiated" subtypes, based on the expression of hepatocyte lineage, epithelial and mesenchymal markers. Poorly differentiated cell lines lost epithelial and hepatocyte lineage markers, and overexpressed mesenchymal markers. Also, they were highly motile and invasive. We compared the expression of 45 Wnt pathway genes between two subtypes. TCF1 and TCF4 factors, and LRP5 and LRP6 co-receptors were ubiquitously expressed. Likewise, six Frizzled receptors, and canonical Wnt3 ligand were expressed in both subtypes. In contrast, canonical ligand Wnt8b and noncanonical ligands Wnt4, Wnt5a, Wnt5b and Wnt7b were expressed selectively in well- and poorly differentiated cell lines, respectively. Canonical Wnt signaling activity, as tested by a TCF reporter assay was detected in 80% of well-differentiated, contrary to 14% of poorly differentiated cell lines. TCF activity generated by ectopic mutant β-catenin was weak in poorly differentiated SNU449 cell line, suggesting a repressive mechanism. We tested Wnt5a as a candidate antagonist. It strongly inhibited canonical Wnt signaling that is activated by mutant β-catenin in HCC cell lines.

Conclusion: Differential expression of Wnt ligands in HCC cells is associated with selective activation of canonical Wnt signaling in well-differentiated, and its repression in poorly differentiated cell lines. One potential mechanism of repression involved Wnt5a, acting as an antagonist of canonical Wnt signaling. Our observations support the hypothesis that Wnt pathway is selectively activated or repressed depending on differentiation status of HCC cells. We propose that canonical and noncanonical Wnt pathways have complementary roles in HCC, where the canonical signaling contributes to tumor initiation, and noncanonical signaling to tumor progression.

Background

Hepatocellular carcinoma (HCC) is an epithelial cancer that originates from hepatocytes or their progenitors. It is the fifth most frequent neoplasm worldwide (>500,000 deaths/year), and its incidence is steadily increasing in the West [1]. Hepatocellular carcinoma is graded into four stages as well-differentiated, moderately differentiated, poorly differentiated and undifferentiated tumors, respectively. HCC arises as a very well differentiated cancer and proliferates with a stepwise process of dedifferentiation. Indeed, well-differentiated histology is exclusively seen in early stage and is rare in advanced HCC. Well-differentiated and moderately differentiated HCC cells are morphologically similar to hepatocytes, and are distinguished only by their smaller size and architectural organization as irregular trabecular or pseudoglandular patterns. In contrast, poorly differentiated and undifferentiated HCC cells are characterized with scanty cytoplasms and pleomorphism [2]. Like in other epithelial tumors, in HCC the progenitors evolve during tumor progression and become more and more autonomous. In this process, the tumor cells change their morphology and behavior; they loose cuboidal shape and polarity, and become more independent from neighboring tissues. Finally, they acquire the capacity to invade the underlying tissue and form distant metastases. These morphological changes are usually associated with progressive loss of biochemical and morphological features of hepatocytes, hence the process is qualified as "dedifferentiation" [3]. Portal venous invasion is significantly associated with poorly differentiated and undifferentiated HCCs and the tumor invasiveness is the most crucial factor in determining the long-term outcome for the patient [4].

Molecular changes involved in HCC dedifferentiation and invasiveness are known only partially. Epithelial markers such as hepatocyte nuclear factors and E-cadherin were reported to be down-regulated in HCC [3,5] and their loss is closely related to tumor invasion and metastasis [5]. In contrast, mesenchymal cell markers such as snail [6], twist [7] and vimentin [8] display positive correlation with HCC invasiveness and/or metastasis. These changes have been considered to represent the epithelial-mesenchymal transition (EMT) in HCC, based on in vitro studies [9-15]. Hepatocyte nuclear factor-4α (Hnf-4α) is essential for morphological and functional differentiation of hepatocytes [16,17], and its expression is downregulated during HCC progression in mice [18]. HCC dedifferentiation process is associated with a progressive accumulation of genomic changes including chromosomal gains and losses, as well as p53 mutations [19]. A rare exception to this picture is the status of the *CTNNB1* gene that encodes β-catenin, a key component of the Wnt/β-catenin (canonical Wnt) signaling pathway.

Independent studies showed that β-catenin mutations are associated with a subset of low grade (well-differentiated) HCCs with a favorable prognosis and chromosome stability [20-25]. Among 366 unifocal HCCs studied by Hsu et al. [20], β-catenin mutations were associated with grade I histogoly. Another study with similarly high number of tumors (n = 372) also indicated that mutant nuclear β-catenin correlated positively with non-invasive tumor and inversely with portal vein tumor thrombi [23]. In addition, β-catenin mutations were associated with significantly better 5-year patient survival in these large cohorts. Direct study of canonical Wnt signaling activity in primary tumors is not possible. However, this can be studied indirectly by using target genes [22]. Using glutamine synthetase (encoded by canonical Wnt signaling target *GLUL* gene) as a sensitive and specific marker, Audard et al. [22] showed that 36% HCCs displayed canonical Wnt activation. These tumors exhibited significant features associated with well-differentiated morphology. The association of β-catenin mutation and nuclear translocation with well-differentiated tumor grade was also reported during hepatocellular carcinogenesis, using several transgenic mouse models [26]. Activation of β-catenin was most frequent in liver tumors from c-myc and c-myc/TGF-β1 transgenic mice. However, it was very rare in faster growing and histologically more aggressive HCCs developed in c-myc/TGF-α mice. Taken together, these studies suggest that nuclear translocation of β-catenin and activation of canonical Wnt signaling are early events in liver carcinogenesis, mostly affecting well-differentiated HCCs.

Mutations of β-catenin gene initially identified in colorectal cancers, cause constitutive activation of canonical Wnt signaling, as a result of aberrant β-catenin protein accumulation. Inactivating mutations of APC gene in colorectal cancer and AXIN1 in HCC also activate canonical Wnt signaling by the same mechanism. Therefore, tumors displaying β-catenin, APC or AXIN1 mutation are considered to display active or constitutive canonical Wnt signaling [27] Activation of canonical Wnt signaling appears to be a common event for colorectal cancer, as opposed to HCC with mutations limited to a subset of these cancers. Interestingly, transgenic mice expressing oncogenic β-catenin in hepatocytes develop only hepatomegaly [28,29], in contrast to intestinal polyposis and microadenoma when expressed in intestinal cells [30].

Taken together, published data indicate that Wnt pathway and β-catenin mutations may play a complex role in HCC. Close association of β-catenin mutation with low tumor grade suggests that canonical Wnt signaling has a dual role in HCC cells, depending on their differentiation state. As an initial attempt to characterize differentiation-dependent functions of Wnt pathway and canonical Wnt signaling in HCC, we used a panel of HCC-derived cell lines. We

first performed gene expression and in vitro cell migration analyses to classify HCC cell lines into two distinct subtypes. The first subtype that we named here as "well-differentiated" was formed by epithelial cell lines with limited motility and invasiveness. Mesenchymal-like cell lines that have lost their epithelial-, hepatocyte-like features clustered into a second subtype named as "poorly differentiated". Next, we compared these two subtypes for the expression of 45 Wnt pathway genes, as well as for the activity of canonical Wnt signaling. Our findings provided evidence for the constitutive activation of canonical Wnt signaling in well-differentiated, but not in poorly differentiated cell lines. We also report the upregulation canonical Wnt3 ligand in the majority of HCC cell lines. Canonical Wnt8b was selectively expressed in well-differentiated cell lines. In contrast, noncanonical Wnt4, Wnt5a, Wnt5b and Wnt7b ligands were expressed selectively in poorly differentiated HCC cell lines. In addition, ectopic expression of noncanonical Wnt5a inhibited canonical Wnt signaling in two different cell lines. Our findings support the differential involvement of canonical and noncanonical Wnt signaling in HCC, depending on tumor cell differentiation state.

Results

Classification of hepatocellular carcinoma cell lines into "well-differentiated" and "poorly differentiated" subtypes

Fuchs et al. [12] have recently classified HCC cell lines into "epithelial" and "mesenchymal" types based on E-cadherin and vimentin expression. We performed a similar analysis using our cell line panel. Initially, we analyzed 15 cell lines (Figure 1). The expression of α-fetoprotein (AFP) was limited to six cell lines (Huh7, Hep40, HepG2, Hep3B, Hep3B-TR, PLC/PRF/5); the other cell lines being either not expressing (SNU182, SNU387, SNU398, SNU423, SNU449, SK-Hep1, Mahlavu, FOCUS) or weakly expressing (SNU475). All AFP-positive (AFP+) cell lines also expressed E-cadherin, whereas only 3/9 (33%) of AFP- cell lines expressed this epithelial marker. Mesenchymal cell markers including vimentin, slug, snail, twist-1 and twist-2 were also positive in most AFP- cell lines. These markers also displayed weakly positive expression in some AFP+ cell lines. For confirmation, we performed immunocytochemical analysis of vimentin protein expression in five AFP+ and five AFP- cell lines (Figure 2). We observed strong and homogenous immunostaining with all five AFP- cell lines. In contrast AFP+ cell lines were either negative or displayed heterogeneously positive immunoreactivity. These findings suggested that all AFP+ HCC cell lines were epithelial-like based on E-cadherin expression, but they also expressed some mesenchymal cell markers at variable degrees. In contrast, AFP- cell lines were usually negative for E-cadherin, and most of them were strongly positive for mesenchymal cell markers. The expression patterns of these mesenchymal markers showed marked heterogeneity. For example, SNU182 was positive for all five markers tested, whereas FOCUS was positive only for vimentin expression.

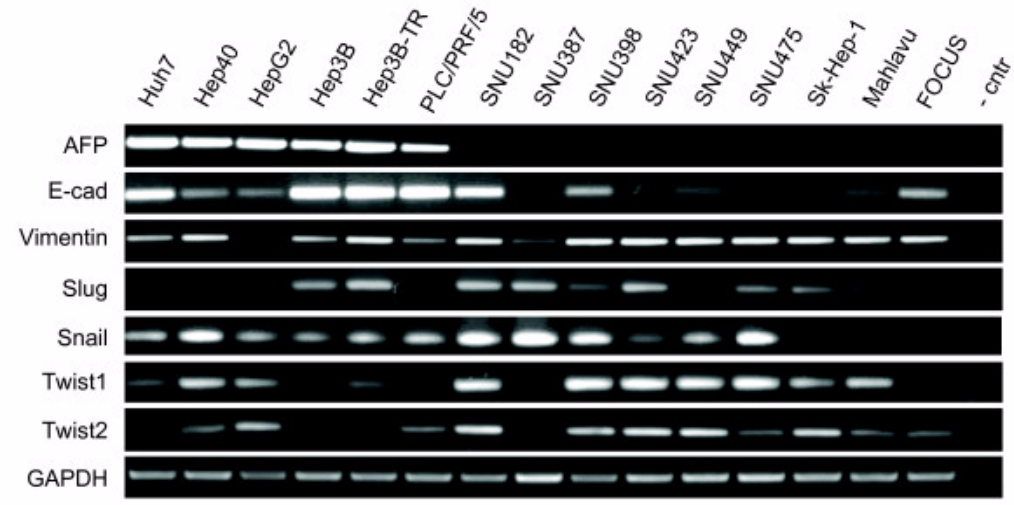

Figure 1

Expression analysis of a-fetoprotein (AFP), E-cadherin and five mesenchymal cell markers in HCC cell lines. Total RNAs were extracted from cell lines and used to detect gene expression by RT-PCR assay. GAPDH was used as a control for expression analyses shown here and in figures 4 to 7.

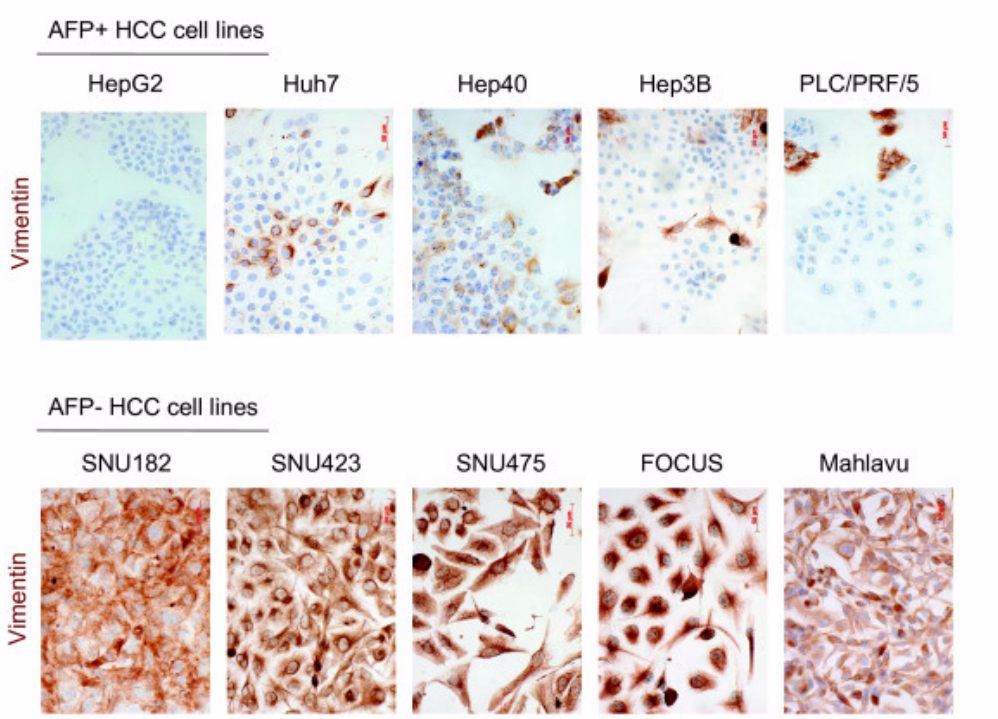

Figure 2
Immunocytochemical analysis of mesenchymal marker vimentin protein in AFP+ and AFP- HCC cell lines. Cells grown on coverslips were subjected to immunoperoxidase assay using anti-vimentin antibody (brown), and counter-stained with hematoxylin (blue).

We selected four AFP+, and seven AFP- cell lines for further analysis. HNF-4α and its downstream target HNF-1α are best known hepatocyte-associated epithelial cell markers [3]. These two genes that are involved in liver development and hepatocyte specification have previously been identified as specific markers for HCC cells with well-differentiated function and morphology [31]. The expression of these HNFs displayed perfect correlation with the expression of AFP (Figure 3a): four AFP+ cell lines (Huh7, Hep3B, HepG2, Hep40) were also highly positive for both HNF-4α and HNF-1α. In contrast, seven AFP- cell lines (SNU398, SNU475, SNU449, SNU387, FOCUS, Mahlavu, SNU182) did not express these factors. SNU449, another AFP- cell line displayed only weak HNF-4α expression. Epithelial cells including hepatocytes show low motility, in contrast to mesenchymal cells that display high motility and invasive behavior. To test whether epithelial and mesenchymal gene expression patterns of HCC cells correlated with their in vitro motility, we used wound-healing assay. After 24 hours of wounding, AFP- HCC cells (Mahlavu, SNU449, SNU475, SNU182) moved through the wound, whereas AFP+ HCC cells (Huh7, Hep3B, Hep G2, Hep40) cells did not (Figure 3b; Hep40 and SNU182 data not shown). A quantitative analysis of this data confirmed that poorly differentiated cell lines display higher motility (Figure 3c).

Based on expression analysis, together with in vitro motility and previously published invasiveness data, we classified our panel of HCC cell lines into two subtypes (Table 1). We qualified HepG2, Huh7, Hep3B and Hep40 as "well-differentiated" HCC cell lines, because they express AFP, E-cadherin, HNF-4α and HNF-1α, and they display low motility and/or low invasiveness. Most of these features are confined to "well-differentiated" HCC tumors ([2,18,32,33]. We qualified the remaining seven cell lines (SNU398, SNU475, SNU449, SNU387, FOCUS, Mahlavu, SNU182) as "poorly-differentiated" HCC cell lines, based on the lack of expression of both hepatocyte lineage and epithelial cell markers analyzed here. In addition, these poorly differentiated cell lines shared many features with mesenchymal cells including the expression of mesenchymal markers (vimentin, slug, snail, twist-1, and twist-2), high motility and invasiveness. These expression

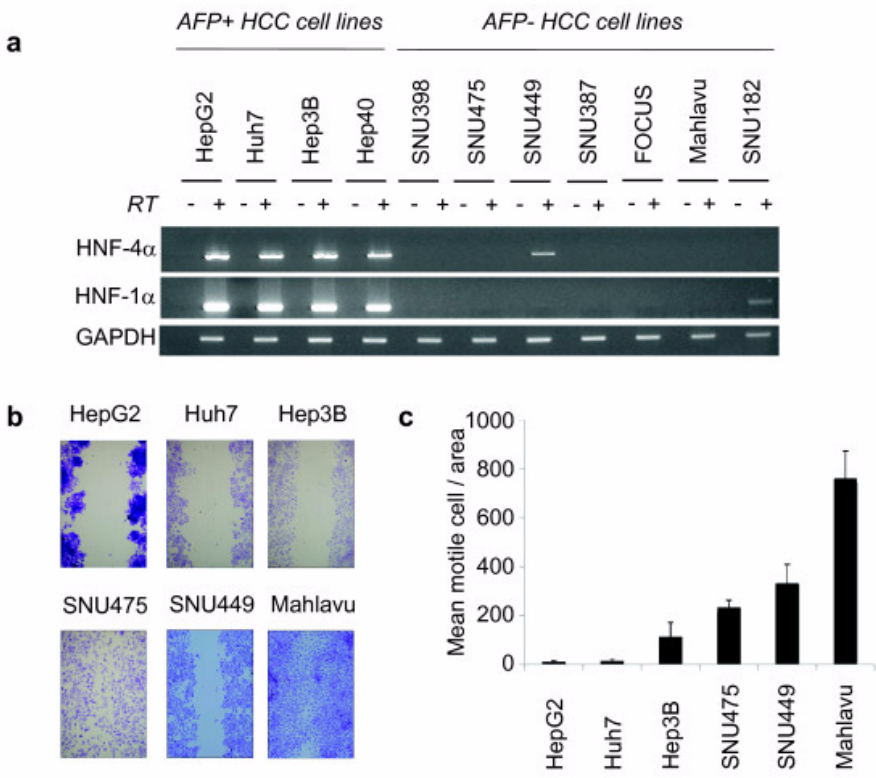

Figure 3

Expression of hepatocyte lineage markers HNF-4α and HNF-1α in HCC cell line correlate with low motility. (**a**)Selective expression of HNF-4α and HNF-1α in AFP+ HCC cell lines. Total RNAs were extracted from cells and used for RT-PCR analysis of HNF-4α and HNF-1α expression. GAPDH RT-PCR was used as a loading control. (**b. c**) Differential motility of AFP+ and AFP- HCC cell lines. Cells were cultured in six-well culture plates, and a single linear wound was made with a pipette tip in confluent monolayer cells. The distances between wound edges were measured at fixed points in each dish according to standardized template. After 24 hours migration, cell migration into the wound was visualized using phase contrast microscopy at ×20 magnification (**b**). The number of cells migrating beyond the wound edge was counted (**c**). Assays in six replicates, error bars; SD. SNU475 cells are larger cells giving rise to visual overestimation of migrating cell number in the picture shown in **b**.

and migratory features are associated with tumor dedifferentiation and confined to poorly differentiated HCCs [6-8,14,34].

Expression TCF/LEF family of transcription factors

Following the identification of well-differentiated and poorly differentiated HCC cell lines, we analyzed the expression of 45 Wnt pathway genes by RT-PCR assay. We first investigated the expression profile of TCF/LEF factors. The TCF-1 and TCF-4 were highly expressed in all HCC cell lines, while TCF-3 expression was limited to a subset of cell lines (Figure 4). LEF-1 transcript expression was weak, except for SNU398 cells. These findings indicated that at least two different nuclear factors mediating canonical Wnt signaling were expressed in any of HCC cell lines tested.

Expression of Frizzled receptors and LRP co-receptors

Next we analyzed the expression of 10 Frizzled receptors and their two co-receptors. Two canonical (Fzd1, Fzd5) and three noncanonical (Fzd3, Fzd4, Fzd6) Frizzled receptors were expressed in all cell lines tested. Also, Fzd2, Fzd7 and Fzd8 were expressed in most cell lines independent of their differentiation status (Figure 5-top). Lrp-5 and Lrp-6 co-receptors also were consistently expressed in all cell lines (Figure 5-bottom). These findings indicated that HCC cell lines were equipped with the expression of several canonical and noncanonial Wnt signaling receptors,

Table 1: Well-differentiated and poorly differentiated HCC cell lines according to hepatocyte lineage, epithelial and mesenchymal markers, and in vitro motility and invasiveness assays

Cell Lines	Fetal Hepatocyte Marker	Epithelial & Hepatocyte Markers			Mesenchymal markers					Motility	Invasiveness
	AFP	**HNF4a**	**HNF1a**	**E-cadherin**	**vimentin**	**slug**	**Snail**	**Twist-1**	**Twist-2**		
Well-differentiated											
HepG2	High	High	High	Low	(-)	Low	Low	Low	High	Low	Low [14]
Huh7	High	High	High	High	Low	(±)	Low	Low	(-)	Low	Low [14]
Hep3B	High	High	High	High	Low	High	Low	(-)	(-)	Low	Low ([74]
Hep40	High	High	High	Low	High	(-)	High	High	Low	Low	n.t.
Poorly differentiated											
SNU398	(-)	(-)	(-)	Low	High	Low	High	High	High	Low	n.t.
SNU475	(±)	(-)	(-)	(-)	High	High	High	High	Low	High	n.t.
SNU449	(-)	Low	(-)	(±)	High	Low	Low	High	High	High	n.t.
SNU387	(-)	(-)	(-)	(-)	Low	High	High	(-)	(±)	n.t.	n.t.
FOCUS	(-)	(-)	(-)	Low	High	Low	(-)	(-)	Low	n.t.	n.t.
Mahlavu	(-)	(-)	(-)	(±)	High	Low	(-)	High	Low	High	High [74]
SNU182	(-)	(-)	(±)	High	high	High	High	High	High	High	n.t.

(-); not detected; ±; traces; n.t.; not tested.

so that each HCC cell line was likely to respond to both canonical and noncanonical Wnt signals.

Differential expression of canonical and noncanonical Wnt ligands

In humans, there are 19 known genes encoding canonical and noncanonical Wnt ligands [35]. We studied the expression profile of the complete list of human Wnt ligands (Figures 6 and 7). From the group of eight known canonical Wnt ligands, only Wnt3 was strongly and uniformly expressed in all cell lines tested. Wnt10b was also strongly expressed, but not in all cell lines (Figure 6). We observed selective expression of canonical Wnt8b in well differentiated cell lins. In contrast, among seven noncanonical Wnt ligands, Wnt4, Wnt5a, Wnt5b and Wnt7b were expressed in almost all poorly differentiated cell lines tested. This contrasted with their poor expression in well differentiated cell lines (Figure 7-top). Signaling specificity of four other Wnt ligands have not yet been clearly established [35]. Among these ligands, Wnt9a expression was detectable in nearly all cell lines tested. In contrast, Wnt9b and Wnt2b expressions were associated to well differentiated and poorly differentiated cell lines, respectively (Figure 7-bottom).

Our comprehensive analysis of Wnt signaling molecules in HCC cell lines revealed several features. First, with the exception of Wnt ligands, most of the major components of Wnt signaling pathway were expressed redundantly in HCC cell lines, independent of their differentiation status. In contrast, Wnt ligand expression displayed two types of selectivity. First, out of eight known canonical only Wnt3 and Wnt10b displayed strong expression in most cell lines, independent of differentiation status. Second, out of seven noncanonical Wnt ligands, four were expressed in HCC cell lines with a high selectivity for poorly differentiated ones. Well-diffferentiated cell lines displayed selective expression of Wnt8b. These findings may have several

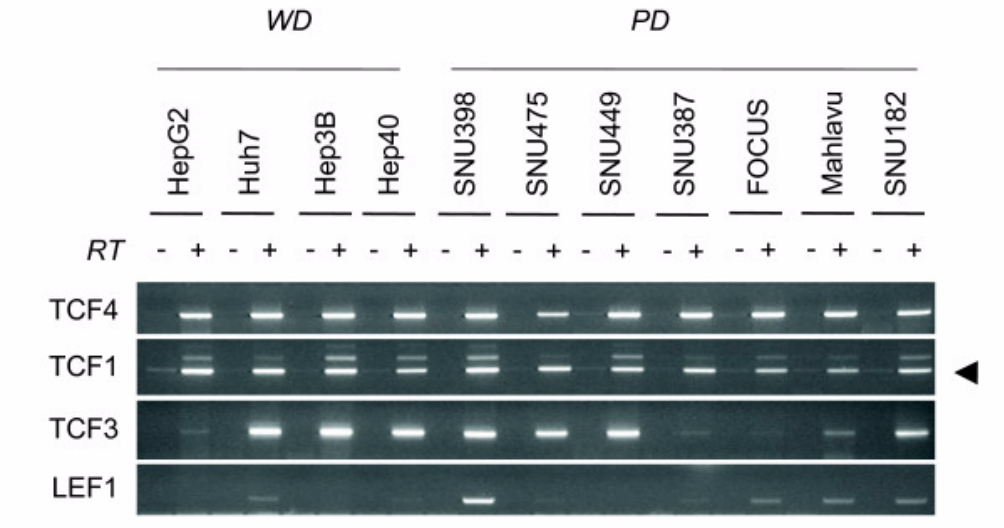

Figure 4
Comparative analysis of TCF/LEF transcription factors in hepatocellular carcinoma cell lines. Total RNAs were extracted from cell lines and used to detect gene expression by RT-PCR assay of four members of TCF/LEF family. See Figure 1 for GAPDH loading control.

implications. Most, in not all HCC cell lines were equipped with an autocrine/paracrine canonical Wnt signaling system, as reported previously for breast and ovarian cancer cell lines [36]. In contrast, because of selective expression of noncanonical Wnt ligands, only poorly differentiated cell lines could serve from an autrocrine noncanonical Wnt signaling system. In addition, poorly differentiated HCC cells could also provide noncanonical Wnt signals to other cells by a paracrine mechanism. Finally, noncanonical Wnt ligands such as Wnt5a might inhibit canonical Wnt signaling in HCC cells, as previously reported in other cell types [37-39].

Autocrine canonical Wnt signaling in well differentiated hepatocellular carcinoma cell lines

Canonical Wnt signaling activates TCF/LEF-dependent transcription, which can be monitored by reporters containing TCF/LEF-responsive elements [27,40]. We surveyed canonical Wnt signaling in HCC cell lines using TCF/LEF reporter pGL3-OT plasmid, as described previously [41]. First, we compared TCF/LEF (TCF) activity in three cell lines with known mutations in canonical Wnt signaling pathway (Figure 8a). Well-differentiated HepG2 cell line displays β-catenin mutation. Poorly-differentiated SNU398 and SNU475 cell lines display β-catenin and AXIN1 mutations, respectively [42,43]. Normalized TCF activity was the highest in HepG2 cells. Compared to HepG2, SNU398 cells displayed 50% less activity. More interestingly, despite a homozygous deletion leading to a loss of Axin1 expression (data not shown; [42,43], there was no detectable TCF activity in SNU475 cells. This contrasted sharply with another well-differentiated AXIN1 mutant HCC cell line, namely PLC/PRF/5 (Alexander) that displayed high TCF activity [42] (additional data not shown).

Next, we compared TCF activity of eight other cell lines that displayed wild-type β-catenin and AXIN1 status [41-43]. Hep40 cells that harbor a missense AXIN1 mutation/polymorphism (R454H) was included in this group, since functional significance of this mutation is unknown [41]. We detected weak, but significant (3-4 fold) TCF activity in well-differentiated Huh7 and Hep3B cell lines. On the other hand, all five poorly differentiated cell lines, as well as well-differentiated Hep40 cells displayed no detectable activity under our experimental conditions (Figure 8b).

Taken together, we collected TCF activity data from 12 HCC cell lines. Independent of β-catenin or AXIN1 status, TCF activity was detected in four out of five (80%) well-differentiated cell lines, whereas only one out of seven (14%) poorly differentiated cell lines had constitutive TCF activity [$P < 0.046$ (one-tailed), 0.071(two-tailed); Fisher Exact Probability Test]. This data supports the hypothesis that well-differentiated HCC cells display an autocrine/paracrine canonical Wnt signaling, probably because they co-express Wnt3 and several canonical Frizzled receptors. However, the great majority of poorly differentiated cell lines failed to generate canonical Wnt signaling activity, although they similarly co-expressed Wnt3 and canonical Frizzled receptors.

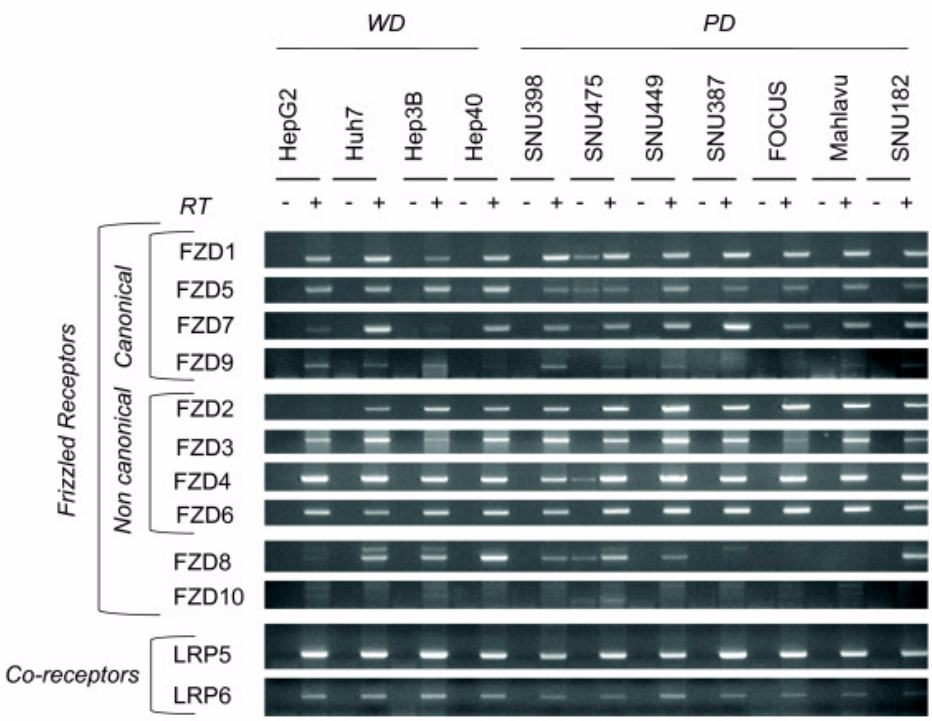

Figure 5

Comparative analysis of Frizzled receptors and LRP co-receptors in hepatocellular carcinoma cell lines. Frizzled receptors involved in canonical and noncanonical Wnt signaling were tested for expression by RT-PCR assay (Top). The expression of LRP co-receptors was analyzed similarly (bottom). Total RNAs were extracted from cell lines and used to detect gene expression by RT-PCR assay. See Figure 1 for GAPDH loading control.

Canonical Wnt signaling is repressed in poorly differentiated hepatocellular carcinoma cells

The lack of canonical Wnt activity in poorly differentiated cells could be due to either lack of sufficient Wnt ligand activity. Alternatively, canonical Wnt signaling could be repressed in these cell lines. A number of proteins downstream to β-catenin such as Axin2, HTLE family, hAES, Chibby, CTBP and ICAT are known to display inhibitory activity on canonical Wnt signaling [44]. We compared the expression of genes encoding these inhibitory proteins, but found no correlation with TCF activity or differentiation state (Figure 9).

Next, we compared TCF activity in Huh7, SNU449 and SNU182 cell lines following transient expression of a mutant (S33Y)-β-catenin (Figure 10). Transfection with S33Y-β-catenin resulted in an increase in total β-catenin protein in Huh7 and SNU449. This increase was less evident in SNU182 cells (Figure 10a). Well-differentiated Huh7 cells responded to S33Y-β-catenin expression by a strong activation of TCF/LEF reporter (130 folds). Under the same experimental conditions, the response of SNU449 cells was minimal (5 folds). More importantly, SNU182 cells were totally unresponsive (Figure 10b). These important differences between well-differentiated Huh7 and two different poorly differentiated cell lines (SNU449 and SNU182) are apparently not due to differences in transient transfection efficiencies, since the measured activities have been corrected for such differences (see material and methods section).

In order to confirm the data on weakened response in poorly differentiated cell lines, we generated a clone from SNU449 cells (SNU449-cl8) with Tet repressor controlled expression of N-terminally truncated β-catenin (aa 98-781). N-terminally truncated β-catenin forms are frequently detected in cancer cells including HCC cells. They lack Ser/Thr phosphorylation sites (aa Ser23, Ser29, Ser33, Ser37, Thr41, Ser45) that are critically involved in its ubiquitin-mediated degradation, and they accumulate in the cell nucleus leading to oncogenic activation canonical Wnt signaling [27]. As shown in figure 11a, SNU449-cl8 cells expressed only wild-type β-catenin in the presence of tetracycline (Tet-on conditions), while expressing both wild-type and truncated β-catenin at comparable levels in Tet-off conditions. The induced expression of truncated β-catenin resulted in only a weak activation (3-4 fold) of TCF reporter activity, similar to data obtained by

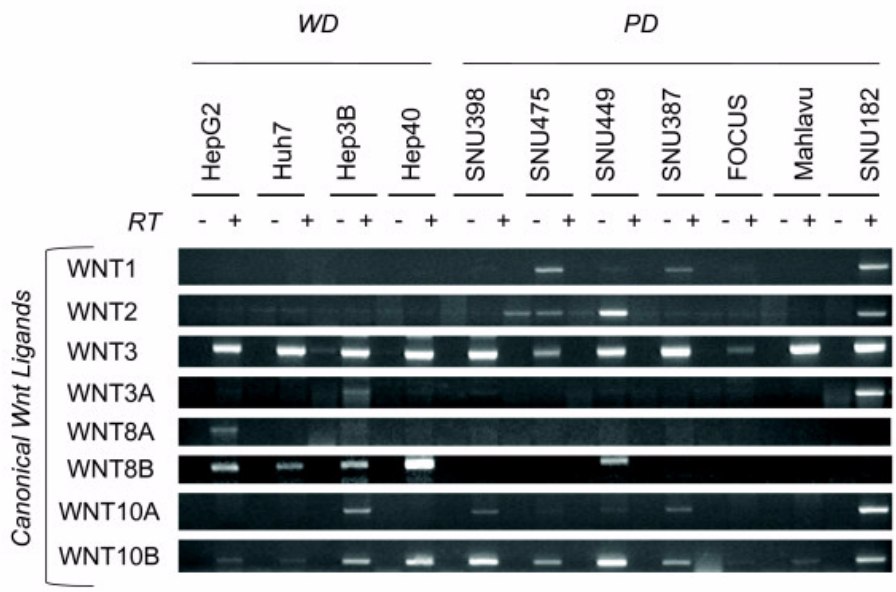

Figure 6
Comparative analysis of canonical Wnt ligands in hepatocellular carcinoma cell lines. Canonical Wnt ligands were tested for expression by RT-PCR assay. Total RNAs were extracted from cell lines and used to detect gene expression by RT-PCR assay. See Figure 1 for GAPDH loading control.

transient transfection experiments (Figure 11b). This low level of activation was similar to that seen in well-differentiated HCC cells in the absence of β-catenin or Axin-1 mutation (Fig. 8b), and strongly suggests that canonical Wnt signaling is actively repressed in this poorly differentiated HCC cell line. For comparison, well-differentiated HepG2 cells expressing wild-type and a similar N-terminally truncated β-catenin (Δ25-140 aa) activated TCF reporter gene by more than 60-fold (Figure 8a). In other words, although both Tet-off SNU449-cl8 and HepG2 cells displayed a heterozygous truncating β-catenin mutation, TCF activation was 15-fold less in poorly differentiated SNU449 background. To test whether this repression was related to cellular localization of β-catenin, we performed immunofluorescence detection using confocal microscopy (Figure 11c). Wild-type β-catenin was localized at the cell membrane with weak nuclear localization. The induction of truncated β-catenin in Tet-off SNU449-cl8 cells did not change this distribution significantly. We observed only weak cytoplasmic accumulation, with slight increases in both membrane and nuclear localization. In sharp contrast with these observations, in colorectal cancer cells (APC-mutated), used as a positive control [45], we detected strong nuclear accumulation of β-catenin by the same technique.

WNT5A inhibits canonical Wnt signaling in HCC cells

Presently, the mechanism of repression of canonical Wnt signaling in poorly differentiated HCC cells is unknown, but it is associated with a lack of nuclear accumulation of β-catenin. Among noncanonical Wnt ligands, Wnt5a is best known for its antagonistic effect on canonical Wnt signaling [46]. Therefore, we tested the effect of ectopic Wnt5a expression on mutant-β-catenin-induced TCF activity in Huh7 cell line. In the absence of Wnt5a, TCF activity was induced more than 160-fold by mutant β-catenin in this cell line. Co-expression of Wnt5a resulted in three-fold repression of TCF activity (Figure 12a). To confirm our observations, we also tested the effects of Wnt5a on TCF activity induced by endogenous mutant β-catenin using HepG2 cell line. The expression of Wnt5a in this cell line caused a significant inhibition of TCF activation mediated by endogenous β-catenin ($P < 0.05$; Figure 12b). We concluded that Wnt5a that is selectively expressed in poorly differentiated HCC cell lines, and probably similarly acting noncanonical Wnt ligands are involved, at least partly, in the repression of canonical Wnt signaling in these cells.

Discussion

Since the initial description of β-catenin mutations in HCCs in 1998 [33], Wnt signaling became a center of interest for these tumors. A large set of Wnt ligands and a large array of receptors are implicated in different cell processes by initiating canonical, but also noncanonical Wnt signals [35]. The antagonism between canonical and noncanonical Wnt pathways has also been reported [37,38,46]. Thus, both β-catenin and Wnt signaling are

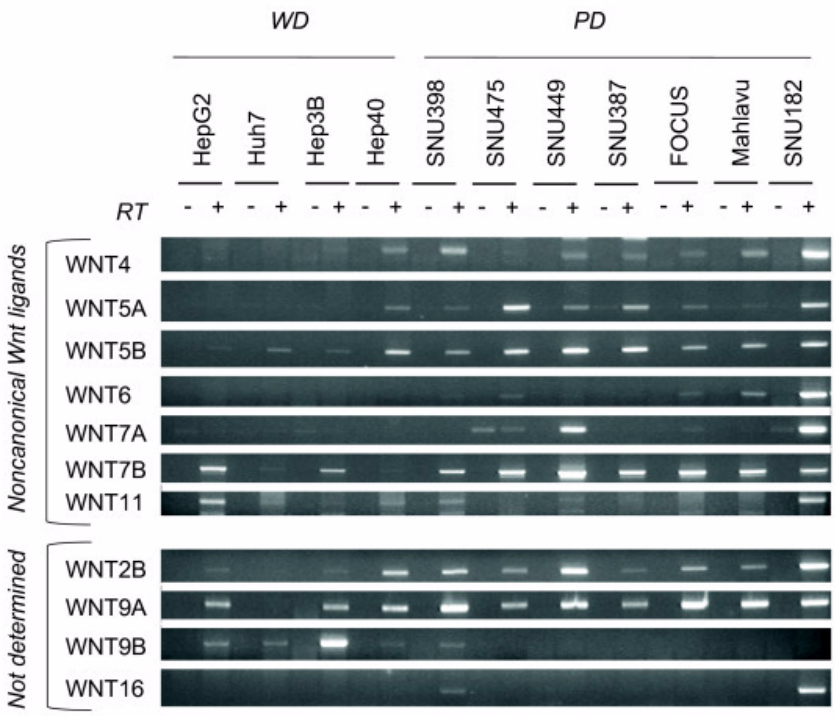

Figure 7
Comparative analysis of noncanonical (top) and unclassified (bottom) Wnt ligands in hepatocellular carcinoma cell lines. Noncanonical and unclassified Wnt ligands were tested for expression by RT-PCR assay. Total RNAs were extracted from cell lines and used to detect gene expression by RT-PCR assay. See Figure 1 for GAPDH loading control.

involved in highly complex cellular events of which only some are mediated by canonical Wnt pathway. This complexity is also observed during liver development and as well as in adult liver homeostatic events. Canonical Wnt signaling contributes to liver growth and regeneration, but also to liver "zonation" by controlling some liver-specific metabolic programs. ([47]). In addition, it contributes to the activation of liver stem or progenitor cells, as well as HCC-initiating cells [48-51].

Mutational activation of canonical Wnt signaling is not a frequent event in HCC, in contrast to hepatoblastoma displaying very high rates [52]. Mutations of β-catenin were restricted to a group of HCCs associated with low p53 mutation rate, negative HBV status and chromosomal stability, as stated earlier. These mutations were also associated with lower histological grade and better patient survival. Unexpectedly, β-catenin mutations are rare in more advanced and poorly differentiated HCCs [20,23]. Therefore, although considered to play an active role in HCC malignancy, the activation of canonical Wnt signaling may not be necessary for, or even repressed in advanced HCCs. Thus, β-catenin mutation and constitutive activation of canonical Wnt signaling may be differentiation-dependent events with mechanistic implications in HCC initiation and progression. We attempted to address this issue by using HCC-derived cell lines.

We first classified 11 HCC cell lines into "well-differentiated" and "poorly differentiated" subtypes using hepatocyte lineage, epithelial and mesenchymal cell markers, and in vitro migration assays. Well-differentiated HCC cell lines shared many features with hepatocytes such as expression of HNF-1α, HNF-4α, and E-cadherin, and epithelial morphology. Poorly differentiated cell lines were usually deficient in the expression of hepatocyte lineage and epithelial markers, but they expressed different mesenchymal markers strongly. These two types of HCC cell lines were also distinguished from each other by their in vitro behaviors. Poorly differentiated cell lines were usually more motile and more invasive than well-differentiated cell lines (Table 1). A global expression profiling study classified HCC cell lines in Group I and Group II [51]. Our well-differentiated and poorly differentiated cell line subtypes showed perfect correlation with Group I and Group II, respectively. Well-differentiated Group I was characterized by the activation of oncofetal promoters leading to increased expression of AFP and IGF-II, whereas poorly differentiated Group II was characterized by overexpression of genes involved in metastasis and

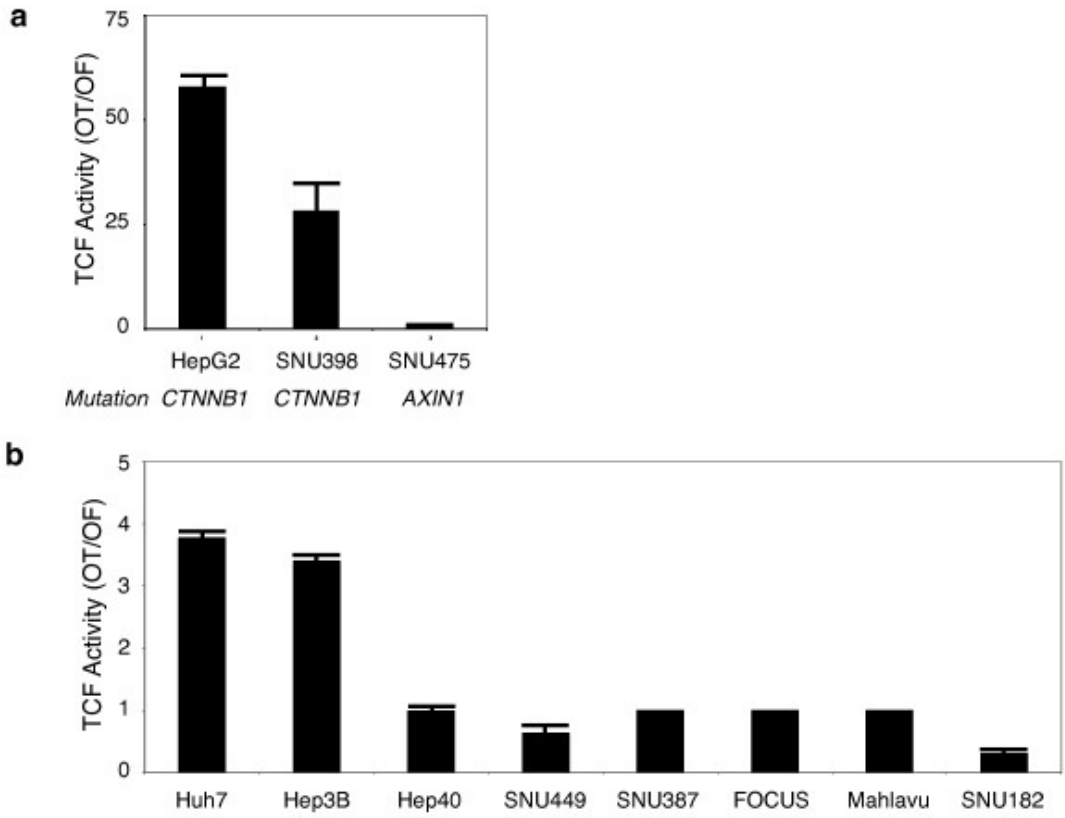

Figure 8

Frequent constitutive activation of canonical Wnt signaling in well-differentiated, but not in poorly differentiated hepatocellular carcinoma cell lines. (**a**) Comparative analysis of the canonical Wnt signaling in hepatoma cell lines with known mutations of β-catenin or Axin-1 genes. TCF reporter assay shows that well-differentiated HepG2 cells display high signaling activity. In contrast, canonical Wnt signaling is attenuated in poorly differentiated SNU398, and undetectable in poorly differentiated SNU475 cell line. Assays in triplicate, error bars; SD. (**b**) Comparative analysis of the canonical Wnt signaling in HCC cell lines with wild-type β-catenin and Axin-1 genes. Huh7 and Hep3B cell lines (both well-differentiated) display weak but significantly increased TCF reporter activity. Other cell lines (all poorly differentiated, except Hep40) display no detectable TCF reporter activity. TCF activity denotes the ratio of signals detected with pGL3-OT (OT) and pGL3-OF (OF) plasmids, respectively. Assays in triplicate, error bars; S. D. Cells were transfected with the reporter gene pGL3-OT (OT) harboring LEF-1/TCF binding sites for β-catenin and the corresponding pGL3-OF (OF) without these sites.

invasion. Our well-differentiated and poorly differentiated subtypes were also in perfect correlation with respectively epithelial and mesenchymal HCC cell line types that have been identified very recently [12]. Mesenchymal cancer cells are considered as the products of EMT that is believed to be a key mechanism for the acquisition of invasive and metastatic capabilities by tumor cells [53]. Higher motility of poorly differentiated HCC cell lines reported here is in line with this concept. Thus, our two classes of cell lines share many similarities with well-differentiated and poorly differentiated HCC tumors. We used this model to compare the status of Wnt pathway according to HCC differentiation status.

A comprehensive analysis of Wnt signaling components in liver or hepatocytes is lacking. However, the expression of Wnt ligands and Frizzled receptors in mouse hepatocytes has been published [54]. Mouse hepatocytes expressed canonical receptors Fzd7 and Fzd9, as well as noncanonical Fzd2, Fzd3, Fzd4 and Fzd6. We observed highly similar pattern of expression in HCC cell lines with the exception of Fzd9 that showed weak expression. In addition, we detected increased expression of canonical Fzd1 and Fzd5 in most HCC cell lines. The expression frequency of these receptors was not associated with HCC cell differentiation status. Mouse hepatocytes expressed canonical Wnt1 and Wnt2, and noncanonical Wnt4, Wnt5a, Wnt5b and Wnt11. All or most HCC cell lines

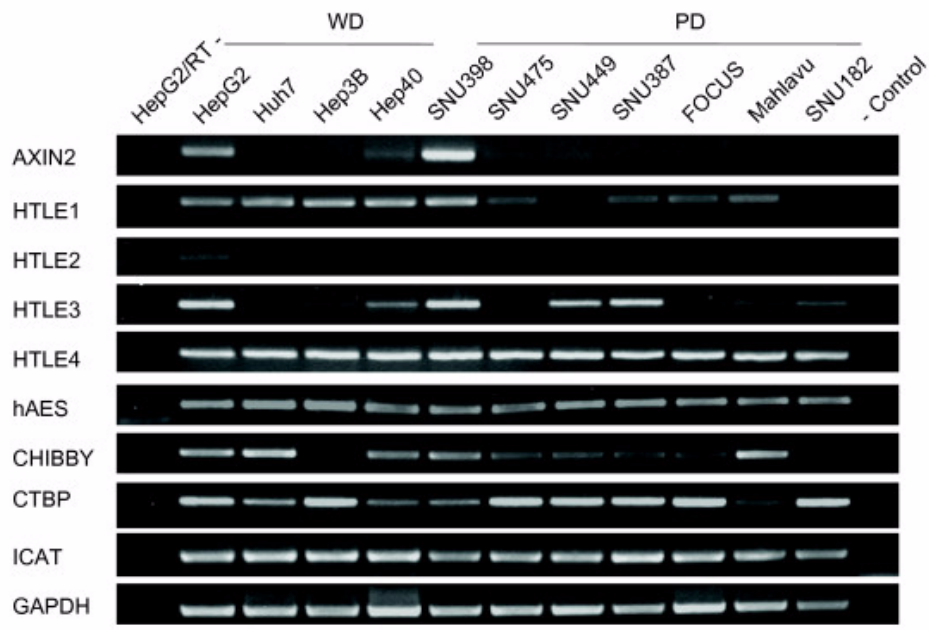

Figure 9
Expression analysis of genes inhibiting canonical Wnt signaling downstream to β-catenin in HCC cells. Total RNAs were extracted from cell lines and used to detect gene expression by RT-PCR assay. GAPDH RT-PCR was used as a loading control.

have lost the expression of canonical Wnt1 and Wnt2, but they displayed increased expression of canonical Wnt3 and Wnt10b ligands. Another canonical ligand, Wnt8b was expressed selectively in well-differentiated cell lines. In contrast, noncanonical Wnt4, Wnt5a and Wnt5b ligands were expressed in the majority of poorly differentiated cell lines, but not in most of well-differentiated cell lines. In addition, most HCC cell lines (poorly differentiated cell lines in particular) also displayed increased expression of noncanonical Wnt7b. Among Wnt ligands and Frizzled receptors that we found to be expressed or upregulated in HCC cell lines, Wnt3, Wnt4, Wnt5a, Fzd3, Fzd6 and Fzd7 have been previously reported to be overexpressed also in primary HCC tumors [55-57]. Overexpression of Wnt10b was also reported in HCC cels [58]. Increased levels of Wnt5a transcripts were detected in chronic hepatitis, cirrhosis and HCC [59]. A C-terminally mutated HBV X protein was shown to upregulate Wnt5a expression in HCC cells [60]. Thus, Wnt5a upregulation observed in clinical samples might be related to HBV at least in HBV-related liver diseases. Based on our observations that associate noncanonical Wnt ligand expression to poorly differentiated HCC cell lines, it will be interesting to test the predictive value of noncanonical Wnt expression for HCC prognosis.

Another important finding of this study is the differential activity of canonical Wnt signaling in different HCC subtypes. Well-differentiated cell lines displayed active canonical Wnt signaling at variable degrees. In addition to strong signaling activity associated to β-catenin and Axin1 mutations in two well differentiated cell lines, we also observed autocrine canonical Wnt signaling in two other well differentiated cell lines, as reported for some other cancer cell lines [36]. The functional significance of autocrine canonical Wnt signaling in these cell lines is not known.

However, small molecule antagonists of Tcf4/beta-catenin complex were shown to inhibit TCF reporter activity and down-regulate the endogenous Tcf4/β-catenin target genes c-Myc, cyclin D1, and survivin in Huh7 cells [61]. This observation strongly suggests that the autocrine canonical Wnt signaling is functional in well-differentiated HCC cell lines. Canonical Wnt signaling has been linked to both stem cell and cancer cell self-renewal in other cancer types. It was proposed that some adult cancers derive from stem/progenitor cells and that canonical Wnt signaling in stem and progenitor cells can be subverted in cancer cells to allow malignant proliferation [62]. Indeed, well-differentiated-HCC cell lines identified

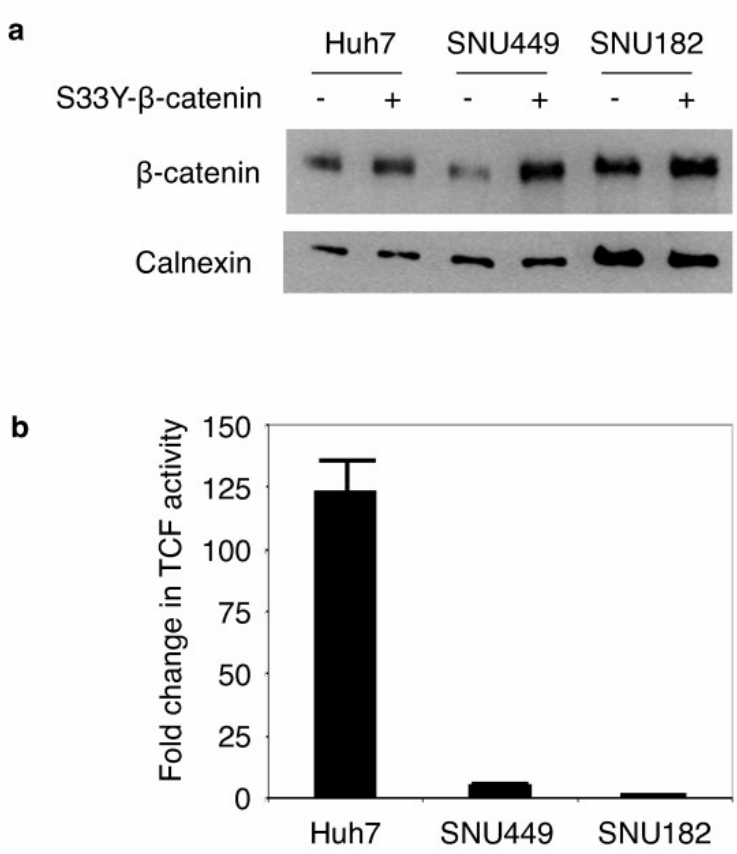

Figure 10

Ectopic expression of mutant β-catenin induces high canonical Wnt activity in well-differentiated, but not in poorly differentiated hepatocellular carcinoma cells. (**a**) Well-differentiated Huh7, and poorly differentiated SNU449 and SNU182 cell lines have been co-transfected with either pCI-neo-mutant β-catenin (S33Y) plasmid (S33Y-β-catenin +) or empty pCI-neo plasmid (S33Y-β-catenin -), and cellular β-catenin levels at post-transfection 48 h were tested by immunoblotting. Calnexin was used as a loading control. (**b**) Cell lines were treated as described, then pCI-neo-mutant β-catenin (S33Y)-transfected cells were subjected to TCF reporter assay. TCF activity denotes the ratio of signals detected with pGL3-OT (OT) and pGL3-OF (OF) plasmids, respectively. Assays in triplicate, error bars; SD. Co-transfections included pGL-OT or pGL-OF, in addition to pCI-neo plasmids in both (a) and (b).

here such as HepG2, Huh7 and PLC/PRF/5 have been reported to harbor HCC stem cells [63]

Our third noteworthy observation was the lack of detectable canonical Wnt signaling activity in six out of seven poorly differentiated cell lines. Even a poorly differentiated cell line with a deleterious Axin1 mutation (SNU475) lacked detectable signaling activity. Thus, most probably, the canonical Wnt signaling was not only inactive, but also repressed in poorly differentiated HCC cell lines. In confirmation of this expectation, transient or Tet-regulated expression of mutant β-catenin failed to generate significant canonical Wnt signaling activity in two different poorly differentiated cell lines. Furthermore, we linked this weak activity to poor nuclear accumulation of β-catenin protein in SNU449.cl8 cell line. Thus, unlike well-differentiated cell lines, poorly differentiated HCC cells displayed strong resistance to canonical Wnt signal activation.

The mechanisms of resistance to canonical Wnt signal activation in poorly differentiated HCC cells are presently unknown. We provide here one potential mechanism. Wnt5a has been previously implicated in canonical Wnt signaling as an antagonist and regulator of β-catenin levels in other cell types [48,49]. Using both ectopic and endogenous mutant β-catenin expression systems in two different cell lines, we demonstrated that co-transfections with Wnt5a-expressing plasmid can significantly inhibit canonical Wnt signaling in HCC cells. The mechanism of Wnt5a antagonism on canonical Wnt signaling in HCC cells is not known. In breast cancer cells, the loss of Wnt5a

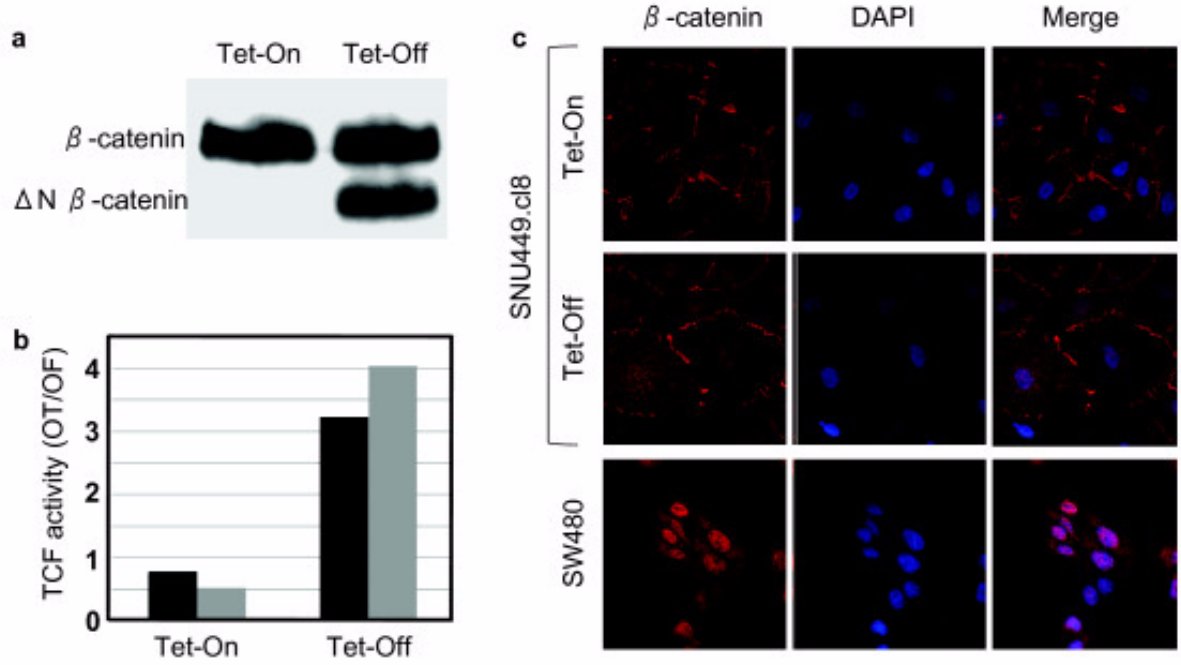

Figure 11
Minimal TCF reporter activity and lack of nuclear accumulation of mutant β-catenin in poorly differentiated SNU449.cl8 cells. SNU449 cells were stably transfected with Tet-responsive ΔN-β-catenin expression vector to obtain SNU448.cl8 cells. (**a**) Induced expression of N-terminally truncated ΔN-β-catenin protein in the Tet-Off conditions, as tested by western blot assay. Total cell lysates were extracted from cells and subjected to western blot assay using anti-β-catenin antibody. (**b**) TCF activity is only weakly induced in Tet-off conditions, as tested by duplicate experiments. (**c**) SNU449.cl8 cells at Tet-On state express wild-type endogenous β-catenin protein principally located at cell membrane. Under Tet-Off conditions the staining pattern remains almost identical despite ΔN-β-catenin expression. Note lack of nuclear accumulation. SW480 cells used as positive control display strong nuclear β-catenin staining. Cells were grown on coverslips, subjected to indirect immunofluorescence assay using anti-β-catenin antibody (red), counterstained with DAPI (blue) and examined by confocal microscopy.

signaling resulted in stabilization of nuclear beta-catenin and expression of Wnt/beta-catenin target genes [64]. However, both ectopically and endogenously expressed mutant β-catenins used in our experiments were N-terminally truncated devoid of their Ser/Thr phosphorylation motifs. Thus, Wnt5a appears to inhibit canonical Wnt signaling in HCC cells, downstream to β-catenin, independent of its glycogen synthase 3-β- and bTrCO-dependent degradation. Wnt5a has been shown to inhibit canonical Wnt signaling either by bTrCP-independent proteasomal degradation [65], or, by downregulating β-catenin-induced reporter gene expression without influencing β-catenin levels [37] in kidney epithelial cells. Wnt5a may use similar mechanisms in Huh7 and HepG2 cells. Further studies with downregulation of noncanonical Wnt ligands in poorly differentiated HCC cell lines may help to better define the implications of such ligands in liver cancer biology.

The role of Wnt5a in cancer is complex. It may play tumor-promoting or tumor-suppressing functions depending on cellular context. Wnt5a has been described as a tumor promoter in melanoma, gastric, pancreas, prostate cancer, but as a tumor suppressor in HCC, neuroblastoma, leukemia, colon, and thyroid cancers [46]. The inability of Wnt5a to transform cells or signal through the canonical β-catenin pathway pointed that it cannot promote tumorigenesis by upregulation of canonical Wnt signaling, unlike canonical Wnt ligands [66]. Our results suggest that Wnt5a, upregulated in poorly differentiated highly motile mesenchymal-like HCC cells may play a role in tumor progression by inducing EMT. Upregulation of Wnt5a expression during EMT has been reported [67]. Furthermore, the Wnt5A/Protein kinase C pathway was shown to mediate motility in melanoma cells via of an EMT [68]. Similarly, CUTL1-upregulated Wnt5a significantly enhanced migration, proliferation and invasiveness

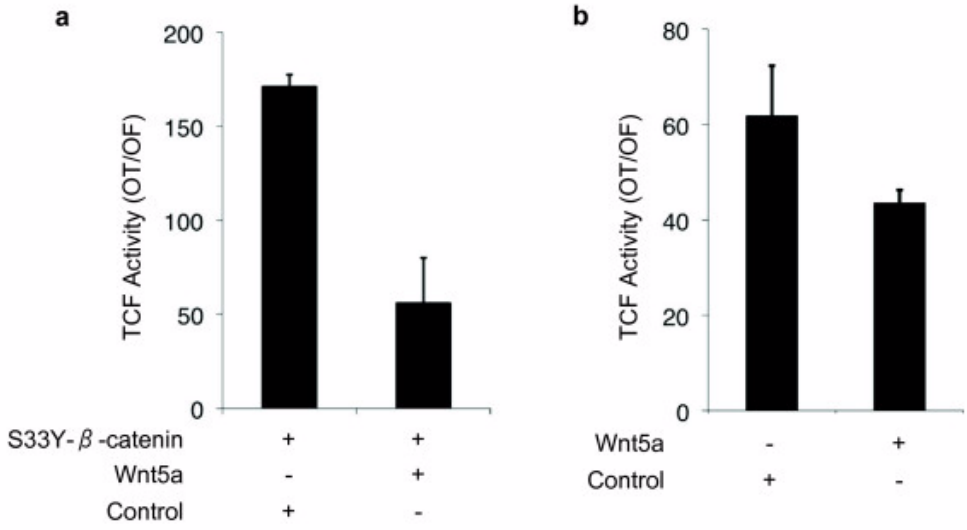

Figure 12

Wnt5a inhibits canonical Wnt signaling activity in Huh7 and HepG2 cells. (**a**) Huh7 cells were co-transfected with either pCI-neo-mutant β-catenin (S33Y) plasmid (S33Y-β-catenin +) along with pShuttle-IRES-WNT5a or empty pShuttle-IRES vector. 48 hours post transfection; cells were subjected to TCF reporter assay. TCF activity denotes the ratio of signals detected with pGL3-OT (OT) and pGL3-OF (OF) plasmids, respectively. Assays in triplicate, error bars; SD. Co-transfections included pGL-OT or pGL-OF, in addition to pCI-neo-S33Y-β-catenin and pIRES plasmids. (**b**) HepG2 experiments were performed under similar conditions, except that pCI-neo-mutant β-catenin (S33Y) plasmid was omitted.

in pancreas cancer cellls [69]. These effects were accompanied by a marked modulation of marker genes associated with EMT. Wnt5a may promote EMT in HCC cells by a similar mechanism.

The expression status of Wnt5a in HCC is not well known. To our knowledge, only one report addressed this issue [59]. Compared to normal tissue, Wnt5a mRNA expression was strongly induced in HCC, as well as in chronic hepatitis and cirrhosis. However, immunostaining of Wnt5a protein showed a bell-shaped pattern: low to undetectable levels were present in normal tissue and in tumor samples, whereas strong immunostaining was seen in chronic hepatitis, cirrhosis and dysplastic liver cells. The reasons of the discrepancy between transcript and protein expression in HCC tissues are not known presently. However, it appears that peritumoral liver tissues express high levels of Wnt5a protein that could trigger noncanonical Wnt signaling in adjacent tumor cells. It will be important to further investigate the role of Wnt5a in HCC tumor progression.

Taken together, our studies demonstrate that canonical Wnt activity is active in well-differentiated, but repressed in poorly differentiated HCC cell lines. This correlates with in vivo tumor studies indicating that β-catenin mutations are prevelant in well-differentiated, but not in poorly differentiated tumors. In addition, we showed that poorly differentiated cell lines express noncanonical Wnt ligands such as Wnt5a acting as an antagonist of canonical Wnt signaling. Thus, it appears that HCC cells may activate or repress their canonical Wnt signaling, using autocrine/paracrine systems based on selective use of canonical and noncanonical Wnt ligands.

We hypothesize that the active canonical Wnt signaling observed in well-differentiated HCC cells contributes to tumor initiation, but not necessarily to tumor progression. Instead, noncanonical Wnt signaling may be used by poorly differentiated HCC tumors to promote cell motility and invasion. Selective use of canonical and noncanonical Wnt signaling at different stages may be a key mechanism involved in hepatocellular carcinogenesis. Recent studies showed that canonical Wnt signaling contributes to the self-renewal and expansion of HCC-initiating cells with stem/progenitor cell features [50,70]. However, the lack of HCC development in β-catenin transgenic mice strongly suggests that canonical Wnt signaling activation has limited tumorigenic potential in liver tissue. Indeed, recent studies showed that canonical Wnt signaling plays a major role in the specification of mature hepatocytes for perivenous-specific gene expression ([71,72]. Such a hepatocyte differentiation function of canonical Wnt signaling may not be compatible with cellular dedifferentiation that goes along with HCC development. Therefore, alternative pathways such as Wnt5a-

mediated noncanonical Wnt signaling may be necessary for sustained growth and progression of HCC tumors. Melanoma may serve as a demonstrated model to our hypothesis. Similar to HCC, canonical Wnt signaling activation is an early event and nuclear β-catenin accumulation is associated with better patient survival in melanoma. Nuclear β-catenin is lost in more aggressive melanomas that express Wnt5a that promotes EMT, cell motility and metastasis[46]. Chien et al. [73] have recently demonstrated that canonical Wnt signaling induces growth inhibition and differentiation in melanoma cells, whereas Wnt5a can antagonize some of these effects. These findings clearly establish a dual function of Wnt signaling in melanoma. In light of these recent developments, our findings call for further investigations on respective roles of canonical and noncanonical Wnt signaling in HCC.

Conclusion

Our observations support the hypothesis that Wnt pathway is selectively activated or repressed depending on differentiation status of HCC cells. We propose that canonical and noncanonical Wnt pathways have complementary roles in HCC, where the canonical signaling contributes to tumor initiation, and noncanonical signaling to tumor progression.

Methods

Cell lines

Hepatocellular carcinoma cell lines Huh7, Hep40, Hep3B, Hep3B-TR, FOCUS, Mahlavu, SNU182, SNU 387, SNU 398, SNU423, SNU 449, SNU 475, PLC/PRF/5, SK-Hep-1, hepatoblastoma cell line HepG2 and colorectal cancer cell line SW480 were cultivated as described previously [41].

Reverse transcription-polymerase chain reaction (RT-PCR) analysis

Total RNAs were extracted from cultured cells using NucleoSpin RNA II Kit (MN Macherey-Nagel, Duren, Germany) according to the manufacturer's protocol. The cDNAs were prepared from total RNA (2 μg) using RevertAid First Strand cDNA Synthesis Kit (MBI-Fermentas, Vilnius, Lithuania). A negative control without reverse transcriptase (1 μl ddH2O instead) was also prepared for each sample. All PCR reactions were carried out using 1 μl cDNA from the reverse transcription mix, for 35 cycles except GAPDH, which was amplified for 24 cycles. Negative controls without reverse transcriptase were included for each set of primers (primer sequence information is available upon request). PCR products were analyzed on a 2% (w/v) agarose gel.

Wound-healing assay

Cells were cultured in six-well culture plates in RPMI 1640 or DMEM with 10% FBS. A single linear wound was made with a p200 pipette tip in confluent monolayer cells. The distances between wound edges were measured at fixed points in each dish according to standardized template. Debris were removed by washing the cells twice with PBS and then cells were incubated in RPMI 1640 or DMEM with 2% FBS. After 24 hours migration, cells were fixed with methanol and stained with 0.2% crystal violet. Cell migration into the wound was visualized using phase contrast microscopy (x20 magnification). The number of cells migrating beyond the wound edge was quantified microscopically in the randomly selected fields for each triplicate well.

Immunocytochemistry

Cells were grown on coverslips, fixed in 4% formaldehyde, permeated with 0.5% saponin/0.1% Triton X-100, and stained with mouse monoclonal anti-human vimentin antibody (Dako) using Envision kit (Dako), developed with diaminobenzidine, and counterstained with hematoxylin.

Confocal microscopy

Cells were grown on slides in 6 well plates and were fixed in 3.5% paraformaldehyde (PFA) for 15 minutes, and permealized using 0,25% Triton-X-100 for 10 min. Non specific protein binding was blocked by 30 minutes of incubation with 5% bovine serum albumin (BSA) in phosphate-buffered saline (PBS) at room temperature. Cells were then incubated 2 hours with monoclonal anti-β-catenin antibody M5.2 (1:200 dilution) in 1% BSA in PBS at room temperature in a moist chamber. Immunofluorescence staining was obtained by incubating for 1 hour with Alexa Fluor® 594 F(ab')2 fragment of rabbit anti-mouse IgG (H+L) (Invitrogen) (dilution 1:750). Cells were counterstained with DAPI (dilution 1:750), slides were mounted using ProLong® Gold antifade reagent (Invitrogen) and examined under Zeiss LSM 510 Meta laser scanning confocal microscope (MPI Freibourg, Germany) using 488 nm and 543 nm laser excitation lines, and photographed.

Plasmids

The pShuttle-IRES-Wnt5a expression plasmid was constructed by subcloning of an EcoRI-cut Wnt5a cDNA fragment from plasmid pGEMTz-Wnt5a vector (a gift from R. Kemler) into BglII site of the pShuttle-IRES-hrGFP-1 vector (Stratagene, USA). pCI-Neo-mutant β-catenin (S33Y) expression plasmid, and pGL3-OT and pGL3-OF reporter plasmids were kindly provided by B. Vogelstein. Other plasmids were pCI-Neo (Promega) and pEGFP-N2 (Clontech, Palo Alto, CA). The pAUCT-ΔN-β-catenin plasmid expressing N-terminally truncated β-catenin (aa 98-781)

under the control of Tet repressor was constructed using pAUCT-CCW vector (gift from Ali Fattaey, USA). A cDNA fragment of XhoI-NotI digestion from pCI-Neo-mutant β-catenin (S33Y) plasmid was inserted into XhoI-NotI site of pAUCT-CCW vector.

Transfections

Endogenous TCF/LEF-dependent transcriptional activity was tested by using pGL3-OT and pGL3-OF reporter plasmids, as described previously [41], except that cells were transfected using Lipofectamin 2000 reagent (Invitrogen), following instructions provide by the supplier. Mutant β-catenin-induced TCF/LEF-dependent transcriptional activity was tested after co-transfection of cells with pCI-Neo-mutant β-catenin (S33Y) expression plasmid (1.75 μg/well) together with the reporter plasmids. pCI-Neo (1.75 μg/well) was used as negative control. The effect of Wnt5a expression on TCF/LEF-dependent transcriptional activity was tested using Huh7 and HepG2 cell lines. Huh7 cell line was co-transfected with pCI-Neo-mutant β-catenin (S33Y) expression plasmid (1 μg/well) together with either pShuttle-IRES-Wnt5a (0.75 μg/well) or the empty vector pShuttle-IRES-hrGFP-1 (0.75 μg/well) and pGL3-OT/pGL3-OF reporter plasmids (0.75 μg/well for each). At 48 h following transfection, luciferase assay was performed by using Luciferase Reporter Gene Assay, constant light signal kit (Roche Diagnostics GmbH., Mannheim, Germany). Luciferase activity was read with The Reporter® Microplate Luminometer (Turner BioSystems Inc., Sunnyvale, CA) and data was normalized according to transfection efficiency obtained with each transfection, as described previously [41]. HepG2 cell line was co-transfected with either pShuttle-IRES-Wnt5a (0.5 μg/well) or the empty vector pShuttle-IRES-hrGFP-1 (0.5 μg/well) and pGL3-OT/pGL3-OF reporter plasmids (0.5 μg/well for each), with an internal control (0.05 μg/well pRL-TK Renilla luciferase vector) in a 12-well plate, using Lipofectamine 2000 Transfection Reagent. Forty-eight hours post-transfection, the cells were washed with PBS, and lysed in passive lysis buffer (Dual Luciferase kit; Promega). The cell lysates were transferred into an Opti-Plate 96-well plate (Perkin-Elmer) and assayed in a 1420-Multilabel counter luminometer, VICTOR3 (Perkin-Elmer) using the Dual-Luciferase kit (Promega). Relative TOP-FLASH luciferase units were measured and normalized against Renilla luciferase activity and further normalized luciferase activity against FOP-FLASH activity. All transfection experiments were performed in triplicate and data were expressed as mean of triplicate values (±S. D.) and p values were calculated. TCF/LEF activity was reported as the ratio of normalized luciferase activities obtained with pGL-OT and pGL-OF plasmids, respectively (mean ± S. D.).

Generation of mutant β-catenin expressing SNU449-cl8 cell line

SNU449 cell line clone ectopically expressing N-terminally truncated (aa 98-781) β-catenin, under the control of Tet repressor was generated by stable transfection with pAUCT-ΔN-β-catenin plasmid. Briefly, SNU449 cells were plated onto 6-well plate and transfected with 2 μg of plasmid DNA using Lipofectamin 2000 reagent (Invitrogen). 24 hours post transfection, cells were transferred to 90 mm dishes and subjected to G418 (0.6 μg/ml) selection in the presence of tetracycline (1 μg/ml) until resistant cell colonies became visible. Several clones were tested by Western blot for the expression of N-terminally truncated (aa 98-781) β-catenin after withdrawing tetracycline from the culture medium to induce the expression of the transgene. Only one clone (SNU449-cl8) displayed Tet-dependent expression of mutant β-catenin, and it was used for further studies.

Western blotting

Detergent-soluble cell lysates were prepared at 48 h post-transfection and used for western blot analysis, as described previously [41]. Antibodies to β-catenin (Santa Cruz Biotechnology, Inc., CA) and calnexin (Sigma) were obtained commercially. ECL kit (Amersham Life Science, Inc., Piscataway, NJ) was used for detection of antigen-antibody complexes. Equal protein loading was verified by Western blot assay with calnexin antibody.

Statistical analysis

The statistical significance of the active TCF reporter activity between well-differentiated and poorly differentiated HCC cell lines was tested by Fisher Exact Probability Test using an on-line tool http://faculty.vassar.edu/lowry/VassarStats.html.

List of abbreviations

AFP: α-fetoprotein; EMT: epithelial to mesenchymal transition; FZD: Frizzled; HCC: hepatocellular carcinoma; HBV: hepatitis B virus; HNF: hepatocyte nuclear factor; PD: poorly differentiated; RT-PCR: reverse transcriptase-polymerase chain reaction; WD: well differentiated

Competing interests

The authors declare that they have no competing interests.

Authors' contributions

HY, KB, SS and EE carried our RT-PCR analyses. HY carried out confocal microscopy and western blot analyses. SS and MY carried out the immunocytochemistry. HY, HB, NO and NT carried out TCF reporter activity assays. KB constructed SNU440.cl8 cell line. EC, AT and NA carried out wound-healing and cell migration assays. KCA contributed to the design of the study. M.O. conceived of, designed and coordinated the study. MO., HY and KB

drafted the manuscript. All authors read and approved the final manuscript.

Authors' information

Nuri Ozturk - present address: Department of Biochemistry and Biophysics, University of North Carolina School of Medicine, Chapel Hill, North Carolina 27599. USA.

Nilgun Tasdemir - present address: Cold Spring Harbor Laboratory, One Bungtown Road, Cold Spring Harbor, NY 11724, USA.

Acknowledgements

This work was supported by a grant from TUBITAK. Additional support was provided by Terry Fox Fund of the Turkish Association for Research and Fight against Cancer, Turkish Academy of Sciences (Turkey), and Institut National de Cancer (France). H.Y. has performed confocal microscopy studies at MPI (Ralf Kemler's Lab, Freibourg, Germany), and was supported by an EMBO Short-term Fellowship. We thank B. Vogelstein for providing pCI-Neo-mutant β-catenin (S33Y), pGL3-OT and pGL3-OF plasmids, and A. Fattaey for the gift of pAUCT-CCW plasmid. We also thank R. Kemler for guidance in confocal microscopy analyses and for providing pGEMTz-Wnt5a plasmid and anti-β-catenin M5.2 antibody.

References

1. Bruix J, Boix L, Sala M, Llovet JM: **Focus on hepatocellular carcinoma.** *Cancer Cell* 2004, **5:**215-219.
2. Kojiro M: **Histopathology of liver cancers.** *Best Pract Res Clin Gastroenterol* 2005, **19:**39-62.
3. Abelev GI, Lazarevich NL: **Control of differentiation in progression of epithelial tumors.** *Adv Cancer Res* 2006, **95:**61-113.
4. Hsu HC, Wu TT, Wu MZ, Sheu JC, Lee CS, Chen DS: **Tumor invasiveness and prognosis in resected hepatocellular carcinoma. Clinical and pathogenetic implications.** *Cancer* 1988, **61:**2095-2099.
5. Osada T, Sakamoto M, Ino Y, Iwamatsu A, Matsuno Y, Muto T, Hirohashi S: **E-cadherin is involved in the intrahepatic metastasis of hepatocellular carcinoma.** *Hepatology* 1996, **24:**1460-1467.
6. Sugimachi K, Tanaka S, Kameyama T, Taguchi K, Aishima S, Shimada M, Tsuneyoshi M: **Transcriptional repressor snail and progression of human hepatocellular carcinoma.** *Clin Cancer Res* 2003, **9:**2657-2664.
7. Lee TK, Poon RT, Yuen AP, Ling MT, Kwok WK, Wang XH, Wong YC, Guan XY, Man K, Chau KL, Fan ST: **Twist overexpression correlates with hepatocellular carcinoma metastasis through induction of epithelial-mesenchymal transition.** *Clin Cancer Res* 2006, **12:**5369-5376.
8. Hu L, Lau SH, Tzang CH, Wen JM, Wang W, Xie D, Huang M, Wang Y, Wu MC, Huang JF, *et al.*: **Association of Vimentin overexpression and hepatocellular carcinoma metastasis.** *Oncogene* 2004, **23:**298-302.
9. Cicchini C, Filippini D, Coen S, Marchetti A, Cavallari C, Laudadio I, Spagnoli FM, Alonzi T, Tripodi M: **Snail controls differentiation of hepatocytes by repressing HNF4alpha expression.** *J Cell Physiol* 2006, **209:**230-238.
10. Giannelli G, Bergamini C, Fransvea E, Sgarra C, Antonaci S: **Laminin-5 with transforming growth factor-beta1 induces epithelial to mesenchymal transition in hepatocellular carcinoma.** *Gastroenterology* 2005, **129:**1375-1383.
11. Lee HC, Tian B, Sedivy JM, Wands JR, Kim M: **Loss of Raf kinase inhibitor protein promotes cell proliferation and migration of human hepatoma cells.** *Gastroenterology* 2006, **131:**1208-1217.
12. Fuchs BC, Fujii T, Dorfman JD, Goodwin JM, Zhu AX, Lanuti M, Tanabe KK: **Epithelial-to-mesenchymal transition and integrin-linked kinase mediate sensitivity to epidermal growth factor receptor inhibition in human hepatoma cells.** *Cancer Res* 2008, **68:**2391-2399.
13. Lahsnig C, Mikula M, Petz M, Zulehner G, Schneller D, van Zijl F, Huber H, Csiszar A, Beug H, Mikulits W: **ILEI requires oncogenic Ras for the epithelial to mesenchymal transition of hepatocytes and liver carcinoma progression.** *Oncogene* 2009, **28:**638-650.
14. Matsuo N, Shiraha H, Fujikawa T, Takaoka N, Ueda N, Tanaka S, Nishina S, Nakanishi Y, Uemura M, Takaki A, *et al.*: **Twist expression promotes migration and invasion in hepatocellular carcinoma.** *BMC Cancer* 2009, **9:**240.
15. Miyoshi A, Kitajima Y, Sumi K, Sato K, Hagiwara A, Koga Y, Miyazaki K: **Snail and SIP1 increase cancer invasion by upregulating MMP family in hepatocellular carcinoma cells.** *Br J Cancer* 2004, **90:**1265-1273.
16. Parviz F, Matullo C, Garrison WD, Savatski L, Adamson JW, Ning G, Kaestner KH, Rossi JM, Zaret KS, Duncan SA: **Hepatocyte nuclear factor 4alpha controls the development of a hepatic epithelium and liver morphogenesis.** *Nat Genet* 2003, **34:**292-296.
17. Battle MA, Konopka G, Parviz F, Gaggl AL, Yang C, Sladek FM, Duncan SA: **Hepatocyte nuclear factor 4alpha orchestrates expression of cell adhesion proteins during the epithelial transformation of the developing liver.** *Proc Natl Acad Sci USA* 2006, **103:**8419-8424.
18. Lazarevich NL, Cheremnova OA, Varga EV, Ovchinnikov DA, Kudrjavtseva EI, Morozova OV, Fleishman DI, Engelhardt NV, Duncan SA: **Progression of HCC in mice is associated with a downregulation in the expression of hepatocyte nuclear factors.** *Hepatology* 2004, **39:**1038-1047.
19. Thorgeirsson SS, Grisham JW: **Molecular pathogenesis of human hepatocellular carcinoma.** *Nat Genet* 2002, **31:**339-346.
20. Hsu HC, Jeng YM, Mao TL, Chu JS, Lai PL, Peng SY: **Beta-catenin mutations are associated with a subset of low-stage hepatocellular carcinoma negative for hepatitis B virus and with favorable prognosis.** *Am J Pathol* 2000, **157:**763-770.
21. Taniguchi K, Roberts LR, Aderca IN, Dong X, Qian C, Murphy LM, Nagorney DM, Burgart LJ, Roche PC, Smith DI, *et al.*: **Mutational spectrum of beta-catenin, AXIN1, and AXIN2 in hepatocellular carcinomas and hepatoblastomas.** *Oncogene* 2002, **21:**4863-4871.
22. Audard V, Grimber G, Elie C, Radenen B, Audebourg A, Letourneur F, Soubrane O, Vacher-Lavenu MC, Perret C, Cavard C, Terris B: **Cholestasis is a marker for hepatocellular carcinomas displaying beta-catenin mutations.** *J Pathol* 2007, **212:**345-352.
23. Mao TL, Chu JS, Jeng YM, Lai PL, Hsu HC: **Expression of mutant nuclear beta-catenin correlates with non-invasive hepatocellular carcinoma, absence of portal vein spread, and good prognosis.** *J Pathol* 2001, **193:**95-101.
24. Wong CM, Fan ST, Ng IO: **beta-Catenin mutation and overexpression in hepatocellular carcinoma: clinicopathologic and prognostic significance.** *Cancer* 2001, **92:**136-145.
25. Laurent-Puig P, Zucman-Rossi J: **Genetics of hepatocellular tumors.** *Oncogene* 2006, **25:**3778-3786.
26. Calvisi DF, Factor VM, Loi R, Thorgeirsson SS: **Activation of beta-catenin during hepatocarcinogenesis in transgenic mouse models: relationship to phenotype and tumor grade.** *Cancer Res* 2001, **61:**2085-2091.
27. Barker N, Clevers H: **Mining the Wnt pathway for cancer therapeutics.** *Nat Rev Drug Discov* 2006, **5:**997-1014.
28. Cadoret A, Ovejero C, Terris B, Souil E, Levy L, Lamers WH, Kitajewski J, Kahn A, Perret C: **New targets of beta-catenin signaling in the liver are involved in the glutamine metabolism.** *Oncogene* 2002, **21:**8293-8301.
29. Harada N, Miyoshi H, Murai N, Oshima H, Tamai Y, Oshima M, Taketo MM: **Lack of tumorigenesis in the mouse liver after adenovirus-mediated expression of a dominant stable mutant of beta-catenin.** *Cancer Res* 2002, **62:**1971-1977.
30. Harada N, Tamai Y, Ishikawa T, Sauer B, Takaku K, Oshima M, Taketo MM: **Intestinal polyposis in mice with a dominant stable mutation of the beta-catenin gene.** *EMBO J* 1999, **18:**5931-5942.
31. Ishiyama T, Kano J, Minami Y, Iijima T, Morishita Y, Noguchi M: **Expression of HNFs and C/EBP alpha is correlated with immunocytochemical differentiation of cell lines derived from human hepatocellular carcinomas, hepatoblastomas and immortalized hepatocytes.** *Cancer Sci* 2003, **94:**757-763.
32. Du GS, Wang JM, Lu JX, Li Q, Ma CQ, Du JT, Zou SQ: **Expression of P-aPKC-iota, E-cadherin, and beta-catenin related to invasion and metastasis in hepatocellular carcinoma.** *Ann Surg Oncol* 2009, **16:**1578-1586.

33. Wang W, Hayashi Y, Ninomiya T, Ohta K, Nakabayashi H, Tamaoki T, Itoh H: **Expression of HNF-1 alpha and HNF-1 beta in various histological differentiations of hepatocellular carcinoma.** *J Pathol* 1998, **184:**272-278.
34. Niu RF, Zhang L, Xi GM, Wei XY, Yang Y, Shi YR, Hao XS: **Up-regulation of Twist induces angiogenesis and correlates with metastasis in hepatocellular carcinoma.** *J Exp Clin Cancer Res* 2007, **26:**385-394.
35. Staal FJ, Luis TC, Tiemessen MM: **WNT signalling in the immune system: WNT is spreading its wings.** *Nat Rev Immunol* 2008, **8:**581-593.
36. Bafico A, Liu G, Goldin L, Harris V, Aaronson SA: **An autocrine mechanism for constitutive Wnt pathway activation in human cancer cells.** *Cancer Cell* 2004, **6:**497-506.
37. Mikels AJ, Nusse R: **Purified Wnt5a protein activates or inhibits beta-catenin-TCF signaling depending on receptor context.** *PLoS Biol* 2006, **4:**e115.
38. Nemeth MJ, Topol L, Anderson SM, Yang Y, Bodine DM: **Wnt5a inhibits canonical Wnt signaling in hematopoietic stem cells and enhances repopulation.** *Proc Natl Acad Sci USA* 2007, **104:**15436-15441.
39. Ishitani T, Kishida S, Hyodo-Miura J, Ueno N, Yasuda J, Waterman M, Shibuya H, Moon RT, Ninomiya-Tsuji J, Matsumoto K: **The TAK1-NLK mitogen-activated protein kinase cascade functions in the Wnt-5a/Ca(2+) pathway to antagonize Wnt/beta-catenin signaling.** *Mol Cell Biol* 2003, **23:**131-139.
40. Morin PJ, Sparks AB, Korinek V, Barker N, Clevers H, Vogelstein B, Kinzler KW: **Activation of beta-catenin-Tcf signaling in colon cancer by mutations in beta-catenin or APC.** *Science* 1997, **275:**1787-1790.
41. Erdal E, Ozturk N, Cagatay T, Eksioglu-Demiralp E, Ozturk M: **Lithium-mediated downregulation of PKB/Akt and cyclin E with growth inhibition in hepatocellular carcinoma cells.** *Int J Cancer* 2005, **115:**903-910.
42. Satoh S, Daigo Y, Furukawa Y, Kato T, Miwa N, Nishiwaki T, Kawasoe T, Ishiguro H, Fujita M, Tokino T, *et al.*: **AXIN1 mutations in hepatocellular carcinomas, and growth suppression in cancer cells by virus-mediated transfer of AXIN1.** *Nat Genet* 2000, **24:**245-250.
43. Cagatay T, Ozturk M: **P53 mutation as a source of aberrant beta-catenin accumulation in cancer cells.** *Oncogene* 2002, **21:**7971-7980.
44. Brantjes H, Roose J, Wetering M van De, Clevers H: **All Tcf HMG box transcription factors interact with Groucho-related co-repressors.** *Nucleic Acids Res* 2001, **29:**1410-1419.
45. Munemitsu S, Albert I, Souza B, Rubinfeld B, Polakis P: **Regulation of intracellular beta-catenin levels by the adenomatous polyposis coli (APC) tumor-suppressor protein.** *Proc Natl Acad Sci USA* 1995, **92:**3046-3050.
46. McDonald SL, Silver A: **The opposing roles of Wnt-5a in cancer.** *Br J Cancer* 2009, **101:**209-214.
47. Nejak-Bowen K, Monga SP: **Wnt/beta-catenin signaling in hepatic organogenesis.** *Organogenesis* 2008, **4:**92-99.
48. Hu M, Kurobe M, Jeong YJ, Fuerer C, Ghole S, Nusse R, Sylvester KG: **Wnt/beta-catenin signaling in murine hepatic transit amplifying progenitor cells.** *Gastroenterology* 2007, **133:**1579-1591.
49. Apte U, Thompson MD, Cui S, Liu B, Cieply B, Monga SP: **Wnt/beta-catenin signaling mediates oval cell response in rodents.** *Hepatology* 2008, **47:**288-295.
50. Yang W, Yan HX, Chen L, Liu Q, He YQ, Yu LX, Zhang SH, Huang DD, Tang L, Kong XN, *et al.*: **Wnt/beta-catenin signaling contributes to activation of normal and tumorigenic liver progenitor cells.** *Cancer Res* 2008, **68:**4287-4295.
51. Lee JS, Thorgeirsson SS: **Functional and genomic implications of global gene expression profiles in cell lines from human hepatocellular cancer.** *Hepatology* 2002, **35:**1134-1143.
52. Armengol C, Cairo S, Fabre M, Buendia MA: **Wnt signaling and hepatocarcinogenesis: The hepatoblastoma model.** *Int J Biochem Cell Biol* 2009 in press.
53. Kalluri R, Weinberg RA: **The basics of epithelial-mesenchymal transition.** *J Clin Invest* 2009, **119:**1420-1428.
54. Zeng G, Awan F, Otruba W, Muller P, Apte U, Tan X, Gandhi C, Demetris AJ, Monga SP: **Wnt'er in liver: expression of Wnt and frizzled genes in mouse.** *Hepatology* 2007, **45:**195-204.
55. Merle P, Kim M, Herrmann M, Gupte A, Lefrancois L, Califano S, Trepo C, Tanaka S, Vitvitski L, de la Monte S, Wands JR: **Oncogenic role of the frizzled-7/beta-catenin pathway in hepatocellular carcinoma.** *J Hepatol* 2005, **43:**854-862.
56. Kim M, Lee HC, Tsedensodnom O, Hartley R, Lim YS, Yu E, Merle P, Wands JR: **Functional interaction between Wnt3 and Frizzled-7 leads to activation of the Wnt/beta-catenin signaling pathway in hepatocellular carcinoma cells.** *J Hepatol* 2008, **48:**780-791.
57. Bengochea A, de Souza MM, Lefrancois L, Le Roux E, Galy O, Chemin I, Kim M, Wands JR, Trepo C, Hainaut P, *et al.*: **Common dysregulation of Wnt/Frizzled receptor elements in human hepatocellular carcinoma.** *Br J Cancer* 2008, **99:**143-150.
58. Yoshikawa H, Matsubara K, Zhou X, Okamura S, Kubo T, Murase Y, Shikauchi Y, Esteller M, Herman JG, Wei Wang X, Harris CC: **WNT10B functional dualism: beta-catenin/Tcf-dependent growth promotion or independent suppression with deregulated expression in cancer.** *Mol Biol Cell* 2007, **18:**4292-4303.
59. Liu XH, Pan MH, Lu ZF, Wu B, Rao Q, Zhou ZY, Zhou XJ: **Expression of Wnt-5a and its clinicopathological significance in hepatocellular carcinoma.** *Dig Liver Dis* 2008, **40:**560-567.
60. Liu X, Wang L, Zhang S, Lin J, Feitelson MA, Gao H, Zhu M: **Mutations in the C-terminus of the X protein of hepatitis B virus regulate Wnt-5a expression in hepatoma Huh7 cells: cDNA microarray and proteomic analyses.** *Carcinogenesis* 2008, **29:**1207-1214.
61. Wei W, Chua MS, Grepper S, So S: **Small molecule antagonists of Tcf4/beta-catenin complex inhibit the growth of HCC cells in vitro and in vivo.** *Int J Cancer* 2009 in press.
62. Reya T, Clevers H: **Wnt signalling in stem cells and cancer.** *Nature* 2005, **434:**843-850.
63. Chiba T, Kita K, Zheng YW, Yokosuka O, Saisho H, Iwama A, Nakauchi H, Taniguchi H: **Side population purified from hepatocellular carcinoma cells harbors cancer stem cell-like properties.** *Hepatology* 2006, **44:**240-251.
64. Roarty K, Baxley SE, Crowley MR, Frost AR, Serra R: **Loss of TGF-beta or Wnt5a results in an increase in Wnt/beta-catenin activity and redirects mammary tumour phenotype.** *Breast Cancer Res* 2009, **11:**R19.
65. Topol L, Jiang X, Choi H, Garrett-Beal L, Carolan PJ, Yang Y: **Wnt-5a inhibits the canonical Wnt pathway by promoting GSK-3-independent beta-catenin degradation.** *J Cell Biol* 2003, **162:**899-908.
66. Shimizu H, Julius MA, Giarre M, Zheng Z, Brown AM, Kitajewski J: **Transformation by Wnt family proteins correlates with regulation of beta-catenin.** *Cell Growth Differ* 1997, **8:**1349-1358.
67. Taki M, Kamata N, Yokoyama K, Fujimoto R, Tsutsumi S, Nagayama M: **Down-regulation of Wnt-4 and up-regulation of Wnt-5a expression by epithelial-mesenchymal transition in human squamous carcinoma cells.** *Cancer Sci* 2003, **94:**593-597.
68. Dissanayake SK, Wade M, Johnson CE, O'Connell MP, Leotlela PD, French AD, Shah KV, Hewitt KJ, Rosenthal DT, Indig FE, *et al.*: **The Wnt5A/protein kinase C pathway mediates motility in melanoma cells via the inhibition of metastasis suppressors and initiation of an epithelial to mesenchymal transition.** *J Biol Chem* 2007, **282:**17259-17271.
69. Ripka S, Konig A, Buchholz M, Wagner M, Sipos B, Kloppel G, Downward J, Gress T, Michl P: **WNT5A--target of CUTL1 and potent modulator of tumor cell migration and invasion in pancreatic cancer.** *Carcinogenesis* 2007, **28:**1178-1187.
70. Yamashita T, Ji J, Budhu A, Forgues M, Yang W, Wang HY, Jia H, Ye Q, Qin LX, Wauthier E, *et al.*: **EpCAM-positive hepatocellular carcinoma cells are tumor-initiating cells with stem/progenitor cell features.** *Gastroenterology* 2009, **136:**1012-1024.
71. Benhamouche S, Decaens T, Godard C, Chambrey R, Rickman DS, Moinard C, Vasseur-Cognet M, Kuo CJ, Kahn A, Perret C, Colnot S: **Apc tumor suppressor gene is the "zonation-keeper" of mouse liver.** *Dev Cell* 2006, **10:**759-770.
72. Burke ZD, Reed KR, Phesse TJ, Sansom OJ, Clarke AR, Tosh D: **Liver zonation occurs through a beta-catenin-dependent, c-Myc-independent mechanism.** *Gastroenterology* 2009, **136:**2316-2324. e2311-2313
73. Chien AJ, Moore EC, Lonsdorf AS, Kulikauskas RM, Rothberg BG, Berger AJ, Major MB, Hwang ST, Rimm DL, Moon RT: **Activated Wnt/beta-catenin signaling in melanoma is associated with decreased proliferation in patient tumors and a murine melanoma model.** *Proc Natl Acad Sci USA* 2009, **106:**1193-1198.

74. Riou P, Saffroy R, Chenailler C, Franc B, Gentile C, Rubinstein E, Resink T, Debuire B, Piatier-Tonneau D, Lemoine A: **Expression of T-cadherin in tumor cells influences invasive potential of human hepatocellular carcinoma.** *FASEB J* 2006, **20:**2291-2301.

OPEN ACCESS Freely available online

PLoS one

The Ability to Generate Senescent Progeny as a Mechanism Underlying Breast Cancer Cell Heterogeneity

Mine Mumcuoglu[1], Sevgi Bagislar[1,2], Haluk Yuzugullu[1,2], Hani Alotaibi[1], Serif Senturk[1], Pelin Telkoparan[1], Bala Gur-Dedeoglu[1], Burcu Cingoz[1], Betul Bozkurt[3], Uygar H. Tazebay[1], Isik G. Yulug[1], K. Can Akcali[1], Mehmet Ozturk[1,2]*

1 BilGen Genetics and Biotechnology Center, Department of Molecular Biology and Genetics, Bilkent University, Ankara, Turkey, **2** INSERM - Université Joseph Fourrier, CRI U823, Grenoble, France, **3** Department of Surgery, Ankara Numune Research and Teaching Hospital, Ankara, Turkey

Abstract

Background: Breast cancer is a remarkably heterogeneous disease. Luminal, basal-like, "normal-like", and ERBB2+ subgroups were identified and were shown to have different prognoses. The mechanisms underlying this heterogeneity are poorly understood. In our study, we explored the role of cellular differentiation and senescence as a potential cause of heterogeneity.

Methodology/Principal Findings: A panel of breast cancer cell lines, isogenic clones, and breast tumors were used. Based on their ability to generate senescent progeny under low-density clonogenic conditions, we classified breast cancer cell lines as senescent cell progenitor (SCP) and immortal cell progenitor (ICP) subtypes. All SCP cell lines expressed estrogen receptor (ER). Loss of ER expression combined with the accumulation of $p21^{Cip1}$ correlated with senescence in these cell lines. $p21^{Cip1}$ knockdown, estrogen-mediated ER activation or ectopic ER overexpression protected cells against senescence. In contrast, tamoxifen triggered a robust senescence response. As ER expression has been linked to luminal differentiation, we compared the differentiation status of SCP and ICP cell lines using stem/progenitor, luminal, and myoepithelial markers. The SCP cells produced CD24+ or ER+ luminal-like and ASMA+ myoepithelial-like progeny, in addition to CD44+ stem/progenitor-like cells. In contrast, ICP cell lines acted as differentiation-defective stem/progenitor cells. Some ICP cell lines generated only CD44+/CD24-/ER-/ASMA- progenitor/stem-like cells, and others also produced CD24+/ER- luminal-like, but not ASMA+ myoepithelial-like cells. Furthermore, gene expression profiles clustered SCP cell lines with luminal A and "normal-like" tumors, and ICP cell lines with luminal B and basal-like tumors. The ICP cells displayed higher tumorigenicity in immunodeficient mice.

Conclusions/Significance: Luminal A and "normal-like" breast cancer cell lines were able to generate luminal-like and myoepithelial-like progeny undergoing senescence arrest. In contrast, luminal B/basal-like cell lines acted as stem/progenitor cells with defective differentiation capacities. Our findings suggest that the malignancy of breast tumors is directly correlated with stem/progenitor phenotypes and poor differentiation potential.

Citation: Mumcuoglu M, Bagislar S, Yuzugullu H, Alotaibi H, Senturk S, et al. (2010) The Ability to Generate Senescent Progeny as a Mechanism Underlying Breast Cancer Cell Heterogeneity. PLoS ONE 5(6): e11288. doi:10.1371/journal.pone.0011288

Editor: Syed A. Aziz, Health Canada, Canada

Received March 16, 2010; **Accepted** June 4, 2010; **Published** June 24, 2010

Funding: This work was supported by TUBITAK (The Scientific and Technological Research Council of Turkey), DPT (State Planning Office of Turkey) and TUBA (Turkish Academy of Sciences). Additional funding was from Institut National de Cancer and INSERM of France. The funders had no role in study design, data collection and analysis, decision to publish, or preparation of the manuscript.

Competing Interests: The authors have declared that no competing interests exist.

* E-mail: ozturkm@ujf-grenoble.fr

Introduction

Human breast tumors are heterogeneous, both in their pathology and in their molecular profiles. Gene expression analyses classify breast tumors into distinct subtypes, such as luminal A, luminal B, ERBB2-positive (ERBB2+) and basal-like [1,2,3]. The prognosis and therapeutic response of each subtype is different. Luminal A cancers are mostly estrogen receptor-α-positive (ER+) and sensitive to anti-estrogen therapy, with the best metastasis-free and overall survival rates. Luminal B tumors have an incomplete anti-estrogen response and lower survival rates. Basal-like and ERBB2+ tumors are ER- and display the worst survival rates [2,3]. The patterns of genetic changes such as chromosomal aberrations and gene mutations observed in breast tumors indicate that breast tumorigenesis does not follow a stepwise linear progression from well-differentiated to poorly differentiated tumors with cumulative genetic aberrations [4]. This suggests that different breast tumor subtypes do not represent different stages of tumor progression, but rather represent the cells from which they initiate [4]. The mammary gland is composed of differentiated luminal and myoepithelial cells that are generated from multi-lineage, luminal-restricted, and myoepithelial-restricted progenitors originating from a hypothetical breast epithelial stem cell. Thus, different types of breast cancers might originate from such stem or progenitor cells at a given stage of commitment and differentiation, as observed in hematological malignancies [4,5]. Without compromising the author's hypothesis, it is also possible that the molecular heterogeneity of breast cancer is due to subtle differences in the ability of tumor-initiating cells to generate differentiated progeny.

Epithelial cells isolated from mammary gland cells undergo two successive senescence states in cell culture, termed "stasis" and "agonescence" [6,7]. In contrast to normal mammary epithelial cells, established breast cancer cells are immortal by definition. They may owe this phenotype of immortalization to genetic and epigenetic inactivation of senescence checkpoints and reactivation of telomerase reverse transcriptase expression [7]. Either in relation to these changes or independently, breast cancer cells may also present a stem/progenitor phenotype that is less subjected or resistant to senescence barriers. However, the abundance of non-tumorigenic and differentiated cells both in breast tumors and cell lines strongly suggests that replicative immortality cannot be assigned to all cells within a tumor or a cancer cell line, and that spontaneous senescence after a limited number of population doublings (PD) is likely to occur. If this hypothesis is correct, then the rate of generation of senescent progeny may reflect the potential of a cancer stem/progenitor cell to produce terminally differentiated progeny. We tested this hypothesis using a panel of luminal and basal-like breast cancer cell lines (Table S1). Although a single cell line is not representative of breast tumor heterogeneity, a panel of cell lines might reproduce the heterogeneity that is observed in primary breast tumors, albeit with some limitations [5,8]. Therefore, we hoped that in vitro studies with a panel of cell lines might help to better understand breast tumor heterogeneity.

Our senescence tests allowed us to classify breast cancer cell lines as senescent cell progenitor (SCP) and immortal cell progenitor (ICP) subtypes. We also show that senescent progeny are observed exclusively in ER-positive cells, as a result of ER inactivation, partly mediated with $p21^{Cip1}$ protein. The ability to produce senescent progeny was associated with the ability to produce luminal-like and myoepithelial-like progeny from stem/progenitor-like cells. In contrast, most of the cell lines lacking senescent progeny were also unable to generate differentiated progeny. Finally, we show that SCP-subtype cells cluster with luminal A and "normal-like" breast tumor types and are less tumorigenic, whereas ICP-subtype cell lines cluster with luminal B and basal-like tumor types and are more tumorigenic.

Materials and Methods

Ethics Statement

We used archival tumor samples remaining from a previous study by BB and IGY described in Gur-Dedeoglu et al. [9], for which the use of the tissue material was approved by the Research Ethics Committee of Ankara Numune Research and Teaching Hospital (decision date: 04/07/2007). The tumor samples in this study were used anonymously. All animals received care according to the Guide for the Care and Use of Laboratory Animals. All animal experiments have been pre-approved by the Bilkent University Animal Ethics Committee (Decision No: 2006/1; Decision date: 10/5/2006).

Clinical samples and cell lines

Freshly frozen tumor specimens were collected at Ankara Numune Hospital. Breast cancer cell lines used in this study were obtained from ATCC (http://www.atcc.org) and listed in Table S1. Cell line authenticity was verified by short tandem repeat profiling, as recommended by ATCC (Dataset S1). Isogenic clones from the T47D (n = 20) cell line were obtained from single cell-derived colonies. Briefly, cells were plated in 96-well plates to obtain single colonies in fewer than 70% of the wells. Isolated colonies were then transferred to progressively larger wells, and to T25 flasks. Clones were subcultivated weekly at 1:4 dilution ratios, and maintained in culture for 25–30 passages to reach >60 PD before testing.

Primary antibodies

The following antibodies were used: anti-CD44 (559046; BD Pharmingen), anti-CD24 (sc53660; Santa Cruz,), anti-ASMA (ab7817; Abcam), anti-CK19 (sc6278; Santa Cruz,), anti-$p21^{Cip1}$ (OP64; Calbiochem), anti-$p16^{Ink4a}$ (NA29, Calbiochem), anti-ERα (sc8002; Santa Cruz).

Low-density clonogenic assays

Cells were seeded as low-density on coverslips in six-well plates (500–2000 cells, according to plating efficiency) and allowed to grow in DMEM supplemented with 10% fetal calf serum (FCS), with medium change every three days, until they formed colonies of a few hundred cells. Depending on the cell line, this took one to two weeks. For bromodeoxyuridine (BrdU) incorporation assays, cells were labeled for 24 h prior to immunocytochemistry, as described previously [10].

Immunocytochemistry

For simple immunoperoxidase assays, cells were fixed with cold methanol for five minutes, then blocked with 10% FCS in phosphate-buffered saline (PBS) for 1 hour. This was followed by incubation with a primary antibody for 1 h. Cells were then washed with PBS three times and subjected to immunostaining using the Dako-Envision-dual-link system and the liquid diaminobenzidine (DAB) substrate chromogen system (Dako, CA, USA), according to the manufacturer's instructions. Hematoxylin was used as a counter-stain when the visualization of cells was necessary. For SABG-immunoperoxidase co-staining studies, unfixed cells were first subjected to SABG assay, and then fixed prior to immunostaining assays. Hematoxylin counter-staining was omitted for co-staining experiments, unless cells were negative for SABG staining.

Immunoblot analyses

Cell pellets were incubated in an NP-40 lysis buffer containing 50 mM Tris–HCl, pH 8.0, 250 mM NaCl, 0.1% Nonidet P-40, and a protease inhibitor cocktail (Roche) for 30 minutes in a cold room. Cell lysates were then cleared by centrifugation, and a Bradford assay was performed to quantify their protein concentration. 30 µg of protein was denatured and resolved by SDS-PAGE using 10% or 12% gels. The proteins were then transferred to the PVDF or nitrocellulose membranes. Membranes were treated for 1 h with a blocking solution of TRIS-buffered saline containing 0.1% Tween-20 and 5% non-fat milk powder (TBS-T) and probed with a primary antibody for 1 h. Next, membranes were washed three times with TBS-T and incubated with an HRP-conjugated secondary antibody for 1 h. Immunocomplexes were then detected by an ECL-plus (Amersham) kit on the membrane. α-tubulin was used as an internal control.

SABG assay and BrdU/SABG co-staining

SABG activity was detected as described [11], except that cells were counterstained with eosin or nuclear fast red following SABG staining. For BrdU/SABG co-staining, cells were first labeled with BrdU (10 µg/ml) for 24 h in a freshly added culture medium as described [10]. Next, cells were subjected to a SABG assay, fixed in 70% methanol, and subjected to BrdU immunostaining.

Estrogen and tamoxifen treatment

Cells were seeded under low-density clonogenic conditions onto coverslips in six-well plates, and cultivated in a standard culture

medium for seven to eight days. Then, cells were fed with phenol red-free DMEM (Gibco) supplemented with 5% charcoal-stripped FCS for 48 h, followed by two successive 48 h treatments with 10^{-9} M estrogen (E2; 17β-estradiol; Sigma), 10^{-6} to 10^{-9} M 4-hydroxytamoxifen (4OHT; Sigma) or an ethanol vehicle, under the same conditions. Colonies were then subjected to a SABG assay. Each experimental condition was conducted in triplicate and experiments were repeated three times.

Generation of estrogen receptor-overexpressing clones

T47D-iso23 cells were transfected with the expression vector pCMV- ERα [12] or an empty vector, using FuGENE-6 (Roche). ER overexpressing and control clones were selected with 500 μg/ml G418 for three weeks. Isolated single cell-derived colonies were picked and expanded in the presence of G418.

Lentiviral infection and generation of $p21^{Cip1}$ knockdown clones

We used mission shRNA plasmid pLKO.1<-puro-p21 (NM_000389.2-640s1c1, Sigma) for $p21^{cip1}$ knockdown experiments. The Control vector shRNA-pGIPz-SCR-puro and a helper packaging mix (Invitrogen) were also used. HEK293T was co-transfected with the appropriate vector and packaging mix, using the CalPhos Mammalian Transfection Kit (Clontech) and following the manufacturer's instructions. After 48 h of culture, virus-containing culture media were collected, filtered, and used to infect T47D-iso23 cells. After 4 h of infection, stable cells were selected with 1 μg/ml puromycin for seven days.

Nude mice tumorigenicity and in vivo senescence assays

T47D and MDA-MB-231 cells (5×10^6) were injected subcutaneously into CD-1 *nude* mice (Charles River). Females (n = 5 for each cell line) and males (n = 4 for each cell line) were used. Tumor sizes were measured up to 47 days post-injection. In addition, four tumors from each cell line were analyzed for the presence of senescent cells by SABG staining, as described previously [10].

Cluster analysis

The two-channel microarray data containing 8102 cDNA genes/clones generated by Sorlie et al. [2] were downloaded from the Stanford Microarray Database (SMD) (http://genome-www.stanford.edu/MicroArray/). In the downloading process, the "log (base 2) of R/G Normalized Ratio (median)" parameter was used for data filtering. We have median-centered expression values for each array. We selected arrays and genes with greater than 75% good data (representing the amount of data passing the spot criteria). Sixty-eight tissue samples were obtained according to this criterion and annotated with the subtypes described by the authors, found in the "Supplementary Information" of the data set in SMD. The expression values of "500 gene signature," defined by the authors, were extracted from the data. Gene expression profiles of 31 breast cancer cell lines performed by Charafe-Jauffret et al. [13], using the whole-genome cDNA microarray Affymetrix HGU-133 plus 2, was obtained from the "Supplementary Table" of the article. The authors filtered genes with low and poorly measured expression, and with low expression variation, retaining 15, 293 genes. After log transformation of the data, we median normalized the data arrays in R language, using the Bioconductor biostatistical package (www.r-project.org/ and www.bioconductor.org/). The "500 gene signature" tumor data [2] and the normalized breast-cancer cell line data [13] were combined with respect to probe IDs using a set of customized perl routines (source codes are available upon request). A set of 175 genes was common. "Median center" normalization of genes was done for the merged data set for the total samples. We performed unsupervised hierarchical clustering with the 99 samples (the 31 breast cell line [13] and 68 breast tumor [2] samples) by the pair-wise complete-linkage hierarchical clustering parameter, using the Gene-Pattern program. The Pearson correlation method was used for distance measurements. Clustering was visualized by java treeview, again using Gene-Pattern (http://www.broad.mit.edu/cancer/software/genepattern/).

Statistical analyses

Significant differences were evaluated using unpaired Student's t test for compared samples sizes of 10 or higher. Otherwise, one-tailed Fisher's exact test was used with 2×2 tables; $P<0.05$ was considered statistically significant. On the graphical representation of the data, y-axis error bars indicate the standard deviation for each point on the graph.

Results

Classification of breast cancer cell lines as senescent-cell progenitor and immortal-cell progenitor subtypes

Clonogenic assays have been successfully used to test the generation and self-renewal abilities of phenotypically distinct progeny of mammary stem/progenitor cells [14]. We previously applied this technique to test the ability of cancer cells to produce progeny with replication-dependent senescence arrest [10]. Cells were plated under low-density clonogenic conditions and cultivated for one to two weeks until individual cells performed eight to ten PDs and generated isolated colonies composed of several hundred cells. This method permits tracing progeny generated by a few hundred cells under the same experimental conditions. We explored a panel of 12 breast cancer cell lines, composed of luminal (n = 7) and basal (n = 5) subtypes (Table S1). Cell lines formed two groups, according to the presence of senescent cells in isolated colonies. One group of cell lines generated colonies with high rates of senescence, while others did not produce appreciable amounts of senescent cells. Representative pictures of colonies subjected to the SABG assay are shown in Fig. 1A. The percent of SABG+ progeny was calculated by manual counting of at least 10 different colonies for each cell line. Colonies derived from five cell lines generated SABG+ cells at high rates (means: 5-40%) Senescence rates were negligible (means <5%) in the progeny of the remaining seven cell lines. The first group, the senescent cell progenitor subtype, included T47D, BT-474, ZR-75-1, MCF-7, and CAMA-1 cell lines. The second group, the immortal cell progenitor subtype, included MDA-MB-453, BT-20, SK-BR-3, MDA-MB-468, HCC1937, MDA-MB-231 and MDA-MB-157 (Fig. 1B).

In order to verify whether the occurrence of senescent cells in the SCP group was intrinsic to each cell line or due to the presence of a side population, we generated clones from the T47D (n = 20) cell line, and subjected them to the SABG assay at different intervals. All clones acted similarly to the parental T47D cell line with similar rates of SABG+ progeny. No clone gained the ICP phenotype. More importantly, none of the clones tested over a long period of time (>60 PDs) entered full senescence (data not shown), unlike normal mammary epithelial cells that undergo two stages of senescence arrest over a period of ~20 PDs [7]. The SABG assay can provide false-positive responses, especially when cells remain under confluence for a long period [15]. Although all our tests used low-density clonogenic conditions, we wanted to confirm the senescence arrest by a long-term (24 h) BrdU labeling assay under mitogenic

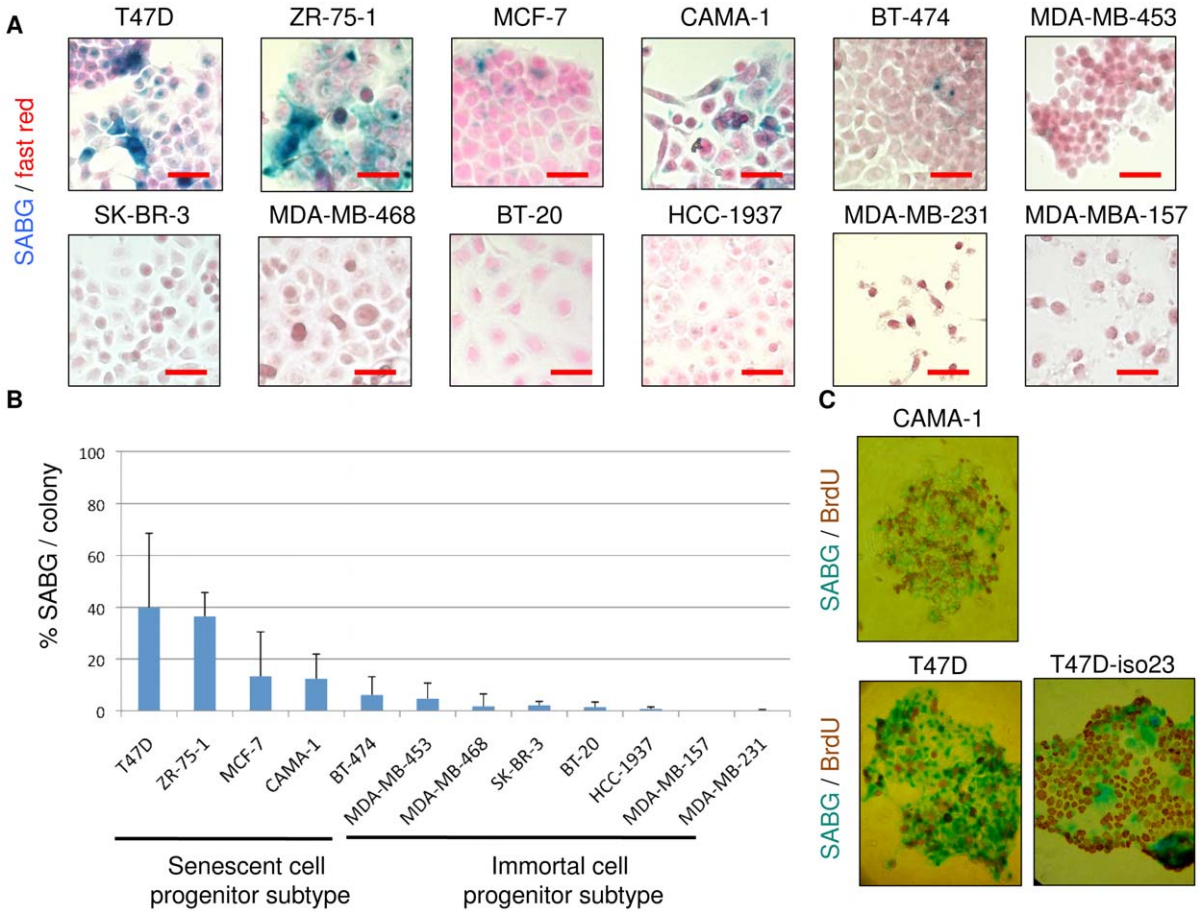

Figure 1. Classification of breast cancer cell lines as senescent cell progenitor and immortal cell progenitor subtypes. (**A**) Examples of SABG staining for senescence of breast cancer cell line colonies obtained after plating at low-density clonogenic conditions. Breast cancer cell lines (Table S1) were plated to obtain a few hundred colonies with 1–2 weeks of cell culturing and were subjected to SABG assay, followed by counterstaining with nuclear fast red. T47D, ZR-75-1, MCF-7, CAMA-1 and BT-474 generated heterogeneous colonies composed of with SABG+ and SABG- cells (shown here), but also fully negative and/or fully positive colonies. All other cell lines produced only SABG- colonies (<5% SABG+ cells). Scale bar: 50 μm. (**B**) Classification of breast cancer cell lines as senescent cell progenitor (SCP) and immortal cell progenitor (ICP) subtypes by quantification of the ability to generate senescent progeny. Cell lines with a mean of SABG+ cells higher than 5% were termed SCP, and the other cell lines as ICP. Colonies that were generated and stained as described in (**A**) were counted manually to calculate % SABG+ cells. At least 10 colonies were counted for each cell line. Error bars represent mean ± SD. (**C**) SABG+ senescent cells displayed terminal growth arrest. CAMA-1, T47D and T47D-iso23 colonies were generated as described in (**A**), labeled with BrdU for 24 h in the presence of freshly added culture medium, and subjected to SABG/BrdU double-staining. SABG+ cells are BrdU-, and *vice versa*. T47D-iso23 is a clone derived from T47D. Note that parental T47D and T47D-iso23 clones displayed similar staining features.
doi:10.1371/journal.pone.0011288.g001

conditions, as senescent cells in permanent cell cycle arrest cannot incorporate BrdU under these conditions [16]. Co-staining of cells for SABG and BrdU from CAMA-1, T47D, and T47D-iso23 colonies provided clear indication that the great majority of SABG+ senescent cells were BrdU-, whereas non-senescent BrdU+ cells were usually SABG- (Fig. 1C). These findings indicated that SABG+ senescent cells were at the terminal differentiation stage with an irreversible loss of DNA synthesis ability. Our observations also indicated that SABG and BrdU tests could be used alternatively to identify senescent (SABG+/BrdU-) and immortal (SABG-/BrdU+) cells under our experimental conditions.

Senescent cell progenitor phenotype association with $p21^{Cip1}$ expression

$p16^{Ink4a}$ and $p21^{Cip1}$ (in a p53-dependent manner or independently) have been shown to be mediators of senescence arrest in different cells, including mammary epithelial cells [6,15,17,18,19]. We therefore analyzed the expression of $p16^{Ink4a}$ and $p21^{Cip1}$ in the cell line panel. Heterogeneously positive nuclear $p21^{Cip1}$ immunoreactivity was observed in four of the five SCP cell lines, but not in any of the seven ICP cell lines (Fig. 2A). The association of $p21^{Cip1}$ expression with the SCP subtype was statistically significant ($P = 0.01$). We also compared the expression of $p16^{Ink4a}$. Three of five SCP cell lines displayed heterogeneously positive immunostaining, whereas three of seven ICP cell lines displayed homogenously positive staining (Fig. S1). The difference of $p16^{Ink4a}$ expression between the two groups was not significant ($P = 1$). These observations indicated that the SCP phenotype was associated with $p21^{Cip}$ expression in breast cancer cell lines.

To test whether $p21^{Cip1}$ was directly involved in the senescence observed in SCP cells, we first performed $p21^{Cip1}$/SABG staining in T47D-iso23 cells (hereafter termed T47D). $p21^{Cip1}$, but not $p16^{Ink4a}$ staining, was associated with SABG staining (Fig. S2). Next, we generated two derivative cell lines following infection of T47D with lentiviral vectors encoding $p21^{Cip1}$ shRNA (T47D-p21sh) or a scrambled control (T47D-scr). Following the

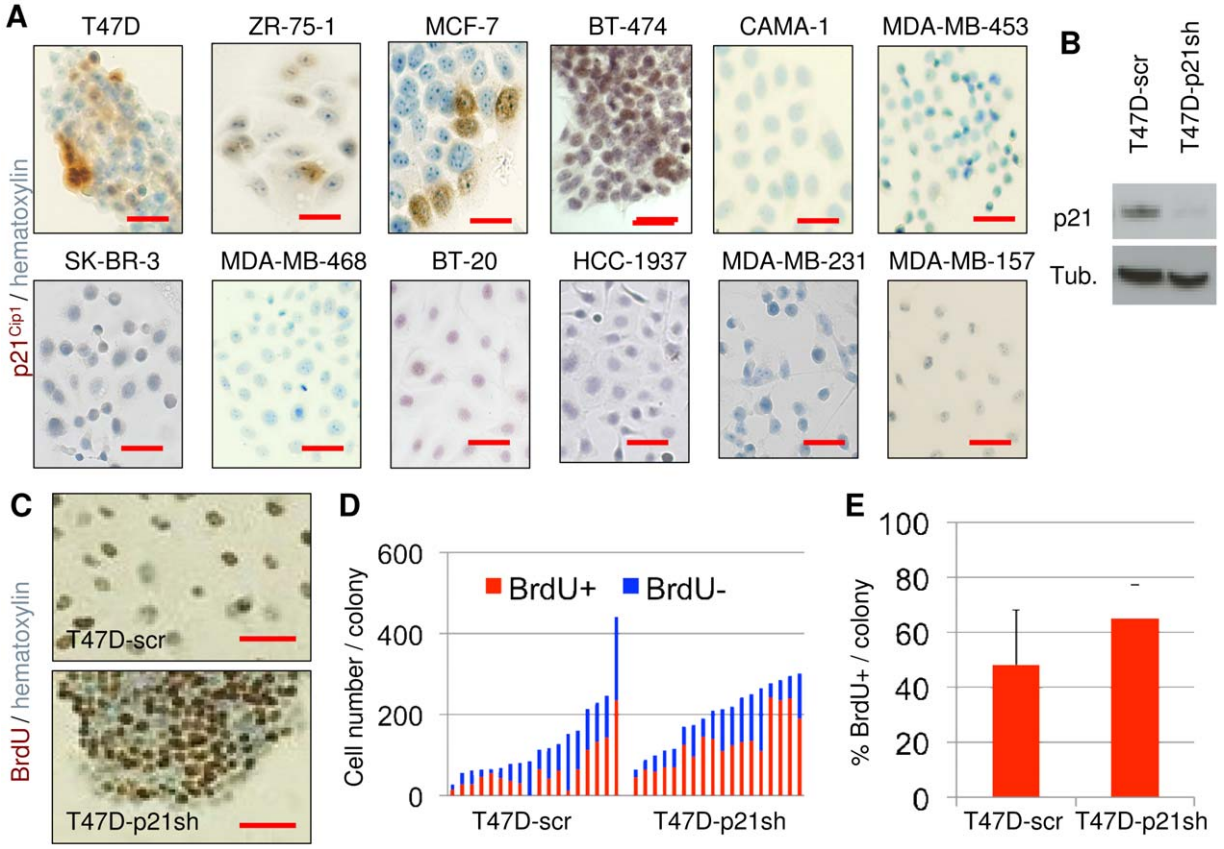

Figure 2. Growth arrest observed in senescent cell progenitors was inhibited by $p21^{Cip1}$ silencing. (**A**) Four of five senescent SCP cell lines (top four from left) generated colonies with heterogeneous expression of $p21^{Cip1}$; in contrast none of seven ICP cell lines generated $p21^{Cip1}$ cells. Colonies were immunostained for $p21^{Cip1}$, with hematoxylin used as counterstain. Scale bar: 50 μm. (**B–E**) $p21^{Cip1}$ silencing inhibited the production of the terminally arrested progeny of SCP cells. (**B**) shRNA-mediated inhibition of $p21^{Cip1}$ expression. T47D cells were infected with lentiviral vectors encoding $p21^{Cip1}$ shRNA or scrambled shRNA to generate T47D-p21sh and T47D-scr stable cell lines, and tested for $p21^{Cip1}$ knockdown by western blotting. (**C–E**) The ability to generate growth-arrested cells was inhibited by $p21^{Cip1}$ knockdown. Colonies were generated from respective cell lines, labeled with BrdU for 24 h, immunostained for BrdU, and slightly counterstained with hematoxylin to visualize BrdU+ and negative cells. Scale bar: 50 μm. (**C**). Individual colonies were manually counted for quantification of % BrdU cells. Each bar represents one colony (**D**). The silencing of $p21^{Cip1}$ caused a significant increase ($P = 0.0043$) in % ratios of BrdU+ cells (**E**). Mean % BrdU+ cells (± SD) values were calculated from data presented in (**D**). Error bars represent mean ± SD. Tub.; α-tubulin.
doi:10.1371/journal.pone.0011288.g002

demonstration of $p21^{Cip1}$ knockdown in T47D-p21sh cells by western blot assay (Fig. 2B), both cell lines were plated under low-density plating conditions, colonies were grown for 10 days, and subjected to SABG and BrdU staining. It was not possible to quantify SABG+ cells in T47D-p21sh cells because they formed tight clusters in culture (data not shown). We therefore used BrdU staining as an alternative method for senescent cell quantification (Fig. 2C). Randomly selected colonies were counted for the number of BrdU+ and BrdU- cells (Fig. 2D). The T47D-scr cell line generated BrdU+ progeny at a rate of 48±20% per colony (n = 18). Under the same conditions, T47D-p21sh cells displayed BrdU+ progeny at a rate of 65±12% per colony (n = 18), with a significant ($P = 0.0043$) increase in the number of cells escaping terminal arrest (Fig. 2E). These results indicated that $p21^{Cip1}$ was responsible, at least partly, for inducing the senescence observed in the progeny of T47D cells.

The control of senescent cell progeny generation by an estrogen receptor

As stated above, $p21^{Cip1}$ is a downstream target of p53 for senescence, but T47D cells do not express wild-type p53 (Table S1). Estrogen inhibits $p21^{Cip1}$ expression [20] by c-Myc-mediated repression [21], *MYC* gene being a direct target of ER complex [22]. We therefore tested whether ER could be involved in the senescence observed in T47D cells. The data shown in Fig. 3A indicates that T47D cells displayed nuclear ER immunoreactivity in their great majority, but some progeny was ER-. More interestingly, these ER- cells tended to be SABG+, suggesting that senescence occurred in T47D cells as a result of ER loss. Next, we tested whether experimentally modifying ER activity in T47D cells had any effect on senescence response. After plating at low-density clonogenic conditions, cells were grown in a regular cell culture medium that contained weakly estrogenic phenol red [23] for seven days in order to obtain visible colonies. The culture medium was then changed with phenol-free DMEM complemented with charcoal-treated FCS, grown for two more days, and then cultivated for four more days in the presence of E2 (10^{-9} M), OHT (10^{-9} M to 10^{-6} M), or an ethanol vehicle as control. Colonies were subjected to SABG staining (Fig. 3B). Total and SABG+ cells were counted from 20 randomly selected colonies for each treatment (Fig. 3C). Colonies grown in a phenol-free charcoal-treated control medium complemented with an ethanol vehicle only displayed 31±13% SABG+ cells. Complementing this medium with 10^{-9} M

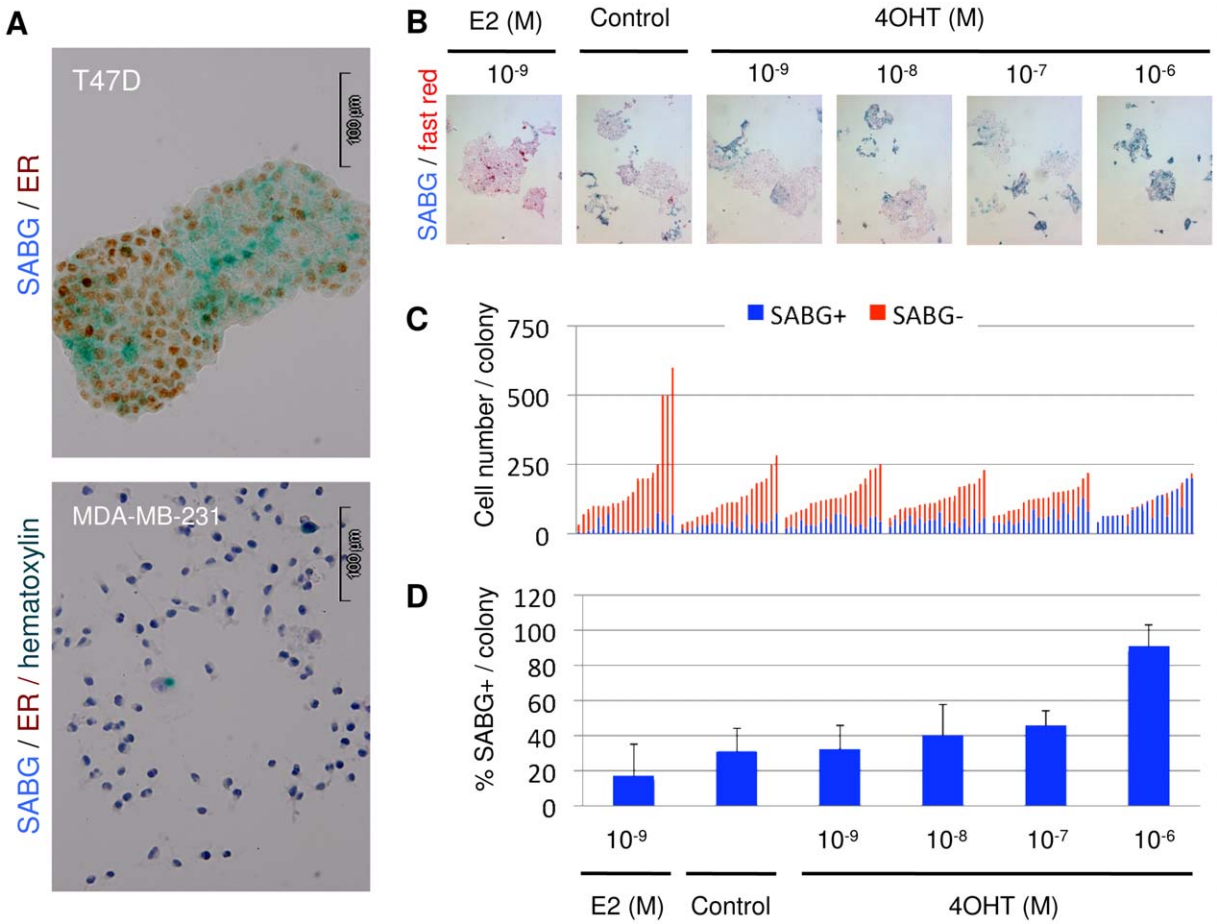

Figure 3. Generation of senescent cell progeny was controlled by the estrogen receptor-α. (**A**) SCP cells (T47D) expressed nuclear ER. Colonies were co-stained for senescence by SABG and for ER expression by immunoperoxidase. The MDA-MB-231 cell line was used as a negative control. (**B–D**) The production of senescent progeny in SCP cells was inhibited by estrogen (E2), but enhanced by tamoxifen (4OHT) treatment. After plating in low-density clonogenic conditions, T47D cells were grown in standard cell culture medium for seven days, followed by phenol-free DMEM complemented with charcoal-treated fetal calf serum for two days, and then cultivated for four days in the presence of E2, OHT, or an ethanol vehicle (control). Colonies were subjected to SABG staining (**B**). Total and SABG+ and SABG- cells were counted from 20 randomly selected colonies (**C**), and mean % SABG+ cells (± SD) values were calculated (**D**). Error bars represent mean ± SD. The inhibition of senescence by E2 and its activation by OHT was statistically significant when compared to ethanol-complemented control cells (*P* values 0.0093, 0.0002 and <0.0001 for 10^{-9} M E2, 10^{-7} M OHT and 10^{-6} M OHT, respectively).
doi:10.1371/journal.pone.0011288.g003

E2 generated colonies with 17±18% SABG+ cells. Senescence inhibition by E2 was nearly 50% and statistically significant when compared to the ethanol-complemented control cells ($P=0.0093$). In contrast to E2, OHT provoked a dose-dependent increase in the proportion of SABG+ cells. At the maximum dose used (10^{-6} M OHT), 90±13% of colony-forming cells displayed a SABG+ signal (Fig. 3D), indicating that tamoxifen-mediated inactivation of ER can induce almost a complete senescence response in these cells ($P<0.0001$). The increase in senescence rate was also significant with 10^{-7} M OHT ($P=0.0002$).

Our findings strongly suggested that the senescence observed in the SCP T47D cell line was due to a loss of expression and/or function of ER in a subpopulation of the progeny of these cells. For confirmation, we constructed ER-overexpressing stable clones from T47D cells. The thhree clones with the highest ER expression were selected. In addition, three clones with endogenous expressions of ER were selected from stable clones obtained with an empty vector (Fig. 4A). Progeny obtained from these six clones were tested by BrdU assay (Fig. S3). Randomly selected colonies (n = 10) from each clone were evaluated for total and BrdU+ number of cells (Fig. 4B). Consistently higher levels of BrdU+ cells were observed with clones ectopically expressing the ER protein (Fig. 4C). Overexpression of ER resulted in a significant increase in the BrdU+ progeny ($P=0.034$). The protective effect of ER overexpression was not as important as the senescence-promoting effects of ER inhibition. This was not unexpected, since the parental cells used for the ER overexpression studies were already expressing high levels of endogenous ER (Fig. 4A), displaying a baseline anti-senescence activity due to the serum estrogen and phenol red found in the cell culture medium.

The close relationship between ER and senescence in the ER+ T47D cell line, and the highly effective treatment of ER+ breast tumors with tamoxifen, which induced senescence in our experimental model, suggested that senescence induction might be a relevant mechanism involved in anti-estrogen treatments. As fresh tumor tissues cannot be obtained from tamoxifen-treated patients for obvious ethical reasons, we analyzed untreated ER+ breast tumor samples for evidence of spontaneously occurring in vivo senescence. We screened a panel of 12 snap-frozen ER+ breast tumor tissues from 11 patients for senescence by an SABG

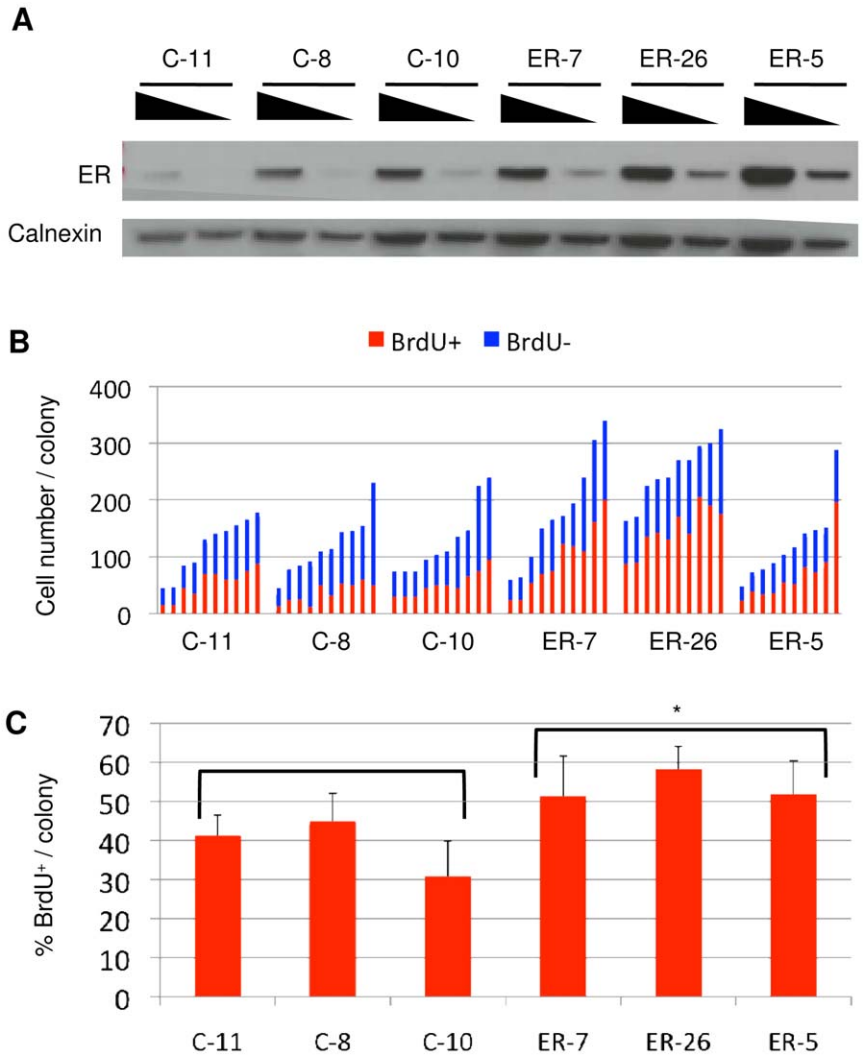

Figure 4. Overexpression of estrogen receptor-α inhibited the production of terminally arrested progeny. (**A**) ER-overexpressing (ER-5, ER-7, ER-26) and control (C-8, C-10, C-11) clones were established from T47D cells and tested for ER expression by western blotting using decreasing amounts of total proteins. Calnexin was used as loading control. (**B–C**). Colonies were generated, labeled with BrdU for 24 h and immunostained for BrdU (shown in Fig. S3). Individual colonies were manually counted for quantification of % BrdU cells (**B**), and mean % BrdU+ cells values were calculated (**C**). Error bars represent mean ± SD. ER overexpression caused a significant increase in % ratio of BrdU+ cells (*three ER clones *versus* three controls; $P = 0.034$).
doi:10.1371/journal.pone.0011288.g004

assay. The mean age of the patients was 58±12 yrs, with a mixed menopause status (Table S2). Two tumors (17%) displayed SABG+ cells that were scattered within the tumor area (Fig. S4). Thus, ER+ breast tumors also produced senescent progeny in vivo, but at a lower rate.

Senescent cell progenitor and immortal cell progenitor subtypes' abilities to differentiate into luminal and myoepithelial cell types

The cellular specificity of ER expression in the mammary epithelial cell hierarchy is poorly understood. Previous data suggests that normal ER+ cells may represent either relatively differentiated luminal cells with limited progenitor capacity or primitive progenitors with stem cell properties in the luminal cell compartment [4,24,25]. Based on the close association between senescence (which can be considered a manifestation of terminal differentiation) and loss of ER positivity, we hypothesized that ER+ SCP cells may differ from ER- ICP cells by their differentiation potential. We surveyed a few hundred single-cell-derived colonies from each of the 12 cell lines for production of stem/progenitor-like, luminal-like, and myoepithelial-like cells. We used CD44 as a positive stem/progenitor cell marker [26,27], CD24, ER, and CK19 as luminal lineage markers [27,28,29], and ASMA as a myoepithelial lineage marker [29].

Representative examples of marker studies by immunoperoxidase staining in SCP and ICP cell lines are shown in Fig. 5. All five SCP cell lines displayed a heterogeneous pattern of positivity for CD44; some colonies were fully positive, some fully negative, and others were composed of both positive and negative cells. CD44/CD24 double immunofluorescence studies with the T47D cell line indicated that SCP cells produce also CD44+/CD24- stem/progenitor cells, as expected (data not shown). In sharp contrast, five of the seven ICP cell lines generated only fully positive CD44 colonies, indicating they do not produce CD44- cells. One cell line was totally CD44-. Only one cell line displayed

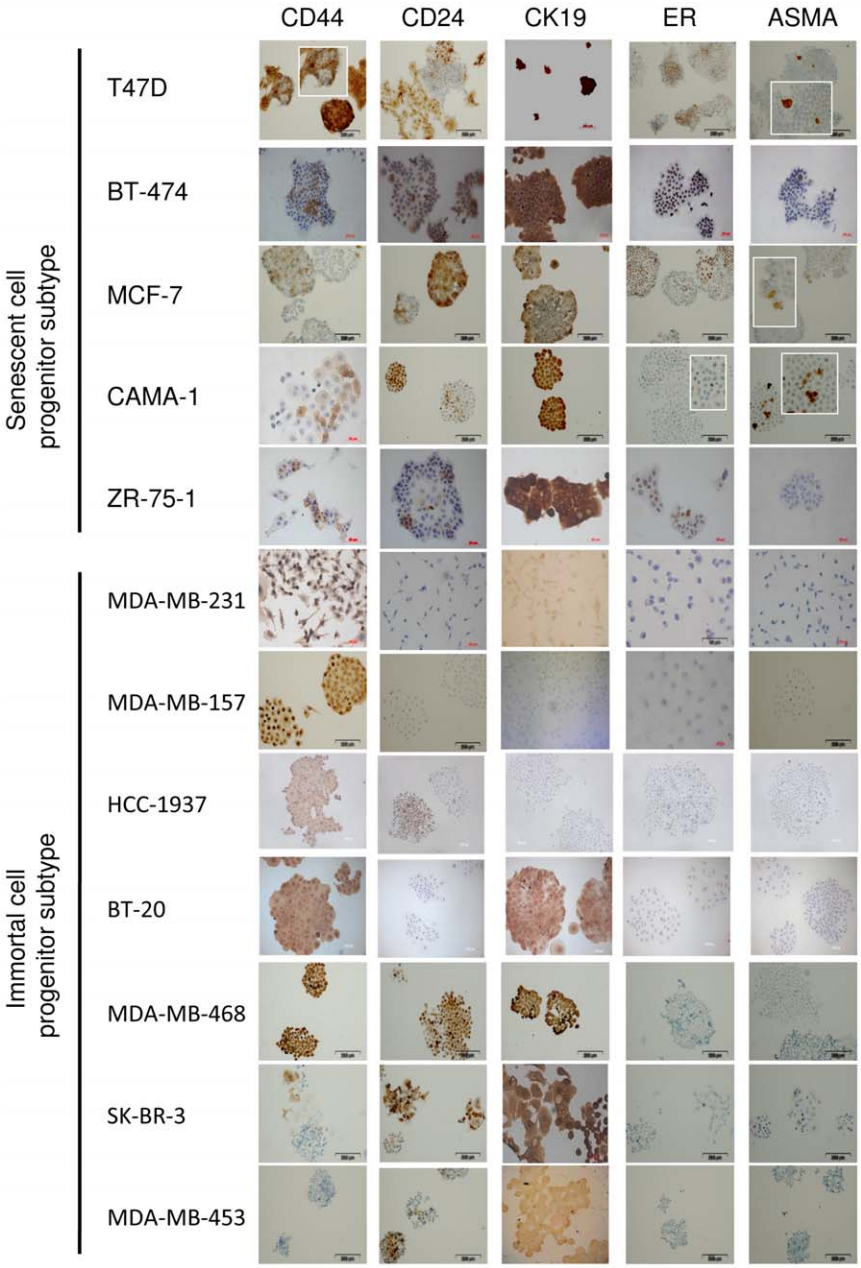

Figure 5. Senescent cell progenitor and immortal cell progenitor subtypes greatly differed in their ability to differentiate into luminal and myoepithelial lineage cells. Senescent cell progenitor and immortal cell progenitor subtype cell lines were studied by immunoperoxidase staining using CD44 and markers for luminal epithelial (CD24, CK19, ER) and myoepithelial (ASMA) lineages. Insets: magnified views of positive cells. Both subtypes have CD44+ cells. Senescent cell progenitor cell lines produced both progenitor-like (CD44+; CD24−), as well as ER+ luminal-like and ASMA+ myoepithelial-like cells (except ZR-75-1 for myoepithelial-like cells). Immortal cell progenitor cell lines were defective for generation of ER+ luminal-like or ASMA+ myoepithelial-like cells. Moreover, five of seven cell lines could not generate CD44- cells. The expression of CD24 and CK19 markers did not differ significantly between the two subgroups, except that some immortal cell progenitor subtype cell lines did not express CD24 or CK19.
doi:10.1371/journal.pone.0011288.g005

a pattern similar to that of SCP cell lines. A comparison of the two subtypes indicated that the ability to generate both CD44+ and CD44- progeny was significantly associated with the SCP phenotype ($P = 0.0046$). All five SCP cell lines displayed heterogeneous, but mostly positive ER immunostaining, whereas all seven ICP cell lines never generated ER+ cells. The expression of ER was also significantly associated with the SCP subtype ($P = 0.0012$), as well as the ability to produce ASMA+ progeny ($P = 0.0046$). The ICP cell lines did not generate ASMA+ cells, while four out of five SCP cell lines generated rare ASMA+ cells under low-density clonogenic conditions. Interestingly, the abundance of ASMA+ cells was much higher in the two SCP cell lines that were tested at high cell density (Fig. S5). This suggests that either the production of ASMA+ cells is enhanced at high cell density, or these myoepithelial-like cells display limited survival under long-term culture conditions. We did not find a strong association between the expression of CD24 and CK19 markers and cell subtype. All five SCP cell lines and three ICP cell lines

generated heterogeneously staining colonies for CD24 expression. Similarly, all five SCP cell lines, as well as three ICP cell lines, expressed CK19, but homogenously.

Typical features of senescent progenitor and immortal progenitor breast cancer cell lines

As summarized in Fig. 6, SCP and ICP subtype cell lines displayed several subtype-specific features. All SCP cell lines produced differentiated and senescent cells, in addition to putative CD44+/CD24− stem/progenitor cells. Indeed, all of them produced ER+ and CD24+ luminal-like cells and most of them (n = 4/5) also produced ASMA+ myoepithelial-like cells. In contrast, five of the seven ICP cell lines never produced CD44- cells, suggesting they cannot generate differentiated progeny under the experimental conditions tested. In confirmation of this hypothesis, four ICP cell lines only produced CD44+/CD24−/ER-/CK19-/ASMA- stem/progenitor-like, but never differentiated cells. Furthermore, all seven ICP cell lines were unable to produce ASMA+ myoepithelial-like, ER+ luminal-like or SABG+ senescent cells. CD24 and CD19 luminal lineage markers were expressed in three cell lines, one of which was fully positive for the CD44 stem/progenitor marker.

SCP and ICP subtype cell lines correlate with distinct breast tumor subtypes

Distinct cell-type features associated with SCP and ICP subtypes suggest that they may be phenocopies of molecularly defined breast tumor subtypes [1,2,3,30]. As the prognosis and therapeutic response of each subtype is different [2,3], we questioned whether we could assign SCP and ICP cell lines to known molecular subtypes of breast tumors. Using cell line and primary tumor gene expression datasets, we conducted a hierarchical clustering analysis. The "intrinsic gene set" data generated by Sorlie et al. [2] to classify breast tumors into five molecular subtypes was used to filter cell line data generated by Charafe-Jauffret et al. [13]. A set of 175 genes was common between the two data sets. Sixty-eight tumors and 31 cell lines were subjected to pair-wise complete-linkage hierarchical clustering and distance measurements. This tumor–cell line combined analysis produced two major clusters. One cluster was composed of basal and luminal B subtype tumors and five of six ICP cell lines. The other cluster included luminal A, ERBB2+, and "normal-like" subtype tumors and all five SCP subtype cells. Four cell lines clustered with the luminal A tumor subclass. Finally. one cell line clustered with the "normal-like" subclass (Fig. 7A). A full list of clustered tumors and cell lines is provided in Fig. S6.

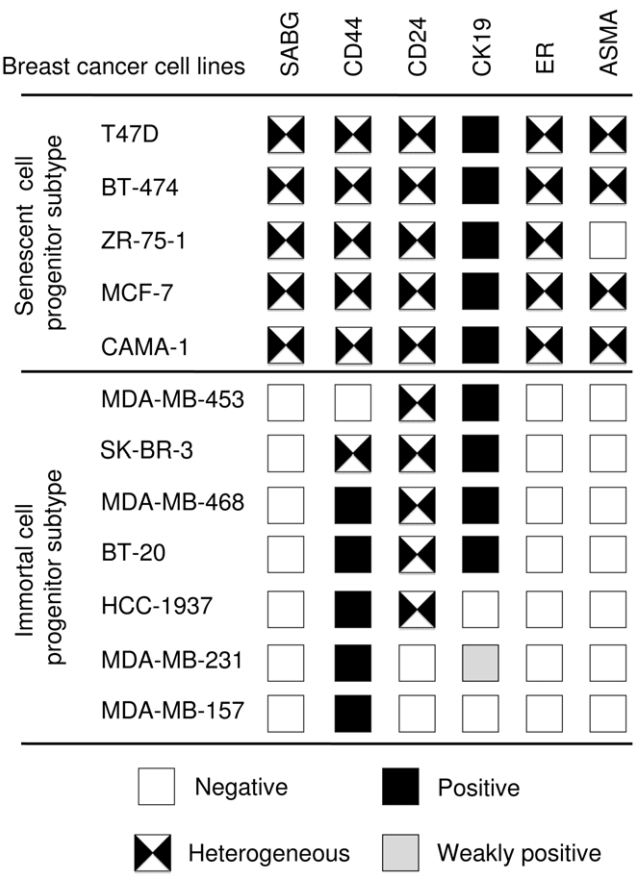

Figure 6. Typical features of senescent progenitor and immortal progenitor breast cancer cell lines.
doi:10.1371/journal.pone.0011288.g006

Luminal A tumors clustering with our SCP subtype cell lines displayed the longest tumor-free, distant metastasis-free, and overall survival rates. In contrast, basal and luminal B tumors clustering with our ICP subtype cell lines had the worst prognosis, with shorter tumor-free, distant metastasis-free, and overall survival times [2]. Our cluster analysis suggested that the ability to generate differentiated and senescent progeny characterized breast cancers with poor tumorigenicity, and that resistance to differentiation and senescence was indicative of more aggressive tumorigenicity. We compared in vivo intrinsic tumorigenic behaviors of the SCP cell line T47D and the ICP cell line MDA-MB-231 in female (n = 5 for each cell line) and male (n = 4 for each cell line) CD1 *nude* mice Fig. 7B). MDA-MB-231 cells displayed higher tumorigenicity than T47D cells. In total, we observed progressively growing tumors in five of nine animals injected with MDA-MB-231. In contrast, T47D formed smaller and regressing tumors in nine of nine animals ($P<0.03$). Interestingly, the difference in tumorigenicity between these two cell lines was more pronounced in male animals ($P<0.05$ after 20 days post-injection). To test whether the difference in tumorigenicity between MDA-MB-231 and T47D cells was correlated with spontaneous in vivo senescence, we analyzed four tumors from each cell line. Two T47D tumors displayed positive SABG staining, whereas no positive staining was observed with all four MDA-MB-231 tumors (Fig. S7).

Discussion

In recent years, phenotypic heterogeneity of breast cancers has been correlated with genetic and molecular heterogeneity [1,3]. Breast cancer subtypes may represent cancers originating from different progenitor cells. Molecular and phenotypic heterogeneity and associated clinical manifestations of breast tumor subtypes have been related to the type of hypothetical tumor progenitor cells originating from a hypothetical mammary epithelial stem cell or from downstream progenitor cells [4,5]. This hypothesis has not been fully validated, mainly because a hierarchical map of cells involved in mammary epitheliogenesis has not yet been established.

To better understand phenotypic differences between breast cancer subtypes, we applied senescence as a surrogate marker for the potential to generate terminally differentiated progeny. We completed these studies with markers for breast stem/progenitor and differentiated luminal and myoepithelial lineage cells. The use of low-density clonogenic conditions allowed us to follow the fate

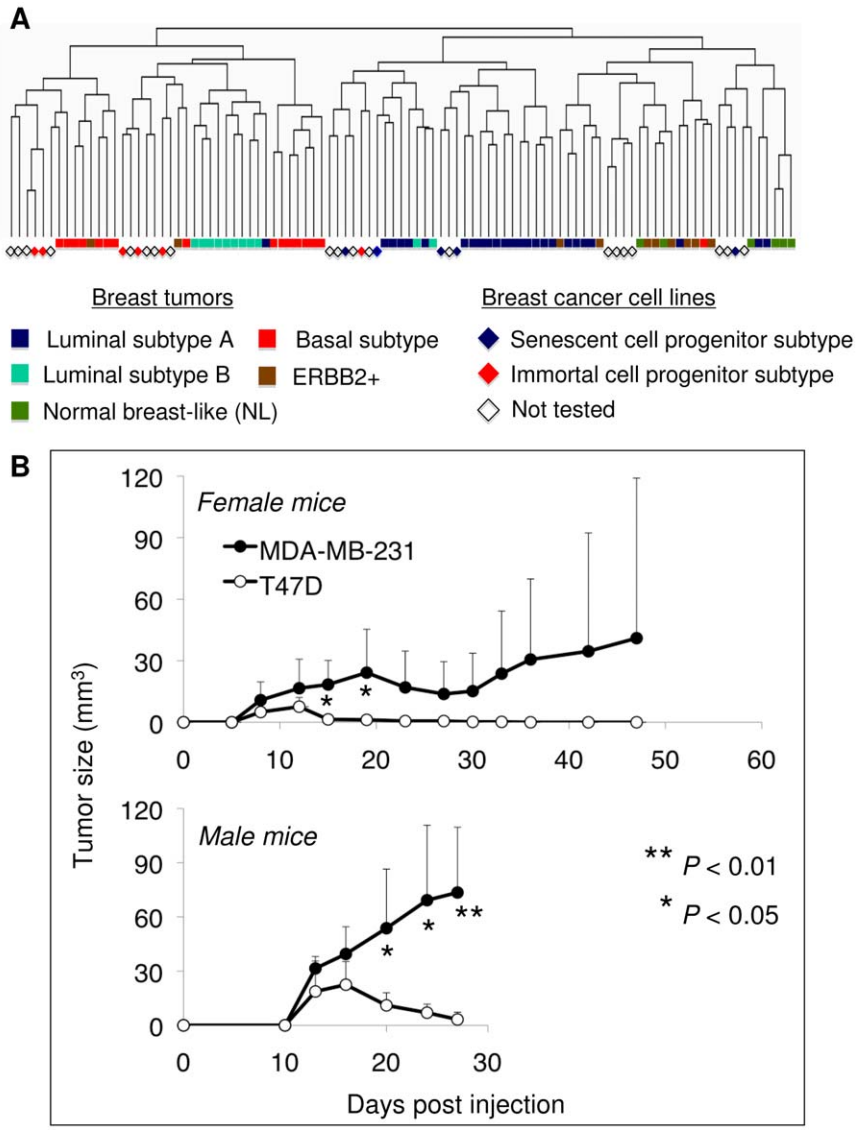

Figure 7. Senescence cell progenitor and immortal cell progenitor subtype cell lines correlate with distinct breast tumor subtypes. (**A**) Unsupervised hierarchical clustering of breast tumor and cell line gene expression data were obtained from Sorlie et al [2] and Charafe-Jauffret et al [25]. Dendrogram displaying the relative organization of tumor and cell line data demonstrated that ICP cell lines cluster with basal and luminal A tumors in the same branch, except for MDA-MB-453. In contrast, SCP cell lines clustered with luminal A (BT-474, CAMA-1, MCF-7, T47D) and "normal-like" tumors (ZR-75-1). No data was available for MDA-MB-468. A dendrogram with sample IDs was provided in Fig. S6. The "intrinsic gene set" data generated by Sorlie et al. [2] was used to filter cell line data generated by Charafe-Jauffret et al. [13]. A set of 175 genes was common between the two data sets. Sixty-eight tumors and 31 cell lines were subjected to pair-wise complete-linkage hierarchical clustering and distance measurements. (**B**) Immortal cell progenitor MDA-MB-231 was more tumorigenic than the SCP type T47D cell line. Female (n = 5 per cell line) and male (n = 4 per cell line) CD1*nude* mice received 5×10^6 cells by subcutaneous injection and observed up to 47 days for tumor formation. Chart displays mean tumor sizes (± S.D.) generated by MDA-MB-231 and T47D cell lines, respectively in female (top) and mala (bottom) mice. T47D cells formed smaller tumors that regressed and completely resolved within 30 days. Tumors formed by MDA-MB-231 were larger in size and did not show total resolution. Note that this cell line was more tumorigenic in male mice.
doi:10.1371/journal.pone.0011288.g007

of a large number of progeny for each cell line studied. From these approaches, we draw several important conclusions. First, breast cancer cell lines form two distinct groups: SCP and ICP subtypes. The SCP cell lines produce non-senescent and senescent progeny, whereas the ICP cell lines produce only non-senescent progeny. Second, SCP and ICP cell lines are exclusively ER+ and ER- cell lines, respectively. Senescence occurs as a result of ER loss associated with $p21^{Cip1}$ induction in SCP cells. Inversely, experimental activation of ER by E2 protects from senescence, whereas its inactivation by tamoxifen aggravates it. Thus, senescence in ER-dependent cells appears to result from the loss of survival signals generated by transcriptional activity of ER. A similar type of senescence has been reported for lymphoma, osteosarcoma, and hepatocellular carcinoma tumors upon c-*MYC* inactivation [31]. Third, SCP cells generate ER+, CD24+, or CK19+ luminal-like, as well as ASMA+ myoepithelial-like progeny. These findings strongly suggest that most, if not all, SCP cells have the capacity to give rise to two major types of differentiated cells that are found in normal mammary epithelium. In sharp contrast, ICP cells never produce ER+ luminal-like or

ASMA+ myoepithelial-like cells. Indeed, some ICP cells generate only CD44+ stem/progenitor-like cells and never CD44−, CD24+, CK19+, ER+, or ASMA+ cells. These findings indicate that ICP cells have limited differentiation ability, at least under in vitro conditions. The differentiation ability of ICP cells appears to be lost completely or partially, so that they do not differentiate fully while they self-renew as stem/progenitor-like cells. Fourth, SCP cell lines form the same molecular cluster with luminal A and "normal-like" breast tumors. This suggests that SCP cell lines are phenocopies of these relatively benign and/or anti-estrogen-responsive tumors. The poor tumorigenicity of SCP cells in *nude* mice correlates with better tumor-free and metastasis-free survival of patients with luminal A type tumors. In contrast, ICP cell lines cluster with luminal B and basal-like breast tumor subtypes, and they are more tumorigenic, as expected for luminal B and basal-like tumor cells. It is presently unknown whether breast tumor subtypes that cluster with SCP or ICP cell lines are also composed of either differentiating or mostly self-renewing stem/progenitor cells. Recent studies reported that breast tumors may contain only CD44+, or only CD24+ cells, as well as mixed cell populations, and that CD44+ tumor cells express many stem-cell markers [27,32]. In addition, an association between basal-like breast cancer and the presence of CD44+/CD24− cells has been established [32].

The mechanisms of the differentiation block observed in ICP cell lines are not known. One might argue that cell lines that produce only CD44+, but never differentiation marker-positive cells, cannot be defined as stem/progenitor cells. However, such cell lines are not completely inert to differentiation stimuli, and may undergo differentiation under special conditions. For example, MDA-MB-231 and MDA-MB-468 cells (identified as ICP cell lines here) can be induced to differentiate into ER+ cells by Wnt5a treatment, and MDA-MB-231 cells then become sensitive to tamoxifen [33].

Most of the findings reported here are derived from in vitro studies performed with established cancer cell lines. Presently, it is unknown to what extent these findings are also relevant for breast tumors. We provide here some promising data that supports in vivo relevance of our conclusions. First, our cluster analyses associated SCP cell types with luminal A and "normal-like" breast tumors, whereas ICP cell types shared similar gene expression profiles with luminal B and basal-like breast tumors. Second, ICP-type MDA-MB-231 cells were more tumorigenic than SCP-type T47D cells. T47D cells formed smaller tumors in some animals, and all tumors displayed regression between 10 and 15 days post-injection. Accordingly, we observed positive SABG staining in two out of four T47D tumors, but not in MDA-MB-231 tumors. Obviously, ICP-like and SCP-like tumors in affected women may or may not display similar tumorigenic potentials, depending on the women's hormonal status and treatment conditions. However, as most SCP-like luminal A or ER+ tumors are successfully treated with tamoxifen [34], their less aggressive behavior could be related to their highly effective senescence response to tamoxifen treatment, as shown here with T47D cells under in vitro conditions (Fig. 3). It will be interesting to examine whether the success of anti-estrogenic treatments is indeed associated with senescence induction in breast tumors. If this is the case, senescence-inducing treatments could be considered for breast cancer.

In conclusion, our analyses reveal that the in vitro ability to generate senescent progeny permits discrimination between cells that share molecular and tumorigenic similarities with luminal A subtype breast tumors from cells related to basal/luminal B subtype tumors. We also provide in vitro evidence for classifying breast cancers into two major groups based on the ability to generate differentiated progeny. Less-tumorigenic SCP cell lines generate both luminal- and myoepithelial-like cells. In contrast, more-tumorigenic ICP cell lines are defective in their ability to generate differentiated progeny. Our findings may have prognostic relevance and serve as a basis for therapeutically inducing differentiation and senescence in breast cancer.

Supporting Information

Dataset S1 STR analysis data that shows the authenticity of breast cancer cell lines used in this study.
Found at: doi:10.1371/journal.pone.0011288.s001 (1.50 MB XLS)

Table S1 Gene clusters, genetic mutations and epigenetic changes of breast cancer cell lines used in this study.
Found at: doi:10.1371/journal.pone.0011288.s002 (0.05 MB DOC)

Table S2 Estrogen receptor (ER) status, main pathological features of senescence staining (SABG) of breast tumors used in this study.
Found at: doi:10.1371/journal.pone.0011288.s003 (0.05 MB DOC)

Figure S1 p16Ink4a expression in colonies obtained from breast cancer cell lines. There was no correlation between p16Ink4a expression and progenitor subtype.
Found at: doi:10.1371/journal.pone.0011288.s004 (3.39 MB TIF)

Figure S2 Co-staining experiments indicate that SABG staining is associated with p21Cip1, but with p16Ink4a expression in SCP cells. Colonies were generated from T47D and MB-MDA-231 cells and subjected to SABG staining, followed by p21Cip1 or p16Ink4a immunoperoxidase (brown) staining. MDA-MB-231 cells were used as negative control.
Found at: doi:10.1371/journal.pone.0011288.s005 (2.74 MB TIF)

Figure S3 Effect of estrogen receptor-overexpression on the production of BrdU-negative terminally arrested cell progeny. ER-overexpressing (ER-5, ER-7, ER-26) and control (C-8, C-10, C-11) stable clones were established from T47D cells. Following transfection with ER expression and control vectors, colonies were generated from respective cell lines, labeled with BrdU for 24 h, immunostained for BrdU (brown), and slightly counterstained with hematoxylin to visualize BrdU+ and BrdU- cells.
Found at: doi:10.1371/journal.pone.0011288.s006 (6.57 MB TIF)

Figure S4 Detection of SABG+ senescent cells in estrogen receptor-positive breast tumors. Snap-frozen tumors were used to obtain 6 μ thick sections and used directly to detect SABG+ cells. H&E: hematoxylin-eosin staining.
Found at: doi:10.1371/journal.pone.0011288.s007 (9.45 MB TIF)

Figure S5 ASMA+ myoepithelial-like cells are produced frequently in senescent cell progenitor T47D and MCF-7 cell lines under confluent conditions. ASMA was tested by immunoperoxidase.
Found at: doi:10.1371/journal.pone.0011288.s008 (4.08 MB TIF)

Figure S6 Unsupervised hierarchical clustering of breast tumor and cell line gene expression data that is described in Fig. 7A. Dendrogram shown here includes tumor and cell line sample IDs.
Found at: doi:10.1371/journal.pone.0011288.s009 (1.05 MB TIF)

Figure S7 Tumors derived from T47D but not from MDA-MB-231 display SABG (+) senescent cells. Two of four T47D tumors

displayed SABG+ cells. All four MDA-MB-231 tumors lacked SABG+ cells.
Found at: doi:10.1371/journal.pone.0011288.s010 (7.97 MB TIF)

Acknowledgments

We thank Rana Nelson for editorial help.

Author Contributions

Conceived and designed the experiments: MO. Performed the experiments: MM SB HY HA SS PT BGD BC. Analyzed the data: MM UHT IGY CA MO. Contributed reagents/materials/analysis tools: BB. Wrote the paper: MM MO.

References

1. Perou CM, Sorlie T, Eisen MB, van de Rijn M, Jeffrey SS, et al. (2000) Molecular portraits of human breast tumours. Nature 406: 747–752.
2. Sorlie T, Tibshirani R, Parker J, Hastie T, Marron JS, et al. (2003) Repeated observation of breast tumor subtypes in independent gene expression data sets. Proc Natl Acad Sci U S A 100: 8418–8423.
3. Sotiriou C, Pusztai L (2009) Gene-expression signatures in breast cancer. N Engl J Med 360: 790–800.
4. Stingl J, Caldas C (2007) Molecular heterogeneity of breast carcinomas and the cancer stem cell hypothesis. Nat Rev Cancer 7: 791–799.
5. Vargo-Gogola T, Rosen JM (2007) Modelling breast cancer: one size does not fit all. Nat Rev Cancer 7: 659–672.
6. Romanov SR, Kozakiewicz BK, Holst CR, Stampfer MR, Haupt LM, et al. (2001) Normal human mammary epithelial cells spontaneously escape senescence and acquire genomic changes. Nature 409: 633–637.
7. Stampfer MR, Yaswen P (2003) Human epithelial cell immortalization as a step in carcinogenesis. Cancer Lett 194: 199–208.
8. Neve RM, Chin K, Fridlyand J, Yeh J, Baehner FL, et al. (2006) A collection of breast cancer cell lines for the study of functionally distinct cancer subtypes. Cancer Cell 10: 515–527.
9. Gur-Dedeoglu B, Konu O, Kir S, Ozturk AR, Bozkurt B, et al. (2008) A resampling-based meta-analysis for detection of differential gene expression in breast cancer. BMC Cancer 8: 396.
10. Ozturk N, Erdal E, Mumcuoglu M, Akcali KC, Yalcin O, et al. (2006) Reprogramming of replicative senescence in hepatocellular carcinoma-derived cells. Proc Natl Acad Sci U S A 103: 2178–2183.
11. Dimri GP, Lee X, Basile G, Acosta M, Scott G, et al. (1995) A biomarker that identifies senescent human cells in culture and in aging skin in vivo. Proc Natl Acad Sci U S A 92: 9363–9367.
12. Alotaibi H, Yaman EC, Demirpence E, Tazebay UH (2006) Unliganded estrogen receptor-alpha activates transcription of the mammary gland Na+/I− symporter gene. Biochem Biophys Res Commun 345: 1487–1496.
13. Charafe-Jauffret E, Ginestier C, Monville F, Finetti P, Adelaide J, et al. (2006) Gene expression profiling of breast cell lines identifies potential new basal markers. Oncogene 25: 2273–2284.
14. Stingl J (2009) Detection and analysis of mammary gland stem cells. J Pathol 217: 229–241.
15. Campisi J, d'Adda di Fagagna F (2007) Cellular senescence: when bad things happen to good cells. Nat Rev Mol Cell Biol 8: 729–740.
16. Wei W, Sedivy JM (1999) Differentiation between senescence (M1) and crisis (M2) in human fibroblast cultures. Exp Cell Res 253: 519–522.
17. Kiyono T, Foster SA, Koop JI, McDougall JK, Galloway DA, et al. (1998) Both Rb/p16INK4a inactivation and telomerase activity are required to immortalize human epithelial cells. Nature 396: 84–88.
18. Beausejour CM, Krtolica A, Galimi F, Narita M, Lowe SW, et al. (2003) Reversal of human cellular senescence: roles of the p53 and p16 pathways. EMBO J 22: 4212–4222.
19. Garbe JC, Holst CR, Bassett E, Tlsty T, Stampfer MR (2007) Inactivation of p53 function in cultured human mammary epithelial cells turns the telomere-length dependent senescence barrier from agonescence into crisis. Cell Cycle 6: 1927–1936.
20. Cariou S, Donovan JC, Flanagan WM, Milic A, Bhattacharya N, et al. (2000) Down-regulation of p21WAF1/CIP1 or p27Kip1 abrogates antiestrogen-mediated cell cycle arrest in human breast cancer cells. Proc Natl Acad Sci U S A 97: 9042–9046.
21. Mukherjee S, Conrad SE (2005) c-Myc suppresses p21WAF1/CIP1 expression during estrogen signaling and antiestrogen resistance in human breast cancer cells. J Biol Chem 280: 17617–17625.
22. Dubik D, Shiu RP (1992) Mechanism of estrogen activation of c-myc oncogene expression. Oncogene 7: 1587–1594.
23. Berthois Y, Katzenellenbogen JA, Katzenellenbogen BS (1986) Phenol red in tissue culture media is a weak estrogen: implications concerning the study of estrogen-responsive cells in culture. Proc Natl Acad Sci U S A 83: 2496–2500.
24. Booth BW, Smith GH (2006) Estrogen receptor-alpha and progesterone receptor are expressed in label-retaining mammary epithelial cells that divide asymmetrically and retain their template DNA strands. Breast Cancer Res 8: R49.
25. Shyamala G, Chou YC, Cardiff RD, Vargis E (2006) Effect of c-neu/ErbB2 expression levels on estrogen receptor alpha-dependent proliferation in mammary epithelial cells: implications for breast cancer biology. Cancer Res 66: 10391–10398.
26. Al-Hajj M, Wicha MS, Benito-Hernandez A, Morrison SJ, Clarke MF (2003) Prospective identification of tumorigenic breast cancer cells. Proc Natl Acad Sci U S A 100: 3983–3988.
27. Shipitsin M, Campbell LL, Argani P, Weremowicz S, Bloushtain-Qimron N, et al. (2007) Molecular definition of breast tumor heterogeneity. Cancer Cell 11: 259–273.
28. Sleeman KE, Kendrick H, Ashworth A, Isacke CM, Smalley MJ (2006) CD24 staining of mouse mammary gland cells defines luminal epithelial, myoepithelial/basal and non-epithelial cells. Breast Cancer Res 8: R7.
29. Yeh IT, Mies C (2008) Application of immunohistochemistry to breast lesions. Arch Pathol Lab Med 132: 349–358.
30. Sotiriou C, Neo SY, McShane LM, Korn EL, Long PM, et al. (2003) Breast cancer classification and prognosis based on gene expression profiles from a population-based study. Proc Natl Acad Sci U S A 100: 10393–10398.
31. Wu CH, van Riggelen J, Yetil A, Fan AC, Bachireddy P, et al. (2007) Cellular senescence is an important mechanism of tumor regression upon c-Myc inactivation. Proc Natl Acad Sci U S A 104: 13028–13033.
32. Honeth G, Bendahl PO, Ringner M, Saal LH, Gruvberger-Saal SK, et al. (2008) The CD44+/CD24− phenotype is enriched in basal-like breast tumors. Breast Cancer Res 10: R53.
33. Ford CE, Ekstrom EJ, Andersson T (2009) Wnt-5a signaling restores tamoxifen sensitivity in estrogen receptor-negative breast cancer cells. Proc Natl Acad Sci U S A 106: 3919–3924.
34. (1998) Tamoxifen for early breast cancer: an overview of the randomised trials. Early Breast Cancer Trialists' Collaborative Group. Lancet 351: 1451–1467.

Cancer Letters 286 (2009) 103–113

Contents lists available at ScienceDirect

Cancer Letters

journal homepage: www.elsevier.com/locate/canlet

Mini-review

Senescence and immortality in hepatocellular carcinoma

Mehmet Ozturk [a,b,*], Ayca Arslan-Ergul [a], Sevgi Bagislar [a,b], Serif Senturk [a], Haluk Yuzugullu [a,b]

[a] Department of Molecular Biology and Genetics, Bilkent University, 06800 Ankara, Turkey
[b] Centre de Recherche INSERM-Université Joseph Fourrier U823, Institut Albert Bonniot, 38042 Grenoble, France

ARTICLE INFO

Article history:
Received 26 March 2008
Received in revised form 23 June 2008
Accepted 29 October 2008

Keywords:
Liver cancer
Senescence
Telomeres
DNA damage
p53
$p16^{INK4a}$
$p21^{Cip1}$
Retinoblastoma
Cirrhosis
Hepatocytes
Telomerase reverse transcriptase

ABSTRACT

Cellular senescence is a process leading to terminal growth arrest with characteristic morphological features. This process is mediated by telomere-dependent, oncogene-induced and ROS-induced pathways, but persistent DNA damage is the most common cause. Senescence arrest is mediated by $p16^{INK4a}$- and $p21^{Cip1}$-dependent pathways both leading to retinoblastoma protein (pRb) activation. p53 plays a relay role between DNA damage sensing and $p21^{Cip1}$ activation. pRb arrests the cell cycle by recruiting proliferation genes to facultative heterochromatin for permanent silencing. Replicative senescence that occurs in hepatocytes in culture and in liver cirrhosis is associated with lack of telomerase activity and results in telomere shortening. Hepatocellular carcinoma (HCC) cells display inactivating mutations of p53 and epigenetic silencing of $p16^{INK4a}$. Moreover, they re-express telomerase reverse transcriptase required for telomere maintenance. Thus, senescence bypass and cellular immortality is likely to contribute significantly to HCC development. Oncogene-induced senescence in premalignant lesions and reversible immortality of cancer cells including HCC offer new potentials for tumor prevention and treatment.

1. Introduction

Senescence is an evolutionary term meaning "the process of becoming old"; the phase from full maturity to death characterized by accumulation of metabolic products and decreased probability of reproduction or survival [1]. The term "cellular senescence" was initially used by Hayflick and colleagues to define cells that ceased to divide in culture [2]. Today, cellular senescence is recognized as a response of proliferating somatic cells to stress and damage from exogenous and endogenous sources. It is characterized by permanent cell cycle arrest. Senescent cells also display altered morphology and an altered pattern of gene expression, and can be recognized by the presence of senescence markers such as senescence-associated β-galactosidase (SABG), $p16^{INK4A}$, senescence-associated DNA-damage foci and senescence-associated heterochromatin foci (for a review see Ref. [3]). This cellular response has both beneficial (anti-cancer) and probably deleterious (such as tissue aging) effects on the organism. Most of our knowledge of cellular senescence is derived from in vitro studies performed with fibroblasts, and some epithelial cells such as mammary epithelial cells. Animal models are increasingly being used to study cellular senescence in vivo. Telomerase-deficient mouse models lacking RNA subunit (TERC−/−) have been very useful in demonstrating the critical role of telomeres in organ aging and tumor susceptibility [4]. Other mouse models including tumor suppressor gene-deficient and oncogene-expressing mice were also used extensively.

Compared to other tissues and cancer models, the role of senescence in liver cells and its implications in hepatocellular carcinogenesis have been less explored. One of

* Corresponding author. Address: Centre de Recherche INSERM-Université Joseph Fourrier U823, Institut Albert Bonniot, Grenoble 38000, France. Tel.: +33 (0) 4 76 54 94 10; fax: +33 (0) 4 76 54 94 54.
E-mail address: ozturkm@ujf-grenoble.fr (M. Ozturk).

0304-3835/$ - see front matter © 2008 Elsevier Ireland Ltd. All rights reserved.
doi:10.1016/j.canlet.2008.10.048

the main obstacles is the lack of adequate in vitro systems. As hepatocytes can not divide in cell culture, the study of their replicative senescence mechanisms is not easy. Nevertheless, these cells are able to quit their quiescent state in vivo and proliferate massively in response to partial hepatectomy or liver injury [5]. This capacity can be explored to study in vivo senescence of hepatocytes using rodent models. Studies with clinical samples indicate that hepatocyte senescence occurs in vivo in patients with chronic hepatitis, cirrhosis and HCC [6–8]. In contrast to the paucity of studies directly addressing cellular senescence, the critical role of telomere shortening (as a feature associated with replicative senescence) in cirrhosis and HCC development is well established [9]. Telomeres in normal liver show a consistent but slow shortening during aging. In contrast, hepatocyte DNA telomere shortening is accelerated in patients with chronic liver disease with shortest telomeres described in cirrhotic liver and HCC. Telomerase-deficient mice have also been used elegantly to demonstrate the critical roles of telomerase and telomeres in liver regeneration and experimentally induced cirrhosis [10,11]. A major accomplishment in recent years was the demonstration of critical role played by senescence for the clearance of ras-induced murine liver carcinomas following p53 restoration [12].

Despite a relatively important progress, the mechanisms of hepatocellular senescence and the role of cellular immortality in HCC remain ill-known issues. As one of the rare tissues with ample clinical data on senescence-related aberrations, liver may serve as an excellent model to further explore the relevance of cellular senescence in human biology. Moreover, a better understanding of senescence and immortality in hepatic tissues may help to develop new preventive and therapeutic approaches for severe liver diseases such as cirrhosis and HCC. Here we will review recent progress on senescence and immortality mechanisms with a specific emphasis on hepatocellular carcinogenesis.

2. Senescence pathways

Cellular senescence has long been considered as a mechanism that limits the number of cell divisions (or population doublings) in response to progressive telomere shortening. Most human somatic cells are telomerase-deficient because of the repression of telomerase reverse transcriptase (TERT) expression. Therefore, proliferating somatic cells undergo progressive telomere DNA erosion as a function of their number of cell divisions. This form of senescence is now called as replicative or telomere-dependent senescence (Fig. 1).

Human chromosome telomere ends are composed of TTAGGG repeats (5–20 kb) in a DNA-protein complex formed by six telomere-specific proteins, called "shelterin" [13]. Telomeric DNA has a structure called "t-loop" which is formed as a result of invasion of the single stranded G-rich sequence into the double-stranded telomeric tract. Since the 1930s, it has been known that telomeres, with telomere-binding proteins, prevent genomic instability and the loss of essential genetic information by "capping" chromosome ends. They are also indispensable for proper recombination and chromosomal segregation during cell division. Telomeres become shorter with every cell division in somatic cells, because of replication complex's inability to copy the ends of linear DNA, which also makes them a "cell cycle counter" for the cell [14]. Telomeres are added to the end of chromosomes with a complex containing the RNA template TERC and the reverse transcriptase TERT [15]. Most somatic cells lack telomerase activity because the expression of TERT is repressed, in contrast to TERC expression. The lack of sufficient TERT expression in somatic cells is the main cause of telomere shortening during cell replication. This telomerase activity also helps to maintain telomere integrity by telomere capping [15].

The loss of telomeres has long been considered to be the critical signal for senescence induction. It is now well known that telomere-dependent senescence is induced by a change in the protected status of shortened telomeres, whereby the loss of telomere DNA contributes to this change [16]. The loss of telomere protection or any other cause of telomere dysfunction results in inappropriate chromosomal end-to-end fusions through non-homologous end joining or homologous recombination DNA repair pathways [17]. These DNA repair pathways are used principally to repair double-strand DNA breaks (DSBs). Thus, it is highly likely that the open-ended telomere DNA is sensed as a DSB by the cell machinery when telomere structure becomes dysfunctional. Accordingly, dysfunctional telomeres elicit a potent DSB type DNA damage response by recruiting phosphorylated H2AX, 53BP1, NBS1 and MDC1 [18].

Telomere-dependent senescence is not the only form of senescence. At least two other forms of telomere-independent senescence are presently known: (1) oncogene-induced senescence; and (2) reactive oxygen species (ROS)-induced senescence (Fig. 1).

Oncogene-induced senescence had initially been identified as a response to expression of Ras oncogene in normal cells ([19], for a recent review see [20]). The expression of oncogenic Ras in primary human or rodent cells results in permanent G1 arrest. The arrest was accompanied by accumulation of p53 and $p16^{INK4a}$, and was phenotypically indistinguishable from cellular senescence. This landmark observation suggested that the onset of cellular senescence does not simply reflect the accumulation of cell divisions, but can be prematurely activated in response to an oncogenic stimulus [19]. In 10 years following this important discovery, telomere-independent forms of senescence have become a new focus of extensive research leading to the recognition of senescence as a common form of stress response. Moreover, oncogene-induced senescence is now recognized as a novel mechanism contributing to the cessation of growth of premalignant or benign neoplasms to prevent malignant cancer development [21]. In addition to Ras, other oncogenes including Raf, Mos, Mek, Myc and Cyclin E also induce senescence [20]. Conversely, the loss of PTEN tumor suppressor gene also leads to senescence [22]. Similar to telomere-dependent senescence, oncogene-induced senescence is also primarily a DNA damage response (Fig. 1). Experimental inactivation of DNA damage response abrogates Ras-induced senescence

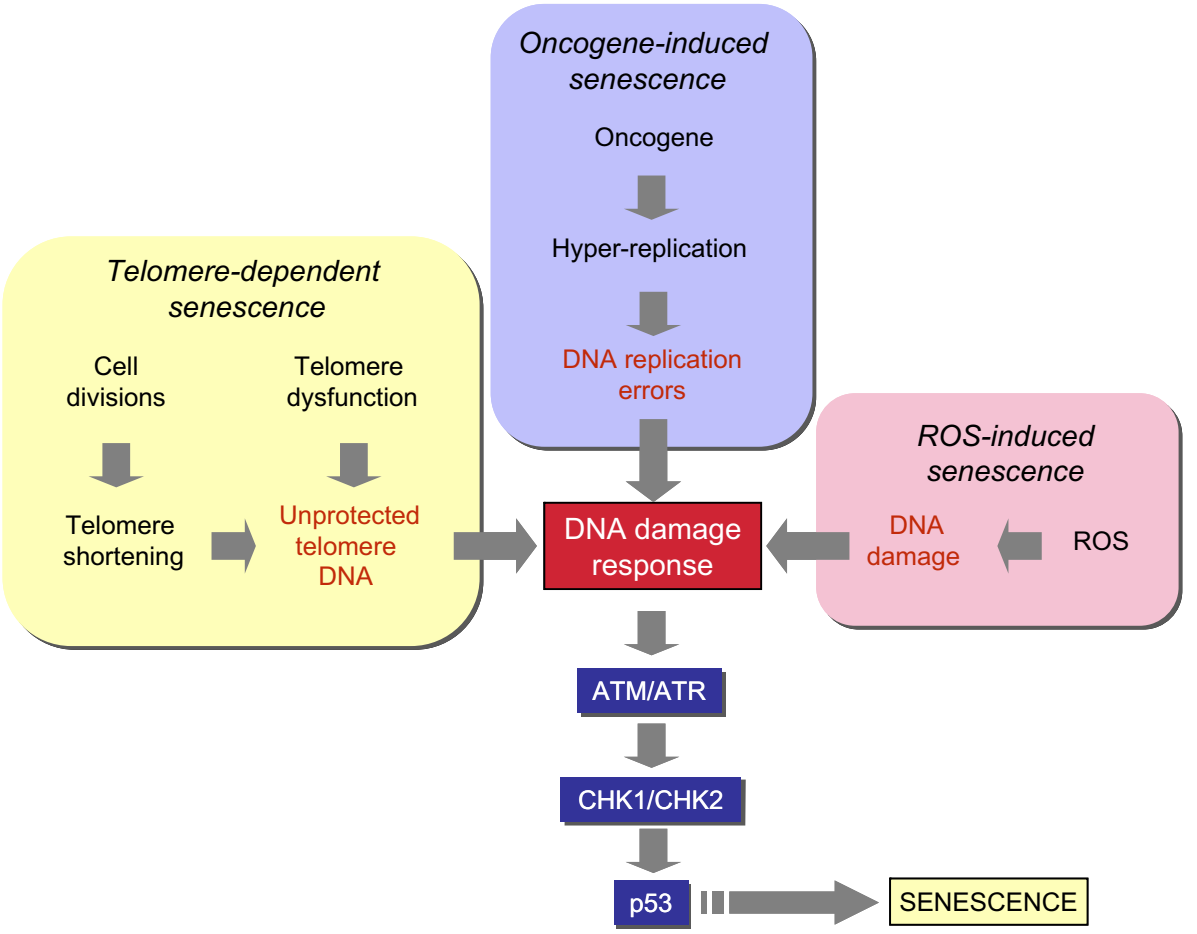

Fig. 1. DNA damage and p53 activation play a central role in different senescence pathways. DNA damage (often in the form of double-strand breaks) activate upstream kinases (ATM and ATR) leading to p53 phosphorylation by CHK1 and CHK2 kinases. Phosphoryated p53 is released from MDM, and stabilized in order to induce senescence arrest or apoptosis (not shown here).

and promotes cell transformation. DNA damage response and oncogene-induced senescence are established following DNA hyper-replication immediately after oncogene expression. Senescent cells arrest with partly replicated DNA, where DNA replication origins have fired multiple times, prematurely terminated DNA replication forks and DNA double-strand breaks are present [23,24].

ROS-induced senescence, the other telomere-independent senescence pathway is gaining importance (for a recent review see Ref. [25]). Mitochondria are the major intracellular sources of ROS which are mainly generated at the respiratory chain. Therefore, ROS have been suspected for many years as cellular metabolites involved in organismal aging [26]. ROS are also generated in the cytoplasm by the NOX family of enzymes [27]. Experimental induction of ROS accumulation in cells (for example by mild H2O2 treatment or glutathione depletion) induces senescence-like growth arrest in different cell types, whereas anti-oxidant treatment can inhibit senescence [25]. More importantly, ROS have been identified as critical mediators of both telomere-dependent and oncogene-induced senescence. Telomere-dependent senescence arrest is accelerated in cells grown under high O_2 conditions. Inversely, cells grown under low O_2 conditions display increased lifespan ([28], see Ref. [25]). ROS also play a critical role in Ras-induced senescence [29,30].

Currently, mechanisms of ROS-induced senescence are not fully understood. It is generally accepted that oxidative stress and ROS eventually cause DNA damage, whereby DNA damage response may contribute to senescence induction. The relationship between mitochondrial dysfunction, ROS, DNA damage and telomere-dependent senescence has recently been demonstrated [31]. However, ROS may also induce modifications in the cellular signaling pathways resulting in senescence arrest. For example, ROS induce senescence in hematopoietic stem cells by activating p38 MAPK [32].

Whether induced by telomere dysfunction, DNA replication stress following oncogene activation, or ROS accumulation, DNA damage is one of the common steps in the generation of senescence arrest via p53 activation (Fig. 1). Upstream checkpoint kinases, such as ATM or ATR are activated in response to DNA damage in the form of double-stand breaks. These kinases phosphorylate

downstream factors including CHK1 and CHK2 that in turn phosphorylate p53. Phosphorylation of p53 results in its activation by the displacement of the MDM2 protein. Critical involvement of this p53 activating pathway has been reported for both telomere-dependent [33], and oncogene-induced senescence [34].

Other mechanisms of senescence that are apparently not driven by DNA damage should also be discussed here. Of particular interest is the INK4 locus encoding two inhibitors of cyclin-dependent kinases ($p16^{INK4a}$, $p15^{INK4b}$), and ARF, a p53 regulatory protein (for a review see Ref. [35]). $p16^{INK4a}$ and $p15^{INK4b}$ connect some senescent initiating signals to the retinoblastoma (Rb) pathway, independent of p53 activation. These proteins are easily activated in cell culture and induce senescence arrest. Cells that escape senescence often display inactivation of $p16^{INK4a}$, and sometimes $p15^{INKb}$ and ARF either by homozygous deletion or by shutting-down gene expression. A prominent role for $p16^{INK4a}$ in senescence and tumor suppression in humans has emerged, despite some confusion due to the fact that a relatively small DNA segment encodes the 3 proteins of the INK4 locus. $p16^{INK4a}$ is activated during telomere-dependent and oncogene-induced senescence [19,36]. Moreover, its expression is induced in aging tissues [37]. The mechanisms of regulation of $p16^{INK4a}$ expression are not well known. Although individual components of INK4 locus can respond independently to positively – (for example to Ras) or negatively – (for example c-Myc) acting signals, the entire INK4 locus might be coordinately regulated by epigenetic mechanisms (reviewed in Ref. [35]).

A very recent addition to the list of senescence mechanisms is to be qualified as "senescence induced by secreted proteins". It was reported many years ago that TGF-β is a mediator of oncogene-induced senescence [38]. This mechanism of induction is of particular interest, because it suggests that not only intrinsic cellular factors, but also extracellular or secreted proteins can induce senescence. Recent discovery of several other secreted proteins, including IGFBP7 and IL6 as autocrine/paracrine mediators of oncogene-induced senescence arrest, provide strong support for an extracellularly induced form of senescence [39–41]. This new form of senescence regulation is reminiscent of the so called active apoptosis induction by death ligands. Thus, an active form of cellular senescence induced by "aging ligands" could be a major physiological regulator of tissue/organism aging.

3. Cyclin-dependent inhibitors as common mediators of senescence arrest

We have already stated that senescence and apoptosis share interesting similarities. Another similarity between these cellular processes is the convergence of different pathways in a common place to induce the same cell fate, independent of the initial signal. Similarly to caspase activation, prior to apoptosis induction by different stimuli, most if not all senescence pathways result in the activation of cyclin-dependent kinase inhibitors (CDKIs) in order to induce permanent cell cycle arrest. Senescent cells accumulate at G1 phase of the cell cycle due to an inability to enter into S phase in order to initiate DNA synthesis. The transition of proliferating cells from G1 to S phase requires the release of E2F factors from their inhibitory partner retinoblastoma protein (pRb) following phosphorylation by cyclin-dependent kinases (CDKs), in particular by CDK4/CDK6 and CDK2 at this stage of the cycle [35]. The senescence arrest is mediated by inhibition of pRb phosphorylation by CDK4 and CDK2. The activities of these enzymes are controlled by different mechanisms, but the major proteins involved in the control of senescence arrest are CDKIs. Almost all known CDKIs have been reported to be implicated in senescence arrest, but three of them are best characterized: $p16^{INK4a}$ and $p15^{INK4b}$ which inhibit CDK4/CDK6, and $p21^{Cip1}$ which inhibits CDK2 (Fig. 2).

$p21^{Cip1}$ is one of the main targets of p53 for the induction of cell cycle arrest following DNA damage [42]. Pathways that generate DNA damage response and p53 activation use $p21^{Cip1}$ as a major mediator of cellular senescence to control pRb protein [43]. Exceptionally, $p21^{Cip1}$ can be activated by p53-independent pathways to induce senescence [44].

The Rb protein plays two important and complementary roles that are necessary to initiate and to permanently maintain the cell cycle arrest in senescent cells. pRb proteins firstly contribute to the exit from the cell cycle by arresting cells at G1 phase, as expected [45]. In senescent cells, this exit is complemented with a dramatic remodeling of chromatin through the formation of domains of facultative heterochromatin called SAHF [46–48]. SAHF contain modifications and associated proteins characteristic of transcriptionally silent heterochromatin. Proliferation-promoting genes, such as E2F target genes are recruited into SAHF in a pRb protein-dependent manner. This recruitment is believed to contribute to irreversible silencing of these proliferation-promoting genes [49].

4. Senescence of hepatocytes and chronic liver disease

Hepatocytes in the adult liver are quiescent cells, they are renewed slowly, approximately once a year, as estimated by telomere loss which is 50–120 bp per year in healthy individuals [50,51]. However, the liver has an extremely powerful regenerative capacity, as demonstrated experimentally in rodents, and as observed in patients with chronic liver diseases [5]. This regenerative capacity is due mostly to the ability of mature hepatocytes to proliferate in response to a diminution of total liver mass either experimentally, or following exposure to viral and non viral hepatotoxic agents. In addition, the adult liver seems to harbor hepatocyte-progenitor cells (<0.10% of total hepatocyte mass) that are able to restore liver hepatocyte populations [52]. However, hepatocytes, like any other somatic cells, do not have unlimited replicative capacity, due to the lack of telomerase activity that is needed to avoid telomere shortening during successive cell divisions. This is best exemplified by decreased hepatocyte proliferation in liver cirrhosis stage of chronic liver diseases [53], providing in vivo evidence for the exhaustion of hepatocyte proliferation capacity. Senescence mechanisms in hepatocytes and in liver tissue are not well known. However, a limited

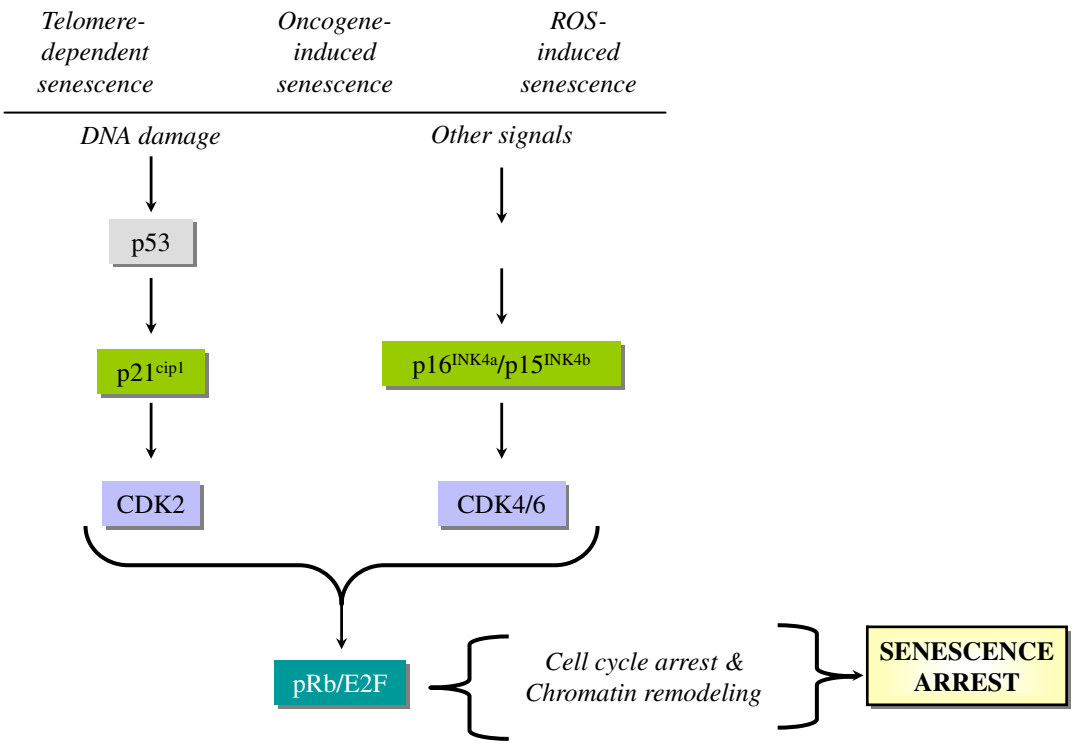

Fig. 2. All known senescence pathways converge at the level of activation of CDKIs ($p15^{INK4b}$, $p16^{INK4a}$ and $p21^{Cip1}$) that keep the pRb protein under the active form. The pRb protein inhibits E2F action and prevents the expression of growth-promoting genes for cell cycle exit. Furthermore, pRb recruits growth-promoting genes into a facultative chromatin structure for permanent silencing and growth arrest.

number of in vitro studies with hepatocytes, as well as numerous descriptive in vivo studies in liver tissue provide sufficient evidence that hepatocytes can undergo senescence type changes.

In vitro senescence in hepatocytes: as stated earlier, limited proliferative capacity of somatic cells is controlled by replicative senescence. The experimental study of replicative senescence is done traditionally by serial culture of primary cells. Initially observed in fibroblasts, this phenomenon has also been well understood in some epithelial cells, mammary epithelial cells in particular [54]. On the other hand, our knowledge of hepatocyte replicative senescence is highly limited. In contrast to in vivo conditions, mature hepatocytes are extremely resistant to cell proliferation in cell culture. Usually, more than 99.9% of adult liver hepatocytes do not divide and can only be maintained in culture for a few weeks at most. A small progenitor-type cell population (so called small hepatocytes) has been shown to proliferate in vitro, but they usually stop growing at passages 5–7, with an ill-defined senescence-like phenotype [55].

Fetal hepatocytes display better proliferation capacity in culture. A few studies have shown that these fetal cells enter replicative senescence, as shown by senescence-associated β-galactosidase assay (SABG) at population doubling (PD) 30–35 [55]. This is accompanied by progressive shortening of telomeres down to ~6 kbp, as these cells like adult hepatocytes lack telomerase activity. However, it was possible to immortalize these fetal hepatocytes by stable expression of TERT [55]. Such immortalized cells have been expanded beyond known senescence barriers (>300 PD).

In vivo senescence in liver tissue: in contrast to in vitro studies, in vivo senescence of human hepatocytes is better known. Indeed, the liver is one of the rare tissues where in vivo evidence for senescence has been convincingly and independently demonstrated by different investigators [6–9]. Replicative senescence (as tested by SABG assay) displayed a gradual increase from 10% in normal liver, to 84% in cirrhosis ([6,7]. It was also detected in 60% HCCs [6]. It has also been demonstrated that telomere shortening in cirrhosis is restricted to hepatocytes and this hepatocyte-specific shortening was correlated with SABG staining [7].

Potential mechanisms of senescence in hepatocytes and the liver: as presented in detail in the previous section, multiple pathways of senescence have been described in different experimental systems. Key molecules that are already involved in senescence arrest have also been summarized. The published data on different senescence pathways in the liver is fragmented and control mechanisms involved in hepatocyte senescence are not completely understood. Therefore, existing data on hepatocellular senescence together with potential mechanisms that may be involved in this process will be presented.

For reasons previously described, almost nothing is known about molecular mechanisms involved in replicative senescence and immortalization of hepatocytes in cul-

ture. There are only a few demonstrations of hepatocyte immortalization in vitro. Thus, ectopically expressed TERT may induce hepatocyte immortalization. However, as the published data using TERT immortalization is scarce, it is highly likely that the immortalization of hepatocytes is not an easy task even with a well-established protocol that works with other epithelial cell types such as mammary epithelial cells. The mechanisms of in vitro senescence induction in hepatocytes are also mostly unknown. Rapid induction of a senescence arrest in cultured hepatocytes suggests that these cells display robust telomere-independent senescence-inducing systems that are functional in vitro. However, they remain to be discovered. It is highly likely that, similar to other somatic cells, p53 and RB pathways in general, and some CDKIs in particular are also involved in hepatocyte senescence, but the evidence is lacking for the time being.

Telomere shortening during aging is slow (55–120 base pairs per year) and stabilizes at mid age in healthy liver, so that the loss of telomeric DNA does not reach a level to induce telomere dysfunction and DNA damage response [50,51]. Other forms of telomere-independent senescence such as ROS-induced senescence may also be rare under normal physiological conditions. On the other hand, telomere loss is accelerated in chronic liver disease to reach lowest levels in the cirrhotic liver [7,51]. Therefore, one plausible mechanism involved in cirrhosis is probably telomere-dependent senescence, or replicative senescence. The relevance of replicative senescence to liver tissue aging has been demonstrated experimentally using telomerase-deficient mice. Late generation telomerase-deficient mice display critically shortened telomeres and an impaired liver growth response to partial hepatectomy. A subpopulation of telomere-shortened hepatic cells displayed impaired proliferative capacity that is associated with SABG activity [11,56]. On the other hand, it has been reported that mouse liver cells are highly resistant to extensive telomere dysfunction. Conditional deletion of the telomeric protein TRF2 in hepatocytes resulted in telomeric accumulation of phospho-H2AX and frequent telomere fusions, indicating loss of telomere protection. However, there was no induction of p53 and liver function appeared unaffected. The loss of TRF2 did not compromise liver regeneration after partial hepatectomy. Liver regeneration occurred without cell division involving endoreduplication and cell growth, thereby circumventing the chromosome segregation problems associated with telomere fusions. Thus, it appears that hepatocytes display intrinsic resistance to telomere dysfunction, although they are apparently vulnerable to severe telomere loss [57].

Hepatocyte senescence that is observed in severe chronic liver diseases such as cirrhosis may also be induced by telomere-independent pathways. Chronic liver injury observed under such conditions is accompanied with inflammation, cell death, and oxidative stress [58–60]. Some of the etiological factors such as HCV and alcohol induce mitochondrial dysfunction may result in ROS accumulation [61,62]. Thus, ROS-induced senescence may also occur during cirrhosis, although this has not yet been reported. The status of DNA damage in chronic liver disease is less well-known. 8-Hydroxydeoxyguanosine, an indicator of DNA lesions produced by ROS, was reported to be increased in chronic liver disease [63]. On the other hand, the upregulation of DNA repair enzymes in cirrhosis has also been reported [64]. Increased DNA repair activity in cirrhosis which may reflect increased DNA damages as a consequence of chronic liver injury, but also inhibition of DNA damage responses such as senescence were observed. Taken together, these observations suggest that the primary cause of senescence in cirrhotic patients is telomere dysfunction and that ROS may also play additional roles.

Among senescence-related proteins, $p16^{INK4a}$ and $p21^{Cip1}$ expression was found to be high in cirrhosis, as compared to normal liver and tumor tissues [65], suggesting that these major senescence-inducing proteins accumulate in the cirrhotic liver. Promoter methylation of these CDKIs was also studied. Chronic liver disease samples displayed lower levels of methylation as compared to HCCs [66]. Thus, the progression of chronic liver disease towards cirrhosis is accompanied with a progressive activation of different CDKIs, as expected.

5. Senescence pathway aberrations and telomerase reactivation in hepatocellular carcinoma

As stated earlier, p53 and retinoblastoma (Rb) pathways play a critical role in senescence arrest as observed in different in vitro and in vivo models. Indirect evidence suggests that these pathways may also be important in hepatocellular senescence. The accumulation of p21 and p16 in cirrhotic liver tissues has been reported independently by different reports. On the other hand, HCC rarely develops in liver tissues absent of chronic liver disease. More than 80% of these cancers are observed in patients with cirrhosis [9]. As the appearance of proliferating malignant cells from this senescence stage requires the bypass of senescence, the status of both p53 and RB pathways in HCC is of great importance in terms of molecular aspects of hepatocellular carcinogenesis.

HCC is one of the major tumors displaying frequent p53 mutations [67,68]. The overall p53 mutation frequency in HCC is around 30%. Both the frequency and the spectrum of p53 mutations show great variations between tumors from different geographical areas of the World. A hotspot mutation (codon 249 AGG → AGT) has been linked to exposure to aflatoxins which are known to be potent DNA damaging agents (for a review see Ref. [67]). Although, it is unknown whether aflatoxins are able to generate a DNA damage-dependent senescence response in hepatocytes, their association with DNA damage and p53 mutation provides indirect evidence for such an ability. Other p53 mutations described in HCCs from low aflatoxin areas may similarly be correlated with other DNA damaging agents, such as ROS which are known to accumulate in the livers of patients with chronic liver diseases, including cirrhosis.

Another player of senescence arrest, the p16 gene is rarely mutated in HCC, but its epigenetic silencing by promoter methylation is highly frequent in this cancer. More than 50% of HCCs display de novo methylation of the promoter of CDKN2A gene, encoding p16 protein, resulting in

loss of gene expression [67]. Major components of p53 and Rb pathways in the same set of HCCs with different etiologies have been analyzed [69]. Retinoblastoma pathway alterations (p16 ^{INK4a}, p15^{INK4b} or RB1 genes) were present in 83% of HCCs, whereas p53 pathway alterations (p53 or ARF genes) were detected in only 31% of tumors. Alterations in both Rb and p53 pathways were present in 30% of HCCs. Thus, it appears that either the Rb and/or the p53 pathway are affected in the great majority of HCCs, and that both pathways are affected in at least one third of these tumors. Unfortunately, p53 and p16^{INK4a} aberrations observed in HCC have not yet been studied in relation to senescence aberrations. However, these observations provide supporting evidence on the critical role of senescence-controlling pathways in the development of HCC.

The lack of telomerase activity in normal and cirrhotic liver correlates with progressive loss of telomere sequences ending up with a senescence arrest. The emergence of malignant hepatocytes from this senescence-dominated cirrhotic milieu would require not only the bypass of senescence, but also a way of survival despite critically shortened telomeres. Additionally, the proliferative expansion of neoplastic cells in order to form sustained tumor masses would require telomeres at a minimal length required to maintain intact chromosomal structures.

Many studies showed that telomerase activity is a hallmark of all human cancers, including 80–90% of HCCs [70–72]. It is currently unclear how the TERT expression is repressed and released in normal hepatocytes and HCC cells, respectively. The integration of HBV DNA sequences into TERT gene provides evidence for a virus-induced deregulation of TERT expression, but this appears to rarely occur, as only four cases have been reported thus far [73–75]. Hbx and PreS2 proteins may upregulate TERT expression [76,77]. The molecular mechanisms involved in TERT suppression in somatic cells and its reactivation in cancer cells are ill-known. The TERT promoter displays binding sites for a dozen of transcriptional regulators: estrogen receptor, Sp1, Myc and ER81 acting positively, and vitamin D receptor, MZF-2, WT1, Mad, E2F1 and SMAD interacting protein-1 (SIP1, also called ZEB-2 or ZFHX1B) acting negatively [78]. Despite high telomerase activity, telomeres in HCC were repeatedly found to be highly shortened [65,79,80]. However, 3′ telomere overhangs were found to be increased in nearly 40% HCCs [80]. Moreover, the expression of several telomeric proteins is increased in HCC [80,81].

Another ill-known aspect of TERT activity in HCC cells is the cellular origin of these malignant cells. It is presently unclear whether HCC arises from mature hepatocytes which lack telomerase activity, or stem/progenitor cell-like cells that may already express TERT at sufficient levels to maintain telomere integrity. In the non-tumor area surrounding the cancer tissue, telomerase activity could not be detected, or was detected at very low levels.

The importance of telomerase activity in HCC development has been studied experimentally using telomerase-deficient mouse model. These mice show increased susceptibility to adenoma development (tumor initiation), but they are quite resistant to fully malignant tumor development [82]. Likewise, telomerase deletion limits the progression of p53-mutant HCCs with short telomeres [83]. These observations suggest that the aberrations affecting telomerase activity and senescence controlling genes such as p53 may cooperate during hepatocellular carcinogenesis.

In summary, HCC is characterized by mutational inactivation of p53, a major player in DNA damage-induced senescence. In addition, p15^{INK4b}, p16^{INK4a}, p21^{Cip1} CDKIs are often inactivated in this cancer mostly by epigenetic mechanisms involving promoter methylation. These changes may play a critical role in the bypass of senescence that is observed in most cirrhosis cases, allowing some initiated cells to escape senescence control and proliferate. In the absence of telomerase activity such cells would probably not survive due to telomere loss. However, since more than 80% of HCCs display telomerase activity, it is highly likely that the telomerase reactivation, together with the inactivation of major CDKIs, plays a critical role in HCC development by conferring premalignant or malignant cells the ability to proliferate indefinitely (Fig. 3). However, cellular immortality is not sufficient for full malignancy [84]. Thus, senescence-related aberrations that are observed in HCC cells, may confer a partial survival advantage that would need to be complemented by other genetic or epigenetic alterations.

6. Senescence as an anti-tumor mechanism in hepatocellular carcinoma

Senescence in normal somatic cells and tissues is expected. How about cancer cells and tumors? Initial studies using different cancer cell lines provided ample evidence for the induction of senescence by different genetic as well as chemical or biological treatments [85]. Thus, it appeared that cancer cells, immortalized by definition, do have a hidden senescence program that can be revealed by different senescence-inducing stimuli. These studies provided preliminary evidence for considering senescence induction as an anti-cancer therapy. The in vivo relevance of these observations and expectations became evident only very recently. Senescence was observed in tumors or pre-neoplastic lesions. SABG activity as well as several other senescence markers were detected in lung adenomas, but not in adenocarcinomas observed in oncogenic Ras "knock-in" mice [86]. Ras-driven mouse T-cell lymphomas entered senescence after drug therapy, when apoptosis was blocked [87]. The first direct evidence of cellular senescence in humans was reported for the melanocytic nevus [88].

Senescence response of HCC cells was not the subject of intensive study until very recently. Therefore the potential role of senescence in these tumors is less well understood. Treatment of HCC cell lines with 5-aza-2-deoxycytidine induced the expression of p16^{INK4a}, hypophosphorylation of pRb and G1 arrest associated with positive SABG staining [89]. Recent findings indicate that senescence induction is a powerful mechanism of HCC regression. Xue et al. expressed H-ras oncogene and suppressed endogenous p53 expression in mouse hepatoblasts which produced massive

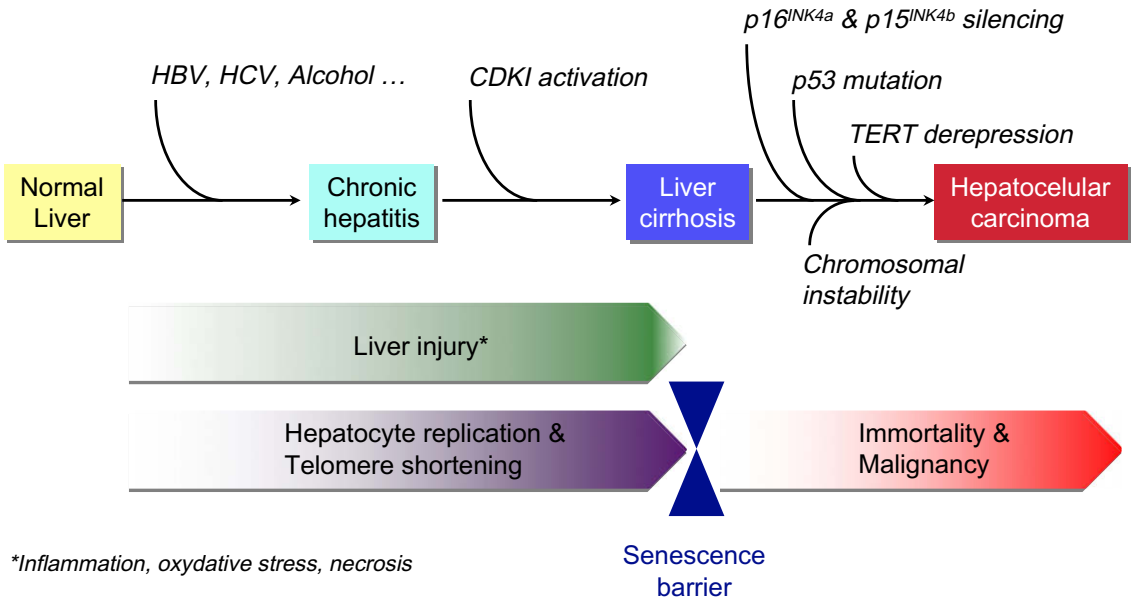

Fig. 3. Role of cellular senescence and immortalization in hepatocellular carcinogenesis. Chronic liver injury (triggered by major etiological factors HBV, HCV and alcohol) leading to cirrhosis is a common cause of HCC. Hepatocytes having no telomerase activity undergo progressive telomere shortening and DNA damage during this process. Consequently, CDKIs (primarily $p16^{INK4a}$ and $p21^{Cip1}$) are activated gradually to induce senescence in the preneoplastic cirrhosis stage. Mutation and expression analyses in HCC strongly suggest that neoplastic cells bypass the senescence barrier by inactivating major senescence-inducing genes (p53, $p16^{INK4a}$ and $p15^{INK4b}$). Moreover, they acquire the ability of unlimited proliferation (immortality) by re-expressing the TERT enzyme. Chromosomal instability that is generated by telomere erosion may contribute to additional mutations necessary for tumor progression.

HCCs upon implantation into livers of athymic mice [12]. However, these tumors regressed rapidly upon restoration of p53 expression. Tumor regression was due to differentiation and massive senescence induction, followed by immune-mediated clearance of senescent cells. These observations may indicate that oncogene-induced senescence is also involved in HCC. On the other hand, HCCs induced by tet-regulated c-Myc activation in mouse liver cells differentiate into mature hepatocytes and biliary cells or undergo senescence [90]. Thus, senescence induction may also be relevant to oncogene inactivation in HCC. In this regard, c-Myc down-regulation and senescence induction in several HCC cell lines as a response to TGF-β was observed (S. Senturk, M. Ozturk, unpublished data).

So far, all the reported examples of senescence induction in HCC cells are in the form of a telomere-independent permanent cell cycle arrest. Until recently, it was unknown whether replicative senescence could also be induced in immortal cancer cells. Ozturk et al. reported recently that immortal HCC cells can revert spontaneously to a replicative senescence phenotype [91]. Immortal HCC cells generated progeny that behaved, in vitro, similar to normal somatic cells. Such senescence-programmed progeny lacked telomerase activity due to TERT repression (probably mediated by SIP1 gene), and displayed progressive telomere shortening in cell culture, resulting in senescence arrest. It will be interesting to test whether such spontaneous reversal of replicative immortality is involved in well known tumor dormancy and/or spontaneous tumor regression.

7. Concluding remarks

Cellular senescence has gained great interest in recent years following the demonstration that it also occurs in vivo. It is also highly interesting that senescence can be mediated by a large number of pathways and molecules, as is the case for apoptosis. Recent findings that implicate secreted molecules in senescence induction strongly suggest that cellular senescence is not just a cellular event, but also a physiologically relevant process for the whole organism. In terms of tumor biology, oncogene-induced senescence that may serve as anti-tumor mechanism in pre-neoplastic lesions underlines its clinical relevance. On the other hand, induced or spontaneous senescence that is observed in cancer cells is promising to explore new approaches for tumor prevention and treatment. The role of senescence bypass and cellular immortality in hepatocellular carcinogenesis is not well defined. But, many findings (inactivation of senescence-mediator genes such as p53, $p16^{INK4a}$ and $p15^{INK4b}$, as well as reactivation of TERT) indicate that senescence mechanisms and their aberrations are critically involved in HCC. We may expect that this field will attract more attention in coming years for a better definition of senescence implications in hepatocellular carcinogenesis.

AcknowledgmentS

Authors' research is supported by grants from TUBITAK, DPT and TUBA (Turkey), and InCA (France). We thank D. Ozturk for language editing.

References

[1] D.E. Crew (Ed.), Human senescence-evolutionary and biocultural perspectives, Cambridge University Press, Cambridge, 2003.
[2] L. Hayflick, The limited in vitro lifetime of human diploid cell strains, Exp. Cell Res. 37 (1965) 614–636.
[3] J. Campisi, F. d'Adda di Fagagna, Cellular senescence: when bad things happen to good cells, Nat. Rev. Mol. Cell Biol. 8 (2007) 729–740.
[4] K.L. Rudolph, S. Chang, H.W. Lee, M. Blasco, G.J. Gottlieb, C. Greider, R.A. DePinho, Longevity, stress response, and cancer in aging telomerase-deficient mice, Cell 96 (1999) 701–712.
[5] G.K. Michalopoulos, Liver regeneration, J. Cell Physiol. 213 (2007) 286–300.
[6] V. Paradis, N. Youssef, D. Dargere, N. Ba, F. Bonvoust, J. Deschatrette, P. Bedossa, Replicative senescence in normal liver, chronic hepatitis C, and hepatocellular carcinomas, Hum. Pathol. 32 (2001) 327–332.
[7] S.U. Wiemann, A. Satyanarayana, M. Tsahuridu, H.L. Tillmann, L. Zender, J. Klempnauer, P. Flemming, S. Franco, M.A. Blasco, M.P. Manns, K.L. Rudolph, Hepatocyte telomere shortening and senescence are general markers of human liver cirrhosis, FASEB J. 16 (2002) 935–942.
[8] V. Trak-Smayra, J. Contreras, F. Dondero, F. Durand, S. Dubois, D. Sommacale, P. Marcellin, J. Belghiti, C. Degott, V. Paradis, Role of replicative senescence in the progression of fibrosis in hepatitis C virus (HCV) recurrence after liver transplantation, Transplantation 77 (2004) 1755–1760.
[9] H.B. El-Serag, K.L. Rudolph, Hepatocellular carcinoma: epidemiology and molecular carcinogenesis, Gastroenterology 132 (2007) 2557–2576.
[10] K.L. Rudolph, S. Chang, M. Millard, N. Schreiber-Agus, R.A. DePinho, Inhibition of experimental liver cirrhosis in mice by telomerase gene delivery, Science 287 (2000) 1253–1258.
[11] A. Satyanarayana, S.U. Wiemann, J. Buer, J. Lauber, K.E. Dittmar, T. Wüstefeld, M.A. Blasco, M.P. Manns, K.L. Rudolph, Telomere shortening impairs organ regeneration by inhibiting cell cycle re-entry of a subpopulation of cells, EMBO J. 22 (2003) 4003–4013.
[12] W. Xue, L. Zender, C. Miething, R.A. Dickins, E. Hernando, V. Krizhanovsky, C. Cordon-Cardo, S.W. Lowe, Senescence and tumour clearance is triggered by p53 restoration in murine liver carcinomas, Nature 445 (2007) 656–660.
[13] T. de Lange, Shelterin: the protein complex that shapes and safeguards human telomeres, Genes Dev. 19 (2005) 2100–2110.
[14] E.H. Blackburn, Structure and function of telomeres, Nature 350 (1991) 569–573.
[15] Y.S. Cong, W.E. Wright, J.W. Shay, Human telomerase and its regulation, Microbiol. Mol. Biol. Rev. 66 (2002) 407–425.
[16] J. Karlseder, A. Smogorzewska, T. de Lange, Senescence induced by altered telomere state, Not telomere loss, Science 295 (2002) 2446–2449.
[17] R.E. Verdun, J. Karlseder, Replication and protection of telomeres, Nature 447 (2007) 924–931.
[18] F. d'Adda di Fagagna, P.M. Reaper, L. Clay-Farrace, H. Fiegler, P. Carr, T. Von Zglinicki, G. Saretzki, N.P. Carter, S.P. Jackson, A DNA damage checkpoint response in telomere-initiated senescence, Nature 426 (2003) 194–198.
[19] M. Serrano, A.W. Lin, M.E. McCurrach, D. Beach, S.W. Lowe, Oncogenic ras provokes premature cell senescence associated with accumulation of p53 and p16INK4a, Cell 88 (1997) 593–602.
[20] R. Di Micco, M. Fumagalli, d'Adda F. di Fagagna, Breaking news: high-speed race ends in arrest-how oncogenes induce senescence, Trends Cell Biol. 17 (2007) 529–536.
[21] W.J. Mooi, D.S. Peeper, Oncogene-induced cell senescence-halting on the road to cancer, N. Engl. J. Med. 355 (2006) 1037–1046.
[22] Z. Chen, L.C. Trotman, D. Shaffer, H.K. Lin, Z.A. Dotan, M. Niki, J.A. Koutcher, H.I. Scher, T. Ludwig, W. Gerald, C. Cordon-Cardo, P.P. Pandolfi, Crucial role of p53-dependent cellular senescence in suppression of Pten-deficient tumorigenesis, Nature 436 (2005) 725–730.
[23] R. Di Micco, M. Fumagalli, A. Cicalese, S. Piccinin, P. Gasparini, C. Luise, C. Schurra, M. Garre', P.G. Nuciforo, A. Bensimon, R. Maestro, P.G. Pelicci, F. d'Adda di Fagagna, Oncogene-induced senescence is a DNA damage response triggered by DNA hyper-replication, Nature 444 (2006) 638–642.
[24] J. Bartkova, N. Rezaei, M. Liontos, P. Karakaidos, D. Kletsas, N. Issaeva, L.V. Vassiliou, E. Kolettas, K. Niforou, V.C. Zoumpourlis, M. Takaoka, H. Nakagawa, F. Tort, K. Fugger, F. Johansson, M. Sehested, C.L. Andersen, L. Dyrskjot, T. Ørntoft, J. Lukas, C. Kittas, T. Helleday, T.D. Halazonetis, J. Bartek, V.G. Gorgoulis, Oncogene-induced senescence is part of the tumorigenesis barrier imposed by DNA damage checkpoints, Nature 444 (2006) 633–637.
[25] T. Lu, T. Finkel, Free radicals and senescence, Exp. Cell Res. 314 (2008) 1918–1922.
[26] M. Giorgio, M. Trinei, E. Migliaccio, P.G. Pelicci, Hydrogen peroxide: a metabolic by-product or a common mediator of ageing signals?, Nat Rev. Mol. Cell Biol. 8 (2007) 722–728.
[27] C. Blanchetot, J. Boonstra, The ROS-NOX connection in cancer and angiogenesis, Crit. Rev. Eukaryot. Gene Expr. 18 (2008) 35–45.
[28] T. von Zglinicki, G. Saretzki, W. Döcke, C. Lotze, Mild hyperoxia shortens telomeres and inhibits proliferation of fibroblasts: a model for senescence?, Exp Cell Res. 220 (1995) 186–193.
[29] A.C. Lee, B.E. Fenster, H. Ito, K. Takeda, N.S. Bae, T. Hirai, Z.X. Yu, V.J. Ferrans, B.H. Howard, T. Finkel, Ras proteins induce senescence by altering the intracellular levels of reactive oxygen species, J. Biol. Chem. 274 (1999) 7936–7940.
[30] S. Courtois-Cox, S.L. Jones, K. Cichowski, Many roads lead to oncogene-induced senescence, Oncogene 27 (2008) 2801–2809.
[31] J.F. Passos, G. Saretzki, S. Ahmed, G. Nelson, T. Richter, H. Peters, I. Wappler, M.J. Birket, G. Harold, K. Schaeuble, M.A. Birch-Machin, T.B. Kirkwood, T. von Zglinicki, Mitochondrial dysfunction accounts for the stochastic heterogeneity in telomere-dependent senescence, PLoS Biol. 5 (2007) e110.
[32] K. Ito, A. Hirao, F. Arai, K. Takubo, S. Matsuoka, K. Miyamoto, M. Ohmura, K. Naka, K. Hosokawa, Y. Ikeda, T. Suda, Reactive oxygen species act through p38 MAPK to limit the lifespan of hematopoietic stem cells, Nat. Med. 12 (2006) 446–451.
[33] U. Herbig, W.A. Jobling, B.P. Chen, D.J. Chen, J.M. Sedivy, Telomere shortening triggers senescence of human cells through a pathway involving ATM, p53, and p21(CIP1), but not p16(INK4a) but not p16(INK4a), Mol. Cell. 14 (2004) 501–513.
[34] F.A. Mallette, M.F. Gaumont-Leclerc, G. Ferbeyre, The DNA damage signaling pathway is a critical mediator of oncogene-induced senescence, Genes Dev. 21 (2007) 43–48.
[35] J. Gil, G. Peters, Regulation of the INK4b-ARF-INK4a tumour suppressor locus: all for one or one for all, Nat. Rev. Mol. Cell Biol. 7 (2006) 667–677.
[36] D.A. Alcorta, Y. Xiong, D. Phelps, G. Hannon, D. Beach, J.C. Barrett, Involvement of the cyclin-dependent kinase inhibitor p16 (INK4a) in replicative senescence of normal human fibroblasts, Proc. Natl. Acad. Sci. U S A 93 (1996) 13742–13747.
[37] F. Zindy, D.E. Quelle, M.F. Roussel, C.J. Sherr, Expression of the p16INK4a tumor suppressor versus other INK4 family members during mouse development and aging, Oncogene 15 (1997) 203–211.
[38] R. Tremain, M. Marko, V. Kinnimulki, H. Ueno, E. Bottinger, A. Glick, Defects in TGF-beta signaling overcome senescence of mouse keratinocytes expressing v-Ha-ras, Oncogene 19 (2000) 1698–1709.
[39] N. Wajapeyee, R.W. Serra, X. Zhu, M. Mahalingam, M.R. Green, Oncogenic BRAF induces senescence and apoptosis through pathways mediated by the secreted protein IGFBP7, Cell 132 (2008) 363–374.
[40] J.C. Acosta, A. O'Loghlen, A. Banito, M.V. Guijarro, A. Augert, S. Raguz, M. Fumagalli, M. Da Costa, C. Brown, N. Popov, Y. Takatsu, J. Melamed, F. d'Adda di Fagagna, D. Bernard, E. Hernando, J. Gil, Chemokine signaling via the CXCR2 receptor reinforces senescence, Cell 133 (2008) 1006–1018.
[41] T. Kuilman, C. Michaloglou, L.C. Vredeveld, S. Douma, R. van Doorn, C.J. Desmet, L.A. Aarden, W.J. Mooi, D.S. Peeper, Oncogene-induced senescence relayed by an interleukin-dependent inflammatory network, Cell 133 (2008) 1019–1031.
[42] W.S. el-Deiry, T. Tokino, V.E. Velculescu, D.B. Levy, R. Parsons, J.M. Trent, D. Lin, W.E. Mercer, K.W. Kinzler, B. Vogelstein, WAF1, a potential mediator of p53 tumor suppression, Cell 75 (1993) 817–825.
[43] Y. Deng, S.S. Chan, S. Chang, Telomere dysfunction and tumor suppression: the senescence connection, Nat. Rev. Cancer 8 (2008) 450–458.
[44] L. Fang, M. Igarashi, J. Leung, M.M. Sugrue, S.W. Lee, S.A. Aaronson, p21Waf1/Cip1/Sdi1 induces permanent growth arrest with markers

of replicative senescence in human tumor cells lacking functional p53, Oncogene 18 (1999) 2789–2797.
[45] C. Giacinti, A. Giordano, RB and cell cycle progression, Oncogene 25 (2006) 5220–5227.
[46] M. Narita, S. Nunez, E. Heard, A.W. Lin, S.A. Hearn, D.L. Spector, G.J. Hannon, S.W. Lowe, Rb-mediated heterochromatin formation and silencing of E2F target genes during cellular senescence, Cell 113 (2003) 703–716.
[47] R. Zhang, M.V. Poustovoitov, X. Ye, H.A. Santos, W. Chen, S.M. Daganzo, J.P. Erzberger, I.G. Serebriiskii, A.A. Canutescu, R.L. Dunbrack, J.R. Pehrson, J.M. Berger, P.D. Kaufman, P.D. Adams, Formation of MacroH2A-containing senescence-associated heterochromatin foci and senescence driven by ASF1a and HIRA, Dev. Cell 8 (2005) 19–30.
[48] M. Narita, M. Narita, V. Krizhanovsky, S. Nunez, A. Chicas, S.A. Hearn, M.P. Myers, S.W. Lowe, A novel role for high-mobility group a proteins in cellular senescence and heterochromatin formation, Cell 126 (2006) 503–514.
[49] P.D. Adams, Remodeling of chromatin structure in senescent cells and its potential impact on tumor suppression and aging, Gene 397 (2007) 84–93.
[50] K. Takubo, N. Izumiyama-Shimomura, N. Honma, M. Sawabe, T. Arai, M. Kato, M. Oshimura, K. Nakamura, Telomere lengths are characteristic in each human individual, Exp. Gerontol. 37 (2002) 523–531.
[51] H. Aikata, H. Takaishi, Y. Kawakami, S. Takahashi, M. Kitamoto, T. Nakanishi, Y. Nakamura, F. Shimamoto, G. Kajiyama, T. Ide, Telomere reduction in human liver tissues with age and chronic inflammation, Exp. Cell Res. 256 (2000) 578–582.
[52] R. Utoh, C. Tateno, C. Yamasaki, N. Hiraga, M. Kataoka, T. Shimada, K. Chayama, K. Yoshizato, Susceptibility of chimeric mice with livers repopulated by serially subcultured human hepatocytes to hepatitis B virus, Hepatology 47 (2008) 435–446.
[53] M. Delhaye, H. Louis, C. Degraef, O. Le Moine, J. Devière, B. Gulbis, D. Jacobovitz, M. Adler, P. Galand, Relationship between hepatocyte proliferative activity and liver functional reserve in human cirrhosis, Hepatology 23 (1996) 1003–1011.
[54] M.R. Stampfer, P. Yaswen, Human epithelial cell immortalization as a step in carcinogenesis, Cancer Lett. 194 (2003) 199–208.
[55] H. Wege, H.T. Le, M.S. Chui, L. Lui, J. Wu, G. Giri, H. Malhi, B.S. Sappal, V. Kumaran, S. Gupta, M.A. Zern, Telomerase reconstitution immortalized human fetal hepatocytes without disrupting their differentiation potential, Gastroenterology 124 (2003) 432–444.
[56] A. Lechel, A. Satyanarayana, Z. Ju, R.R. Plentz, S. Schaetzlein, C. Rudolph, L. Wilkens, S.U. Wiemann, G. Saretzki, N.P. Malek, M.P. Manns, J. Buer, K.L. Rudolph, The cellular level of telomere dysfunction determines induction of senescence or apoptosis in vivo, EMBO Rep. 6 (2005) 275–281.
[57] E. Lazzerini Denchi, G. Celli, T. de Lange, Hepatocytes with extensive telomere deprotection and fusion remain viable and regenerate liver mass through endoreduplication, Genes Dev. 20 (2006) 2648–2653.
[58] G. Szabo, P. Mandrekar, A. Dolganiuc, Innate immune response and hepatic inflammation, Semin. Liver Dis. 27 (2007) 339–350.
[59] H. Malhi, G.J. Gores, Cellular and molecular mechanisms of liver injury, Gastroenterology 134 (2008) 1641–1654.
[60] D. Schuppan, N.H. Afdhal, Liver cirrhosis, Lancet 371 (2008) 838–851.
[61] F. Farinati, R. Cardin, M. Bortolami, P. Burra, F.P. Russo, M. Rugge, M. Guido, A. Sergio, R. Naccarato, Hepatitis C virus: from oxygen free radicals to hepatocellular carcinoma, J. Viral Hepat. 14 (2007) 821–829.
[62] A. Reuben, Alcohol and the liver, Curr. Opin. Gastroenterol. 24 (2008) 328–338.
[63] R. Shimoda, M. Nagashima, M. Sakamoto, N. Yamaguchi, S. Hirohashi, J. Yokota, H. Kasai, Increased formation of oxidative DNA damage, 8-hydroxydeoxyguanosine, in human livers with chronic hepatitis, Cancer Res. 54 (1994) 3171–3172.
[64] P. Zindy, L. Andrieux, D. Bonnier, O. Musso, S. Langouët, J.P. Campion, B. Turlin, B. Clément, N. Théret, Upregulation of DNA repair genes in active cirrhosis associated with hepatocellular carcinoma, FEBS Lett. 579 (2005) 95–99.
[65] R.R. Plentz, Y.N. Park, A. Lechel, H. Kim, F. Nellessen, B.H. Langkopf, L. Wilkens, A. Destro, B. Fiamengo, M.P. Manns, M. Roncalli, K.L. Rudolph, Telomere shortening and inactivation of cell cycle checkpoints characterize human hepatocarcinogenesis, Hepatology 45 (2007) 968–976.
[66] M. Roncalli, P. Bianchi, B. Bruni, L. Laghi, A. Destro, S. Di Gioia, L. Gennari, M. Tommasini, A. Malesci, G. Coggi, Methylation framework of cell cycle gene inhibitors in cirrhosis and associated hepatocellular carcinoma, Hepatology 36 (2002) 427–432.
[67] M. Ozturk, Genetic aspects of hepatocellular carcinogenesis, Semin. Liver Dis. 19 (1999) 235–242.
[68] T. Soussi, p53 alterations in human cancer: more questions than answers, Oncogene 26 (2007) 2145–2156.
[69] Y. Edamoto, A. Hara, W. Biernat, L. Terracciano, G. Cathamos, H.M. Riehle, M. Matsuda, H. Fuji, J.M. Scoazec, H. Ohgaki, Alterations of RB1, p53 and Wnt pathways in Hepatocellular carcinomas associated with HCV, HBV and alcoholic liver cirrhosis, Int. J. Cancer 106 (2003) 334–341.
[70] H. Tahara, T. Nakanishi, M. Kitamoto, R. Nakashio, J.W. Shay, E. Tahara, G. Kajiyama, T. Ide, Telomerase activity in human liver tissues: Comparison between chronic liver disease and hepatocellular carcinomas, Cancer Res. 55 (1995) 2734–2736.
[71] H. Kojima, O. Yokosuka, F. Imazeki, H. Saisho, M. Omata, Telomerase activity and telomere length in hepatocellular carcinoma and chronic liver disease, Gastroenterology 112 (1997) 493–500.
[72] J. Nakayama, H. Tahara, E. Tahara, M. Saito, K. Ito, H. Nakamura, T. Nakanishi, E. Tahara, T. Ide, F. Ishikawa, Telomerase activation by hTERT in human normal fibroblasts and hepatocellular carcinomas, Nat. Genet. 18 (1998) 65–68.
[73] D. Gozuacik, Y. Murakami, K. Saigo, M. Chami, C. Mugnier, D. Lagorce, T. Okanoue, T. Urashima, C. Bréchot, P. Paterlini-Bréchot, Identification of human cancer-related genes by naturally occurring Hepatitis B Virus DNA tagging, Oncogene 20 (2001) 6233–6240.
[74] I. Horikawa, JC. Barrett, Transcriptional regulation of the telomerase hTERT gene as a target for cellular and viral oncogenic mechanisms, Carcinogenesis 24 (2003) 1167–1176.
[75] Y. Murakami, K. Saigo, H. Takashima, M. Minami, T. Okanoue, C. Bréchot, P. Paterlini-Bréchot, Large scaled analysis of hepatitis B virus (HBV) DNA integration in HBV related hepatocellular carcinomas, Gut 54 (2005) 1162–1168.
[76] Z.L. Qu, S.Q. Zou, N.Q. Cui, X.Z. Wu, M.F. Qin, D. Kong, Z.L. Zhou, Upregulation of human telomerase reverse transcriptase mRNA expression by in vitro transfection of hepatitis B virus X gene into human hepatocarcinoma and cholangiocarcinoma cells, World J. Gastroenterol. 11 (2005) 5627–5632.
[77] H. Liu, F. Luan, Y. Ju, H. Shen, L. Gao, X. Wang, S. Liu, L. Zhang, W. Sun, C. Ma, In vitro transfection of the hepatitis B virus PreS2 gene into the human hepatocarcinoma cell line HepG2 induces upregulation of human telomerase reverse transcriptase, Biochem. Biophys. Res. Commun. 355 (2007) 379–384.
[78] R. Janknecht, On the road to immortality: hTERT upregulation in cancer cells, FEBS Lett. 564 (2004) 9–13.
[79] N. Miura, I. Horikawa, A. Nishimoto, H. Ohmura, H. Ito, S. Hirohashi, J.W. Shay, M. Oshimura, Progressive telomere shortening and telomerase reactivation during hepatocellular carcinogenesis, Cancer Genet. Cytogenet. 93 (1997) 56–62.
[80] J.E. Lee, B.K. Oh, J. Choi, Y.N. Park, Telomeric 3' overhangs in chronic HBV-related hepatitis and hepatocellular carcinoma, Int. J. Cancer 123 (2008) 264–272.
[81] B.K. Oh, Y.J. Kim, C. Park, Y.N. Park, Up-regulation of telomere-binding proteins, TRF1, TRF2, and TIN2 is related to telomere shortening during human multistep hepatocarcinogenesis, Am. J. Pathol. 166 (2005) 73–80.
[82] A. Satyanarayana, M.P. Manns, K.L. Rudolph, Telomeres and Telomerase: a Dual role in hepatocarcinogenesis, Hepatology 40 (2004) 276–283.
[83] A. Lechel, H. Holstege, Y. Begus, A. Schienke, K. Kamino, U. Lehmann, S. Kubicka, P. Schirmacher, J. Jonkers, K.L. Rudolph, Telomerase deletion limits progression of p53-mutant hepatocellular carcinoma with short telomeres in chronic liver disease, Gastroenterology 132 (2007) 1465–1475.
[84] W.C. Hahn, C.M. Counter, A.S. Lundberg, R.L. Beijersbergen, M.W. Brooks, R.A. Weinberg, Creation of human tumor cells with defined genetic elements, Nature 400 (1999) 464–468.
[85] J.W. Shay, I.B. Roninson, Hallmarks of senescence in carcinogenesis and cancer therapy, Oncogene 23 (2004) 2919–2933.
[86] M. Collado, J. Gil, A. Efeyan, C. Guerra, A.J. Schuhmacher, M. Barradas, A. Benguría, A. Zaballos, J.M. Flores, M. Barbacid, D. Beach, M. Serrano, Tumour biology: senescence in premalignant tumours, Nature 436 (2005) 642.
[87] M. Braig, S. Lee, C. Loddenkemper, C. Rudolph, A.H. Peters, B. Schlegelberger, H. Stein, B. Dörken, T. Jenuwein, C.A. Schmitt, Oncogene-induced senescence as an initial barrier in lymphoma development, Nature 436 (2005) 660–665.

[88] C. Michaloglou, L.C. Vredeveld, M.S. Soengas, C. Denoyelle, T. Kuilman, C.M. van der Horst, D.M. Majoor, J.W. Shay, W.J. Mooi, D.S. Peeper, BRAFE600-associated senescence-like cell cycle arrest of human naevi, Nature 436 (2005) 720–724.
[89] S.I. Suh, H.Y. Pyun, J.W. Cho, W.K. Baek, J.B. Park, T. Kwon, J.W. Park, M.H. Suh, D.A. Carson, 5-Aza-2'-deoxycytidine leads to down-regulation of aberrant p16 RNA transcripts and restores the functional retinoblastoma protein pathway in hepatocellular carcinoma cell lines, Cancer Lett. 160 (2000) 81–88.
[90] C.H. Wu, J. van Riggelen, A. Yetil, A.C. Fan, P. Bachireddy, D.W. Felsher, Cellular senescence is an important mechanism of tumor regression upon c-Myc inactivation, Proc. Natl. Acad. Sci. USA 104 (2007) 13028–13033.
[91] N. Ozturk, E. Erdal, M. Mumcuoglu, K.C. Akcali, O. Yalcin, S. Senturk, A. Arslan-Ergul, B. Gur, I. Yulug, R. Cetin-Atalay, C. Yakicier, T. Yagci, M. Tez, M. Ozturk, Reprogramming of replicative senescence in hepatocellular carcinoma-derived cells, Proc. Natl. Acad. Sci. USA 103 (2006) 2178–2183.